Lakehead University

The Nb-mineralization of the Oka Carbonatite Complex, Quebec

Shannon Hay

A thesis submitted to the Department of Geology in partial fulfilment of the requirements for the Degree Masters of Science

May 2003

Acknowledgements

I would like to thank Dr. Roger Mitchell for his guidance and supervision of this thesis. Ann Hammond, Sam Spivak, Alan MacKenzie and Dr. Pete Hollings have been very helpful with different aspects of this work.

I am thankful to all of my friends and family, here at Lakehead and at home, who have made it all so much easier. Finally, I would like to thank Steve for his loving kindness and support.

Abstract

A representative collection of minerals from two niobium deposits found within the Oka carbonatite complex: the Bond Zone deposit; and the NIOCAN deposit, were analysed using an electron microprobe, and compared with existing data from the St. Lawrence Columbium deposit. These minerals are good indicators of the petrological evolution of alkaline rocks, and can be used to re-evaluate the paragenesis of niobium mineralization, and the relationships between Nb-bearing minerals. In addition, this study has revealed the presence of zirconolite as an accessory mineral in calciocarbonatite.

At Oka, pyrochlore typically occurs as euhedral- to –subhedral crystals, rarely as aggregates and clusters. Back-scattered images, coupled with microprobe analyses, reveal complex compositional zoning in pyrochlore, which undoubtedly reflects changes in the fluid composition during the growth of the mineral. Large compositional variations were observed for the major oxides of the pyrochlores: CaO (ranging from 4.1-34.8 wt. % oxide), TiO_2 (2.3-40.4 wt. %), Nb_2O_5 (20.1-58.1 wt. %), ThO_2 (0.3-18.2 wt. %), and UO_2 (0.1-28.0 wt. %). Ceriopyrochlore, cerium pyrochlore, and uranpyrochlore exhibit the greatest *A*-site vacancies, ranging from 8.1-62.5 %. Of the REEs, only Ce is present at high concentration levels (ranging from 2.1-15.8 wt. %). Of note is the significant content of ZrO_2, which ranges from 0.9-16.3 wt. %. An *A*-site substitution in the pyrochlore-group minerals has been identified between (REE+U+Th) and (Na+Ca), as well as a *B*-site substitution between (Nb+Ti) and Zr.

Latrappite and Nb-rich members of the perovskite-group are found occurring as euhedral- to –subhedral crystals. Both oscillatory and patchy zonation in the Oka perovskites has been identified using back-scattered imaging. Small compositional variations are observed in the major oxides of both the latrappite- and –perovskite end-members. Oka perovskites are slightly enriched in the LREE's, Ce being the dominant LREE (averaging 3.5 wt. % oxide).

Zirconolite is commonly found as lath-shaped discrete crystals or intergrown with perovskite and pyrochlore-group minerals. Oka zirconolites have a large range of Nb_2O_5, ranging from 11.5-25.8 wt. %. Compositional zoning has been identified using back-scattered imaging, correlating with an increase in LREE toward the rim of the crystals. The zirconolite compositions are similar to other calciocarbonatite-hosted zirconolites, with the exception of their higher Nb contents.

The crystallization history of the NIOCAN and Bond Zone deposits cannot be deduced from the observed mineral assemblage. The calciocarbonatite does not represent a liquid composition, as it has a bulk composition which is determined by mixing material derived from several batches of magma. The magmas with gave rise to the NIOCAN and Bond Zone seem more evolved than those forming the pyrochlore-group minerals in the St. Lawrence Columbium deposits, as the pyrochlores from St. Lawrence Columbium are "less-evolved" in relation to the NIOCAN and Bond Zone pyrochlores. The major conclusion of this work is that the calciocarbonatites at NIOCAN and Bond Zone are hybrid rocks. Enrichment of specific mineralized zones is probably dependent upon rheological factors rather than compositional controls.

Table of contents

Table of Figures

Table of Figures continued.

Table of Figures continued.

Table of Tables

Chapter 1: Introduction

1.1. Statement of nature of the work

This research work consists of a detailed mineralogical study of the Oka Carbonatite Complex. The focus of this study is the niobium mineralization within the complex and in particular the niobium deposit recently located by NIOCAN Inc. As a result of this discovery, comparisons can be made between the three niobium deposits found within the carbonatite complex; the St. Lawrence Columbium deposit, the Bond Zone deposit, and the NIOCAN deposit. In addition, the paragenesis of niobium mineralization, and relationships between Nb-bearing minerals can be re-evaluated.

Niocalite, pyrochlore- and perovskite-group minerals are relatively common accessory constituents of sovites at the complex. In addition, this study has revealed the occurrence of zirconolite. This work will be concentrated on these minerals, as they are good indicators of the petrological evolution of alkaline rocks.

1.2. General geology

The Oka carbonatite complex is located 40 kilometres west of Montreal, Quebec, and is a member of the Monteregian petrographic province. The Cretaceous (110 Ma, Shafiqullah *et al.* 1970) carbonatites and feldspathoidal-bearing silicate rocks of the Oka complex intrude the Precambrian basement rocks as what has been interpreted as a double ring structure (Gold 1963, 1967, 1972). The complex is not deformed or metamorphosed, and extends along the axis of the Beauharnois arch (a broad northwest trending arch) in a roughly oval shape. The intersection of the two structural trends, the northwest-trending Beauharnois arch and the eastward-trending faults associated with the Ottawa-Bonnechère graben, probably controlled the emplacement of the complex.

The Oka complex is four and a half miles long by one and a half miles wide, and is elongated northwest-to-southest. Previous interpretations of the complex (Gold *et al.*, 1963, 1967, 1972) suggest that it is composed of four plutons in two intrusive centers (a "figure eight" plan). The silicate rocks occur as ring dikes within the carbonatite, and in the outer zones of the complex. The carbonatites occur mainly in the cores of the two rings, but also as ring dikes in the outer zones of the complex. The entire complex is cut by vertically-dipping alnöite breccia pipes.

Exploration of the Oka carbonatite complex began in 1953. Mining activities began at Oka in the 1960s, when St. Lawrence Columbium and Metals Corp. mined pyrochlore-bearing carbonatite ores for Nb_2O_5 at the St. Lawrence Columbium and Metals Corporation mine up until the middle 1970s. A second deposit, the Bond Zone deposit was explored at the same time, but mining activities were not undertaken. Quebec Columbium Limited own the northern part, and Columbium Mining Products Limited own the southern part of this zone (figure 1.1).

Five main groups of intrusive rocks plus fenite, can be found at the Oka Complex (figure 1.1):

Carbonatites:

On the basis of their mineralogy, most of the carbonatite rocks are coarse grained sovites, with calcite being the main mineral. Accessory minerals found in the carbonatites include aegirine-augite, biotite, apatite, nepheline, monticellite, melilite, pyrochlore, perovskite, niocalite, richterite, pyrite, and pyrrhotite. The sovite carbonatite exhibits modal layering due to varying proportions of magnetite, sodian augite, biotite, hornblende and olivine. In most parts of the complex, hydrothermal veins filled with calcite, biotite, pyrite and rare-earth minerals such as

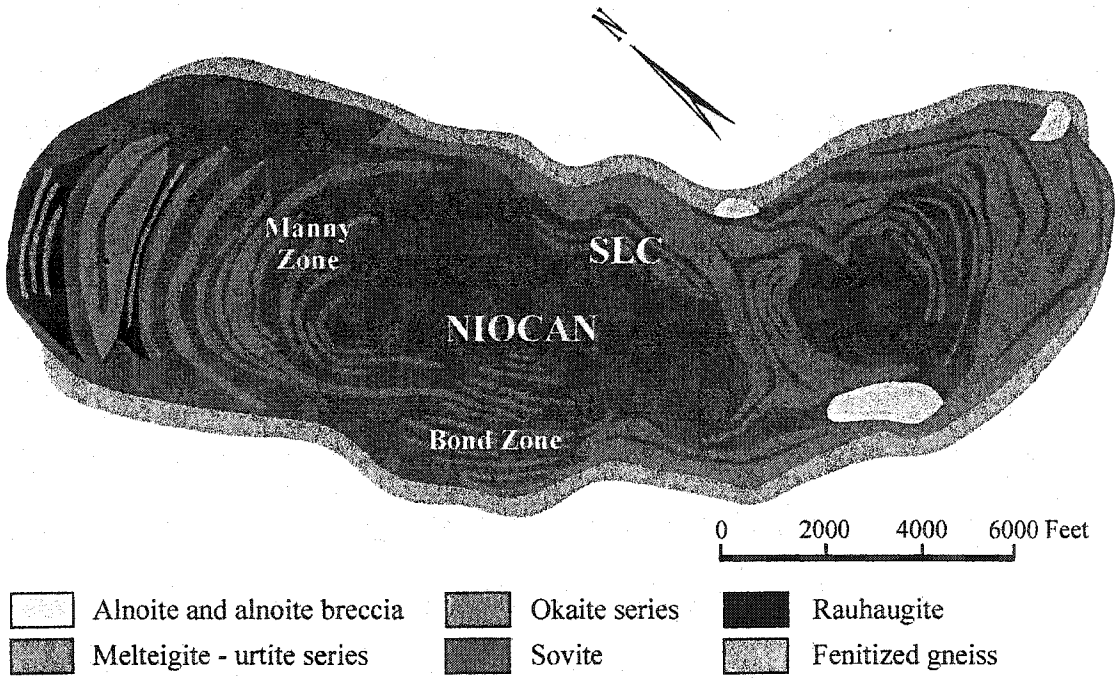

Figure 1.1. Simplified geologic map of the Oka pluton, modified from Gold (1963, 1972). Sample locations shown are: SLC (St. Lawrence Columbian), NIOCAN, and Bond Zone.

bastnaesite, britholite and parisite are present. These veins occur along fractures caused by minor faulting.

Okaite-Jacupirangite Series

This group of rocks is only found in the northern ring of the complex. Melilite and titanaugite are the two main minerals found in this series, along with accessory minerals such as nepheline, haüyne, perovskite, apatite, biotite, magnetite, and calcite.

Ijolite-Urtite Series

This group of rocks is found encompassing the southern ring of the complex, as well as dykes in the northern ring. The rocks are composed principally of aegirine-augite and nepheline with minor or accessory amounts of calcite, melanite, biotite, wollastonite and magnetite.

Glimmerite

Glimmerites occur as zones within ijolite in the St. Lawrence Columbium and Metals Corporation mine, the Manny zone and the Bond zone, and are composed of biotite and calcite with minor zeolites and rare-earth carbonates. Gold (1972) interpreted the glimmerites to have been formed by reaction between late hydrothermal fluids and silicate rocks.

Lamprophyres and intrusive breccias

The lamprophyres and intrusive breccias are made up of polymict breccia comprising country rock fragments within a matrix of country rock with calcite, chlorite or phlogpite, or more commonly massive alnöite with phenocrysts of olivine, augite, phlogopite and hornblende within a calcite –rich matrix.

Fenite

The country rocks around the complex have undergone metasomatic alteration. The alteration is characterized by replacement of alkali-feldspar, plagioclase and quartz by aegirine and nepheline. Fracture systems controlled the alteration.

Gold (1972) postulated the following sequence of events in the formation of the Oka carbonatite complex.

1. Gneissic country rocks underwent fentinization, followed by the emplacement of early carbonatites as dikes and ring dikes.
2. Ijolitization of the enclosed country rock.
3. The okaite-jacupirangite series rocks intruded as pods and arcuate dikes.
4. The main pyrochlore-bearing carbonatite intrudes, followed by the intrusion of the monticellite-carbonatite.
5. The ijolite and micro-ijolite dikes intrude into the complex.
6. Biotitization occurs as a result of the hydrothermal activity along fractures in the complex, forming glimmerites and deposition of thorian pyrochlore.
7. Late carbonatite dikes are emplaced.
8. Alnöite and alnöite breccia pipes and dikes are emplaced.

1.3. Analytical methods

NIOCAN Inc. contributed over 200 drill core samples. Samples were collected from 4 different drilling sites, with depths of the samples ranging from 10-500 metres (Appendix I). Thin sections of the samples were prepared, then carbon coated for analysis using the electron microprobe.

The minerals described in the present work were identified using X-ray energy-dispersion spectrometry (EDS). All mineral compositions were determined using a JEOL 5900 scanning electron microscope equipped with a LINK ISIS analytical system incorporating a Super ATW Light Element Detector. Raw EDS spectra were acquired for 60-300 seconds (live time) with an accelerating voltage of 20 kV and a beam current of 0.86 nA. The spectra were processed with the LINK ISIS SEMQUANT software, with full ZAF corrections applied. The following well-characterized natural standards were employed for analysis: loparite (Na, Nb, La, Ce, Pr, Nd), perovskite (Ca, Fe, Ti), corundum (Al), orthoclase (K), benitoite (Ba), jadeite (Si), metallic Pb, Ta, Th, and U. X-ray diffraction methods were not used as the pyrochlore- and perovskite-group minerals exhibit significant alteration and large differences in intra-granular variation in composition.

1.4. Introduction to the mineralogy of the complex

Petrographic analysis of thin sections indicate all of the samples studied are coarse-grained, calcite-rich rocks, containing euhedral- to -subhedral oxide and silicate minerals in a hypidiomorphic matrix of calcite. Minerals identified from individual drill core are listed in table 1.1. Complete drill core logs are given in Appendix 3. The carbonatite consists mainly of calcite, apatite, and manganese-bearing magnetite, with monticellite, latrappite, Nb-rich perovskite, pyrochlore, biotite, niocalite, and zirconolite as accessory phases.

Calcite is typically present in amounts varying from 40 to about 65 volume percent, and is found as subhedral and anhedral crystals, and as inclusions within apatite, pyrochlore and magnetite. Calcite is also found to host many different mineral inclusions such as: apatite; magnetite; barite; pyrite; galena; pyrochlore; zirconolite; and sphalerite. Apatite is typically present in amounts varying from 20 to about 30 volume percent, and is found as subhedral and

Table 1.1. Minerals identified in the drill cores investigated from the NIOCAN and Bond Zone deposits

Drill core #01	Drill core #31	Drill core #36	Drill core #52
Apatite	Ankerite	Apatite	Apatite
Baddeleyite	Apatite	Baddeleyite	Barite
Barite	Baddeleyite	Barite	Biotite
Biotite	Barite	Biotite	Calcite
Calcite	Biotite	Calcite	Calzirtite
Diopside	Calcite	Diopside	Diopside
Geothite	Galena	Dolomite	Dolomite
Ilmenite	Geothite	Geothite	Geothite
Magnetite	Ilmenite	Magnetite	Ilmenite
Pyrochlore	Magnetite	Niocalite	Magnetite
Sphalerite	Monticellite	Pyrochlore	Monticellite
Zirconolite	Niocalite	REE Carbonate	Niocalite
	Perovskite	Richterite	Perovskite
	Pyrite	Sphalerite	Pyrite
	Pyrochlore	Zirconolite	Pyrochlore
	REE Carbonate		Pyrrhotite
	Siderite		REE Carbonate
	Sphalerite		Sphalerite
	Zirconolite		Zirconolite

euhedral crystals; and as inclusions within calcite. It is commonly associated with high concentrations of pyrochlore, magnetite and other accessory minerals such as sulfides. Most of the apatite is unzoned and homogeneous in composition. The apatite is ubiquitous, occurring both as bands and disseminated crystals. Analysis indicates that zoned apatite grains show compositional variation, with REE-enrichment towards the outer zones of the grains.

Chapter 2: Mineralogy and composition of Pyrochlore-group minerals

2.1. Pyrochlore

2.1.1. Introduction

Pyrochlore is a common accessory mineral of carbonatites, and is a member of a group of cubic ($Fd\bar{3}m$) Nb-Ta-Ti oxides with the general structural formula, $A_{16-x}B_{16}O_{48}(O,OH,F)_{8-y} \cdot zH_2O$, where x and y are vacant sites in the unit cell and x, y and z are non-rational. Pyrochlore structures are capable of accommodating a wide variety of cations. *A*-sites can be occupied by As, Ba, Bi, Ca, Cs, K, Mg, Mn, Na, Pb, REEs, Sb, Sn, Sr, Th, U and Y. *B*-site atoms include Nb, Ta, Ti, and V. The assignment of Al, Fe, Si, and Zr is uncertain (Hogarth, 1989a).

The IMA-CNMMN pyrochlore subcommittee recommended that three subgroups of pyrochlore (See table 2.1 for the complete classification scheme) could be recognized:

Pyrochlore	Nb + Ta >2Ti, Nb >Ta;
Microlite	Nb + Ta >2Ti, Ta ≥ Nb;
Betafite	2Ti ≥ Nb + Ta

2.2. Oka Pyrochlore: NIOCAN and Bond Zone deposit

Further classification within the pyrochlore-subgroup depends on whether any of the *A*-site cations, other than Na or Ca, exceeds 20 atomic (at.) % of the total occupancy in the *A*-site (Hogarth, 1989a). The NIOCAN and Bond Zone (BZ) pyrochlores have been classified using the occupancy of the *A*-site cations. Samples containing >20 at. % of Th, Ce, and U have been identified, and have a prefix attached to the pyrochlore name, and are termed thorpyrochlore, ceriopyrochlore, and uranpyrochlore respectively. Samples containing less than 20 at. % are named thorium pyrochlore, cerium pyrochlore, and uranium pyrochlore, respectively.

Table 2.1. Classification of the pyrochlore group; species found in carbonatites are in capitals (*after* Hogarth, 1989a)

***A*-ions characteristic of species**		**Pyrochlore subgroup**	**Microlite subgroup**	**Betafite subgroup**
Na+Ca but no other *A*-atom		PYROCHLORE	microlite	CALCIOBETAFITE
One or more *A*-atoms other than Na or Ca; >20% total *A*-atoms	K	KALIPYROCHLORE		
	Cs		cestibtantite	
	Sn		stannomicrolite	
	Ba	BARIOPYROCHLORE	bariomicrolite	
	Sr	unnamed		
Species named by most abundant *A*-atom, other than Na or Ca	REE ΣCe>ΣY REE	yttropyrochlore		yttrobetafite
	Bi		bismutomicrolite	
	Sb			stibobetafite
	Pb	PLUMBOPYROCHLORE		plumbobetafite
	U	URANPYROCLORE	uranmicrolite	BETAFITE
	Th	unnamed		

REE= lanthanides + Y; ΣCe = (La → Eu), ΣY = (Gd → Lu) + Y.

At Oka, pyrochlore typically occurs as euhedral- to -subhedral crystals, more rarely as aggregates and clusters. Pyrochlore is present in amounts varying from 2 to 15 vol. percent, and in apatite-rich bands approaches 25 vol. percent. The constant association of apatite, biotite, and pyrochlore, has led Kalogeropoulos (1977), to conclude that Nb-fluorine complexes play a leading role in Nb-transportation. Back-scattered electron images (figure 2.1), coupled with detailed microprobe analyses, reveal complex compositional zoning in pyrochlore which undoubtedly reflects changes in the fluid composition during growth of the mineral. In contrast, a small percentage of the pyrochlore minerals are devoid of detectable zoning. The following criteria have been used to describe the various types of zoning and alteration present (Hogarth *et al.*, 2000).

Primary zonation: Crystals vary in composition, and may change systematically from core- to -rim. Crystals exhibit sharply defined narrow zones of compositional banding.

Low-Temperature alteration: Crystals exhibit an irregular amount of discoloured material at the crystal margin, and show bleached zones around microfractures. Discoloured, turbid patches can be observed within the crystal. Commonly, significant *A*-site vacancy is present.

Metamictization: The leaching of Na and Ca generates a significant *A*-site vacancy, which can only be detected by electron microprobe. Crystals with >10% UO_2 or ThO_2 are commonly metamict.

In the NIOCAN and Bond Zone deposits, pyrochlore is found to be up to 150-200 μm in diameter, and can occur intergrown with zirconolite and baddeleyite. The modal percentage of pyrochlore varies considerably from sample to sample. No more than two different subgroups of pyrochlore were found together within one sample. Cerium pyrochlore and uranoan pyrochlore were most commonly identified within the same section. The pyrochlore can occur as discrete

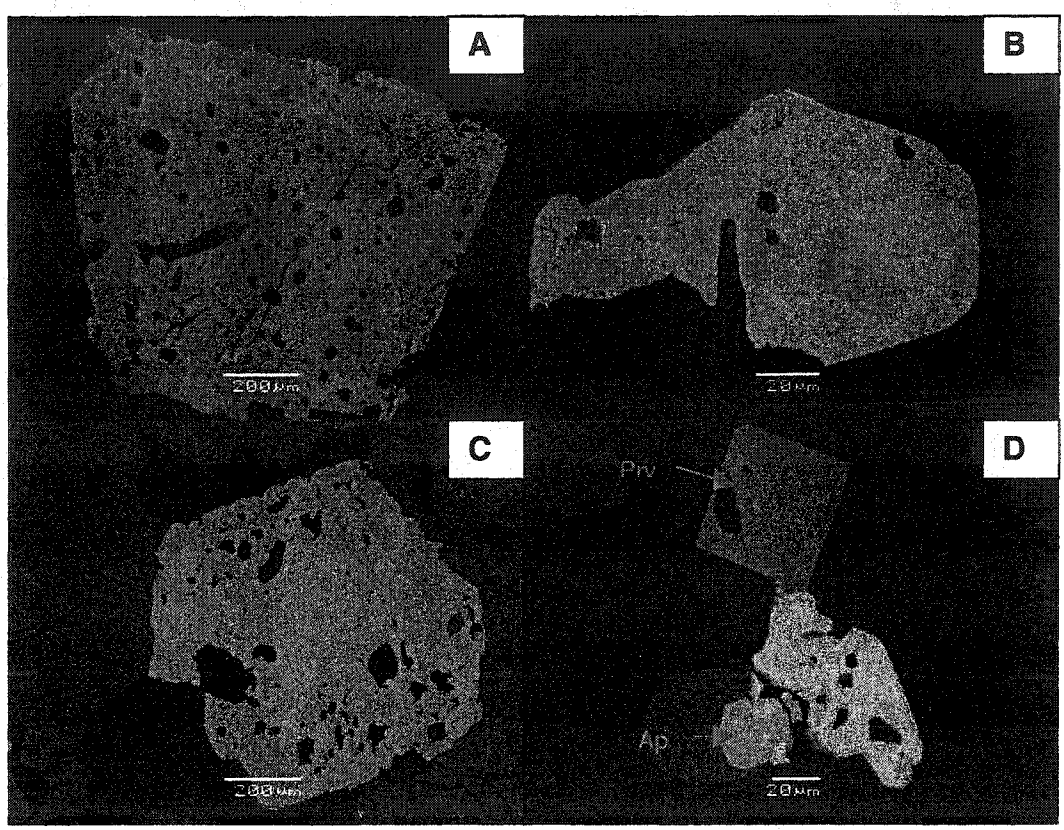

Figure 2.1. Pyrochlore-group minerals from the NIOCAN and Bond Zone deposits (BSE images). (a) oscillatory zoned, euhedral uranoan pyrochlore, (b) patchy-zoned, subhedral cerium pyrochlore, (c) oscillatory zoned, altered, euhedral cerium pyrochlore, (d) two-zone cerium anhedral pyrochlore shown associated with perovskite (Prv) and apatite (Ap).

grains or as a cluster of grains. Euhedral, subhedral and anhedral grains are found individually and associated together within samples of carbonatite. Some grains contain inclusions of calcite, apatite, baddeleyite and zirconolite. Associated minerals include calcite, apatite, magnetite, perovskite and biotite (figure 2.1).

Compositional ranges have been determined from over 120 microprobe analyses of pyrochlores from the NIOCAN and BZ deposits. All pyrochlore analyses are shown in Appendix II. Representative data are given in table 2.2, for which the formulae have been calculated to a total of two *B*-site cations. Extremely large compositional variations were observed for the major oxides:

CaO (range 4.09-34.77 wt. % oxide)

TiO_2 (2.28-40.36 wt. %)

Nb_2O_5 (20.09-58.12 wt. %)

ThO_2 (0.28-18.17 wt. %)

UO_2 (0.1-27.98 wt. %)

These variations result from the alteration of primary magmatic pyrochlore, and demonstrate that naturally-occurring pyrochlore can tolerate an exceptionally high density of vacancies in the *A*-site. The Oka pyrochlores have an *A*-site vacancy ranging from 0 (completely filled) to 62.5% vacant (table 2.3). Ceriopyrochlore, cerium pyrochlore and uranpyrochlore are the groups that exhibit the greatest *A*-site vacancies.

Of the REEs, only cerium is present at high concentration levels (ranging 2.08-15.75 wt. %) and only trace amounts of Nd and La can be found. Of note also is the significant content of ZrO_2, which ranges from 0.96 to 16.27 wt. %. NIOCAN and BZ pyrochlores contain insignificant amounts of Ta_2O_5 (<2 wt. %), in common with pyrochlore-group minerals from

Table 2.2. Representative compositions of Pyrochlore-group minerals from the NIOCAN and Bond Zone deposits of the Oka carbonatite complex

	31-350.2d Pyrochlore	52-14.4b-j Thorpyrochlore	52-155.57b Uranpyrochlore	36-270.85a Thorium Pyrochlore	31-155.15a Cerium Pyrochlore	36-358.3-p3-1 Uranoan Pyrochlore	31-211A Ceriopyrochlore
Na_2O	6.96	1.79	0.00	3.53	3.66	2.78	1.46
Al_2O_3	0.00	0.37	0.00	0.07	0.00	0.40	0.00
SiO_2	0.66	0.35	0.00	0.34	1.52	1.75	1.85
CaO	17.26	10.17	7.22	11.46	12.74	15.67	17.28
TiO_2	5.50	2.15	11.44	4.21	11.06	7.56	7.82
MnO	0.00	0.85	0.36	0.99	0.47	0.24	0.16
Fe_2O_3	0.24	1.91	2.00	2.70	0.71	2.13	1.83
SrO	0.00	0.18	2.25	0.00	0.00	0.00	0.00
ZrO_2	1.66	16.27	5.41	6.25	2.87	0.00	5.10
Nb_2O_5	64.74	34.41	34.60	43.81	42.89	43.28	43.51
BaO	0.00	0.07	0.00	0.21	0.00	0.00	0.20
La_2O_3	0.11	1.25	0.00	1.24	2.44	0.00	1.46
Ce_2O_3	1.29	6.20	2.91	7.23	15.42	6.74	10.28
Nd_2O_3	0.00	2.27	0.00	2.00	2.53	0.83	1.84
PbO	0.41	0.00	0.00	0.00	0.00	0.00	0.00
Ta_2O_5	0.00	0.04	6.37	0.38	0.00	0.00	0.00
ThO_2	0.62	21.05	0.00	12.42	1.81	4.32	2.22
UO_2	0.00	0.51	24.46	0.28	1.27	12.48	2.92
Sum	99.45	99.84	97.02	97.12	99.41	98.18	97.93
Na	0.770	0.254	0.000	0.479	0.455	0.371	0.181
Ca	1.055	0.797	0.514	0.859	0.876	1.155	1.184
Mn	0.000	0.053	0.020	0.059	0.026	0.014	0.009
Sr	0.000	0.008	0.087	0.000	0.000	0.000	0.000
Ba	0.000	0.002	0.000	0.006	0.000	0.000	0.005
La	0.002	0.034	0.000	0.032	0.058	0.000	0.034
Ce	0.027	0.166	0.071	0.185	0.362	0.170	0.241
Nd	0.000	0.059	0.000	0.050	0.058	0.020	0.000
Pb	0.006	0.000	0.000	0.000	0.000	0.000	0.000
Th	0.008	0.350	0.000	0.198	0.026	0.068	0.032
U	0.000	0.009	0.361	0.004	0.018	0.191	0.042
ΣA	1.869	1.731	1.053	1.872	1.880	1.988	1.770
A-def	0.131	0.269	0.947	0.128	0.120	0.012	0.230
Al	0.000	0.032	0.000	0.006	0.000	0.032	0.000
Si	0.038	0.026	0.000	0.340	0.098	0.120	0.118
Ti	0.236	0.118	0.571	0.222	0.534	0.391	0.376
Fe	0.010	0.105	0.100	0.142	0.034	0.110	0.088
Zr	0.046	0.580	0.175	0.213	0.090	0.000	0.159
Nb	1.670	1.138	1.039	1.386	1.245	1.346	0.005
Ta	0.000	0.001	0.115	0.007	0.000	0.000	0.000
ΣB	2.000	2.000	2.000	2.000	2.000	2.000	2.000

Total Fe expressed as Fe_2O_3. F detected, but not analysed.
All data calculated on 2 B-site cations.

Table 2.3. *A*-site vacancy ranges in the NIOCAN and Bond Zone pyrochlore-group minerals

	Drill section	Zoning	*A*-site vacancy range (a.p.f.u)	*A*-site vacancy range (%)
Ceriopyrochlore	31, 36	oscillatory	0.311 - 1.288	15.6 - 64.4
Cerium pyrochlore	01, 36, 31, 52	oscillatory, patchy	0 - 1.251	0 – 62.6
Pyrochlore	31	patchy	0.131 – 0.287	6.6 – 14.4
Thorpyrochlore	52	oscillatory	0.269 – 0.296	13.5 – 14.8
Thorium pyrochlore	52, 36	oscillatory	0.126 – 0.243	6.3 – 12.2
Uranpyrochlore	36, 52	oscillatory, patchy	0.132 – 1.028	6.6 – 51.4
Uranoan pyrochlore	35, 52, 31	oscillatory, patchy	0.012 – 0.374	0.6 – 18.7

other calciocarbonatites (Nasraoui and Bilal, 2000). Low amounts of SiO_2 (<4 wt. %) were found in the NIOCAN and BZ pyrochlore-group minerals.

An *A*-site substitution is illustrated in figure 2.2, a bivariate diagram with (REE) vs-(Na+Ca) (a.p.f.u.). Figure 2.2 shows that the pyrochlore-group minerals with increased amounts of REE (uranpyrochlore, ceriopyrochlore and thorpyrochlore) have lower amounts of (Na+Ca) within their *A*-site.

The proportions of B atoms (Nb, Ta, and Ti) are presented in figure 2.3. NIOCAN and BZ pyrochlores plot in the pyrochlore subgroup and have an insignificant amount of Ta, and varying amounts of Ti and Nb in the *B*-site. Figure 2.4 is a ternary diagram with apices (*A*-vacancy)-(Na+Ca)-(U+Th). No correlation is evident between the amount of U+Th and *A*-site vacancy in the individual pyrochlore groups. However, uranpyrochlores and ceriopyrochlores all plot along a line with approximately 20 % (U+Th), with varying amounts of *A*-site vacancy.

Cation substitutions involving pyrochlore-group minerals from calciocarbonatites are discussed by Nasraoui and Bilal (2000). Figure 2.5 is a planar vector representation of substitutions involving pyrochlores from calciocarbonatites (*after* Nasraoui and Bilal, 2000). NIOCAN and BZ pyrochlores have a large range of Ti, Na and REE (figure 2.6). Any combination of the substitutions may have occurred with the pyrochlore-group minerals from the NIOCAN and BZ deposits. REE may have been incorporated into the pyrochlore structure by a coupled substitution involving only the *A*-site cations in the reaction:

$$[1]\ Na^{+} + REE^{3+} = 2Ca^{2+}$$

With constant Nb and Ti, the ceriopyrochlore end-member, $REE_{0.5}Na_{0.5}CaNb_2O_6(OH,F)$ can be generated. The end-member $(REE)NaTiNbO_6(OH,F)$ can be generated by a coupled substitution involving the cations of both sites *A* and *B*, when Na is constant, with the reaction:

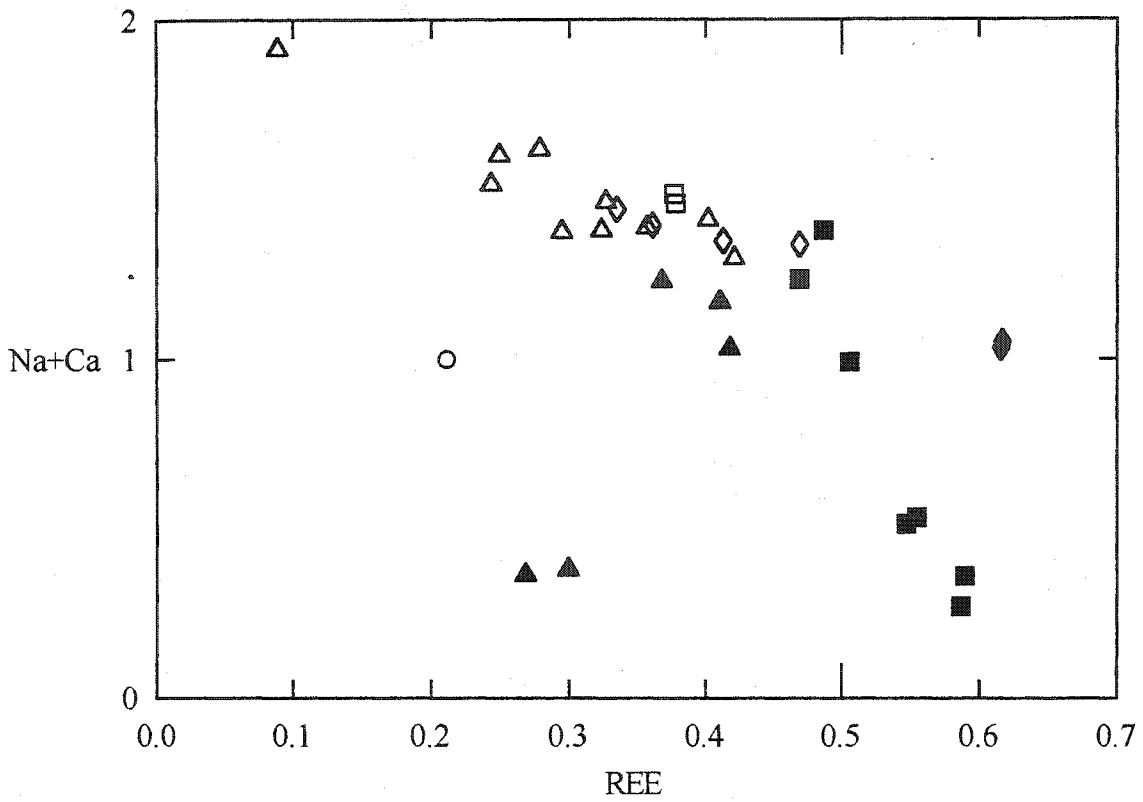

Figure 2.2. Na +Ca (a.p.f.u.) vs. REE (a..p.f.u.) for NIOCAN and Bond Zone pyrochlore-group minerals. ◆: thorpyrochlore, ◇: thorium pyrochlore,: ■: uranpyrochlore, □: uranoan pyrochlore, ▲: ceriopyrochlore, △: cerium pyrochlore.

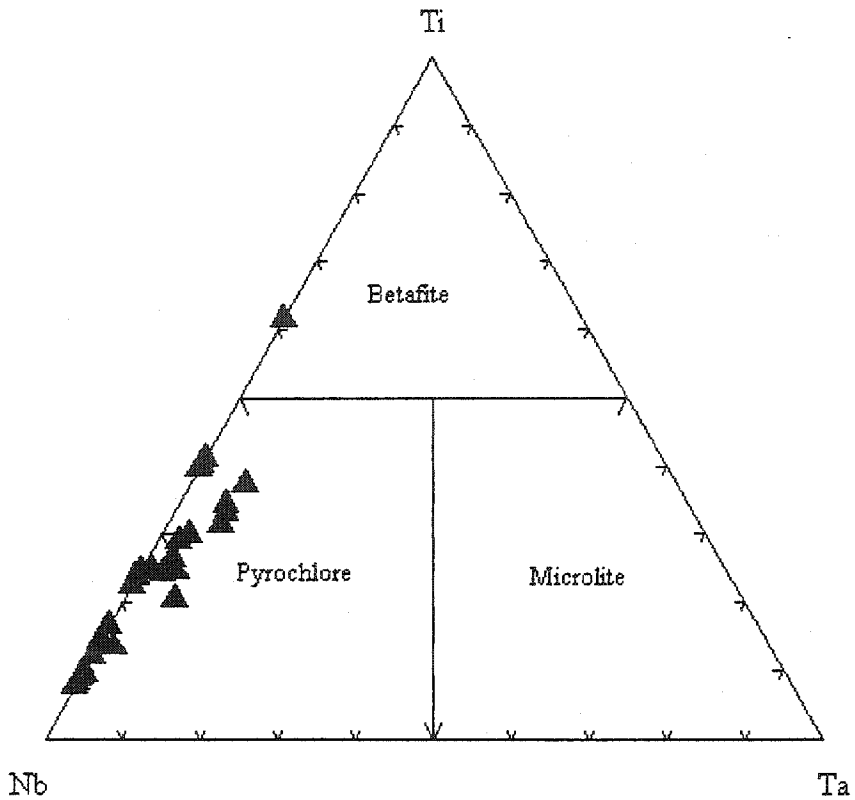

Figure 2.3. Ternary plot of elements in the *B*-position in the pyrochlore formula. Solid triangles represent pyrochlore –group minerals from the NIOCAN and Bond Zone deposits.

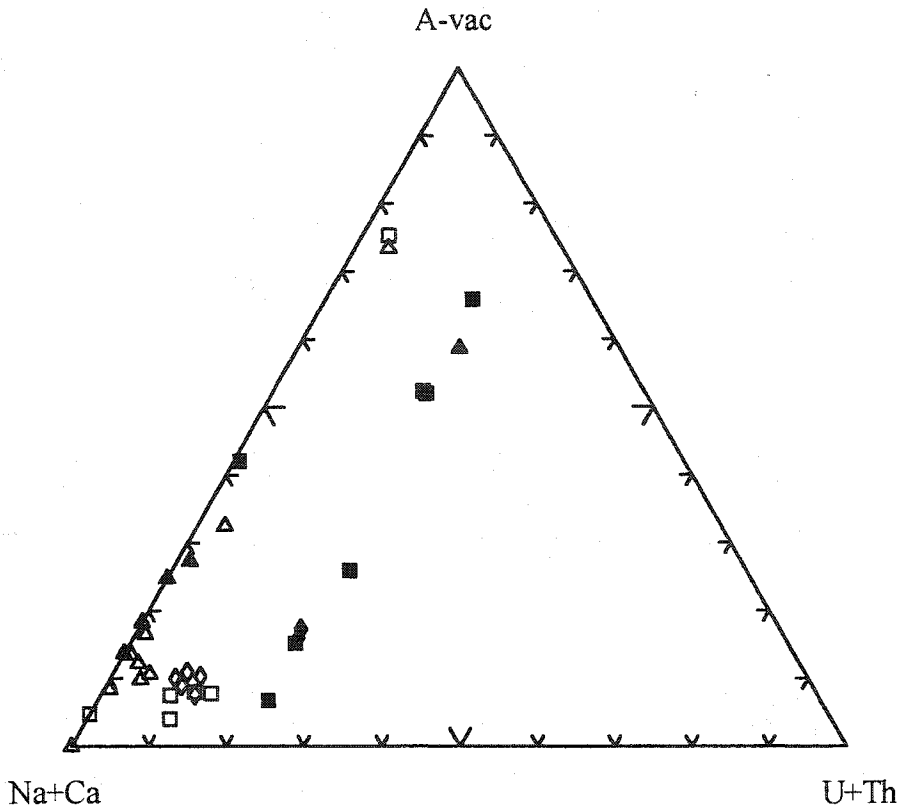

Figure 2.4. Ternary plot of (Na+Ca)-(U+Th)-(*A*-vac) for NIOCAN and Bond Zone pyrochlores. ◆: thorpyrochlore, ◇: thorium pyrochlore, ■: uranpyrochlore, □: uranoan pyrochlore, ▲: ceriopyrochlore, △: cerium pyrochlore.

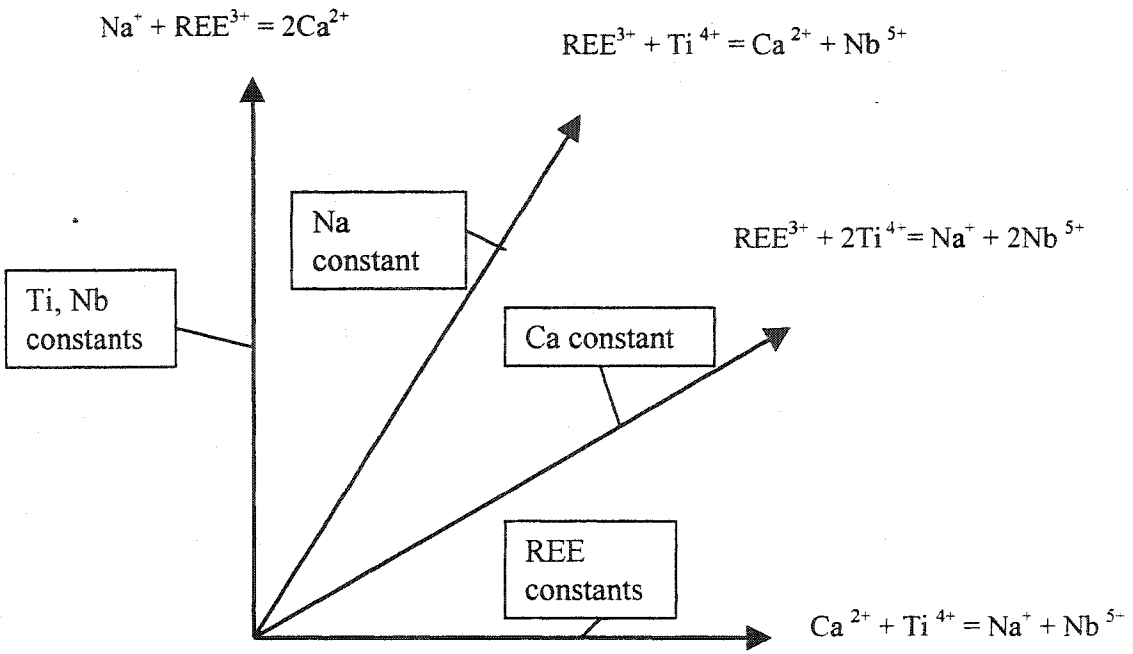

Figure 2.5. Planar vector representation of substitutions involving calciocarbonatite pyrochlore-group minerals (*after* Nasraoui and Bilal, 2000)

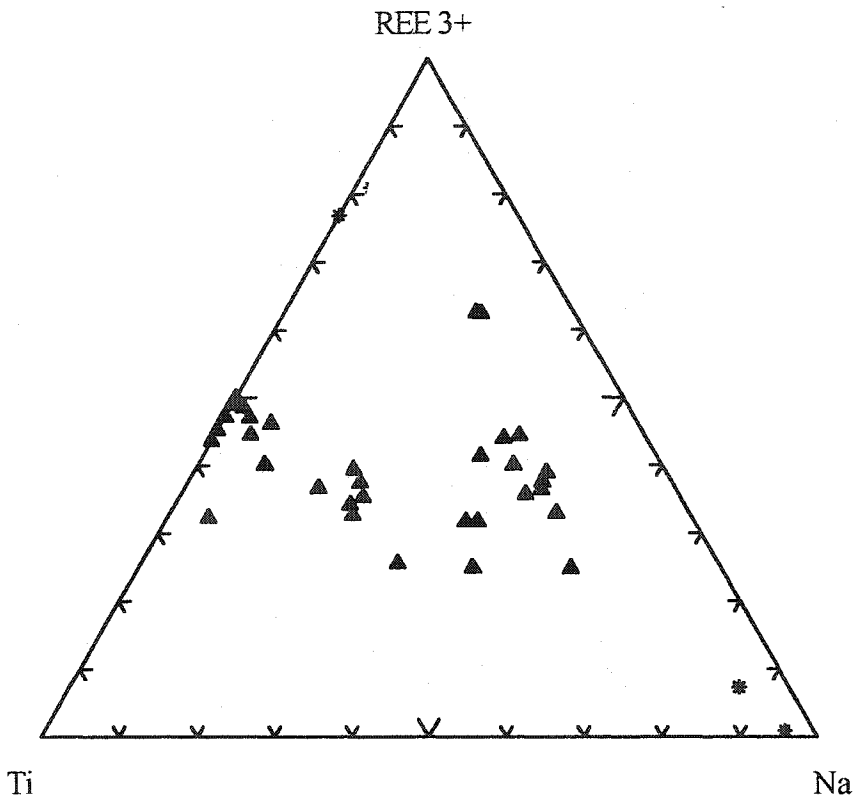

Figure 2.6. Ternary plot REE^{3+}-Ti-Na (a.p.f.u.) for NIOCAN and Bond Zone deposit pyrochlore-group minerals (▲) (Representative analyses are shown for clarity).

$$[2]\ REE^{3+} + Ti^{4+} = Ca^{2+} + Nb^{5+}$$

With constant Ca, the end-member $Ca(REE)Ti_2O_6(OH,F)$ can be generated by a coupled substitution according to:

$$[3]\ REE^{3+} + 2Ti^{4+} = Na^{+} + 2Nb^{5+}$$

With REE constant, another coupled substitution can be deduced from the previous substitutions [2] and [3], where the calciobetafite (Ca_2TiNbO_6 (OH,F)) end-member is generated:

$$[4]\ Ca^{2+} + Ti^{4+} = Na^{+} + Nb^{5+}$$

In the ternary plot REE-Ti-Na (figure 2.6.) pyrochlores from NIOCAN and BZ deposit are scattered showing no definitive trends, indicating that any combination of the substitutions described above by Nasraoui and Bilal (2000) have taken place, with no particular substitution being dominant.

It is necessary to compare the compositional information with the textural information of the pyrochlore-group minerals from the NIOCAN and Bond Zone deposits at Oka. Lumpkin and Ewing (1995) describe alteration trends in pyrochlore from a range of parageneses and weathering environments. Lumpkin and Ewing (1995) identified three trends relating to "primary", "transitional", and "secondary" alterations, using ternary diagrams with apices corresponding to divalent *A*-site cations (A^{2+}) filled by Ca, Sr, Ba, Pb, and Fe, monovalent *A*-site cations (A^{+}) filled mainly by Na and K, and *A*-site vacancies. Lumpkin and Ewing (1995) report that pyrochlores that display oscillatory zonation generally correspond to a "transitional" trend, whereas pyrochlores displaying patchy zonation generally correspond to an "alteration" trend. NIOCAN and Bond Zone pyrochlore textures, however, do not correlate to the "transitional" and "alteration" trends described by Lumpkin and Ewing (1995). Pyrochlores from the NIOCAN and Bond Zone deposits were grouped by their textures: oscillatory zoning, patchy zoning or

where zoning was absent. The groups of textures were plotted on ternary diagrams with apices (A^{2+})-(*A*-vacancy)-(A^{+}) and (Ca+Na)-(All other *A*-cations)-(*A*-vacancy) (figures 2.7 and 2.8, respectively). No correlation could be made, as they plotted randomly on the diagrams.

2.2.1. Uranoan Pyrochlore

Uranoan pyrochlores are commonly found as metamict, mantled crystals, exhibiting primary zonation, patchy zonation and low temperature alteration. The uranoan pyrochlore have been found associated with zirconolite, commonly intergrown with each other. Generally, they are found as large (1.0-1.5 mm) intensively fractured grains. Uranoan pyrochlore are abundant within the NIOCAN and BZ deposit, comprising about 2% of the modal abundance of the rock. Figure 2.9 is a ternary diagram with apices (A-vacancy)-(Ca)-(Na). Uranoan pyrochlores have low Na (a.p.f.u) and a low *A*-site vacancy, and plot mainly in the magmatic field, as represented by Nasraoui and Bilal (2000).

Microprobe analyses were completed on a traverse from the rim to the core of a mantled uranoan pyrochlore (figure 2.10). The mantled rim (dark BSE zone) shows the highest value of uranium and zirconium, which both decrease toward the center of the grain. Cerium peaks at 15 μm, which corresponds to the bright BSE zone analysed. Calcium is depleted and the *A*-site vacancy increases at 10μm, which corresponds to the altered zone that was analysed. Niobium increases from the rim to the core of the grain. In contrast, other uranoan pyrochlore grains analysed showed uranium contents, which slightly increased toward the core of the grain. Some uranoan pyrochlores exhibited distinct zoning shown by BSE imaging, however subsequent analyses of these grains showed no patterns, with fairly constant or very little variation in the UO_2 content across the grains.

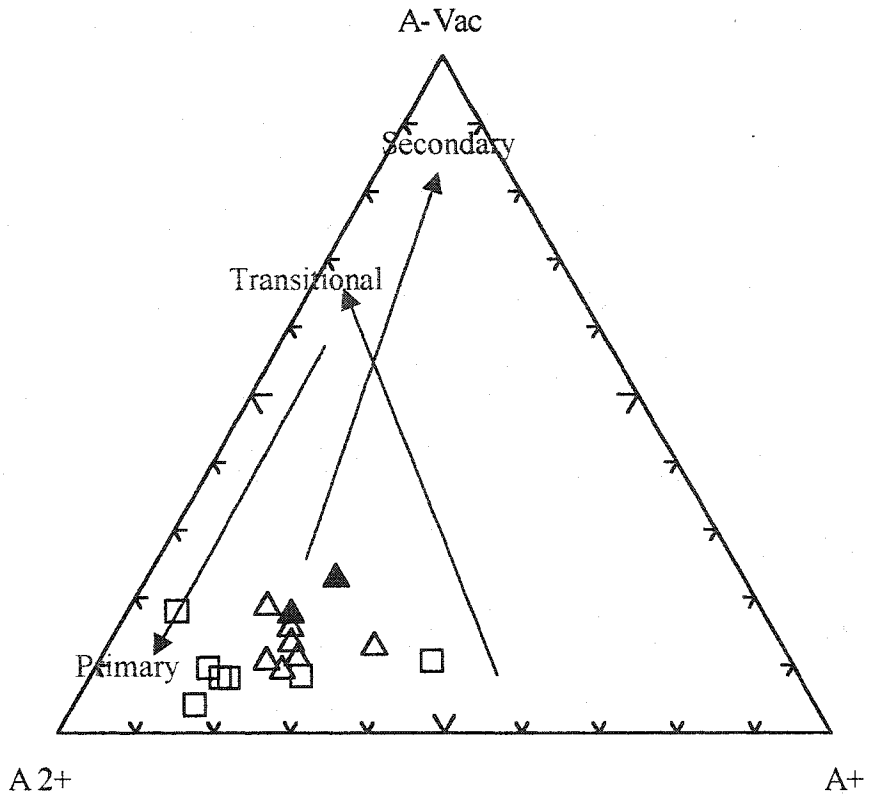

Figure 2.7. Ternary diagram with apices (A^{2+})-(*A*-vacancy)-(A^{+}) for NIOCAN and Bond Zone pyrochlores from the Oka carbonatite complex. Pyrochlores exhibiting △: patchy zonation, ▲: oscillatory zonation, and □: devoid of zoning (Representative analyses are shown for clarity). Alteration vectors (*after* Lumpkin and Ewing, 1995) are shown as arrows pointing toward the altered composition.

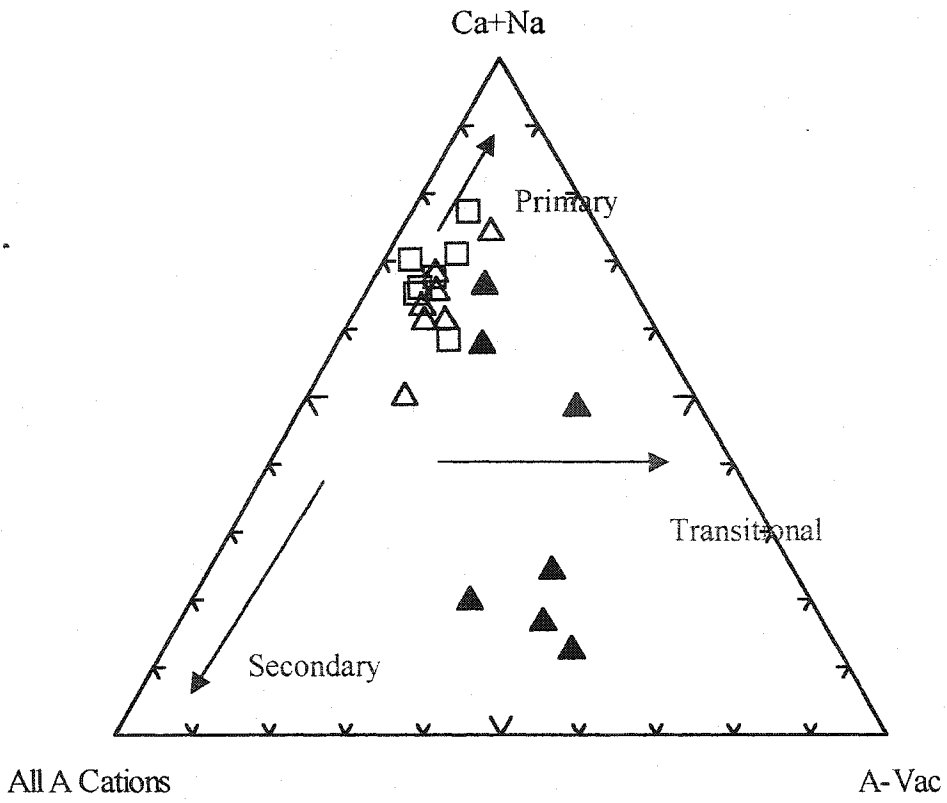

Figure 2.8. Ternary diagram with apices (all *A*-site Cations)-(Ca+Na)-(*A*-vacancy) for NIOCAN and Bond Zone pyrochlores from the Oka carbonatite complex. Pyrochlores exhibiting △: patchy zonation, ▲: oscillatory zonation, and □: devoid of zoning (Representative analyses are shown here for clarity). Alteration vectors (*after* Lumpkin and Ewing, 1995) are shown as arrows pointing toward the altered composition.

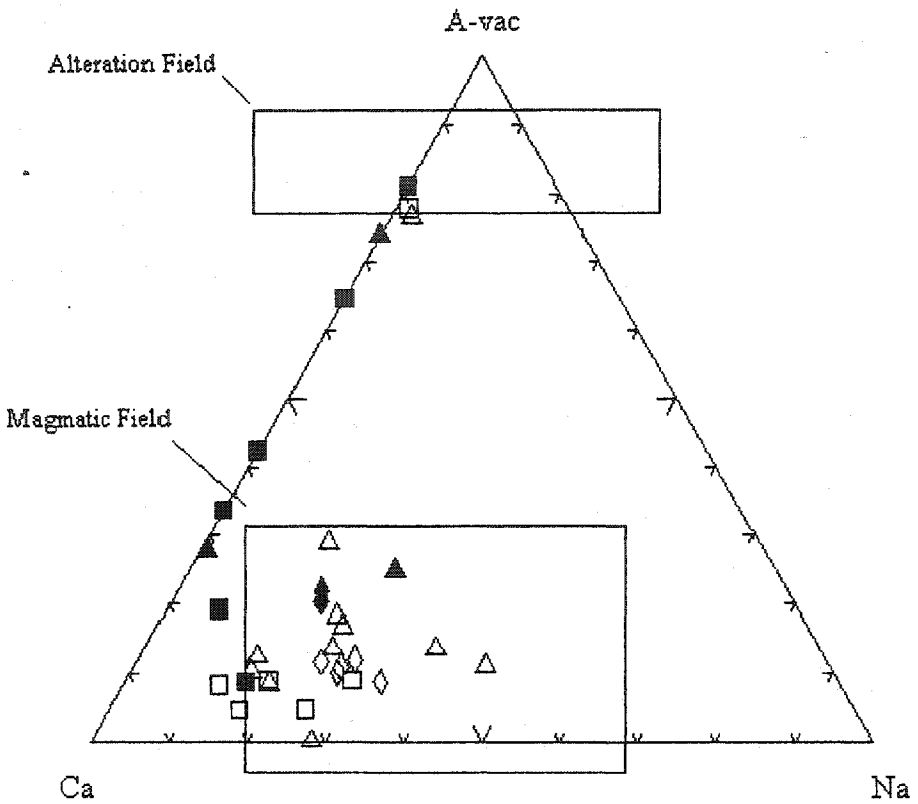

Figure 2.9. Ternary plot of (Ca)-(Na)-(*A*-site vacancy) for NIOCAN and Bond Zone pyrochlores. ◆: thorpyrochlore, ◇: thorium pyrochlore,: ■uranpyrochlore, □: uranoan pyrochlore, ▲: ceriopyrochlore, △: cerium pyrochlore.

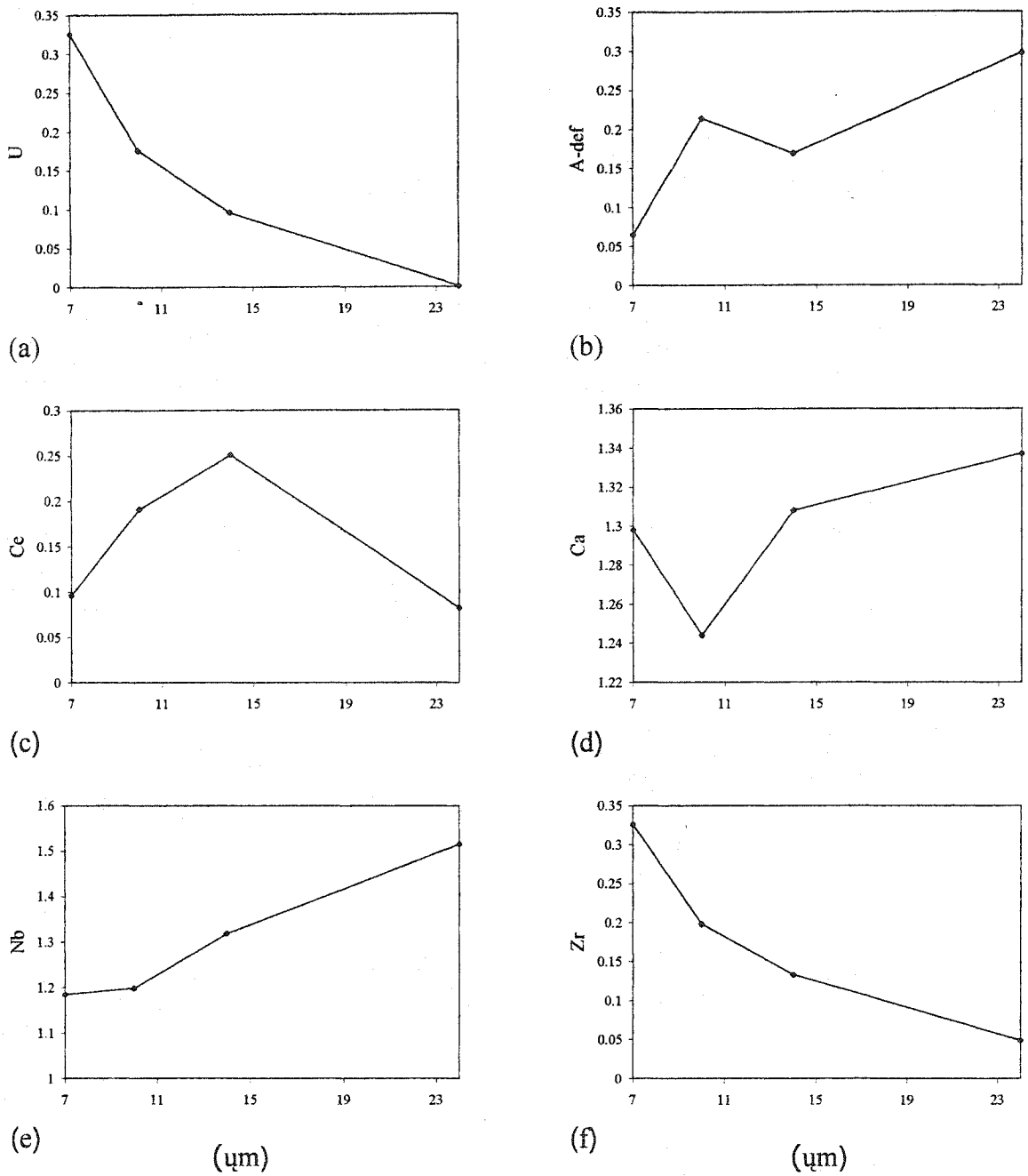

Figure 2.10. Distribution of (a) Uranium, (b) *A*-site deficiency, (c) Cerium, (d) Calcium, (e) Niobium, and (f) Zirconium from the rim to the core of a mantled Uranoan pyrochlore.

Uranoan pyrochlores have a small range of niobium and titanium (1.5-1.7 a.p.f.u), compared to that of the other pyrochlore-group minerals (figure 2.11). A *B*-site substitution between niobium and titanium with zirconium within the uranoan pyrochlore, is shown in figure 2.12. As the amount of Zr (a.p.f.u) increases, the (Nb+Ti) decreases. This plot (Nb+Ti) vs. (Zr) shows a good negative correlation (correlation coefficient = -0.74) confirming this substitution of Zr for (Nb+Ti) within the *B*-site. In the uranoan pyrochlore, moderately high concentrations of Zr occur with up to 9% Zr^{4+} present in the *B*-site.

2.2.2. Uranpyrochlore

Uranpyrochlores are commonly found exhibiting primary zonation, patchy zonation and low temperature alteration. They are found as both intensively fractured, discrete grains and as clusters of smaller grains. Uranpyrochlore comprise about 2% of the modal abundance within the NIOCAN and BZ deposits. In figure 2.9, uranpyrochlores contain insignificant Na, have ranges of *A*-site vacancy, including the second highest *A*-site vacancy of all of the pyrochlore subgroups. Figure 2.9 indicates that uranpyrochlores plot in two separate fields as represented by Nasraoui and Bilal (2000), the alteration field and the magmatic field. This can be explained by a mantled pyrochlore, in which the core of the grain plots in the magmatic field, and the altered rim (with large *A*-site vacancy) plots within the alteration field. A possibility for other uranpyrochlore data that plot within the two separate fields is that they belong to two separate uranpyrochlore groups that either crystallized at different times or were derived from different batches of carbonatite magma.

Analyses reveal that there is a small range of niobium and titanium for uranpyrochlores, ranging from approximately 1.5 to 1.7 a.p.f.u (figure 2.11). A *B*-site substitution between niobium and titanium with zirconium within the uranpyrochlore, is shown in figure 2.12. With

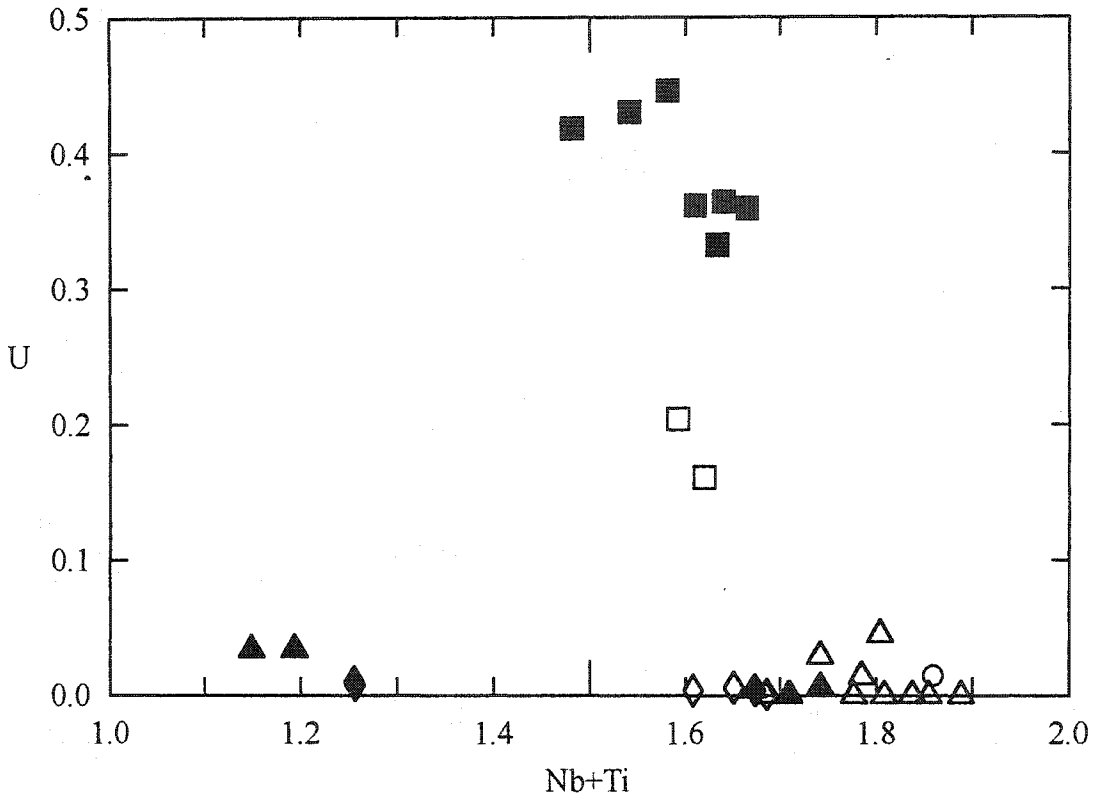

Figure 2.11. U vs. (Nb + Ti) (a.p.f.u) for NIOCAN and Bond Zone pyrochlore-group minerals. ◆: thorpyrochlore, ◇: thorium pyrochlore, ■: uranpyrochlore, □: uranoan pyrochlore, ▲: ceriopyrochlore, △: cerium pyrochlore.

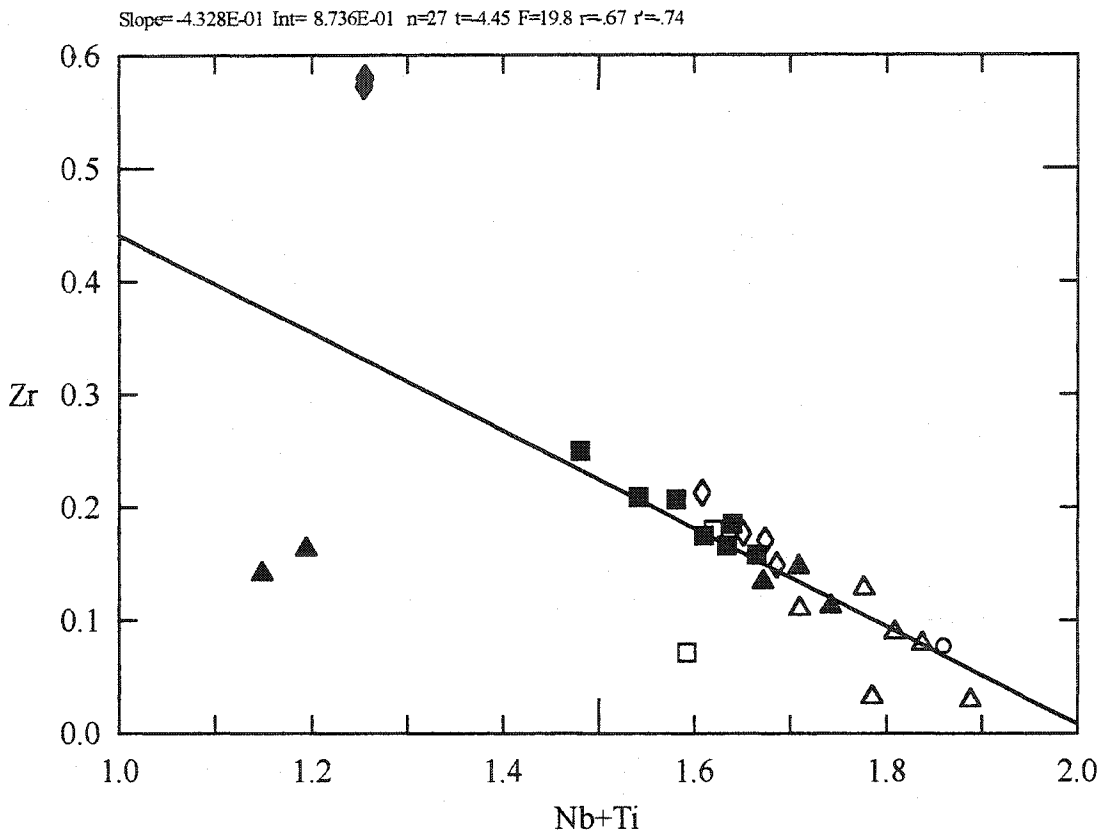

Figure 2.12. Zr vs. (Nb + Ti) (a.p.f.u.) for NIOCAN and Bond Zone pyrochlore-group minerals: ◆: thorpyrochlore, ◇: thorium pyrochlore, ■: uranpyrochlore, □: uranoan pyrochlore, ▲: ceriopyrochlore, △: cerium pyrochlore.

increasing amounts of zirconium (a.p.f.u.) there is a decrease in niobium and titanium. In uranpyrochlore, high concentrations of zirconium occur with up to 16.25 % Zr^{4+} present within the *B*-site.

2.2.3. Cerium Pyrochlore

Cerium pyrochlores are found exhibiting primary and patchy zonation. Bleached zones around microfractures and discoloured, turbid patches can be seen in BSE images, which are features of low temperature alteration as defined by Hogarth *et al.* (2000). They are frequently found as small subhedral clusters (0.1-0.22 mm). The larger cerium pyrochlores (~1.4 mm) contain apatite and calcite inclusions, and are intensively fractured. Cerium pyrochlores are the most abundant of the pyrochlore-group minerals found in the Oka carbonatite, comprising ~9% of the modal abundance (cerium pyrochlore constitutes over 60% of all pyrochlore-group minerals in the Oka carbonatite complex). Cerium pyrochlores exhibiting primary zonation have Ce contents that increase toward the rim of the crystal. In a few cases, cerium pyrochlore forms the core of the primary zoned crystals, with ceriopyrochlore occurring in the rim of the crystal. Some cerium pyrochlore crystals show primary zonation, with fairly constant Ce contents across the crystal. Figure 2.9 illustrates that the cerium pyrochlores have a range of Na (a.p.f.u.) and vacancies within the *A*-site. Cerium pyrochlore, along with ceriopyrochlore, exhibits the second largest *A*-site vacancies of the Oka pyrochlore-group minerals (table 2.3). In figure 2.9, most cerium pyrochlore data plot within the magmatic field as represented by Nasraoui and Bilal (2000), with the exception of a rim of an oscillatory zoned grain, which plots within the alteration field.

Although the cerium pyrochlores do not have a lot of variation within the *B*-site, a *B*-site substitution occurs between niobium and titanium with zirconium (figure 2.12). Cerium

pyrochlores have the lowest contents of zirconium of all the pyrochlore-group minerals from the Oka complex (figure 2.12), averaging 3.9 % Zr^{4+} present within the *B*-site.

2.2.4. Ceriopyrochlore

Ceriopyrochlore are found exhibiting primary zonation, patchy alteration and low temperature alteration. They are found as large, fractured, discrete grains and as clusters of smaller subhedral grains. Ceriopyrochlore are not very abundant within the NIOCAN and Bond Zone deposits, comprising approximately 0.3 ± 0.1 % of the modal abundance of the carbonatite. In figure 2.9, ceriopyrochlore grains plot in the magmatic field, represented by Nasraoui and Bilal (2000), with an exception of an outer zone of a ceriopyrochlore grain, which plots within the alteration field.

A *B*-site substitution between niobium and titanium with zirconium within the ceriopyrochlore, is shown in figure 2.12. Ceriopyrochlores have moderate zirconium contents, in comparison to the other pyrochlore-group minerals from the NIOCAN and Bond Zone deposits (figure 2.12), averaging 4.39 % Zr^{4+} within the *B*-site.

2.2.5. Thorium Pyrochlore

Thorium pyrochlore are found exhibiting primary zonation, and patchy zonation. Generally, the grains are smaller (~0.4 mm) and subhedral. The thorium pyrochlore are rare within the NIOCAN and Bond Zone deposits, comprising about 0.2% of the modal percentage of the carbonatite. In figure 2.4, thorium pyrochlores are found grouped together with low amounts of (U+Th) and low *A*-site vacancies. This corresponds to the low degree of alteration found in the thorpyrochlores and the thorium pyrochlores. In contrast to other pyrochlore-group minerals from the NIOCAN and Bond Zone deposits, there is no significant intra- and intergrain

compositional variation. In figure 2.9, all thorium pyrochlore plot within the magmatic field represented by Nasraoui and Bilal (2000).

A *B*-site substitution between niobium and titanium with zirconium within the thorium pyrochlore, is shown in figure 2.12. Thorium pyrochlores have higher zirconium contents as compared to the other pyrochlore-group minerals from the NIOCAN and BZ deposits (figure 2.12) ranging from 7.3 – 10.65 % Zr^{4+} within the *B*-site.

Figure 2.13 shows the distribution of diverse elements along a traverse of an oscillatory zoned thorium pyrochlore. Thorium remains relatively constant across the traverse, varying from 0.04 to 0.16 a.p.f.u. From 0.4 – 0.6 mm there is an increase in cerium, which is correlated with a decrease in calcium, a result of substitution within the *A*-site. Niobium decreases from 0.04 - 0.06 mm, and this is correlated with an increase in zirconium, a result of the substitution in the *B*-site described above.

2.2.6. Thorpyrochlore

Thorpyrochlore are found exhibiting patchy alteration. Generally, the grains are small (~0.4 mm) and subhedral. The thorpyrochlore are also rare within the NIOCAN and Bond Zone deposits, where only a few grains have been identified. In figure 2.9, thorpyrochlore plots within the magmatic field, represented by Nasraoui and Bilal (2000).

A *B*-site substitution between niobium and titanium with zirconium within the thorpyrochlore, is shown in figure 2.12. Figure 2.12 shows that thorpyrochlores have the highest contents of zirconium among the pyrochlore-group minerals, with up to 29 % Zr^{4+} within the *B*-site.

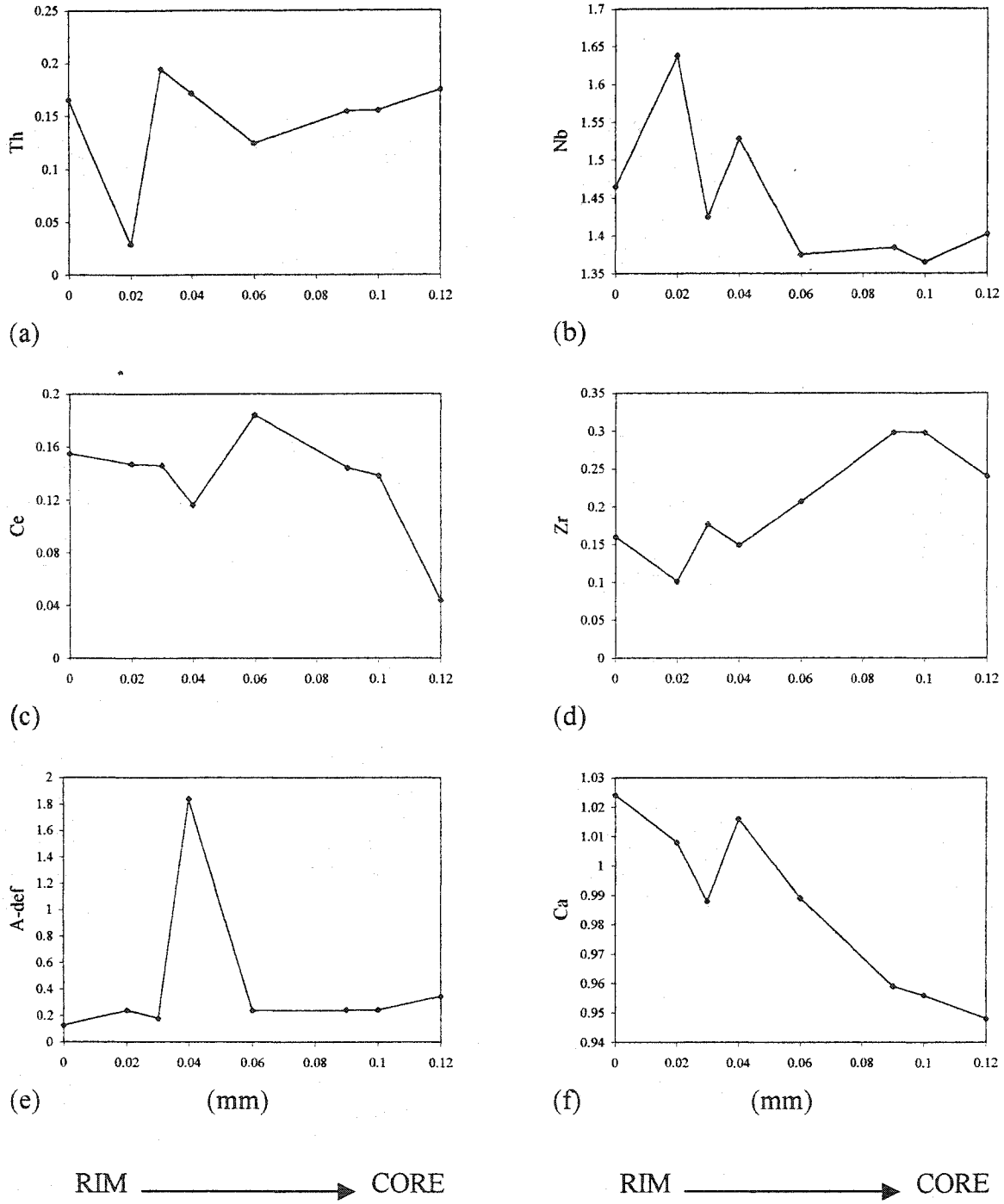

Figure 2.13. Distribution of (a) Thorium, (b) Niobium, (c) Cerium, (d) Zirconium, (e) *A*-site deficiency, and (f) Calcium from the rim to the core of a zoned thorium pyrochlore.

2.3. Pyrochlore from the St. Lawrence Columbium deposit, Oka, Quebec.

In order to compare and contrast the pyrochlore-group minerals within the Oka complex, data for pyrochlores originating from the St. Lawrence Columbium Deposit (figure 1.1) were used for comparison. Electron microprobe analyses of homogeneous and zoned pyrochlores were completed by Petruk and Owens (1975), and Kalogeropoulos (1977).

Petruk and Owens (1975), studied eight separate pyrochlore grains from the St. Lawrence Columbium Deposit (SLC). Representative compositions from their data are listed in Appendix V. Three homogeneous grains, two zoned grains, two uranoan pyrochlore and one uranpyrochlore grain were analysed with a Materials Analysis Company (MAC) electron microprobe. All pyrochlore grains studied showed only minor alteration and were found as euhedral-to-subhedral grains. Analyses revealed small amounts of Si^{4+}, which was considered to be an impurity, present as minute inclusions of a silicate.

Kalogeropoulos (1977), describes the Oka SLC pyrochlore-group minerals as occurring as disseminated idiomorphic crystals and more rarely aggregates and clusters throughout the gangue, as well as intergrowths with calcite. Pyrochlore-group minerals from SLC are typically present in amounts varying from 0.2 to about 5 percent, with the exception of apatite-rich bands, where the modal abundance approaches 12 percent (Kalogeropoulos, 1977). Energy-dispersive and wavelength-dispersive electron microprobe analyses are included in Appendix IV. Kalogeropoulos (1977) describes the pyrochlore-group minerals as euhedral-to-subhedral, exhibiting resorption textures (possibly metamict), and containing numerous inclusions of calcite, apatite, and geothite (?).

Figure 2.14 is a ternary diagram with apices Nb-Ti-Ta. The SLC data have high Nb-content and belong to the pyrochlore subgroup. The Nb contents for the SLC deposit, when

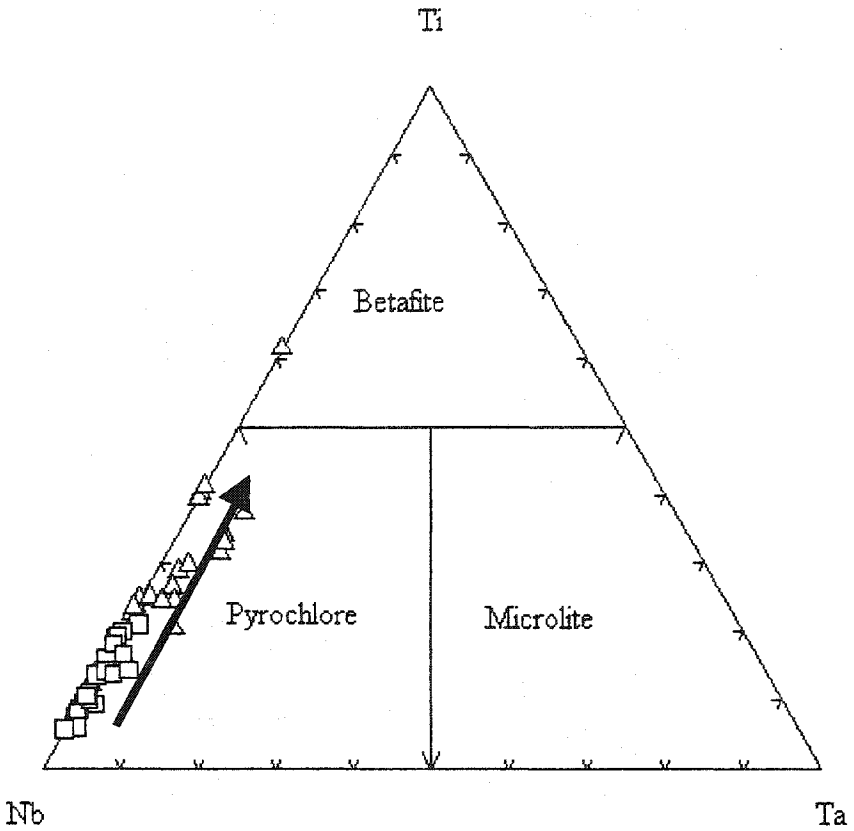

Figure 2.14. Ternary diagram with apices Nb-Ti-Ta. St. Lawrence Columbian Deposit (SLC) pyrochlore-group minerals are represented by (□), NIOCAN and Bond Zone deposit pyrochlore-group minerals are represented by (△). An evolutionary trend is shown by the arrow.

compared to the NIOCAN and Bond Zone deposits, are slightly higher and less variable. Therefore the main constituent in the *B* position of the pyrochlore-group formula is Nb, with slight Ti-substitution.

SLC pyrochlore-group minerals have low amounts of U+Th, and a low *A*-site vacancy (figure 2.15). This indicates that *A*-site substitution is absent, which corresponds to relatively unaltered pyrochlores. An evolutionary trend is shown in figure 2.16, a ternary diagram with apices REE^{3+}-Ti-Na. The SLC pyrochlore-group minerals plot in the Na-enriched corner, with low REE^{3+}. With increasing amounts of REE^{3+}, the SLC data trends towards the composition of pyrochlore in the NIOCAN and Bond Zone deposits.

SLC pyrochlore-group minerals have very low Zr contents as shown by figure 2.17 (<1 wt. %). *B*-site substitution is not evident for the SLC pyrochlores.

Petruk and Owens (1975) conclude that the compositional and physical variations of the SLC pyrochlore may reflect pauses in the evolution of the carbonatite, where equilibrium was attained and specific types of pyrochlore crystallized in response to the thermodynamic and crystallochemical condition associated with the pauses. They also conclude that the presence of zoned pyrochlore grains suggests that conditions for depositing the low-uranium pyrochlores of one zone alternated with the conditions for depositing the uranium-free pyrochlore of the other zone. They report that similar fluctuations existed for the deposition of low-thorian pyrochlores.

Kalogeropoulos (1977) concluded by classifying each of the different varieties of pyrochlore-group minerals from the SLC deposit. Furthermore, a paragenetic sequence of the mineralization of the SLC deposit was constructed. The trace element content, the essential lack of independent rare-earth minerals, and the abundance of pyrochlore, were used to suggest the pyrochlore-group minerals are middle-stage crystallization products of the carbonatite complex.

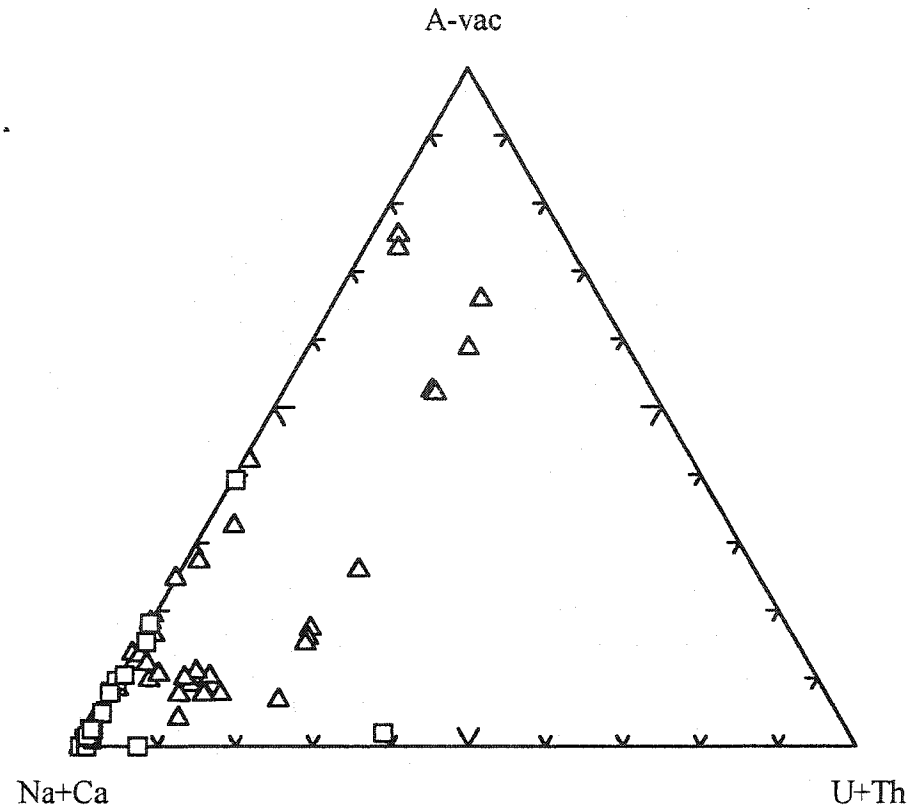

Figure 2.15. Ternary diagram with apices (Na+Ca)-(A-site vacancy)-(U+Th). St. Lawrence Columbian Deposit (SLC) pyrochlore-group minerals are represented by (□), NIOCAN and Bond Zone deposit pyrochlore-group minerals are represented by (△).

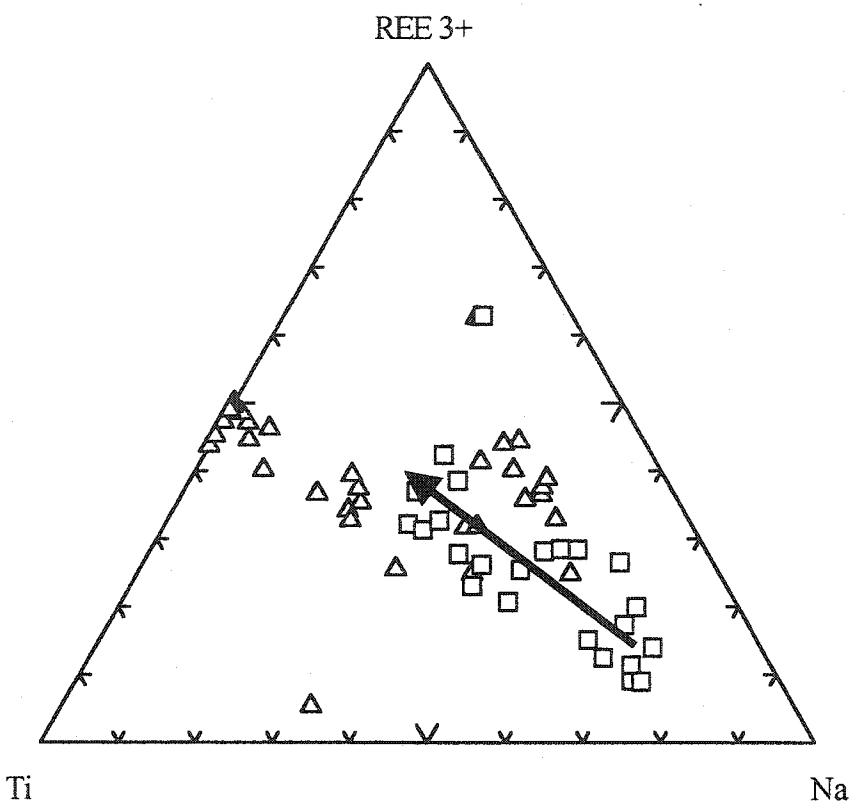

Figure 2.16. A ternary diagram with apices Ti-REE^{3+}-Na. St. Lawrence Columbian Deposit (SLC) pyrochlore-group minerals are represented by (□), NIOCAN and Bond Zone deposit pyrochlore-group minerals are represented by (△). An evolutionary trend is shown by the arrow.

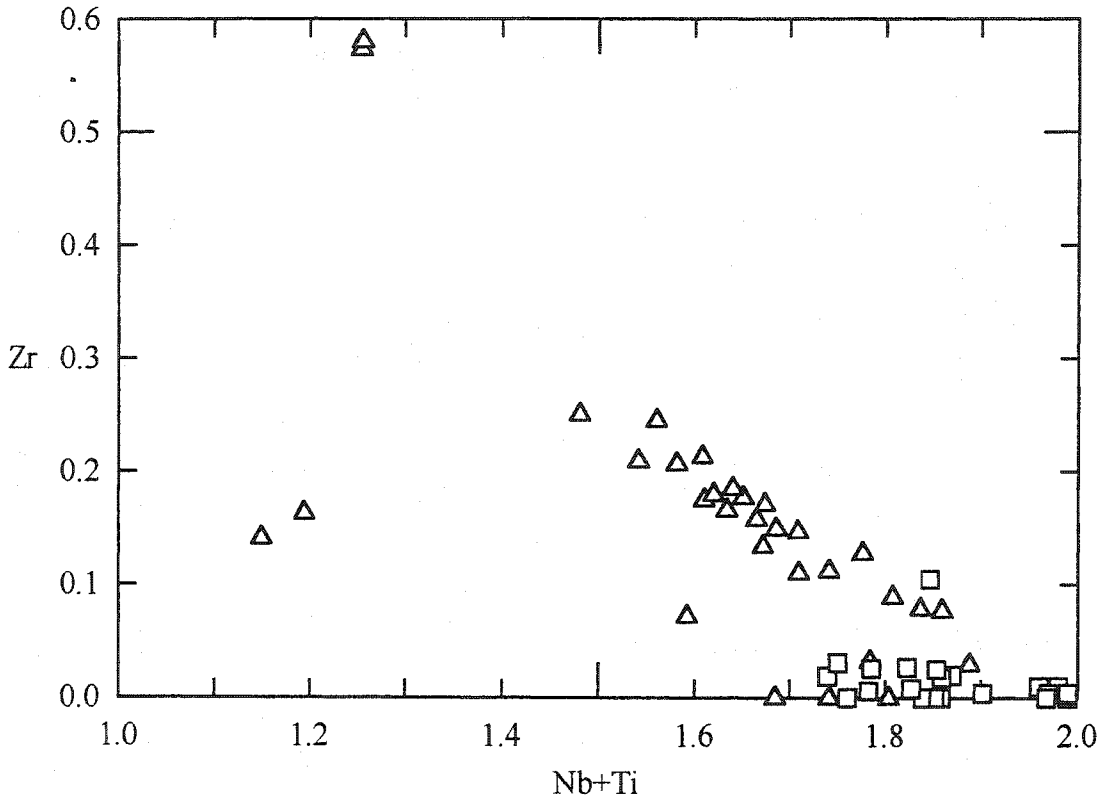

Figure 2.17. Zr vs. (Nb+Ti) (a.p.f.u.). St. Lawrence Columbian Deposit (SLC) pyrochlore-group minerals are represented by (□), NIOCAN and Bond Zone deposit pyrochlore-group minerals are represented by (△).

Furthermore, Kalogeropoulos (1977) infers that the main portion of pyrochlore seems to have been deposited after the main period of calcite crystallization. The resorption textures reflect a physiochemical change in the carbonatite magma during the period of pyrochlore crystallization (Kalogeropoulos, 1977).

When comparing the SLC to the NIOCAN and Bond Zone pyrochlore-group minerals, many differences can be identified. Overall, the pyrochlores from SLC have a lower modal abundance in their host carbonatite (ranging from 0.2-5 %). They can be found as euhedral to subhedral discrete grains (less commonly found clustered). NIOCAN and Bond Zone pyrochlores are found exhibiting euhedral, subhedral and anhedral habit, as both discrete and clustered grains. SLC pyrochlores are found as both homogeneous and zoned grains, and less commonly show signs of alteration.

SLC pyrochlores are found as inclusions within apatite and calcite, and with inclusions of apatite and calcite. NIOCAN and Bond Zone pyrochlores are less commonly found as inclusions within other minerals. The inclusions found in the NIOCAN and Bond Zone pyrochlores are apatite, calcite, REE carbonates and zirconolites; a much more diverse suite of minerals.

The pyrochlore-group minerals identified in the SLC deposit are cerium, uranoan, and low-thorium pyrochlores. There are small compositional variations within the SLC pyrochlores:

CaO (range 14.17-18.78 wt.% oxide)

TiO_2 (2.12-8.45)

Nb_2O_5 (49.21-65.33)

ThO_2 (0-0.76)

UO_2 (0-8.82)

Si^{4+} is present as minute inclusions of silicate in the SLC pyrochlore. In the NIOCAN and Bond Zone pyrochlore, Si^{4+} is present within the pyrochlore structure (<4 wt. % SiO_2). Inclusions of silicate were not identified by BSE imagery, and considered to be absent.

A-site vacancy ranges in the SLC pyrochlore are from 0 (completely filled) to 13.3%, a small range compared to NIOCAN and Bond Zone, which have vacancies up to 62.5%. Of the REE's, only cerium is present at higher concentration levels (2.56-10.86 wt. % Ce_2O_3) in the SLC pyrochlore. SLC pyrochlores have extremely low zirconium contents compared to the NIOCAN and Bond Zone pyrochlores (0 to 0.94 wt. % ZrO_2). Tantalum contents are low in all three Oka deposits.

Figure 2.18 is a ternary diagram of REE^{3+}-Ti-Na (a.p.f.u.). The SLC pyrochlores have a large range of REE^{3+} and Na, with a small range of Ti. Therefore, REE may have been incorporated into the pyrochlore structure by a coupled substitution involving only the *A*-site cations in the reaction:

$$Na^{+} + REE^{3+} = 2Ca^{2+}$$

With constant Nb and Ti, the ceriopyrochlore end-member, $REE_{0.5}Na_{0.5}CaNb_2O_6(OH,F)$ can be generated (Nasraoui and Bilal, 2000).

2.4. Pyrochlore-group minerals from other carbonatite localities and alkaline complexes worldwide

A better understanding of the magmatic, hydrothermal and low-temperature evolution of carbonatites can be developed through the study of the chemical behaviour of pyrochlores altered under different conditions. Pyrochlore-group minerals hosted by calciocarbonatites, dolomitic carbonatites, and other alkaline rocks around the world have been evaluated and compared to the pyrochlore-group minerals identified from Oka. Table 2.4 is a list of the locations that were used

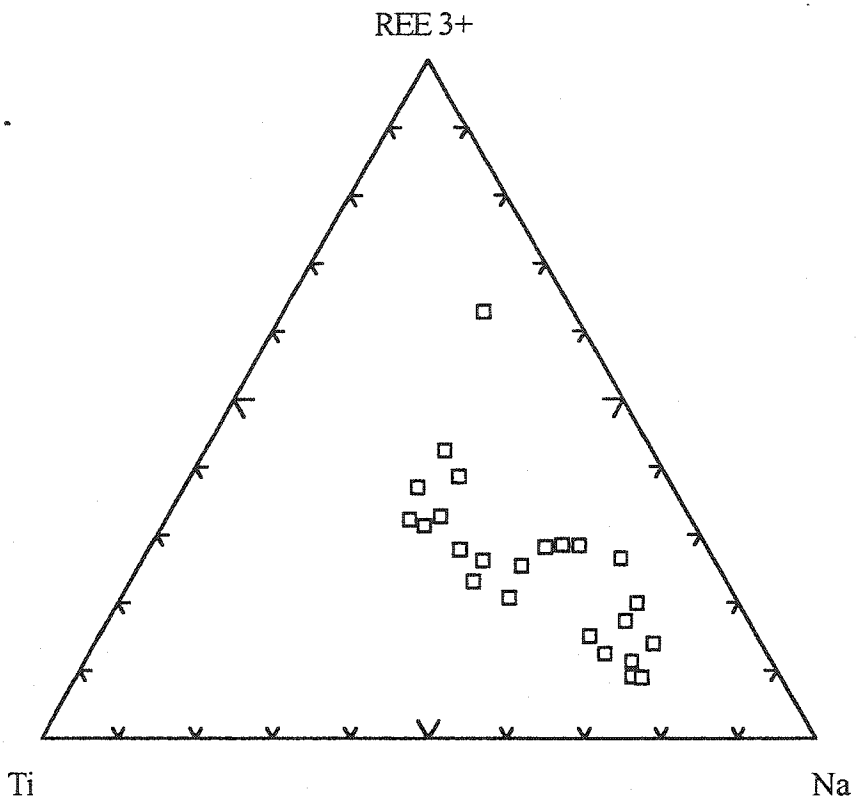

Figure 2.18. Ternary diagram with apices REE^{3+}-Ti-Na for the SLC pyrochlore-group minerals (□).

Table 2.4. Sample data from pyrochlore-group minerals from locations worldwide, used for comparison

Area	Location	General reference	Rock type	Analyses
Lueshe	Dem. Rep. Of Congo	Nasraoui and Bilal, 2000	calciocarbonatite	Lu-mg1, Lu-h2, Lu-w1
Prairie Lake	Northwestern Ontario, Canada	Hammond, 1999	calciocarbonatite	PL-1, PL-2, PL-3, PL-4, PL-5, PL-6, PL-7, PL-8, PL-9, PL-10
Verity and Fir	British Columbia	Simandl et al., 2001	magnesiocarbonatite	Ver-1, Fir-1
Sokli	Northern Finland	Lindqvist et al., 1979	calciocarbonatite	Sok-1, Sok-2
Bingo	Northeastern Zaire	Williams et al., 1997	calciocarbonatite	Bin-1, Bin-2, Bin-3, Bin-4, Bin-5, Bin-6, Bin-7, Bin-8, Bin-9, Bin-10, Bin-11, Bin-12, Bin-13
Mt. Weld	W. Australia	Lottermoser and England, 1988	laterite carbonatite	Mt-W-A, Mt-W-B, Mt-W-C, Mt-W-D, Mt-W-E, Mt-W-E2
Lesnaya Varaka Complex	Kola Penninsula, Russia	Chakhmouradian et al., 1998	apatite- dolomite carbonatite	Kola1, Kola2, Kola3
Kovdor Complex	Kola Penninsula, Russia	C.T. Williams, 1996	alkaline complex	Kov-1, Kov-2, Kov-3
Chilwa I.	Malawi	Hogarth et al., 2000	calciocarbonatite	Chi-1
Fen	Norway	Hogarth et al., 2000	calciocarbonatite	Fen-1, Fen-2, Fen-3, Fen-4
Qaqarssuk	West Greenland	C. Knudsen, 1989	calciocarbonatite	Qaq-1, Qaq-2
Newania	Rajasthan	Viladkar and Ghose, 2002	dolomite carbonatite	New-1, New-2, New-3, New-4, New-5, New-6
Lovozero	Russia	Chakhmouradian and Mitchell, 2002	alkaline complex	Lovo-1, Lovo-2, Lovo-3, Lovo-4, Lovo-5, Lovo-6

for comparison. Representative compositional data for these pyrochlores can be found in Appendix IV.

2.4.1. Dolomitic carbonatite hosts

(a) Newania carbonatite, Rajasthan

Viladkar and Ghose (2002), studied barium- and –uranium pyrochlores from the Newania carbonatite, Rajasthan. The Newania carbonatite is unique because it might represent an unmodified primary mantle-derived melt (Viladkar and Ghose, 2002). Uranpyrochlores (with up to 22.92 wt. % UO_2) are found as fresh, unaltered grains within a dolomitic carbonatite matrix. Analyses of uranpyrochlore from the Newania carbonatite are presented in Appendix IV. The carbonatite consists mainly of dolomite, with calcite, and accessory magnetite, apatite, barium pyrochlore, uranpyrochlore, uranoan pyrochlore, columbite, monazite, zircon, phlogopite, and amphibole. Viladkar and Ghose (2002), conclude that the crystallization of highly uraniferous pyrochlore essentially started in a very early stage (cumulate phase) of crystallization of carbonatite (rauhaugite) magma at Newania, which had elevated concentrations of both Nb and U.

The Newania pyrochlores are useful for comparison with the Oka pyrochlores because of the extremely high UO_2 wt. % found in both occurrences. The proportions of *B* atoms (Nb, Ta, Ti) for pyrochlore-group minerals are presented in figure 2.19. Newania pyrochlores plot in the pyrochlore sub-group and have slightly elevated concentrations of Ta, compared to pyrochlores from other localities. Newania pyrochlores also show a variation in their Ti content (Ti replaces Nb) (figure 2.19). Figure 2.20 indicates that the Newania uranpyrochlores plot in the alteration field from Nasraoui and Bilal (2000). However, Viladkar and Ghose (2002), report that most of the analysed grains in the study were fresh and free from alteration. No explanation was

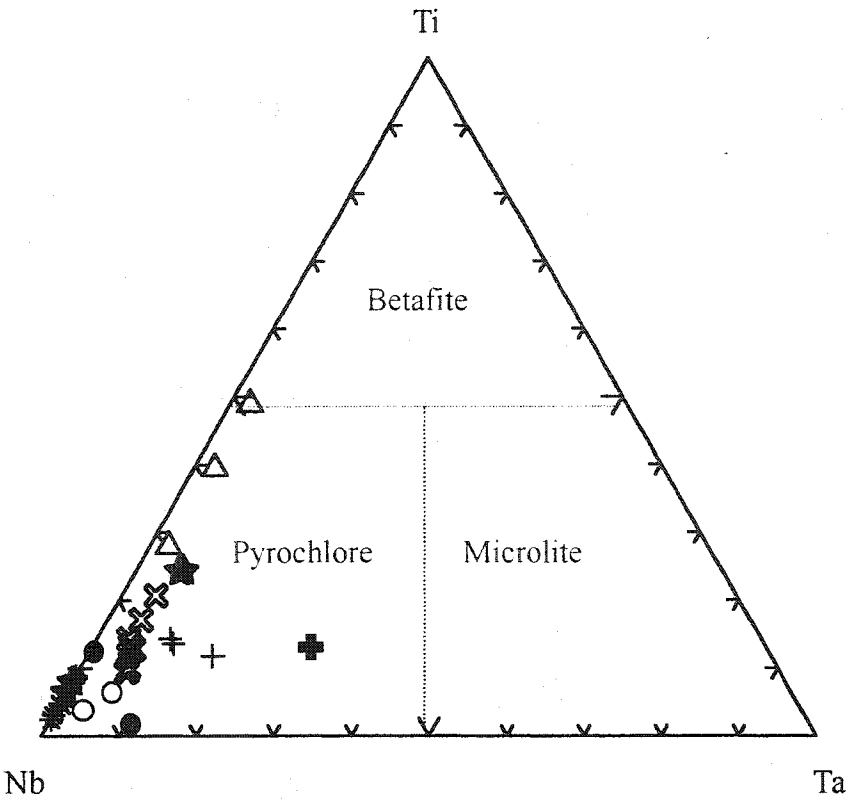

Figure 2.19. Ternary plot of elements in the *B*-position in the pyrochlore formula.

□: Lueshe , ●: Sokli, ○: Blue River, +: Kovdor, ✳: Bingo, △: Prairie Lake,

✖: Newania, ★: Fen, ✙: Kola, ⊠: Qaqarssuk, ◇: Mt. Weld

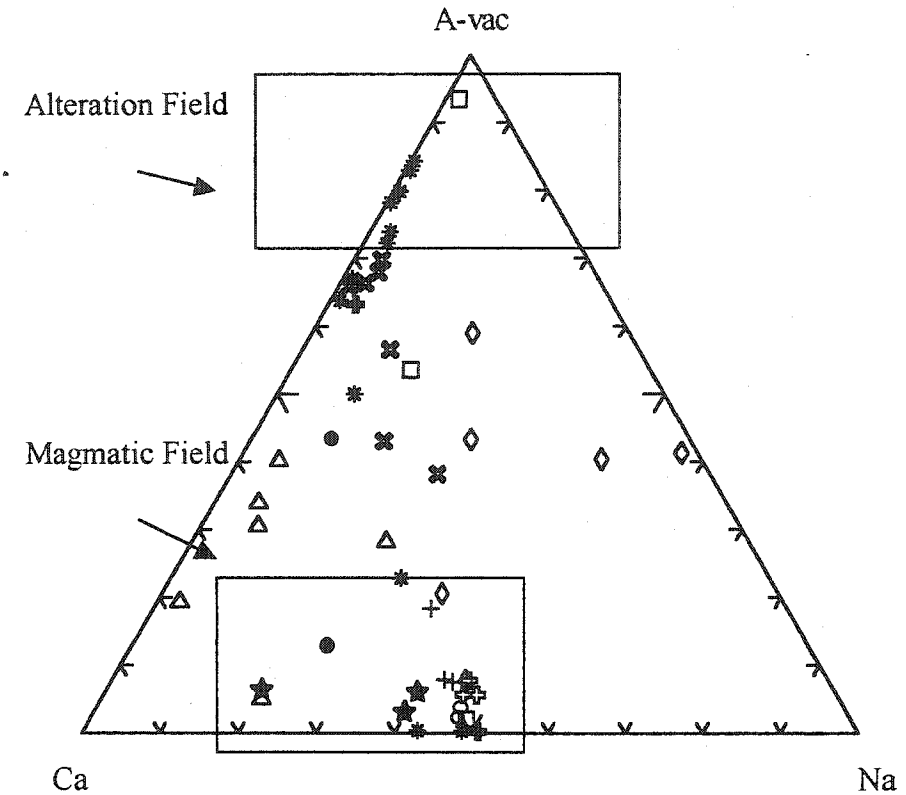

Figure 2.20. Ternary plot of (Ca)-(Na)-(*A*-site vacancy) for pyrochlores from localities worldwide.

□: Lueshe , ●: Sokli, ○: Blue River, ┼: Kovdor, ✳: Bingo, △: Prairie Lake, ✖: Newania, ★: Fen, ✣: Kola, ⊠: Qaqarssuk, ◇: Mt. Weld

given for the large range of *A*-site vacancies within the pyrochlores. Figure 2.21, a ternary diagram with apices Ti-REE^{3+}-Na illustrates Newania pyrochlores as having a small compositional field when compared to Oka pyrochlores. In general, Na_2O abundances are quite low in the Newania pyrochlores (figure 2.21). Figure 2.22, a ternary diagram with apices (Na+Ca)-(*A*-vac)-(U+Th), shows the large range of *A*-site vacancies exhibited by the Newania pyrochlores. In addition, Newania pyrochlores have high (U+Th) (a.p.f.u) contents, which are comparable to those of the Oka uranpyrochlores.

Zr concentration in Newania pyrochlore is extremely low (average ZrO_2 around 0.2 wt. %). A weak, but positive correlation, was found between Zr and Nb in the Newania pyrochlores (Viladkar and Ghose, 2002). Viladkar and Ghose (2002) report that discrete grains of zircon are commonly associated with pyrochlore in bands in rauhaugite, while no Zr is found to be concentrated in the pyrochlore minerals. They conclude that the Zr must be fixed in the zircon grains. Figure 2.23, shows compositional variations at the *B*-site of pyrochlore-group minerals. Newania pyrochlores show a negative correlation, indicating that with an increase in Nb, there is a decrease in Si, Zr, and Ti. However, since extremely low amounts of Si (<0.5 wt. % SiO_2) and Zr (<0.5 wt. % ZrO_2) are present within the Newania pyrochlores, this must represent a *B*-site substitution between Nb and Ti.

Figure 2.24 is a bivariate diagram representing the compositional variations at the *A*-site of pyrochlore-group minerals. Newania pyrochlores show a weak negative correlation between (REE+U+*A*-vac) and (Na+Ca). This indicates that there is a substitution within the *A*-site causing the CaO and Na_2O abundances to be quite low.

Viladkar and Ghose (2002) conclude that most of the Newania pyrochlore seem to have crystallized in the early stages of magmatic crystallization along with apatite, magnetite and

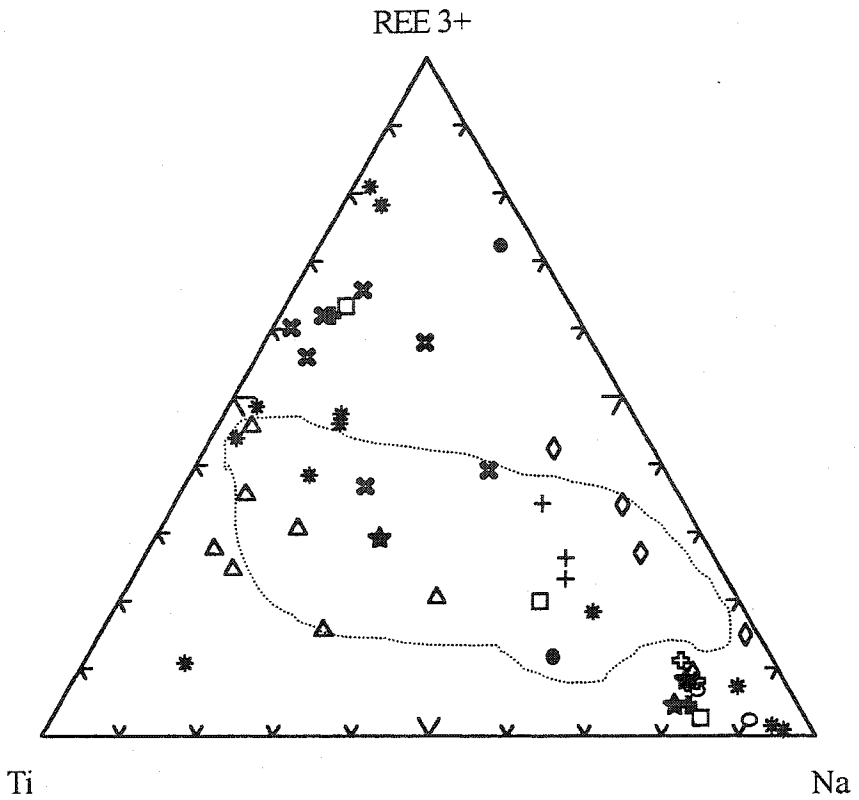

Figure 2.21. Ternary diagram with apices (Ti)-(REE^{3+})-(Na). Dotted line represents the Oka pyrochlore compositional field (Bond Zone, NIOCAN, and St. Lawrence Columbian).

□: Lueshe , ●: Sokli, ○: Blue River, +: Kovdor, ✳: Bingo, △: Prairie Lake, ✖: Newania, ★: Fen, ✙: Kola, ⊠: Qaqarssuk, ◇: Mt. Weld

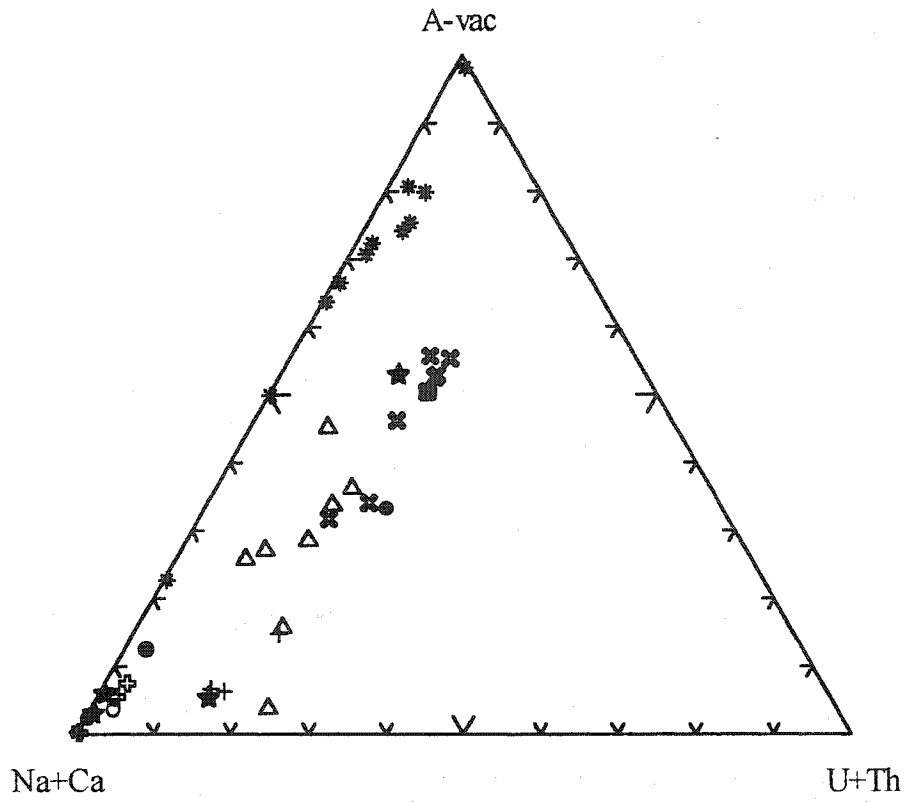

Figure 2.22. Ternary diagram with apices (Na+Ca)-(*A*-site vacancy)-(U+Th) for pyrochlore-group minerals from different localities around the world.

□: Lueshe , ●: Sokli, ○: Blue River, +: Kovdor, ✳: Bingo, △: Prairie Lake, ✖: Newania, ★: Fen, ✙: Kola, ✖: Qaqarssuk, ◇: Mt. Weld

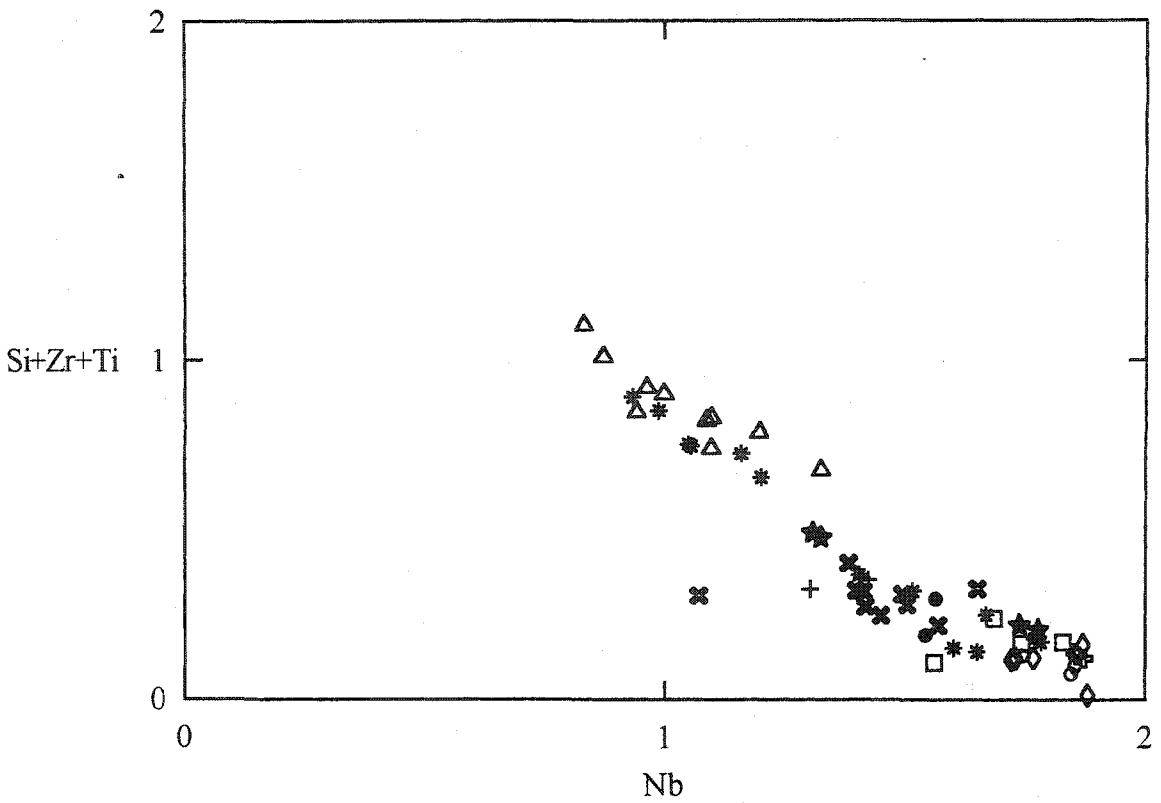

Figure 2.23. Compositional variations at the *B*-site of pyrochlore-group minerals.

□: Lueshe , ●: Sokli, ○: Blue River, +: Kovdor, ✳: Bingo, △: Prairie Lake, ✖: Newania, ★: Fen, ✙: Kola, ⊠: Qaqarssuk, ◇: Mt. Weld

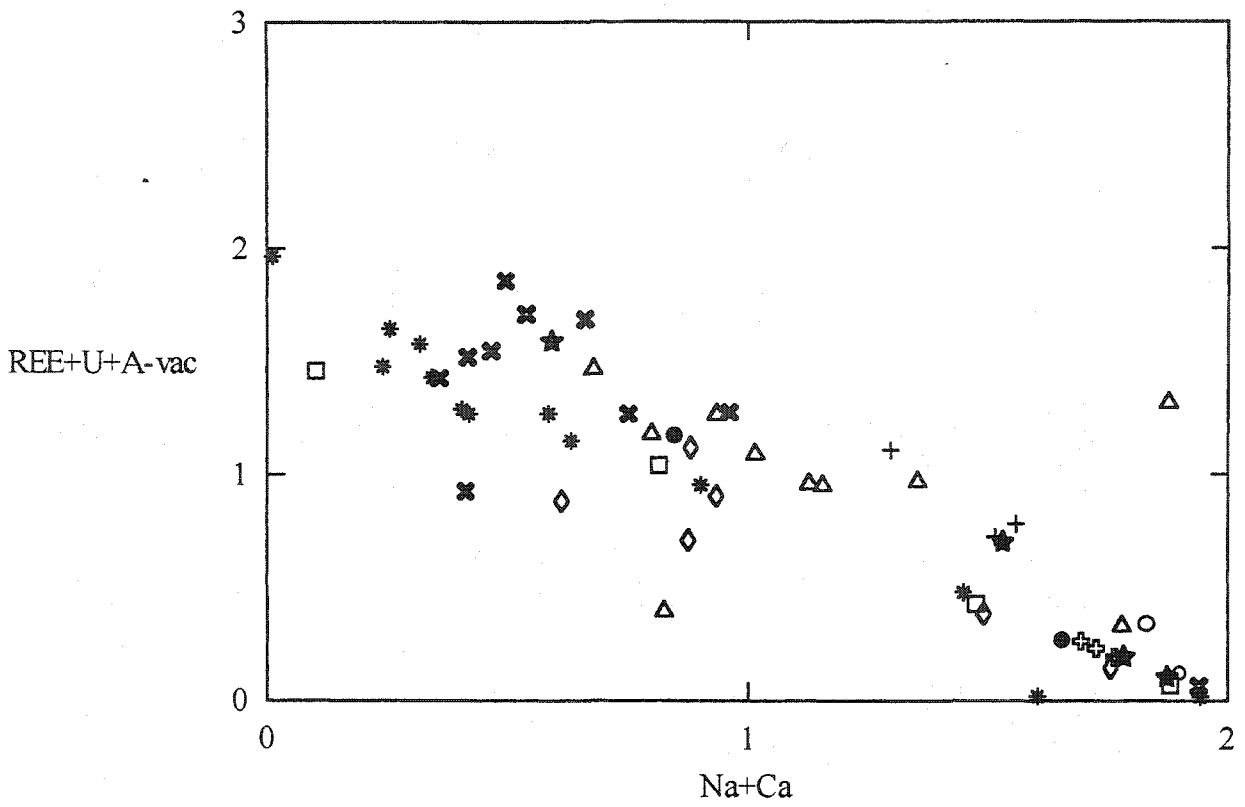

Figure 2.24. Compositional variations at the *A*-site of pyrochlore-group minerals.

□: Lueshe , ●: Sokli, ○: Blue River, +: Kovdor, ✳: Bingo, △: Prairie Lake, ✖: Newania, ★: Fen, ✙: Kola, ⊠: Qaqarssuk, ◇: Mt. Weld

phlogopite. They explain the high modal concentration of U-rich pyrochlore from the early carbonatite to be a product from a carbonatite magma enriched in U and Nb, where the U is progressively depleted during carbonatite development. They conclude that the U content in rauhaugites is high, which explains the highly uraniferous nature of the Newania pyrochlore. However, the large *A*-site vacancy reported does not imply that the U-rich pyrochlores are primary magmatic pyrochlores, other factors were involved during or after crystallization involving the leaching of the *A*-site cations in order to produce significant *A*-site vacancies.

Few similarities can be identified when comparing the U-rich pyrochlores of the Newania carbonatite to the U-rich pyrochlores from Oka. Both pyrochlores have extremely high amounts of U and Nb. At Newania, U-rich pyrochlore is the only Nb-bearing mineral found with a high modal abundance. At Oka, pyrochlore- group minerals, perovskite-group minerals, and niocalite have all been reported in high modal abundances. Oka pyrochlores have higher amounts of Zr held in the *B*-site, in addition to being associated with Zr-bearing minerals such as zirconolite, baddeleyite and calzirtite. Therefore at Oka, the Zr is not fixed in specific minerals, as it occurs in many different minerals. Only one specific pyrochlore-group mineral (uranpyrochlore) has been reported at Newania, in contrast to the variety of pyrochlore-group minerals found at Oka, with varying amounts of Ce, Th, U, and Ca. Oka U-rich pyrochlores are found with varying amounts of alteration, zoning, *A*-site vacancies and impurities. Newania pyrochlores are reported as fresh and free from alteration.

The conclusions of Viladkar and Ghose (2002) for the U-rich pyrochlores are not applicable for the Oka U-rich pyrochlores. In order to account for the various amounts of alteration, zoning, impurities and *A*-site vacancies for the U-rich pyrochlores at Oka, other factors must have been involved, and will be discussed below.

(b) Apatite-dolomite carbonatite, Lesnaya Varaka complex, Kola Peninsula, Russia

Mineral intergrowths composed of lueshite ($NaNbO_3$) in the core and pyrochlore-group minerals in the rim are present within the apatite-dolomite carbonatite at Lesnaya Varaka (Chakhmouradian and Mitchell, 1998). Chakhmouradian and Mitchell (1998) report pyrochlore developing on lueshite and showing a wide compositional range from "normal" almost stoichiometric Na-Ca pyrochlore to Na-poor Sr- and Ba-rich pyrochlore. Representative compositions of the pyrochlore can be found in Appendix IV. The proportions of *B* atoms (Nb, Ta, Ti) for pyrochlore-group minerals are presented in figure 2.19. Lesnaya Varaka pyrochlores plot in the pyrochlore field and do not contain any Ta.

The Na-Ca pyrochlore was found to contain moderate $LREE_2O_3$, SrO and TiO_2 with a small *A*-site vacancy (0.05-0.39 apfu; Chakhmouradian and Mitchell, 1998). The Na-Ca pyrochlores plot in the magmatic field represented by Nasraoui and Bilal (2000) (figure 2.20). Figure 2.21, a ternary diagram with apices Ti-REE^{3+}-Na, shows the Lesnaya Varaka Na-Ca pyrochlores plot in the Na corner, within the Oka pyrochlore compositional field. Chakhmouradian and Mitchell (1998) report that pyrochlores close to the ideal composition, $NaCaNb_2O_6$ (F,OH), with low to moderate *LREE*, Sr, Ti and Th occur in a broad variety of carbonatites. Some Na-Ca pyrochlore is enriched in ThO_2, which is found to have a negative correlation with CaO and no other components, suggesting an *A*-site substitution between Th^{4+} and Ca^{2+}. The Ba-strontiopyrochlore is found developed in peripheral zones and along fractures within the Na-Ca pyrochlore. Ba-strontiopyrochlore exhibits strong compositional variation with respect to CaO, SrO, BaO and Nb_2O_5. Chakhmouradian and Mitchell (1998), conclude that Ba-strontiopyrochlores are products of low-temperature hydrothermal or secondary (hypogene) alteration of the primary mineral assemblage of the carbonatite.

In comparison, the Oka pyrochlore-group minerals contain only trace amounts of Sr and Ba, typically below the detection limit. Pyrochlore-group minerals are found as discrete grains in Oka, not as intergrowths with other Nb minerals. Pyrochlore from the Oka carbonatite complex diverges substantially from the ideal composition in being Ce, U, Th and Zr enriched. Oka does not contain any pyrochlore-group minerals close to the ideal composition $NaCaNb_2O_6(F,OH)$.

(c) Kovdor carbonatite complex, Kola Peninsula, Russia

Uranoan pyrochlore-group minerals (closely associated with zirconolites) from the Kovdor Carbonatite complex, have been described by Williams (1996). Williams (1996) notes the relative abundances of U and Th, and Ce, which is the only detectable REE in the pyrochlore structure. The pyrochlores at Kovdor have Ta-rich cores and U-rich rims. *A*-site occupancies are generally close to 2. Patchy zonation features have not been identified, indicating that the Kovdor pyrochlores have not been subject to any significant degree of sub-solidus cation leaching and hydration (Williams, 1996). However, Williams (1996) reports that the pyrochlores are subhedral and have embayed edges, therefore indicating that some degree of dissolution and corrosion has occurred.

Figure 2.19 is a ternary diagram of elements in the *B*-position in the pyrochlore formula. Kovdor pyrochlores plot in the Nb corner, indicating they belong to the pyrochlore-subgroup. All Kovdor pyrochlores plot in the magmatic field represented by Nasraoui and Bilal (2000) (figure 2.20). Kovdor pyrochlores have elevated values of REE (present as Ce) and plot within the Oka compositional field in figure 2.21. In figure 2.23, no chemical variation is present in the *B*-site of the pyrochlore structure, indicating there is no *B*-site substitution involved with the Kovdor pyrochlores. No substitution is involved in the *A*-site of the pyrochlores from Kovdor,

as there is no variation at the *A*-site shown (figure 2.24). Of note is the elevated concentrations of Zr reported by Williams (1996), with ranges of 0.7 to 4.1 wt. % ZrO_2.

Williams (1996) concludes that accessory minerals such as pyrochlore, zirconolite and baddeleyite are probably major hosts for the incompatible elements in the carbonatite. Furthermore, the Ta-rich cores to the Ta-poor rims reflects the late-stage differentiation of magmas of both alkaline and carbonatitic affinities (Williams, 1996). In contrast, Oka pyrochlores contain little to no detectable Ta. However, the same hypothesis could be possible for the pyrochlores found with Nb-rich cores and Nb-poor rims. Zirconolite is also found associated with Oka pyrochlores, and Zr enrichment in the *B*-site of the Oka pyrochlores has been found to be the result of a substitution with Nb. Of the REE in the Oka pyrochlores, Ce is most enriched and often the only REE present above detectable levels.

2.4.2. Magnesiocarbonatite hosts

(a) Blue River carbonatite complex, British Columbia, Canada

There are twelve carbonatite and syenite complexes known to occur in the Blue River area of Southern British Columbia. Pyrochlore-group minerals from the metamorphosed Verity and Fir magnesiocarbonatite complexes were used in this study for comparison with the Oka pyrochlore-group minerals. Simandl *et al.* (2001) reported on the niobium and tantalum minerals identified at the Verity and Fir deposits. Fine-grained subhedral pyrochlores have been analysed by Simandl *et al.* (2001) and are presented in Appendix IV. Zoned tantalum pyrochlore grains show compositional variations suggesting that the highest Ta concentrations are associated with the highest UO_2 content. Verity and Fir pyrochlores plot within the pyrochlore-subgroup as defined by Hogarth (1989), and plot within the pyrochlore field on the Ti-Nb-Ta diagram (figure 2.19).

Figure 2.20 indicates that the Blue River Ta- and -U-rich pyrochlores plot in the magmatic field represented by Nasraoui and Bilal (2000), having very low *A*-site vacancies. Figure 2.21 defines the Blue River pyrochlores as Na-rich and REE^{3+} poor. Simandl *et al.* (2001) report that the REE contents of both pyrochlore and columbite are relatively low; however, higher amounts of REE were reported in whole rock analyses. They conclude that it is likely that substantial proportions of the total REE indicated by the whole rock analyses, is accounted for by other minerals. No further work has been undertaken on the Blue River pyrochlores, and the variations in Ta, Nb, U and Th compositions of the pyrochlores remain unexplained.

There is very small compositional variation within the *A*-site and *B*-site of the Blue River pyrochlores; therefore no substitution trends can be defined. Minor compositional variation, coupled with both low REE contents and *A*-site vacancies, defines the Blue River pyrochlores as primary magmatic pyrochlores, forming as an accessory phase after crystallization of the carbonate minerals. The carbonatite magma may have been enriched in elements such as U, and Ta, and progressively depleted during carbonatite development.

Comparing the Blue River pyrochlores to the Oka pyrochlores, no similarities are found. Ta-rich pyrochlores have not been reported from Oka. Blue River pyrochlores show little compositional variation, and very low amounts of REE^{3+}. The highest reported UO_2 contents from Blue River pyrochlores is 9.83 wt. % (Verity deposit), and the mean is 4.28 wt. % (n= 10). Oka pyrochlore ranges from 0.1-27.98 UO_2 wt. %. Blue River pyrochlores are unaltered, primary magmatic pyrochlores, perhaps crystallizing in situ simultaneously with Ta-columbite minerals (Simandl *et al.* 2001). Oka pyrochlores display large chemical variations and have a much more complicated history.

2.4.3. Laterite carbonatite hosts

(a) Mount Weld carbonatite laterite, Western Australia

Pyrochlore is present as a residual mineral within a laterite overlying and derived from a carbonatite intrusion (Lottermoser and England, 1988). Pyrochlore has been found associated with resistant primary minerals including Nb-ilmenite, Nb-rutile, baddeleyite, zircon, and magnetite. Lottermoser and England (1988) documented the occurrence and the mineral chemistry of pyrochlore from different parts of the laterite overlying and derived from the Mt. Weld carbonatite. They describe a range of pyrochlores; from fresh, light in colour pyrochlores to dark altered pyrochlores. Textures indicative of complex leaching and re-precipitation processes were reported. Voids were identified in the pyrochlore grains as being infilled with crandallite and beudantite, alunite group minerals. Some grains were shown to be partly- or totally- replaced by crandallite group minerals, destroying their original magmatic texture. Compositions of the Mt. Weld pyrochlores can be found in Appendix IV.

The analysed pyrochlore grains plots in the pyrochlore subgroup of the Nb-Ta-Ti diagram (figure 2.19). Further classification within the pyrochlore subgroup, indicates ceriopyrochlore, plumbopyrochlore and strontium pyrochlore to be present in the Mt. Weld carbonatite laterite. In figure 2.20, a ternary diagram with apices Ca-*A*-vac-Na, the Mt. Weld pyrochlores plot in both the magmatic and alteration field as represented by Nasraoui and Bilal (2000). Large *A*-site vacancies are the result of leaching of *A*-site cations and associated hydration during weathering (Lottermoser and England, 1988). *B*-site deficiencies are reported in fresh pyrochlore from the upper part of the laterite, and are assumed to be the result from the leaching of strongly-bonded Nb from the crystal lattice during weathering, with subsequent replacement by Fe^{3+} (Lottermoser

and England, 1988). This hypothesis is supported by the substantial amounts of Nb found within the secondary crandallite group minerals, anatase, and iron oxides, assuming theses minerals would be the depository for the Nb.

In figure 2.21, a ternary diagram with apices Ti-REE^{3+}-Na, the Mt. Weld pyrochlores plot along the Ti-poor section, and show a large range of REE^{3+}. Mt. Weld pyrochlores show small compositional variations at their *B*-site (figure 2.23), indicating limited *B*-site substitutions between Si, Zr or Ti. In figure 2.24, a bivariate diagram presenting compositional variations at the *A*-site of pyrochlore-group minerals, the Mt. Weld pyrochlores show a negative correlation between (REE+U+*A*-vac) and (Na+Ca). This shows a substitution within the *A*-site involving the leaching of Na+Ca and subsequent replacement by REE (U is not a factor in the substitution as this element was not present at detectable levels by EMP in the Mt. Weld pyrochlores), and resulting in *A*-site vacancies.

Lottermoser and England (1988), conclude that at Mt. Weld, leaching of the *A*-site ions, Na and Ca, from the pyrochlore crystal structure during weathering led to vacancies in the lattice which were subsequently filled by mobilized Sr and Ce. Furthermore, they claim the leaching of strongly bonded *B*-site Nb occurred and the vacant *B*-sites became occupied by Fe^{3+}. They suggest that there is mobility of Nb in humid weathering environments, even though Nb is generally considered to be immobile in geological processes.

Both the Oka pyrochlores and the Mt. Weld pyrochlores are found as both primary magmatic and altered types (figures 2.9 and 2.20, respectively). However, pyrochlores identified within a laterite host should be expected to have experienced varying degrees of alteration. The pyrochlores from Oka were hosted by a calciocarbonatite. The Mt. Weld pyrochlores exhibited a large variation in the amount of REE^{3+}, and this has been correlated with different zones in the

laterites (higher degree of alteration, higher amounts of REE). At Oka, the pyrochlores less commonly exhibited a large variation in the REE^{3+}, however no correlation is present between the surrounding host rock of the pyrochlores and the amount of REE they contain. There is a *B*-site substitution present in the Oka pyrochlores between Zr and (Nb+Ti) (figure 2.12). Lottermoser and England (1988) present a *B*-site substitution between Fe^{3+} and Nb, and a *B*-site vacancy resulting from the leaching of strongly-bonded Nb? However, the *B*-site vacancies reported could be filled with Si, present as a *B*-site cation (Si was not analysed in their study). Si has generally been considered a contaminant present as minute inclusions of silicate. Lottermoser and England (1988) provide no evidence supporting the leaching of Nb from the *B*-site.

Mt. Weld pyrochlores show characteristics directly related to the carbonatite weathering process. Leaching, re-precipitation processes, associated fractionation and differential mobility of the individual elements have produced large variations in the pyrochlore composition. Oka pyrochlores have large variations in their mineral chemistry, however the pyrochlores are NOT associated with laterites or weathering processes.

2.4.4. Calciocarbonatite hosts

(a) Prairie Lake carbonatite complex, Northwestern Ontario, Canada

Hammond (1999) reported pyrochlore from the Prairie Lake carbonatite as varying in size and habit from anhedral irregular to elongate, subhedral or euhedral grains. Pyrochlore grains were reported to be fractured and commonly found in clusters. Associated minerals include titanomagnetite, loparite, ilmenite, calcite, apatite, biotite and sericitized feldspar. Analyses of the Prairie Lake pyrochlores can be found in Appendix IV. Pyrochlore from Prairie Lake is enriched in U, Sr, and Si and Na and Ta poor. The dominant pyrochlore species is

betafite, with uranpyrochlore present as well. For the purposes of comparison, the uranpyrochlores were selected from these data and used for the current study.

In figure 2.19, the Prairie Lake uranpyrochlores plot in the pyrochlore subgroup, extending towards the betafite corner. The uranpyrochlores are therefore highly enriched in Ti. Most of the data for the uranpyrochlores plot in the magmatic field, with some data points extending towards the alteration field represented by Nasraoui and Bilal (2000) (figure 2.20). Figure 2.21, a ternary diagram with apices Ti-REE^{3+}-Na, shows some of the Prairie Lake pyrochlores plotting within the Oka pyrochlore compositional field. Pyrochlore compositions from Prairie Lake that do not plot in the field are enriched in Ti (figure 2.21). Prairie Lake uranpyrochlores have elevated concentrations of U, and varying amounts of *A*-site vacancies (figure 2.22). A bivariate plot of (Nb) vs. (Si+Zr+Ti) shows a negative correlation for the Prairie Lake pyrochlores (figure 2.23). This could represent a substitution within the *B*-site between Ti and Nb. Hammond (1999) has determined that small amounts of Si are present within the *B*-site and might substitute for Nb in the *B*-site. Figure 2.25 is a bivariate plot of (Nb+Ti) vs. Si, showing a very good strong negative correlation between these elements, suggesting that Si does in fact substitute for Nb and Ti in the *B*-site of the Prairie Lake pyrochlore –group minerals. Only small amounts of ZrO_2 were detected in the Prairie Lake pyrochlores, and Zr is therefore assumed not to be involved in a *B*-site substitution with Nb+Ti. A bivariate plot of (Na+Ca) vs. (REE+U+*A*-vac) represents compositional variations at the *A*-site of the Prairie Lake pyrochlore-group minerals (figure 2.24). This bivariate plot shows a negative correlation, suggesting possible *A*-site substitutions. Hammond (1999) reports that Ca contents are generally high, while Na is depleted in the *A*-site.

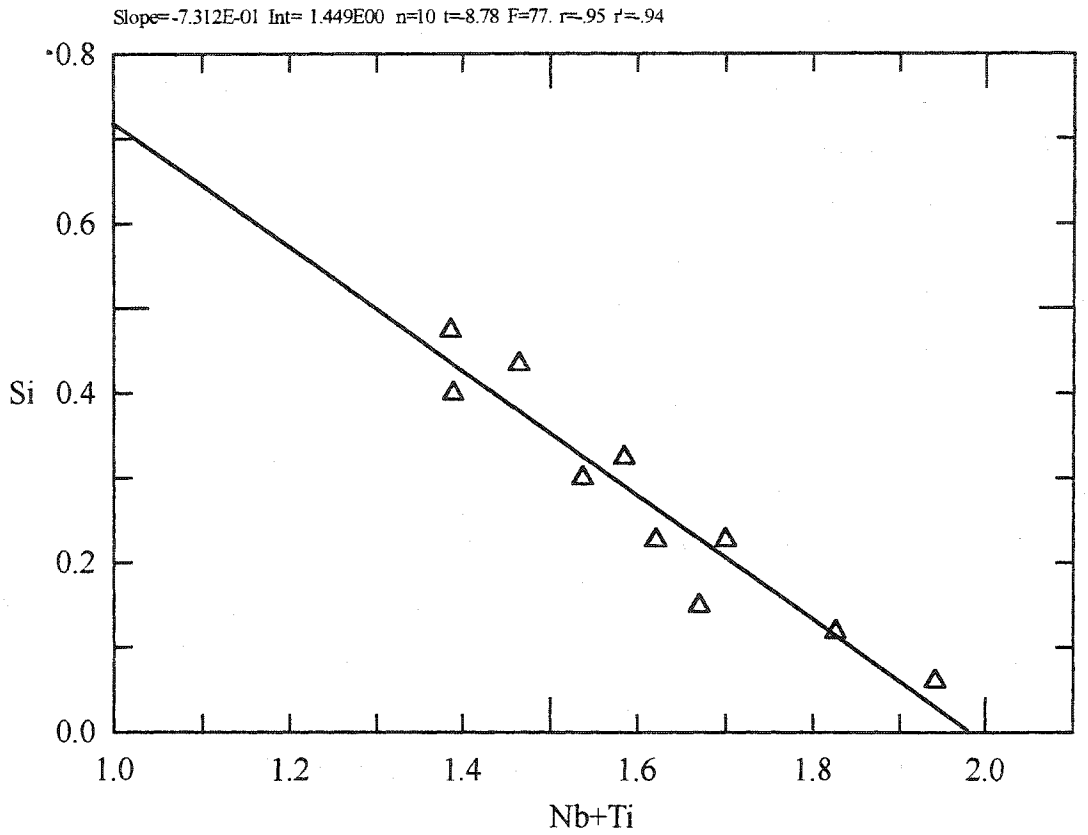

Figure 2.25. Bivariate plot of Si vs. (Nb+Ti) (a.p.f.u.) for pyrochlore-group minerals from the Prairie Lake carbonatite complex.

Hammond (1999) concludes that Prairie Lake pyrochlores are U-rich with moderate Si and Sr contents. Ta is uncommon in the pyrochlores. The Prairie Lake pyrochlores are therefore classified as uranpyrochlore and betafite. Hammond (1999) suggests that compositions of Prairie Lake pyrochlores indicate that after crystallization they have probably undergone some alteration by late-stage magmatic fluids.

Comparing the Prairie Lake uranpyrochlores to Oka uranpyrochlores, there are many similarities. Both pyrochlores have U and Th contents that tend to remain relatively constant (figure 2.22), and both have significantly high UO_2 concentrations for pyrochlores from calciocarbonatites. Both have a wide range of *A*-site vacancies (figure 2.20). However, Oka pyrochlores tend to have higher amounts of REE^{3+} elements in their *A*-site. *B*-site cations in both correlates fairly closely, both have low Fe and Al, and high Nb. However, Oka uranpyrochlores have higher amounts of Zr and lower amounts of Ti in their *B*-site. Ta is uncommon in pyrochlores from Prairie Lake and Oka. The Oka carbonatite complex does not have pyrochlores that belong to the betafite sub-group.

(b) Bingo carbonatite complex, Zaire

Williams *et al.* (1997) described the extensive compositional variation in pyrochlore from the Bingo Carbonatite, Zaire. Pyrochlores are reported to occur in the calciocarbonatite and surrounding laterite, and are generally discrete; euhedral grains typically 20-40 μm in diameter. Patchy alteration is common among the altered pyrochlore. Primary oscillatory magmatic zonation, with a complex interpenetrative twinning in samples of pyrochlore has also been observed. Williams *et al.*(1997) report a large compositional variation observed in the Bingo pyrochlore, ranging from completely filled *A*-sites to 64 % vacant. The laterite pyrochlore at Bingo has been reported to have up to 87% *A*-site vacancy. Using both the textural and

compositional variation, the pyrochlore from the calciocarbonatite at Bingo was classified into five groups: 1) oscillatory-zoned pyrochlore, 2) pyrochlore with low Sr contents, 3) pyrochlore with "medium" Ba contents, 4) pyrochlore with "high" Ba contents, and 5) bariopyrochlore. Analysis of the Bingo pyrochlore-group minerals can be found in Appendix IV.

Bingo pyrochlore compositions plot in the Nb corner of the ternary diagram, therefore belonging to the pyrochlore subgroup defined by Hogarth (1989) (figure 2.19). Three pyrochlore compositions described as "primary magmatic oscillatory zoned" by Williams *et al.* (1997), plot in the magmatic field represented by Nasraoui and Bilal (2000) (figure 2.20). Other pyrochlore compositions from Bingo, described as "patchy zoned", plot in the alteration field (figure 2.20). Pyrochlore compositions from Bingo show a large compositional field on the ternary diagram Ti-REE-Na (figure 2.21). Bingo pyrochlores have low amounts of U+Th, and a large range of *A*-site vacancies (figure 2.22). A negative correlation at the *B*-site is found with Bingo pyrochlore-group minerals (figure 2.23). This indicates that there is a *B*-site substitution between (Si+Zr+Ti) and (Nb) (all of which are present at detectable levels). Since there are elevated amounts of Si in the Bingo pyrochlore, it has been suggested that it is involved in the *B*-site substitution with Nb+Ti. Figure 2.26 is a bivariate plot of Si vs. (Nb+Ti) showing a strong negative correlation, suggesting that Si is involved in a B-site substitution with (Nb+Ti). A negative correlation is also found at the *A*-site of Bingo pyrochlore-group minerals (figure 2.24), indicating an *A*-site substitution involving the leaching of Na+Ca, and subsequent replacement with REE, resulting in an *A*-site vacancy.

Williams *et al.* (1997), conclude that the oscillatory-zoned pyrochlore from Bingo follows a "compositional" trend similar to the "transitional" trend of Lumpkin and Ewing (1995), which is considered to be post-magmatic. In addition, the patchily-altered pyrochlore from

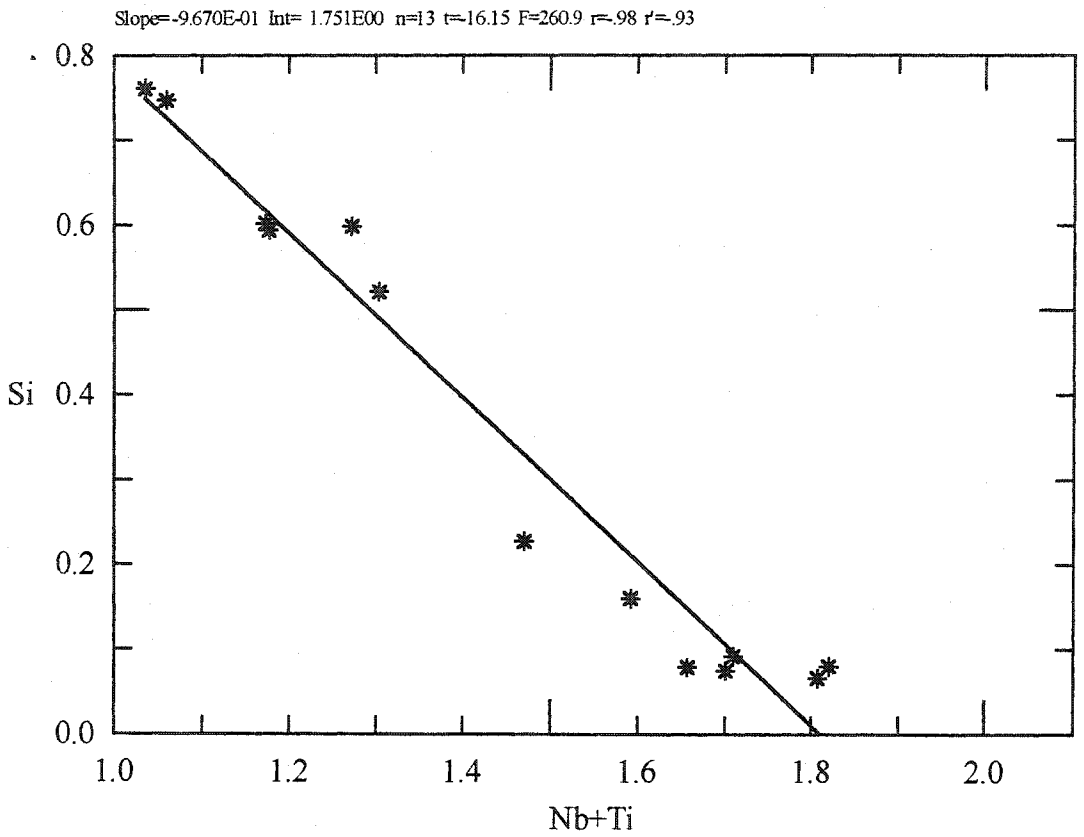

Figure 2.26. Bivariate plot of Si vs. (Nb+Ti) (a.p.f.u.) for the pyrochlore-group minerals from the Bingo calciocarbonatite.

Bingo follows the "altered" trend described by Lumpkin and Ewing (1995). The pyrochlore paragenesis at Bingo has not been completely described.

Oka and Bingo pyrochlore-group minerals both belong to a calciocarbonatite host, and have extremely large compositional variation and vacancies within the *A*-site. However, the altered pyrochlore from Bingo is rich in Ba and Si, whereas the altered pyrochlore from Oka is rich in Th, Ce and U. Oka and Bingo both have multiple sub-groups of pyrochlores, and complicated textures and alteration features. The pyrochlores from both complexes have complicated histories involving multiple magma batches, magma differentiation and secondary alteration processes.

(c) Qaqarssuk carbonatite complex, West Greenland

Knudsen (1989) reports the occurrence of pyrochlore-group minerals from the Qaqarssuk calciocarbonatite complex. Pyrochlore-group minerals are located in the late-carbonatite phase of the complex, found in close association with apatite, magnetite and zircon. The main intrusive phase of the carbonatite is devoid of pyrochlore-group minerals, however, the late-stage carbonatite contains pyrochlore –group minerals, which Knudsen (1989) interprets as a Nb and Ta enrichment in the residual fluids.

The most common pyrochlore at Qaqarssuk has a composition close to the end member $NaCaNb_2O_6$ (O, OH, F). Other pyrochlore-group minerals identified are bariopyrochlore, uranpyrochlore, betafite, and a Ba-betafite. Analyses of the pyrochlore-group minerals from Qaqarssuk carbonatite complex can be found in Appendix IV. Knudsen (1989) describes zoning defined by varying amounts of inclusions, as well as zoning defined by alternating opaque and pale brown transparent pyrochlore. Varying degrees of alteration have been reported. Figure 2.20 shows the Qaqarssuk pyrochlore-group minerals plotting in both the magmatic and

alteration field represented by Nasraoui and Bilal (2000). Figure 2.21 shows the wide compositional variation within the Qaqarssuk pyrochlores, with the Na-Ca end member plotting in the Na corner, betafite end members plotting in the Ti corner, and the U- and –Ta rich pyrochlores plotting towards the REE corner. Knudsen (1989) reports a variation in the amount of Ta and Ti substituting for Nb in the *B*-site in pyrochlore; as well as U, Th, Ba and lanthanides substituting for Na and Ca in the *A*-position. Furthermore, Knudsen (1989) reports that the late stage sovite and ferrocarbonatite pyrochlore-group minerals have a compositional zonation with respect to the *A*-cations and *B*-cations. The Ta and Ti concentrations decrease in the rim, parallel to the evolution in the concentrations of elements such as U, Th, Ba and lanthanides in the *A*-position. Negative correlations for the substitutions in both the *B*-and *A*-sites of the pyrochlore-group minerals are shown in figures 2.23 & 2.24, respectively.

Knudsen (1989) concludes that the precipitation of pyrochlore took place in the late-stage carbonatite. Pyrochlore has precipitated simultaneously with apatite, and this is shown by a rapid decrease in the concentration of the complexing ligands responsible for keeping the elements Nb, Ta, U, Th, and lanthanides in solution. The most abundant pyrochlore in the carbonatite has a composition close to $NaCaNb_2O_6(OH,F)$. The contents of Ta and Ti in the pyrochlore can be correlated with the contents of tri- and tetravalent ions in the *A*-position.

In comparison to the Oka pyrochlore-group minerals, some similarities are seen. Both carbonatites are hosts to a large compositional variation of pyrochlore-group minerals. Various degrees of zoning and alterations are observed at both locations. *A*- and *B*-site substitutions are present in both, however, Zr is present as a *B*-site substituting element in the pyrochlore-group minerals from Oka. The contents of Ta and Ti do correlate with the contents of tri- and tetravalent ions in the *A*-position of the uranpyrochlore and uranoan pyrochlore-group minerals

from Oka however, no other pyrochlore subgroup displays this correlation. Oka pyrochlore-group minerals have been identified in many sections of the carbonatite, and therefore are not unique to any particular host rock, making it extremely difficult to determine factors that would have controlled the crystallization of the pyrochlores.

(d) Fen carbonatite complex, Norway

The Fen carbonatite complex is located in Telemark, SE Norway. Hogarth *et al.* (2000) present a compositional study of primary zoning in pyrochlore-group minerals from nine carbonatites, including the Fen complex. Analyses for pyrochlore-group minerals from Fen are included in Appendix IV. Hogarth *et al.* (2000) classified the pyrochlore-group minerals according to their *A*-site cations, determining Fen to be host to uranoan pyrochlore, uranpyrochlore, and nearly stoichiometric pyrochlore. Uranoan pyrochlore has been analysed in the core of crystals, with uranpyrochlore occurring around the rim of the crystals. Nearly stoichiometric pyrochlore is observed as having sharp zones across the entire crystal, with slight enrichment of Ce, while other specimens of nearly stoichiometric pyrochlore were devoid of any detectable zoning. Uranpyrochlore exhibits oscillatory zonation with highly altered crystal rims.

Figure 2.20 shows Fen pyrochlores plotting in the magmatic field represented by Nasraoui and Bilal (2000), with the exception of the highly altered uranpyrochlore rims which plot in the alteration field. The pyrochlore-group minerals from Fen have large compositional variation, and all plot in the Oka pyrochlore compositional field (figure 2.21). Fen uranoan and uranpyrochlores have enrichment in U, and have U+Th contents very similar to Oka uranoan and uranpyrochlores (figure 2.22). A negative correlation is present in figure 2.23, a diagram representing the chemical variations at the *B*-site of pyrochlore-group minerals. This is probably due to a substitution of Ti for Nb in the *B*-site, as very minor amounts of Si and Zr were analysed

(SiO_2 wt. % ranging from <0.5 to 0.56; ZrO_2 wt. % <0.1 to 3.24). A negative correlation is also present in figure 2.24, a diagram representing the compositional variations at the *A*-site of pyrochlore-group minerals. REE, U, and *A*-site vacancy all could have been involved in substitutions with Na and Ca, as all are present in the *A*-site of the pyrochlores from Fen.

In comparison, the zoning in Oka pyrochlores is not nearly so straightforward. Oscillatory-zoned pyrochlores from Oka do not show consistent zoning patterns. Grains are more likely to be zoned to higher UO_2 contents from the core to the rim, however the opposite does occur, resulting in higher UO_2 contents in the rim. In addition, in many cases fairly constant UO_2 content occurs across the crystal. This is not only the case with the uranoan and uranpyrochlores of the complex, but also with cerium, cerio-, thor-, and thorium pyrochlore group minerals from Oka. Oka pyrochlores tend to be intensively altered and fractured. It is not uncommon to find an euhedral, zoned pyrochlore next to an altered and fractured anhedral pyrochlore, either of the same sub-group or different pyrochlore sub-group.

(e) Lueshe carbonatite complex, Democratic Republic of Congo.

The Lueshe syenite-carbonatite complex is located in the Rwindi Mountains in the northeastern part of the Democratic Republic of Congo. Nasraoui and Bilal (2000) have completed a study of the magmatic pyrochlores from the complex. Nasraoui and Bilal (2000), describe euhedral, discrete grains (0.1-2 mm in diameter) that may contain inclusions of calcite, dolomite and apatite. The modal percentage of pyrochlore varies considerable not only in the different rocks of the complex but also within the same rock type. Nasraoui and Bilal (2000), describe the occurrence of kali-, bario-, strontio-, and ceriopyrochlore that have been the direct result of supergene alteration, involving the complete leaching of Na and Ca. Magmatic, hydrothermal and weathered pyrochlore grains are reported from calciocarbonatite, pyroxenite,

syenite and laterite in the complex. Electron microprobe analyses from Lueshe pyrochlore-group minerals can be found in Appendix IV.

Magmatic pyrochlores from Lueshe have limited chemical variations in terms of Ta, Ti, Si, and REE contents (Nasraoui and Bilal, 2000). In figure 2.20, magmatic pyrochlores from Lueshe plot in the magmatic field, with low *A*-site vacancy. Hydrothermally altered pyrochlores plot in the alteration field in figure 2.20. Nasraoui and Bilal (2000), describe the hydrothermally altered pyrochlores as having undergone the leaching of elements from all three sites (*A*-site, *Y*-site, and *X*-site) due to substitution reactions. This pyrochlore group exhibits extremely large *A*-site vacancies. Supergene pyrochlores from Lueshe plot in the alteration field in figure 2.20. This group of pyrochlores is enriched in the LREE, Sr and Ba. Na-poor pyrochlore has also been identified, and is considered to be of intermediate variety corresponding to an alteration stage between hydrothermal and weathered pyrochlores.

Nasraoui and Bilal (2000) have interpreted the pyrochlore-group minerals at Lueshe to represent the stages of different alteration conditions that have occurred during and after carbonatite emplacement. They have defined trends of alteration by correlating larger scale events to pyrochlore textures and compositional variation. They conclude that pyrochlore-group minerals at Lueshe represent chemico-mineralogical transformations, and can be used to define different alteration conditions that may have occurred over time.

Considering the large variation of both composition and alteration that occurs in the Oka pyrochlores, and the complex history of carbonatite emplacement and crystallization, the conclusions of Nasraoui and Bilal (2000) may be of particular significance. No doubt Oka pyrochlores represent geochemical markers of different conditions, exhibiting various degrees of alteration and zoning, however, trends that are defined by Nasraoui and Bilal (2000) are not

shown with the Oka pyrochlores. Other factors may be involved which cause further "chemico-mineralogical" transformations, such as magma mixing. Evidence for this is found in Oka, with two different pyrochlores being found together in a small area. This will be further discussed below. One aspect that can be ruled out is hydrothermal and supergene alteration trends. Nasraoui and Bilal (2000), describe supergene pyrochlores as pyrochlores with nearly 100% *A*-site vacancy, due to the complete leaching of Na+Ca. This is not a factor at Oka, all pyrochlore-group minerals are devoid of these characteristics, and the carbonatite itself has not undergone "alteration" of any kind.

(f) Sokli carbonatite complex, Northern Finland

Calcite-rich carbonate rocks are dominant at the Sokli carbonatite complex in Northern Finland. Pyrochlore-group minerals are present in all the main types of carbonatite, and commonly contain magnetite inclusion (Lindqvist *et al.*, 1979). Euhedral pyrochlores are reported to vary in size from 0.15 mm to as large as 5 mm. Zoning is reported in the pyrochlore grains, however there are no significant differences in the distribution of the main components. Pyrochlore and uranpyrochlore are the two types of pyrochlore end members identified at Sokli (Lindqvist *et al.*, 1979). Uranpyrochlore is believed to be the product of extensive weathering within the carbonatite complex. The pyrochlore-group minerals were found to contain a notable amount of tantalum. The Nb_2O_5/Ta_2O_5 ratio for pyrochlores is between 4.9 and 177.9. The low Nb_2O_5/Ta_2O_5 ratio is interpreted to indicate that pyrochlore was crystallized in a relatively undifferentiated magma (Lindqvist *et al.*, 1979).

Sokli pyrochlore-group minerals plot in the Nb-corner of the Nb-Ta-Ti ternary diagram in figure 2.19. This indicates that the pyrochlores belong to the pyrochlore sub-group. In figure 2.20, the Sokli pyrochlores plot in the magmatic field represented by Nasraoui and Bilal (2000),

which agrees with the results from Lindqvist *et al.* (1979). Figure 2.22 shows the elevated concentrations of U+Th in the Sokli uranpyrochlores, very similar to Oka pyrochlores (figure 2.4). Sokli pyrochlores occur in weathering environments, and are interpreted to be derived from a relatively undifferentiated magma. Neither of these conditions occurs at Oka, and comparison between the pyrochlores is not useful.

2.5. Discussion

NIOCAN and Bond Zone pyrochlores have *A*-sites commonly occupied by Ca, Na, REEs, Th, and U; and rarely by Mn, Sr, and Ba. *B*-sites are commonly occupied by Nb, Ti, Fe, and Zr; and less commonly by Al and Si. All NIOCAN and Bond Zone pyrochlores belong to the pyrochlore-subgroup. The pyrochlores exhibit primary zonation, low temperature alteration, and metamictization. Many pyrochlores exhibit complex compositional zonation, whereas others are devoid of zoning. Therefore, changes in the fluid composition during the growth of the pyrochlores must have occurred. The NIOCAN and Bond Zone pyrochlores show extremely large compositional variations; and represent the largest recorded variations of any pyrochlores hosted by calciocarbonatites.

Ce is the dominant REE present in pyrochlore at Oka. High concentrations of Zr have been found in the NIOCAN and Bond Zone pyrochlores, and Zr minerals are found associated with these pyrochlores. Therefore, Zr is not fixed in specific minerals, it is found in many minerals at Oka, and may have been very mobile in the fluid system. All pyrochlores from Oka are Ta-poor.

A-site substitutions of U, Ce, and Th with Na and Ca occurred. No particular substitution is dominant, and any combination of substitutions may have occurred. When comparing

compositional information and textural information between the NIOCAN and Bond Zone pyrochlores, no trends are identified.

Cerium pyrochlores are the most common of the pyrochlore-group minerals found at the NIOCAN and Bond Zone deposits. Exhibiting primary zonation and low temperature alteration, they plot in the magmatic field represented by Nasraoui and Bilal (2000). Analyses of the cerium pyrochlores show low Zr concentrations.

Uranoan pyrochlores are the second most common pyrochlore group mineral occurring in the NIOCAN and Bond Zone deposits. Although the uranoan pyrochlores are considered to be the most extensively altered, they are found to plot only in the magmatic field as defined by Nasraoui and Bilal (2000). Uranoan pyrochlores exhibit metamictization features. A *B*-site substitution with Zr is present.

Uranpyrochlores are extensively altered and plot in the magmatic and alteration field defined by Nasraoui and Bilal (2000). Uranpyrochlores exhibit metamictization features. Some uranpyrochlores are mantled, indicating recrystallization of pyrochlore.

Ceriopyrochlores are not abundant in the NIOCAN and Bond Zone deposits. They are most commonly found as large, discrete euhedral- to –subhedral minerals. Analyses of the ceriopyrochlores show moderate Zr concentrations.

Thorium pyrochlores are rare in the NIOCAN and Bond Zone deposits. Generally smaller grains have low *A*-site vacancies that correspond to the low degree of alteration. There is insignificant intra- and intergrain compositional variation.

Thorpyrochlores are also rare in the NIOCAN and Bond Zone deposits, and commonly exhibit patchy zonation. Thorpyrochlores plot in the magmatic field defined by Nasraoui and Bilal (2000). Thorium rich pyrochlores are not characteristic of carbonatites and have only been

encountered in a few localities; Vuorijarvi, Kola and Guli, Siberia. (Chakhmouradian and Mitchell, 1998).

St. Lawrence Columbium pyrochlores have low *A*-site vacancies corresponding to their low degree of alteration. They have a low modal abundance in the deposit. They have low Zr, and do not have a *B*-site substitution. SLC pyrochlores exhibit minor compositional variations. Evolutionary trends have been identified between the SLC pyrochlore-group minerals and the NIOCAN and Bond Zone pyrochlore-group minerals. The first evolutionary trend is an increase in Ti from the SLC pyrochlores to the NIOCAN and Bond Zone pyrochlores. This is a trend towards a betafite subgroup of pyrochlore-group minerals. The second evolutionary trend involves an increase in REEs from SLC to NIOCAN and Bond Zone pyrochlores.

The pyrochlore-group minerals are interesting because of the range of compositions within a single section. Two or more compositional and textural varieties of pyrochlores are found in very close proximity to each other, implying that they could not have crystallized in situ. These pyrochlore-group minerals probably crystallized in another area of the carbonatite, possibly derived from a different batch of magma intruding the complex, and were later transported to their final location.

The wide variety of pyrochlore-group minerals that have been identified throughout the Oka carbonatite complex infer that the carbonatite complex formed from several batches of carbonatite magma. Each batch, slightly different in composition probably intruded the complex one after another, allowing for pauses in evolution, possibly mixing with another and changing the crystallochemical conditions each time. The pauses in the evolution of the Oka carbonatite are reflected by composition and physical variations. The SLC pyrochlores appear to be from an undifferentiated magma, rich in Ce and U. Evolutionary trends prove them to be

primary magmatic defect pyrochlores. NIOCAN and Bond Zone pyrochlores may be products of a more evolved magma, due to the changes caused by new batches of magma intruding into the complex. They have undergone significant changes, probably crystallizing far from their final deposition site. Each stage of differentiation causing an enrichment in one or more element would crystallize a different pyrochlore-group mineral. NIOCAN and Bond Zone pyrochlores have undergone the leaching of *A*-site cations such as Na and Ca, with subsequent replacement with Ce, U, and Th. Observed textures in the pyrochlores clearly support this hypothesis. Transportation of the pyrochlores would subject them to changes in pressure and temperature and different elemental compositions, therefore causing fracturing, mantling, metamictization, bleached zones and recrystallization.

Chapter 3: Mineralogy and composition of Perovskite-group minerals

3.1. Perovskite

3.1.1. Introduction

Perovskites are one of the most important mineral hosts for the rare earth elements (REE) and all natural perovskites contain these elements in concentrations ranging from trace through minor to major elements amounts (Mitchell, 1996). On the basis of the structures of natural and synthetic perovskites, Mitchell (1996, 2002) presented a revised classification of perovskite group minerals in addition to describing the extensive compositional variation of naturally-occurring REE-bearing perovskites. Perovskites have the general structural formula ABX_3, where A and B are cations and X represents anions. Structural distortions are easily tolerated in the framework of the perovskite structure, and as a result, a wide variety of cations may occupy the A and B sites. In natural perovskites, A-site cations include Na^{+}, K^{+}, Ca^{2+}, Sr^{2+}, rare earth elements $(REE)^{3+}$, Pb^{2+}, Th^{4+}, and Ba^{2+}, while B-site cations include Ti^{4+}, Nb^{5+}, Fe^{3+}, Ta^{5+} and Zr^{4+} (Mitchell, 2002). Complex multi-component solid solutions between many end-members of natural perovskite occur (Mitchell, 2002). Table 3.1 lists end-member compositions of natural perovskites.

3.1.2. Nomenclature of perovskite-group minerals

Perovskite-group minerals are named on the basis of the "50 % rule" for dominant end-member molecules. Mitchell (2002) recommended that prefixes be added to the basic name to reflect the dominant cations present in the ternary solid solutions, permitting descriptions of the compositional variations found within particular perovskite solid solutions. Prefixes are assigned in order of decreasing abundance of elements. Perovskites which contain more than 90 mol. % of a particular end-member are considered to be "pure" end member compounds (Mitchell,

Table 3.1. End-member perovskite compositions (*after* Mitchell, 1996)

Composition	Name	Type Locality	Reference
$CaTiO_3$	Perovskite	Ural Mtns, Russia	Rose (1839)
$(Na_{0.5}Ce_{0.5})TiO_3$	Loparite	Khibina, Kola, Russia	Kuznetsov (1925)
$NaNbO_3$	Lueshite	Lueshe, Zaire	Safiannikoff (1959)
$Ca(Fe_{0.5}Nb_{0.5})O_3$	Latrappite	Oka, Quebec	Nickel (1964)
$PbTiO_3$	Macedonite	Crni Kaman, Macedonia	Radusinović and Markov (1971)
$SrTiO_3$	Tausonite	Murun complex, Russia	Vorobyev *et al.* (1984)
$KNbO_3$		Synthetic	
$BaTiO_3$		Synthetic	
$Ce_2Ti_2O_7$		Synthetic	
$Ca_2Nb_2O_7$		Synthetic	
$CaZrO_3$		Synthetic	
$CaThO_3$		Synthetic	

1996). The majority of perovskite compositions can be expressed in terms of the molecular percentages of seven end-members (table 3.1) (Mitchell, 2002).

Perovskite, lueshite, loparite and tausonite are used as informal names for end-member compounds and correspond to IMA-approved mineral names. The other compounds listed are well known as synthetic materials, which are not given mineral names. The total iron content of perovskites is usually expressed as Fe^{3+}, as Mössbauer studies of natural perovskites have shown this to be the only species present (Mitchell, 2002).

3.1.3. Paragenesis of perovskite

Perovskites are a common accessory mineral in a wide variety of undersaturated alkaline rocks and carbonatites (Nickel and McAdam, 1963; Vlasov, 1966; Kapustin, 1980; Haggerty and Mariano, 1983; Mitchell, 1986; Ulrych *et al.* 1988; McCallum, 1989; Mitchell and Bergman, 1991; Mitchell and Vladykin, 1993; Mitchell, 1996). Occurring as discrete crystals, perovskites are commonly intergrown with other oxide minerals. Therefore, perovskites form mantles on oxide minerals and may also be mantled by oxide minerals (Mitchell, 1996).

Mitchell (1996) describes the paragenesis of perovskites in alkaline rocks as:

1. Single phase, early crystallizing discrete euhedral-to-subhedral crystals. In kimberlites, olivine lamproites, melilitites and alnöites they are found as weakly-zoned crystals which are poor in REE. In perovskite pyroxenites, ultrapotassic syenites and carbonatites they are found commonly as strongly-zoned crystals which may be REE-rich.
2. Discrete, early-forming euhedral-to-subhedral REE- and Nb-poor crystals with subhedral overgrowths of a second generation of REE and Na-rich perovskite.
3. Poikiolitic late-stage groundmass plates, found only in some lamproites and orangeites.

3.1.4. Perovskite in alkaline rocks

Mitchell (1996), describes perovskite compositional variation with reference to three ternary systems and one quaternary system, and shows that perovskites in alkaline rocks fall into four compositional groups:

1. Nb-poor, Ca-, Sr- and REE-rich perovskites which represent solid solutions between perovskite, loparite, and tausonite.
2. Sr-poor, Nb-, Ca- and REE-rich perovskites which represent solid solutions between perovskite, loparite and lueshite.
3. Ca-poor, Na-, REE-, Nb- and Sr-rich perovskites which represent solid solutions between lueshite, loparite and tausonite.
4. Sr-poor, Na-, Ca- and Nb- rich perovskites which represent solid solutions between lueshite, latrappite, perovskite and the layered perovskite $Ca_2Nb_2O_7$.

3.2. Previous work on perovskites from the Oka carbonatite complex

Studies on perovskite from the Oka Carbonatite Complex have been completed by Nickel and McAdam (1963); Nickel (1964); Chakhmouradian (1997); Mitchell (1996); and Mitchell *et al.* (1998). Nickel and McAdam (1963) described a new niobium-bearing variety of perovskite from Oka. The nomenclature of niobium-bearing perovskites was inadequate in the older literature. Previously, niobium-bearing perovskite was termed knopite, niboloparite, or dysanalyte. Nickel and McAdam (1963) abandoned the terms knopite and dysanalyte on the grounds that these minerals were members of the loparite-perovskite solid-solution series. Mitchell *et al.* (1996) showed niboloparite to be niobian calcian loparite and/or niobium loparite, therefore discrediting this term. Currently, the correct terminology for the niobium-rich variety of perovskite is niobium perovskite.

Nickel (1964) named the niobium-rich perovskite occurring at Oka, latrappite, due to the Nb content being greater than the Ti content. The International Mineralogical Association (IMA) accepted the name latrappite on this basis as an approved name for the mineral species. There are only two known occurrences of Ca-Nb-rich perovskite-group mineral; the Oka carbonatite complex and the Kaiserstuhl alkaline complex (Mitchell, 1998). However, Nickel (1964) did not define a distinct compositional end-member representing the latrappite component of the complex solid solution. Mitchell *et al.* (1998) presented compositional data for latrappite and other niobium-rich perovskite group minerals from the Oka (Bond Zone deposit and okaite), Kaiserstuhl and Magnet Cove carbonatite complexes (table 3.2). Mitchell *et al.* (1998) consider latrappite to be a member of a continuous solid-solution involving $CaTiO_3$, $NaNbO_3$, $Ca_2NbFe^{3+}O_6$ and $Ca_2Nb_2O_7$, and on the basis of ^{57}Fe Mössbauer spectrometry, only ferric iron is present.

3.3. Oka Perovskite: NIOCAN and Bond Zone deposit

Perovskite typically occurs as small euhedral- to -subhedral crystals, which exhibit patchy and slight compositional oscillatory zonation. NIOCAN and Bond Zone perovskites are commonly fractured and contain inclusions of calcite and magnetite (figures 3.1 and 3.2). Some perovskite grains are found occurring adjacent to anhedral pyrochlore grains (figure 2.1 (d)). The modal percentage of perovskite in the carbonatite ranges from 0.5 – 2 vol. %.

The NIOCAN and BZ perovskite have been classified according to the recommendations of Mitchell (1996). Appendix II includes 100 perovskite compositions from the NIOCAN and Bond Zone deposit. All data are expressed in terms of molecular percentages of end-member components. Fifteen are "pure" perovskite, or perovskite $CaTiO_3$-*sensu stricto,* and latrappite was found in very minor amounts in both deposits, whereas the majority of compositions are of

Table 3.2. Representative compositions of Latrappite from the Bond Zone deposit at Oka

Wt. %	1	2	3	4	5	6	7	8	9	10
Nb_2O_5	47.60	46.44	47.61	47.91	40.53	39.12	35.23	49.7	47.9	43.90
Ta_2O_5	0.24	0.32	n.d.	n.d.	n.d.	n.d.	0.11	n.d.	n.d.	n.d.
TiO_2	9.73	8.94	10.39	8.89	11.71	13.96	17.51	9.8	9.3	10.05
ThO_2	n.d.	n.d.	0.04	0.07	n.d.	n.d.	n.d.	n.d.	0.1	n.d.
Fe_2O_3	6.16	8.39	6.26	6.89	9.91	9.77	10.09	5.8	5.9	9.71
La_2O_3	0.52	0.53	0.49	0.45	0.70	0.77	1.11	0.3	1.1	-
Ce_2O_3	1.04	1.25	1.10	0.98	1.66	1.76	2.36	0.7	1.5	2.03
Pr_2O_3	0.06	0.11	0.08	0.05	0.10	0.22	0.24	0.5	0.8	-
Nd_2O_3	0.27	0.29	0.26	0.26	0.36	0.48	0.71	0.6	0.4	-
MnO	0.41	0.32	0.30	0.34	0.27	0.24	0.26	0.3	0.5	0.77
MgO	2.16	1.67	1.80	1.89	1.54	1.15	0.88	2.1	2.2	2.20
CaO	26.65	27.06	25.24	26.97	29.82	28.25	28.29	24.3	24.2	25.95
SrO	0.17	0.11	0.18	0.22	0.19	0.19	0.24	0.2	0.3	n.d.
Na_2O	3.94	3.85	4.79	3.96	2.33	3.09	2.90	4.9	4.3	4.03
Total	98.95	99.28	98.54	98.88	99.12	99.00	99.93	100.1	99.3	98.64
Structural Formulae based on 3 atoms of oxygen										
Nb	0.573	0.560	0.575	0.574	0.486	0.468	0.420	0.597	0.588	0.529
Ta	0.003	0.002	-	-	-	-	-	-	-	-
Ti	0.195	0.179	0.209	0.177	0.234	0.278	0.347	0.194	0.190	0.202
Fe	0.123	0.169	0.126	0.153	0.198	0.195	0.180	0.116	0.114	0.194
Mn	0.009	0.007	0.007	0.008	0.006	0.005	0.006	0.007	0.011	0.017
Mg	0.086	0.066	0.072	0.075	0.061	0.045	0.035	0.083	0.089	0.088
ΣB	0.989	0.983	0.989	0.987	0.985	0.991	0.988	0.997	0.992	1.030
La	0.005	0.005	0.005	0.004	0.007	0.007	0.011	0.003	0.011	-
Ce	0.010	0.012	0.011	0.009	0.016	0.018	0.023	0.007	0.015	0.020
Pr	0.001	0.001	0.001	0.001	0.001	0.002	0.002	0.004	0.008	-
Nd	0.003	0.003	0.003	0.003	0.003	0.005	0.007	0.006	0.004	-
Ca	0.760	0.774	0.722	0.766	0.848	0.801	0.800	0.693	0.704	0.742
Sr	0.003	0.002	0.003	0.003	0.003	0.003	0.004	0.003	0.005	-
Na	0.203	0.199	0.248	0.204	0.120	0.159	0.148	0.253	0.226	0.208
ΣA	0.985	0.996	0.993	0.990	0.998	0.995	0.995	0.969	0.973	0.970
Mol. % end-members										
$SrTiO_3$	0.25	0.16	0.26	0.32	0.27	0.27	0.34	0.29	0.45	-
LOP	3.07	3.47	3.07	2.73	4.41	4.84	6.68	2.85	6.32	2.39
LU	20.82	20.24	25.04	20.90	11.31	15.06	13.27	25.68	22.38	21.84
LATRAP	14.74	20.14	14.70	18.21	23.48	22.76	20.98	13.61	13.78	23.57
PEROV	21.55	19.07	22.79	19.54	24.67	29.43	35.66	21.22	16.54	23.90
$Ca_2Nb_2O_7$	39.57	36.92	34.16	38.31	35.86	27.64	23.08	36.37	40.53	28.30

Total Fe calculated as Fe_2O_3; LOP = $Na(REE)Ti_2O_6$; LU = $NaNbO_3$; LATRAP = Ca_2NbFeO_6; PEROV = $CaTiO_3$.
Compositions: 1-3, Mitchell (1998); 4, Mitchell (1996); 5-7, Mitchell (1998); 8-9, Chakhmouradian (1996); 10, Nickel and McAdam (1964). Totals of compositions 8 & 9 include 1.0 and 0.8 wt. % ZrO_2, respectively
n.d. = not detected. *From*: Mitchell (1998).

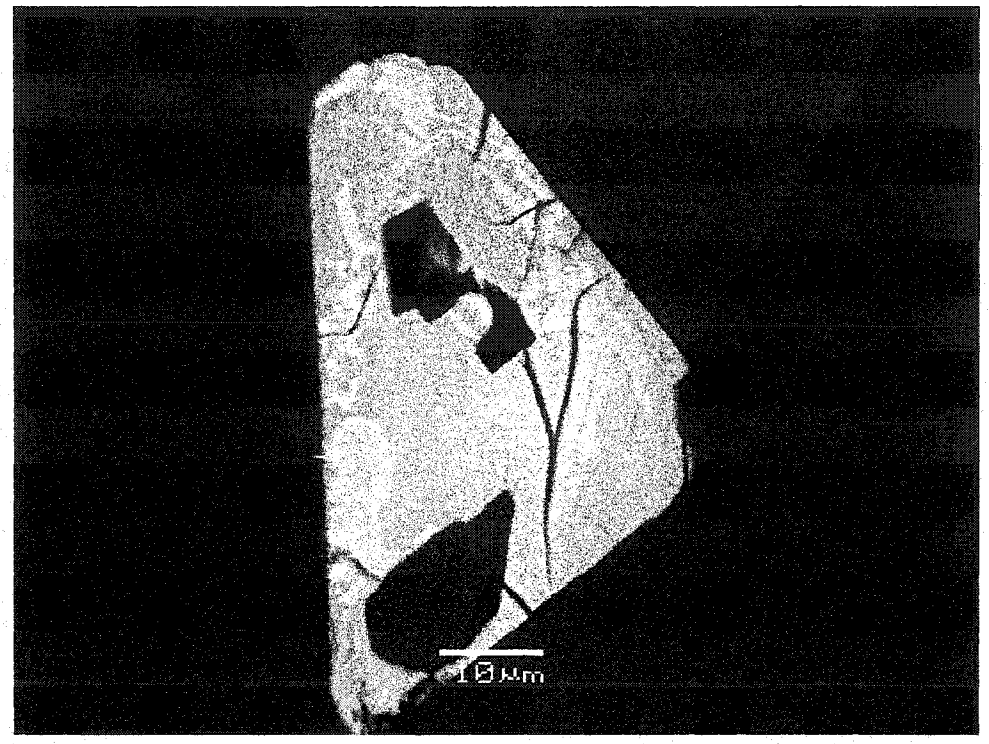

Figure 3.1. Niobium perovskite from NIOCAN deposit at Oka (BSE image) displaying zonation and resorption textures.

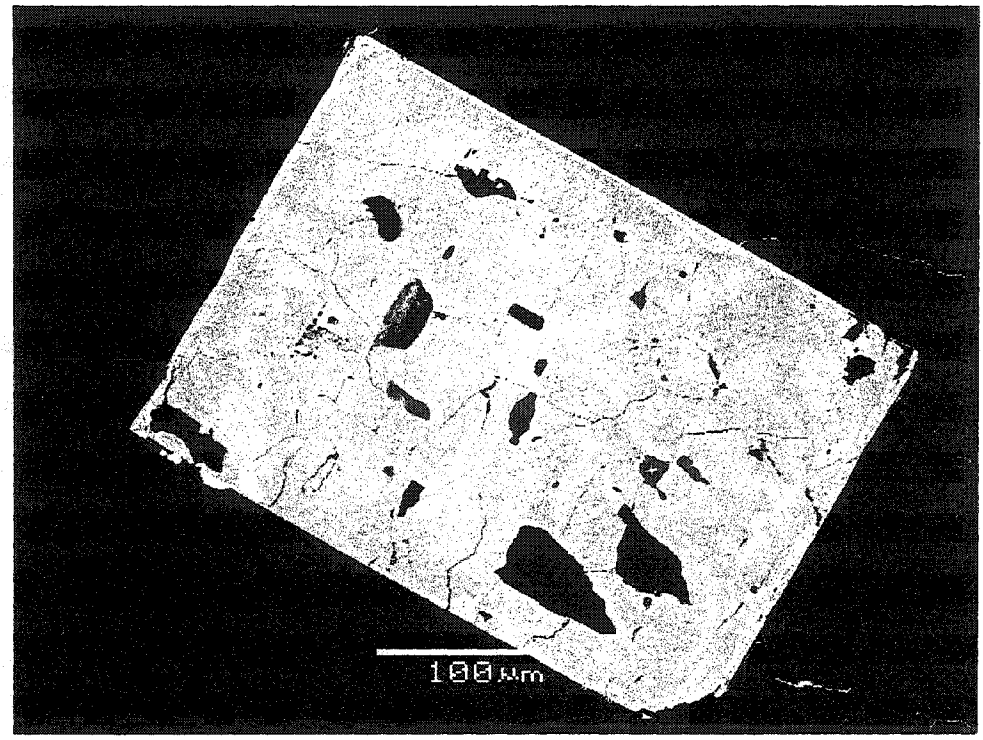

Figure 3.2. Niobium perovskite from NIOCAN deposit at Oka (BSE image) displaying patchy zonation.

niobium perovskite. Table 3.3 lists representative compositions of pure perovskite and niobium perovskite from the NIOCAN and Bond Zone deposits. The perovskite enriched in the $Ca_2Fe^{3+}NbO_6$ and $Ca_2Nb_2O_7$ components previously found in the Bond Zone at Oka (Mitchell *et al.*, 1998) was rare in this study.

Electron microprobe analyses show NIOCAN and Bond Zone perovskite to exhibit a moderate range in composition (table 3.4). Perovskite *sensu stricto* from NIOCAN and Bond Zone exhibits a large range of Nb_2O_5 and TiO_2 (wt. %), while CaO and Fe_2O_3 (wt. %) remain essentially constant. Niobium perovskite from NIOCAN and Bond Zone exhibits a large range in the content of Nb_2O_5, CaO, Na_2O and TiO_2 (wt.%) (table 3.4).

Perovskite-*sensu stricto* analyzed from the NIOCAN and Bond Zone deposits contain Fe_2O_3 ranging from 2.75 to 5.78 wt. %, with a mean (n=15) of 4.0 wt. % Fe_2O_3 (table 3.4). The niobium perovskite contains Fe_2O_3 ranging from 0.4 to 9.05 wt. %, with a mean (n=91) of 5.73 wt. % (table 3.4). Mitchell (2002) reports that with the exception of latrappite, perovskites generally do not contain much Fe (<1 wt. %). Unusually high Fe^{3+} may be considered to be an enrichment of Fe^{3+} in the carbonatite magma.

SiO_2,, ZrO_2 and MgO were each detected at levels of <3 wt. %. Previously, low amounts of SiO_2 and MgO have been interpreted as contamination with minor amounts of other minerals (Nickel and McAdam, 1963). Mitchell *et al.* (1998) report that calcite, pyrochlore, magnetite and clinohumite may be present as inclusions in samples of latrappite from Oka. Inclusions of calcite, pyrochlore, magnetite, and other accessory phases such as zirconolite and baddeleyite, are found in niobium perovskite from the NIOCAN and Bond Zone deposits (this work). Therefore, the minor amounts of Mg and Si could reflect contamination of the analysed material. The presence of co-existing baddeleyite and zirconolite suggests that the Oka carbonatite

Table 3.3. Representative compositions of perovskite and Nb-perovskite from NIOCAN and Bond Zone deposits

Wt. %	1	2	3	4	5	6	7
Nb_2O_5	3.26	1.79	14.46	19.70	24.53	21.60	15.30
Ta_2O_5	0.00	0.00	0.00	0.17	0.74	1.17	1.16
TiO_2	46.54	49.51	38.90	37.78	34.73	32.64	35.85
ThO_2	0.07	0.00	0.00	0.00	0.00	0.00	1.11
Fe_2O_3	4.79	3.78	5.25	3.57	3.67	6.88	6.05
La_2O_3	2.61	4.23	1.70	1.20	1.71	0.00	0.74
Ce_2O_3	9.17	6.47	2.40	2.57	3.21	2.39	2.28
Pr_2O_3	0.00	0.00	0.00	0.00	0.00	0.00	0.00
Nd_2O_3	0.00	1.85	1.00	1.08	1.13	0.00	0.86
MnO	0.00	0.01	0.06	0.00	0.00	0.00	0.22
MgO	0.00	0.00	0.00	0.14	0.29	0.00	0.20
CaO	31.93	30.80	33.39	28.73	25.07	32.28	34.01
SrO	0.00	0.36	0.00	0.39	0.39	0.00	0.25
Na_2O	0.78	0.57	1.73	3.74	4.65	2.15	0.84
Total	99.15	99.37	98.89	99.07	100.12	99.11	98.66
Structural Formulae based on 3 atoms of oxygen							
Nb	0.032	0.019	0.161	0.220	0.265	0.234	0.162
Ta	0.000	0.000	0.000	0.001	0.005	0.008	0.008
Ti	0.873	0.914	0.720	0.703	0.651	0.618	0.682
Fe	0.099	0.077	0.108	0.074	0.076	0.145	0.128
Mn	0.000	0.000	0.001	0.000	0.000	0.000	0.005
Mg	0.000	0.000	0.000	0.005	0.010	0.000	0.008
ΣB	1.00	1.01	0.99	1.00	1.00	1.00	0.99
La	0.025	0.038	0.015	0.011	0.015	0.000	0.007
Ce	0.084	0.058	0.022	0.021	0.029	0.022	0.021
Pr	0.000	0.000	0.000	0.000	0.000	0.000	0.000
Nd	0.000	0.016	0.009	0.009	0.010	0.000	0.008
Ca	0.842	0.811	0.875	0.735	0.669	0.872	0.921
Sr	0.000	0.005	0.000	0.006	0.005	0.000	0.004
Na	0.038	0.027	0.056	0.180	0.225	0.105	0.041
ΣA	0.99	0.96	0.98	0.98	0.95	0.99	1.00
Mol. % end-members							
$SrTiO_3$	-	0.59	-	0.05	0.52	-	0.33
LOP	8.22	6.24	7.61	6.46	8.90	2.43	5.08
LU	-	-	3.24	16.51	20.62	10.00	2.48
LATRAP	-	-	12.34	8.55	8.94	16.60	14.43
PEROV	91.74	93.17	66.63	62.90	54.61	60.25	67.89
$CaThO_3$	0.04	-	-	-	-	-	-
$Ca_2Nb_2O_7$	-	-	10.17	5.07	6.41	10.72	9.80

Total Fe calculated as Fe_2O_3; LOP = $Na(REE)Ti_2O_6$; LU = $NaNbO_3$; LATRAP = Ca_2NbFeO_6; PEROV = $CaTiO_3$.

Compositions: 1-2, Perovskite, 3-7, Niobium Perovskite

Table 3.4. Compositional variations of NIOCAN and Bond Zone perovskites.

$CaTiO_3$ Perovskite or Perovskite *sensu stricto* n=15		
Wt. % Oxide	**Range**	**Mean**
Na_2O	0.00-2.06	0.92
SiO_2	0.00-0.78	0.29
CaO	29.13-36.83	32.47
TiO_2	16.96-49.51	42.84
Nb_2O_5	1.79-19.98	6.85
Ce_2O_3	2.15-9.17	4.93
Ta_2O_5	0.00-2.14	0.28
Fe_2O_3	2.75-5.78	4.00
Niobium Perovskite n=91		
Wt. % Oxide	**Range**	**Mean**
Na_2O	0.00-7.28	3.19
SiO_2	0.00-1.69	0.48
CaO	22.43-34.52	30.49
TiO_2	20.95-48.08	30.97
Nb_2O_5	3.91-42.15	22.80
Ce_2O_3	0.00-7.55	2.82
Ta_2O_5	0.00-3.49	0.70
Fe_2O_3	0.40-9.05	5.73

magmas were enriched in Zr. Therefore, Zr analysed in the perovskite is actually present and occupies the *B*-site of the perovskite structure.

In the niobium perovskite, BaO was not detected, with the exception of a few of the examples containing BaO at trace levels (<2 wt. % oxides). Several perovskite grains analysed are found to co-exist with small anhedral barite grains. Barite is a common accessory mineral throughout the NIOCAN and Bond Zone deposits. Reasons why Ba does not substitute at the *A*-site of naturally-occurring perovskite is not known (Mitchell, 2002).

Figure 3.3 shows the distribution of elements from the rim-to-core of an oscillatory-zoned niobium perovskite. Previous work by Mitchell *et al.* (1998) has shown that minor zoning in niobium perovskites and latrappite from Oka is represented by Nb fluctuations. The perovskite grains from NIOCAN and Bond Zone exibiting zoning were found to represent Nb contents, increasing from the rim to the core of the grain (figure 3.3f). A small spike in the Nb and Fe occurs in the fourth zone towards the core (at 19 μm), which corresponds with a small decline in Ti at the fourth zone (figure 3.3 c). This could represent an exchange of Nb and Fe for Ti in the *B*-site of the perovskite structure. A large Ca spike occurs also in the fourth zone towards the core (at 19 μm), which corresponds to the decline of Na at this zone (figure 3.3 a, b). This could represent an exchange of Ca for Na in the *A*-site of the perovskite structure. Figure 3.3 e, g) shows Ce and La both decreasing toward the core of the perovskite grain.

Ce is the dominant REE in perovskite at the NIOCAN and Bond Zone deposit. La, Nd and Sm are present in trace amounts. Previously, inaccurate analytical techniques for analysing REEs in perovskites, have resulted in poor data on the relative distribution of REEs in perovskite. However, more recent studies show perovskite-group minerals are more likely to be enriched in LREE relative to HREE (Mitchell, 2002).

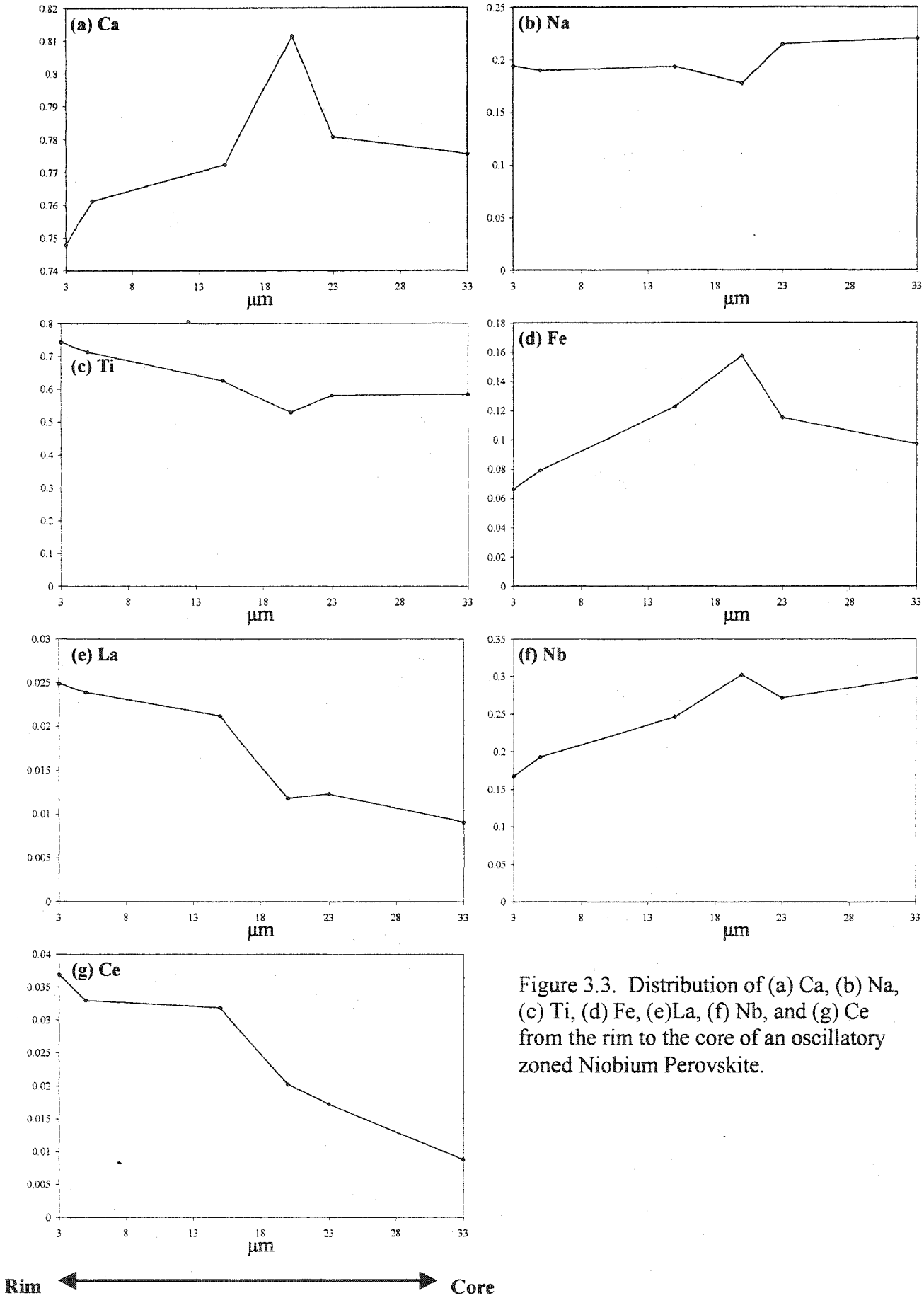

Figure 3.3. Distribution of (a) Ca, (b) Na, (c) Ti, (d) Fe, (e)La, (f) Nb, and (g) Ce from the rim to the core of an oscillatory zoned Niobium Perovskite.

3.4. Discussion

The significant feature of the perovskite-group minerals at the NIOCAN and Bond Zone deposits is the extreme enrichment of Nb, and the low REE contents. Their compositions do not reflect any solid solutions toward loparite, and therefore belong to the quaternary system: Perovskite-Ca_2FeNbO_6-$Ca_2Nb_2O_7$-Lueshite. In figure 3.4, the compositional variations of the perovskite-group minerals from Oka NIOCAN and Bond Zone deposit have been plotted using this quaternary system. Perovskites from three carbonatite complexes only can be depicted using this system: the Oka calciocarbonatite; the Kaiserstuhl carbonatite complex (Germany); and the Magnet Cove carbonatite complex (Arkansas) (Mitchell *et al.* 1998). Previous work by Mitchell *et al.* (1998) show perovskite compositions from the these carbonatites depicted in the quaternary system (figure 3.5). Kaiserstuhl and Magnet Cove plot close to the perovskite corner, while Oka Bond Zone perovskites trend towards Na- , Fe- and Nb-enrichment. Table 3.5 shows that compositions of Nb-perovskites and latrappite from Kaiserstuhl and Magnet Cove, are very similar in composition to the Oka perovskite-group minerals. However, perovskites from Husereau Hill okaites at Oka plot at the perovskite corner of the diagram. Mitchell (2002) defines a trend of increasing $NaNbO_3$, Ca_2FeNbO_6 and $Ca_2Nb_2O_7$ from initial calcian sodian niobian perovskite. Increasing Nb is accompanied by increasing Fe^{3+}, which reflects substantial solid solution with the Ca_2FeNbO_6 component (Mitchell, 2002). The Oka NIOCAN and Bond Zone data presented from this study plots closer to the perovskite corner than previous data from this complex (figures 3.4 and 3.5). This could be interpreted as a trend of an initial calcian sodian niobian perovskite evolving to a more Nb-, Fe- rich perovskite (see blue arrow, figure 3.4). The evolutionary trend of increasing Na, Nb, and LREE contents has been described in a

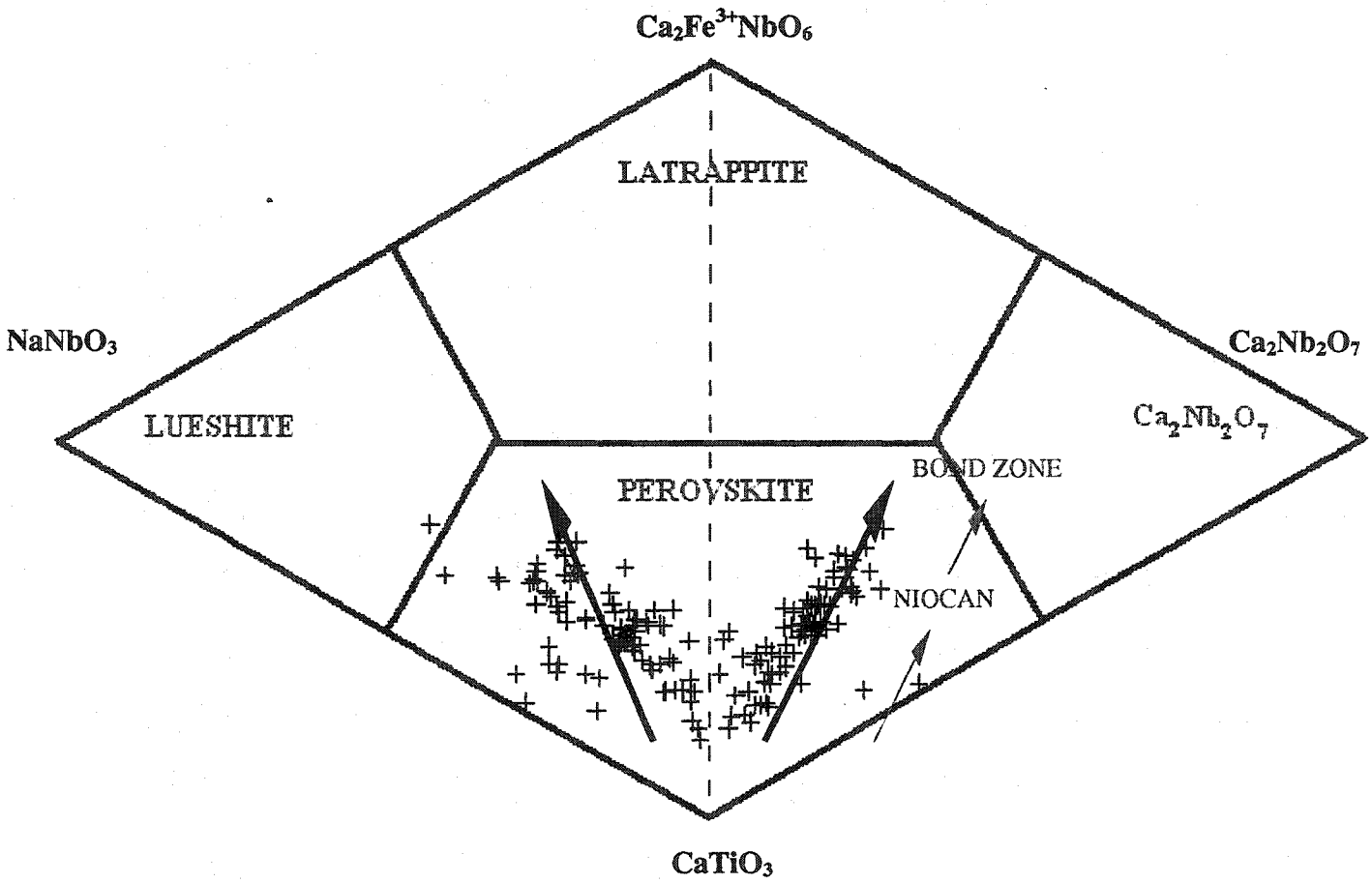

Figure 3.4. Compositional variation (mol. %) of Nb-rich perovskite and latrappite from Oka NIOCAN deposit (+), depicted in the quaternary system $NaNbO_3$-$CaTiO_3$-$Ca_2Nb_2O_7$-Ca_2FeNbO_6. Arrow represents possible evolutionary trend.

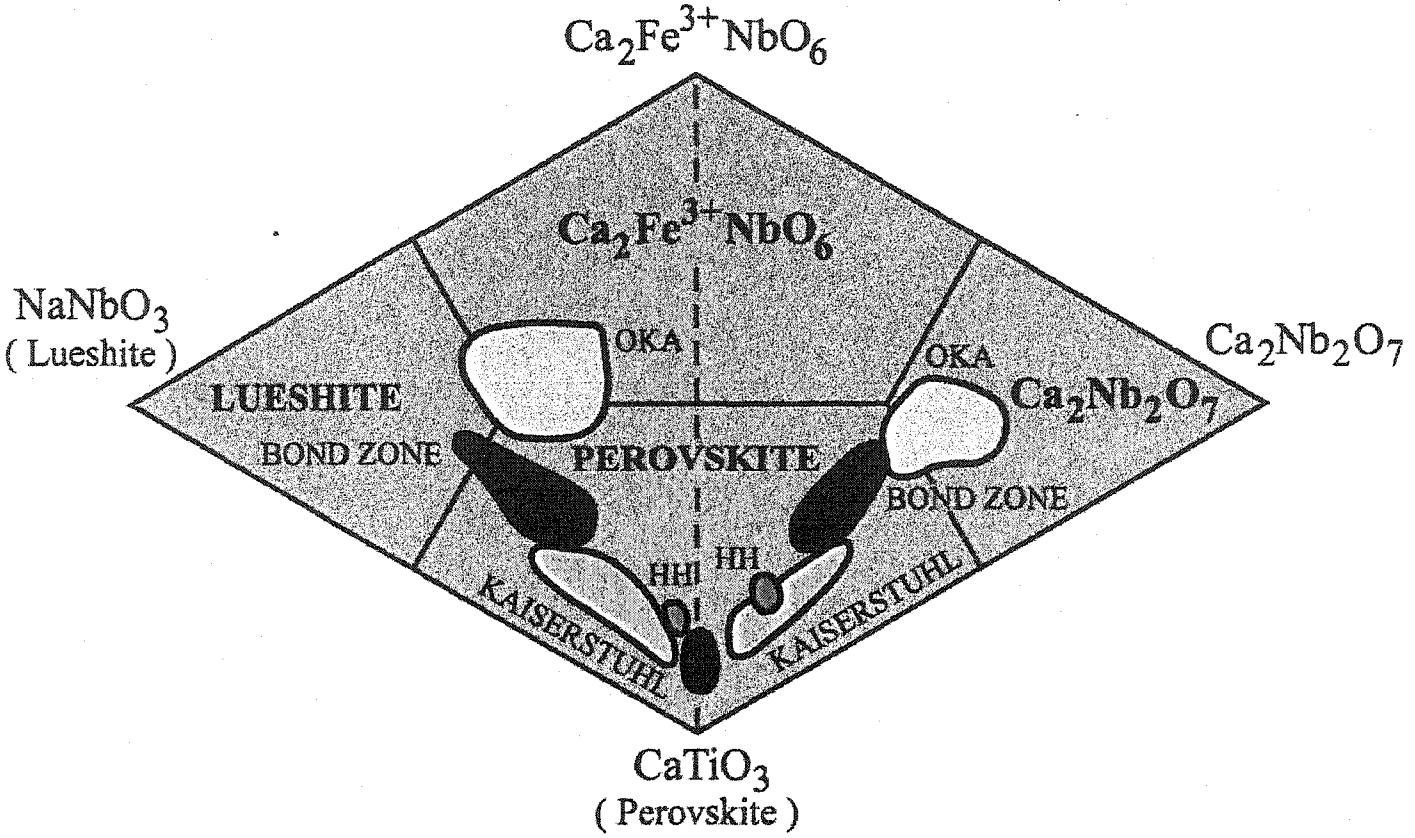

Figure 3.5. Compositional variation (mol. %) of Nb-rich perovskite and latrappite from the Oka (red, green and yellow fields), Kaiserstuhl (orange field), and Magnet Cove (blue field) carbonatite complexes depicted in the quarternary system $NaNbO_3$-$CaTiO_3$-$Ca_2Nb_2O_7$-Ca_2FeNbO_6. (after Mitchell *et al.* 1998).

Table 3.5. Compositions of Nb-perovskite and latrappite from other carbonatite complexes.

Wt. %	**1**	**2**	**3**
Na_2O	0.15	2.20	3.82
CaO	37.49	31.87	28.06
SrO	0.33	0.08	0.17
MgO	n.d.	0.12	0.25
MnO	n.d.	n.d.	0.20
Fe_2O_3	5.70	5.03	5.23
La_2O_3	1.60	0.56	0.36
Ce_2O_3	2.38	1.61	0.97
Pr_2O_3	n.d.	0.17	0.05
Nd_2O_3	0.38	0.46	0.13
ThO_2	0.12	n.a.	n.a.
TiO_2	42.44	33.18	25.06
ZrO_2	n.a.	0.18	0.30
Nb_2O_5	9.38	22.02	33.63
Ta_2O_5	0.33	2.02	1.12
Total	100.30	99.38	98.90
Mol.% End-member components			
$SrTiO_3$	0.05	0.10	0.23
$NaNbO_3$	-	9.59	18.89
$NaREETi_2O_6$	2.09	3.77	2.15
Ca_2FeNbO_6	11.48	10.72	11.60
$REE_2Ti_2O_7$	1.44	-	-
$Ca_2Nb_2O_7$	7.19	14.97	20.68
$CaTiO_3$	77.70	60.85	46.45

1 Calgon Pit, Magnet Cove, Arkansas;
2-3 Kaiserstuhl complex, Germany.
All data from Mitchell *et al.* 1998)
n.d. = not detected; n.a. = not analysed.

diversity of alkaline-ultramafic and carbonatitic rocks (Platt, 1994; Chakhmouradian and Mitchell, 1997, 1998b).

It is proposed that the Nb-perovskites at NIOCAN and Bond Zone crystallized at a middle stage in the evolution of the carbonatite, relative to the other Nb mineralization in the complex. Petrographic evidence for this is shown by the numerous inclusions of groundmass calcite and apatite within the perovskite grains. The moderate range of compositions in the perovskites (including the larger Nb_2O_5 range) is interpreted as crystallizing under fluctuating P-T conditions, with the fluctuating conditions being the result of intruding batches of magma. The perovskites may have become more evolved (Na-, Nb-, and REE-rich) from the interaction of the compositionally primitive generations of this mineral with a second melt, produced as a result of magma mixing, and enriched in Na, Nb, and REE. Petrographic evidence supporting this theory is shown by the resorption textures and alterations exhibited by the perovskites. Some perovskites have escaped the interaction of secondary melts, and have therefore remained perovskite *sensu stricto,* while others are more evolved as a result of the interaction.

Chapter 4: Mineralogy and composition of Zirconolite minerals

4.1. Zirconolite

4.1.1. Introduction

Zirconolite is a rare accessory mineral that can be found in a wide range of geological environments. Zirconolite is a calcium zirconium titanium oxide with the structural formula $CaZrTi_2O_7$. Zirconolite commonly exhibits compositional zoning patterns that are good indicators of the changes taking place in a geological environment (Gière and Williams, 1992). Zirconolite has been considered as a matrix for the immobilization of high-level radioactive wastes (Synroc zirconolite) (Gière and Williams, 1992). Therefore, studies conducted on this mineral species are of great mineralogical and economic importance.

4.1.2. Nomenclature of Zirconolite-group minerals

Zirconolite can exist as three polytypes with monoclinic, orthorhombic and trigonal symmetry (Bayliss *et al.*, 1989). Zirconolite is difficult to identify using optical microscopy because it forms small crystals and can easily be mistaken for ilmenite or rutile (Gière *et al.*, 1998). Actinide elements occur in the structure, which can make the mineral partially-or fully - metamict (Bellatreccia *et al.*, 1999). This results in errors in the identification and the classification of polytypes of zirconolites. Bayliss *et al.* (1989) ended the confusion surrounding the nomenclature of the $CaZrTi_2O_7$ minerals by creating a new nomenclature scheme, which was approved by the IMA-CNMMN. The revised nomenclature scheme is as follows (*after* Bayliss *et al.*, 1989):

1. The metamict mineral / or undetermined polytype of $CaTiZr_2O_7$ is called zirconolite.
2. The orthorhombic mineral of $CaZrTi_2O_7$ is called zirconolite-3O (3-octahedral layers in a crystallographic repeat).

3. The trigonal mineral of $CaZrTi_2O_7$ is called zirconolite-3T (3-octahedral layers in a crystallographic repeat).
4. The monoclinic mineral of $CaZrTi_2O_7$ is called zirconolite-2M (2-octahedral layers in a crystallographic repeat).
5. Polymignite is synonymous with zirconolite.
6. The cubic mineral with composition (Ti, Ca, Zr) O_{2-x} shall be called zirkelite.

4.1.3. Petrographic features and compositional characteristics of Zirconolite

According to Gière *et al.* (1998), zirconolite is always found as an accessory mineral, usually <100 μm in size. It can be the only Zr-bearing phase, or it can be intergrown with other Zr-bearing phases, *i.e.* calzirtite, baddeleyite. The mineral is typically biaxial negative, exhibiting high birefringence and straight extinction with negative elongation.

The structure of zirconolite is compositionally very flexible, leading Gière *et al.* (1998) to conclude that the availability of specific components becomes a key factor in controlling the composition of zirconolite. Bayliss *et al.* (1989) reports the end-member formula to be: $^{VIII}Ca_2{}^{VII}Zr_2{}^{Vi}Ti_4O_{14}$. There is extensive substitution involving mainly the rare earth elements, the actinides, Nb and Fe into natural zirconolite structures (Gière *et al.*, 1998). According to Bayliss *et al.* (1989), major replacements are trivalent REEs and tetravalent actinides in the ^{VIII}(Ca) site are, Nb and Ta in the ^{VI}(Ti) site, and Fe in the ^{IV}(Ti) site. Table 4.1 lists the ideal composition of zirconolite and the actual compositional variations found in natural zirconolite. Gière *et al.* (1998) separated all potential components and defined new variables by grouping bivalent, trivalent and pentavalent metal ions together.

$$Me^{2+} = Mg^{2+} + Fe^{2+} + Mn^{2-} + Zn^{2+}$$

$$Me^{3+} = Al^{3+} + Fe^{3+} + Cr^{3+}$$

Table 4.1. Zirconolite stoichiometry (from Gière *et al.* 1998)

	CaO (wt. %)	**ZrO_2 (wt. %)**	**TiO_2 (wt. %)**
Theoretical	16.5	36.3	47.2
Actual Range found in Natural Zirconolite Samples	2.63-16.5	24.3-45.4	13.6-45.9

$Me^{5+} = Nb^{5+} + Ta^{5+}$

$ACT = U^{4+}$

$REE = Ln^{3+} + Y^{3+}$

Therefore, the components are Ca, Zr, Ti, ACT, REE, Me^{2+}, Me^{3+}, Me^{5+}, W, Hf and O. This allowed Gière *et al.* (1998) to describe natural zirconolite with the following end-members:

$CaZrTi_2O_7$

$CaZr[Me^{5+}Me^{3+}]O_7$

$ACTZrTi[Me^{2+}]O_7$

$REEZrTi[Me^{3+}]O_7$

$REEZr[Me^{5+}Me^{2+}]O_7$

Using these end-members Gière *et al.* (1998) described the compositional space of natural zirconolite graphically using a double tetrahedron (figure 4.1). The upper right part of the double tetrahedron is Me^{3+} dominated, whereas the lower left is Me^{2+} dominated. Chemographic relationships have been studied by Gière *et al.* (1998) for the ternary system $CaO\text{-}ZrO_2\text{-}TiO_2$ (figure 4.2). This diagram shows that if zirconolite is associated with other Zr-bearing minerals theoretically, one of the following three phase assemblages should be present.

(a) zirconolite + baddeleyite + calzirtite

(b) zirconolite + baddeleyite + perovskite

(c) zirconolite +calzirtite + perovskite

In the NIOCAN and Bond Zone deposit, zirconolite is found associated with baddeleyite and perovskite, *i.e.* assemblage (b).

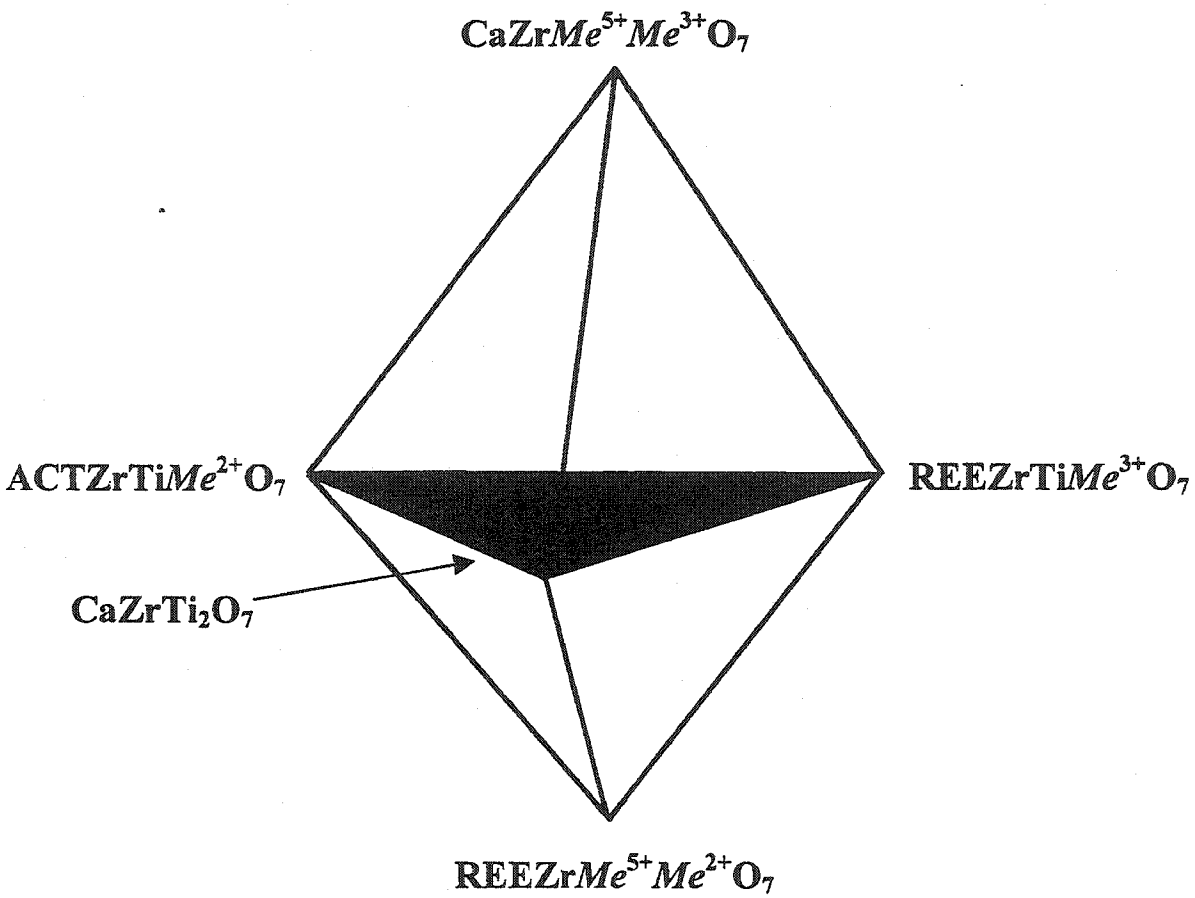

Figure 4.1. Compositional space for natural zirconolite (from Gière *et al.*, 1998).

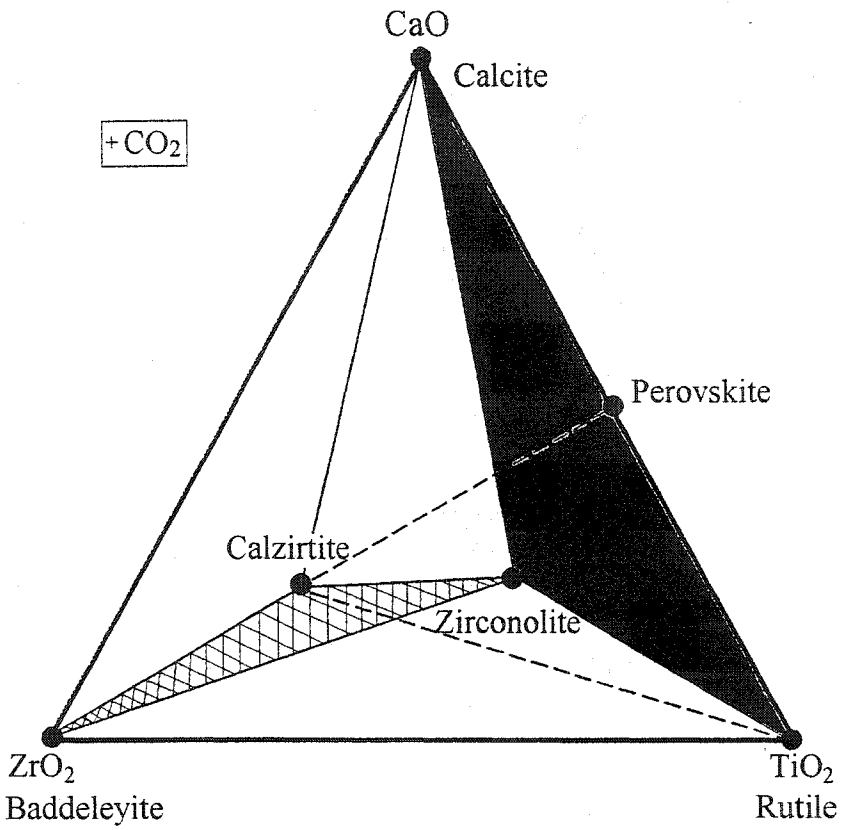

Figure 4.2. Chemographic diagram for the system CaO-ZrO_2-TiO_2-CO_2. Cross-hatched three-phrase assemblage observed in the carbonatite at Schryburt Lake, ON. Dark shaded field represents the assemblage found in the metasomatic veins at Adamello, Italy (from Gière *et al.*, 1998).

4.1.4. Paragenesis of zirconolite

Zirconolite is most commonly reported as a late-stage phase that crystallizes from a trace element-enriched magma in mafic cumulate rocks and carbonatites (de Hoog *et al.*, 2000). Various processes can be attributed to the crystallization of zirconolite, involving solid phases, melts or fluids (Gière *et al.*, 1998). Using the simplified CaO-ZrO_2-TiO_2-CO_2 system, Gière *et al.* (1998) listed zirconolite-forming reactions that could take place (table 4.2). Other zirconolite-forming processes possible are solid-melt interactions, which would explain zirconolite rims around baddeleyite crystals, or by solid-solid reactions (i.e. metasomatism), or finally, by reactions involving a fluid phase (Gière *et al.*, 1998).

4.1.5. Zirconolite occurrences

Zirconolite occurs in a wide range of rock types and geological environments, and has been recognized in over 50 terrestrial localities and 13 lunar samples. Williams and Gière, (1996) reviewed zirconolite occurrences and compared their compositions, and noted that all are in rocks that are poor or deficient in SiO_2. Zirconolites have been identified in kimberlites, ultrabasic rocks, gabbro pegmatites, syenites, nepheline syenites, metasomatic rocks, placer deposits, lunar samples, and most commonly, in carbonatites (Williams and Gière, 1996). Table 4.3 is a summary of the localities described by Williams and Gière, (1996). Their comparison of the compositions of zirconolites from various localities concludes that most common occurring elements in zirconolite are (in no particular sequence): Mg; Al; Si; Ca; Ti; Mn; Fe; Y; Zr; Nb; Hf; Ta; W; Pb; Th; U; La; Ce; Pr; Nd; Sm; and Gd.

Table 4.2. Zirconolite-forming reactions (from Gière *et al.* 1998)

[1] perovskite + rutile + baddeleyite ⇔ zirconolite
[2] 3 perovskite + 5 rutile + calzirtite ⇔ 5 zirconolite
[3] calcite + 2 rutile +baddeleyite ⇔ zirconolite + CO_2
[4] 3 calcite + 8 rutile + calzirtite ⇔ 5 zirconolite +3CO_2
[5] calzirtite + 2 rutile ⇔ 2 zirconolite + 3 baddeleyite
[6] calzirtite + 8 perovskite + 5 CO_2 ⇔ 5 zirconolite + 5 calcite
[7] baddeleyite + 2 perovskite + CO_2 ⇔ zirconolite + calcite
[8] calzirtite + CO_2 ⇔ zirconolite + 4 baddeleyite + calcite

Table 4.3. A summary of the localities of zirconolite as given by Williams and Gière, (1996)

Rock Type	Occurrences	Associated Minerals
Kimberlites	• 3 localities in South Africa	• baddeleyite • zircon • ilmenite • armalcolite • calcite
Ultrabasic Rocks	• identified in 2 ultrabasic cumulate complexes in Algeria and Scotland	• baddeleyite • apatite • zircon
Gabbro Pegmatites	• St. Kilda, Scotland	• biotite • epidote • allanite • titanite • apatite • zircon
Syenites	• Glen Dessarry, Scotland • Arbarastakh massif, Aldan, Russia • Fredicksvatn, South Norway • Campo Flegrei, Italy	• Fe Ti oxides • titanite • allanite • apatite • zircon
Nepheline Syenites	• Pine Canyon, Utah, USA • Elk Massif, Poland • Chikala, Malawi • Tchivira, Angola • Pilanesberg, Gauteng, South Africa • Tre Croci, Latiuum, Italy	• hibonite • perovskite • pseudobrookite • apatite • fluorite • pyrochlore • wohlerite • baddeleyite • zircon • rare thorian hellandite
Carbonatites	• Kola Penninsula, Russia • Schryburt Lake, ON, CA • Santiago Island, Cape Verde Republic • Phalaborwa, South Africa • Sokli, Finland • Kaiserstuhl, Germany • Hegau Volcanic Province, Germany • Prairie Lake, ON, CA • Cummins Range, Australia • Howard Creek, BC, CA • Catalaõ, Brazil • Araxa, Brazil	• calzirtite (intergrown) • apatite • magnetite • clinohumite • tetraferriphlogpite • pyrrhotite • richterite • baddeleyite • pyrochlore • glimmerite • zircon • perovskite • betafite • diopside • anatase
Metasomatic Rocks	• Mt. Melbourne Volcanic Field, Anatartica • Berge Aureole, Switzerland • Octztal-Stubai Complex, Austria • Adamello Contact Aureole, Italy • Koberg mine, Sweden	n/a
Lunar Samples	• mainly in peridotites and metamorphosed breccia	• baddeleyite

4.1.6. Carbonatite host rocks

The zirconolite compositional data presented by (Gière *et al.*, 1998) suggests that different substitutions operate in zirconolites in different geological environments. Carbonatites are the most common host rock for zirconolites, with 16 reported occurrences. Zirconolites from carbonatites are highly variable with respect to their contents of REE, ACT and Me^{5+}. The common features of zirconolites from carbonatites are low Al contents, enrichment in LREE, and a higher Fe_{Total} content. Bellatreccia *et al.* (1999) reports that zirconolites associated with carbonatites almost always show compositional zoning.

4.2. NIOCAN and Bond Zone zirconolite minerals

This work has shown that zirconolite is present in the Oka carbonatite. To the best of the author's knowledge, this is the first time the mineral has been documented from this area. Figure 4.3 is a back-scattered electron image of a zirconolite grain from the Bond Zone of the complex. Zirconolite from the NIOCAN and Bond Zone deposit at Oka occurs as small, rare, subhedral- to -anhedral crystals (maximum length ~ 30 μm). Zirconolite is mostly found located in the fractures and cavities of calcite and apatite, and occasionally found rimming pyrochlore and biotite grains. In one instance, a zirconolite grain is found occurring as an overgrowth on the rim of a uranoan pyrochlore grain. Subsequent analysis of this zirconolite revealed low CaO and enriched UO_2 contents. Rarely, the zirconolite exhibits zoning, which reflects slight variations in Nb and $LREE^{3+}$ content.

Sixty analyses of zirconolites from the NIOCAN and Bond Zone deposits are included in Appendix II.3, with representative compositions given in table 4.4. Table 4.5 lists the compositional variations of zirconolites from the NIOCAN and Bond Zone deposits. These data show a large range of TiO_2 content, (6.20-29.36 wt %). Elevated Nb_2O_5 contents are present in

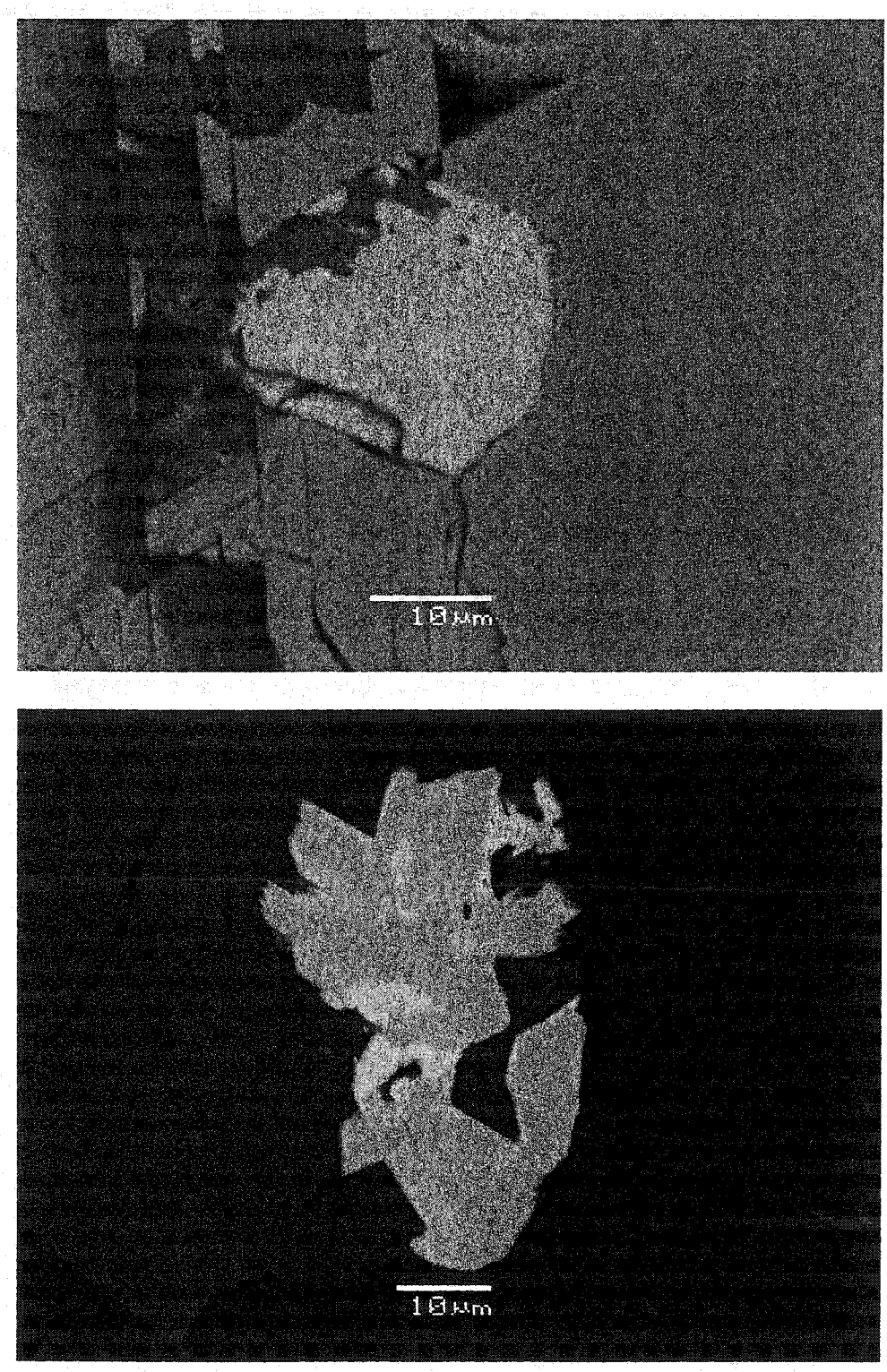

Figure 4.3. BSE images of zirconolite from NIOCAN deposit.

Table 4.4. Representative compositions of zirconolite from NIOCAN and Bond Zone deposits at Oka

Wt. % Oxide	A	B	C	D
MgO	n.d.	n.d.	0.56	0.21
Al_2O_3	n.d.	n.d.	n.d.	0.63
SiO_2	n.d.	n.d.	n.d.	0.50
CaO	14.02	10.03	8.98	13.89
TiO_2	29.36	10.84	12.55	19.91
MnO	n.d.	3.89	3.67	1.65
FeO	6.76	6.24	5.24	7.47
ZrO_2	31.63	32.80	37.10	33.86
Nb_2O_5	11.73	27.47	24.60	21.57
La_2O_3	2.34	n.d.	n.d.	n.d.
Ce_2O_3	n.d.	4.86	2.93	n.d.
Nd_2O_3	1.94	3.19	2.69	n.d.
HfO_2	n.d.	n.d.	n.d.	0.31
ThO_2	n.d.	1.41	0.52	0.13
$(Na,K)_2O$	0.22	n.d.	1.06	0.37
Total	99.06	100.71	99.92	100.60

UO_2 and Ta_2O_5 analysed, but not detected

the NIOCAN and Bond Zone zirconolite, in common with zirconolites from other carbonatite hosts (Gière *et al.*, 1998). Other features characteristic of zirconolites with a carbonatite host, also occur at Oka, i.e. low Al content, LREE>HREE (with the dominant LREE being Ce^{3+}), and $Fe_{Total} > Mg$.

The NIOCAN and Bond Zone zirconolites exhibit a large range in CaO, TiO_2, and ZrO_2 content. Gière *et al.* (1998) notes that the variation in Zr content is large mainly as a result of extensive substitutions taking place at the Ca and Ti sites. These sites can be nearly 80% occupied by other elements, whereas in the majority of cases all of the Zr site is filled by Zr alone. These relationships are shown graphically in figure 4.4, where the NIOCAN and Bond Zone zirconolites plot to the Zr-rich side of the theoretical composition. Figure 4.5 examines the compositional variation at the Ca-site of zirconolites. No correlation is evident in the NIOCAN and Bond Zone zirconolites at Oka, therefore no substitutions between Ca and REE^{3+} are present. With respect to the Ti-site of zirconolites, a strong negative correlation is found between Ti and (Ta+Nb) (figure 4.6). Therefore, of the extensive substitutions discussed by Gière *et al.* (1998) only those on the Ti-sites for zirconolites are present in NIOCAN and Bond Zone zirconolites.

NIOCAN and Bond Zone zirconolites are characterized by low LREE and ACT (figure 4.7, table 4.4). The ACT content for zirconolites from NIOCAN and Bond Zone are typically lower than average (7.9 % ThO_2, <2 % UO_2) compared to zirconolites from other carbonatite complexes. The REE^{3+} content of NIOCAN and Bond Zone zirconolites is average for carbonatite-hosted zirconolites. Figure 4.7 also shows the large range of (Nb+Ta) in the NIOCAN and Bond Zone zirconolites; these having the highest Nb_2O_5 content of any documented zirconolites from carbonatites.

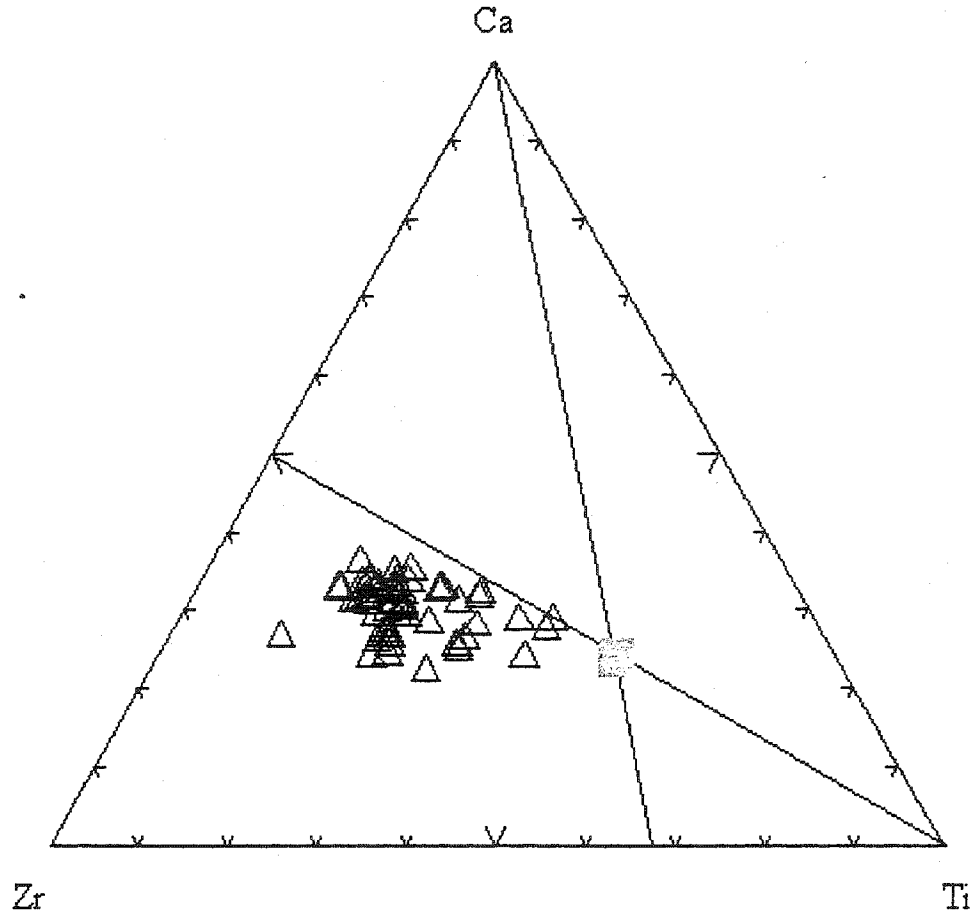

Figure 4.4. Ternary compositional diagram showing the compositional variation of zirconolite from the NIOCAN and Bond Zone, Oka (triangles) with respect to the major components Ca, Zr, and Ti (in atomic %). Orange square represents the theoretical composition of pure $CaZrTi_2O_7$.

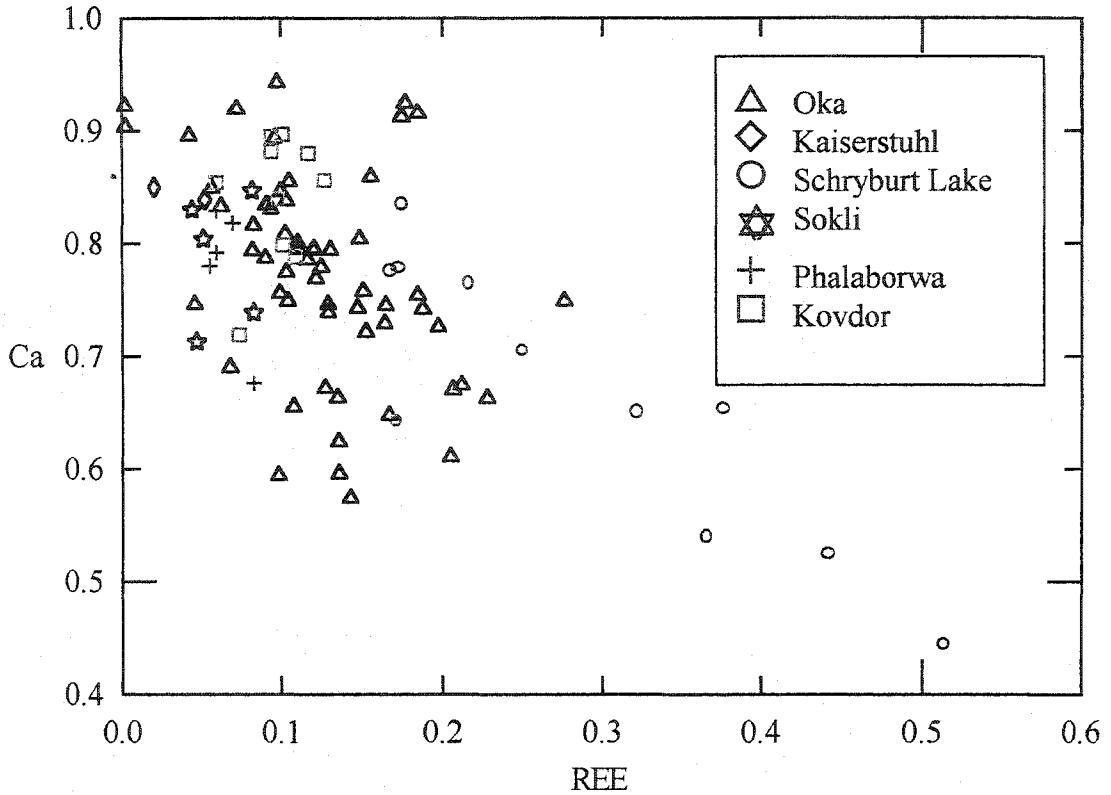

Figure 4.5. Ca (a.p.f.u.) vs. REE (a.p.f.u.) for zirconolite minerals.

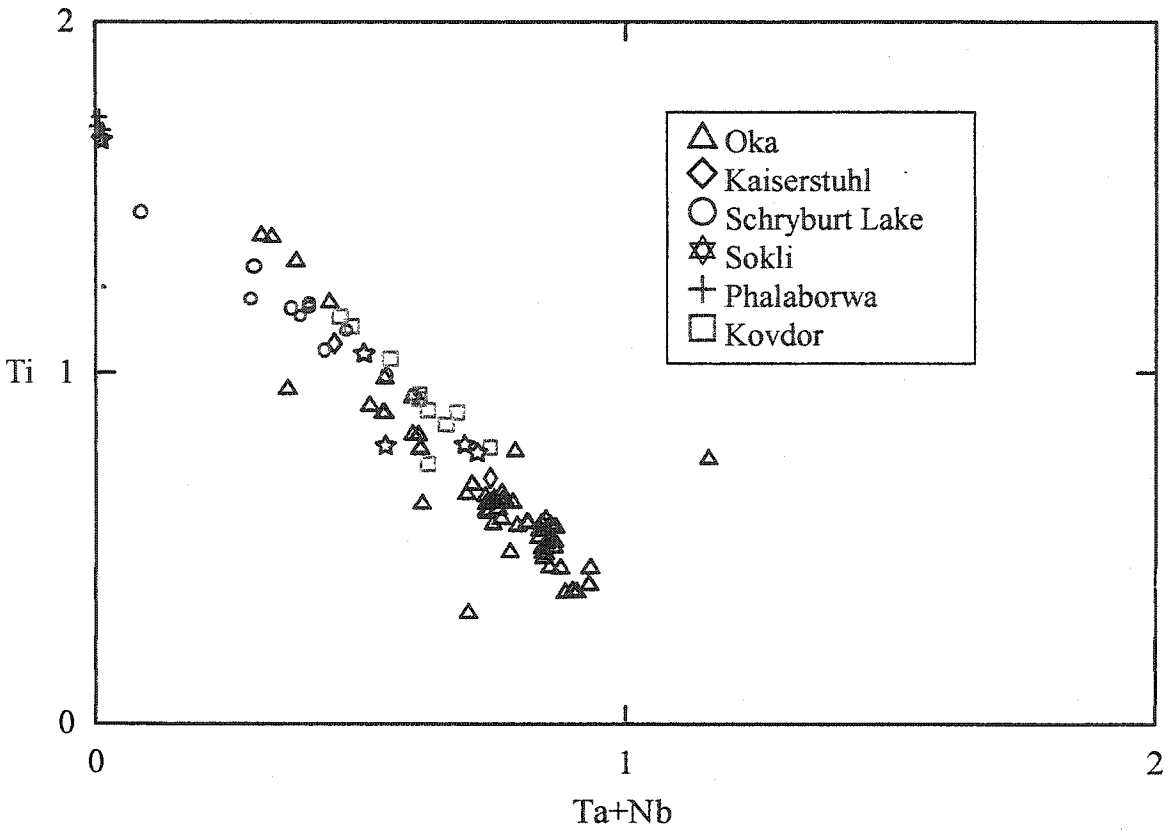

Figure 4.6. Ti (a.p.f.u.) vs. Ta+Nb (a.p.f.u.) for zirconolite minerals.

Table 4.5 Compositional variations of zirconolites from NIOCAN and Bond Zone deposits at Oka

	Compositional Range	Mean
CaO	8.20-14.32 wt. %	10.88 wt. %
TiO_2	6.20-29.36	13.35
FeO	4.48-13.17	6.58
MnO	0.00-4.02	2.68
ZrO_2	30.53-45.04	33.97
Nb_2O_5	11.52-31.10	23.73
Ce_2O_3	trace-6.03	3.01

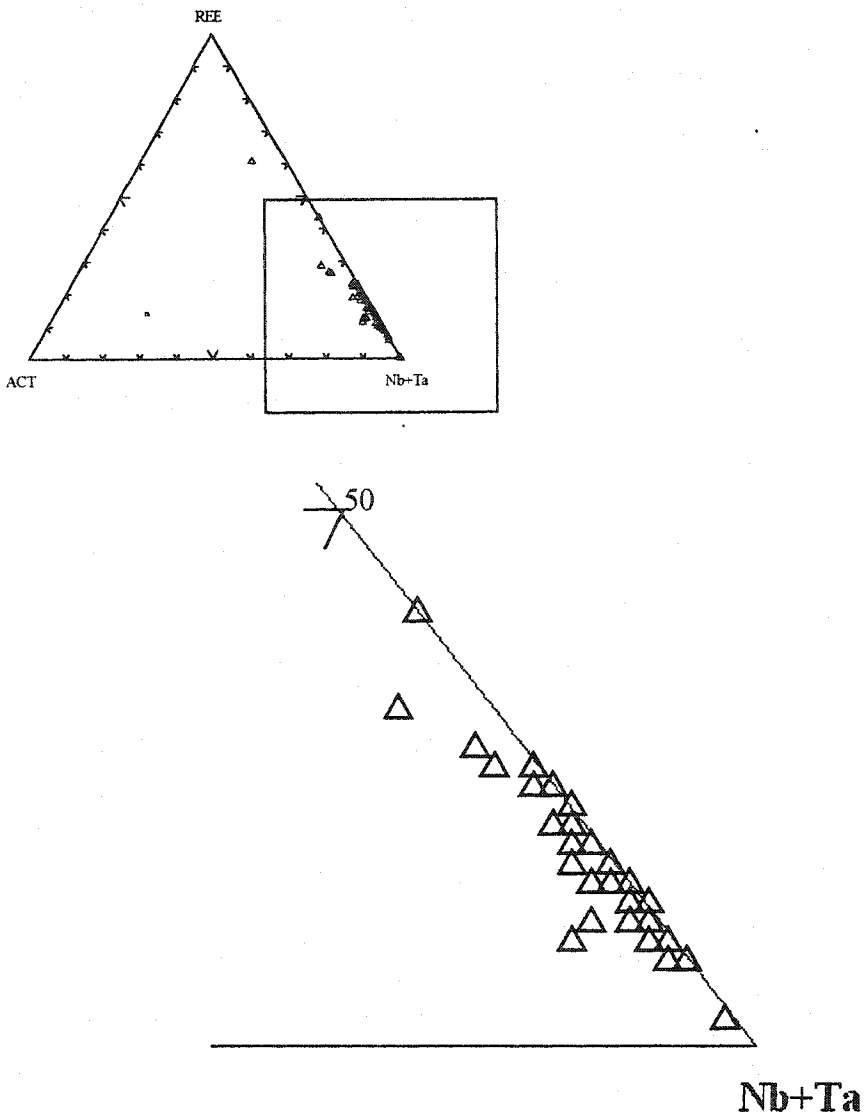

Figure 4.7. Ternary compositional diagram [(ACT)-(REE)-(Nb+Ta)] for NIOCAN and Bond Zone zirconolites.

4.3. Zirconolites from other carbonatite localities worldwide

Appendix VI lists EMPA data for zirconolites from 5 other carbonatite localities worldwide: Kovdor Carbonatite, Russia; Schryburt Lake carbonatite, Canada; Phalaborwa carbonatite, South Africa; Sokli carbonatite, Finland; Kaiserstuhl carbonatite, Germany. Each of the occurrences will be discussed below in order to compare and contrast with the zirconolite occurrence at Oka.

4.3.1. Kovdor carbonatite complex, Kola Peninsula, Russia

At the Kovdor carbonatite complex; zirconolite, pyrochlore and baddeleyite occur as accessory minerals, up to 150-200 μm in diameter, commonly intergrown with each other and usually associated with magnetite and apatite (Williams, 1996). Detailed fine-scale compositional zoning within the zirconolite, and textural relationships between zirconolite and other accessory minerals have been identified at Kovdor. Analysis of the zonation revealed primarily changes in the Nb/Ti ratio (Williams, 1996). Analysis of the REE's revealed little variation from grain-to-grain, or between zones of the grains.

In the Kovdor zirconolite, both Nb and Ta have significantly higher concentrations and are among the highest values reported for these elements thus far in the literature (figure 4.8). The mean for Nb_2O_5 of 18 analyses is 18.64 wt.% (range 13.97-21.21 wt. %). In contrast, the NIOCAN and Bond Zone zirconolites have higher concentrations, with a mean for Nb_2O_5 = 23.73 wt. % (range 11.52-31.10) (table 4.5).

No correlations are present in figure 4.5 and as a result, there is no Ca-site substitution present in the zirconolites from Kovdor. A strong negative correlation is shown in figure 4.6, as Nb+Ta are substitute for Ti in the Kovdor zirconolites.

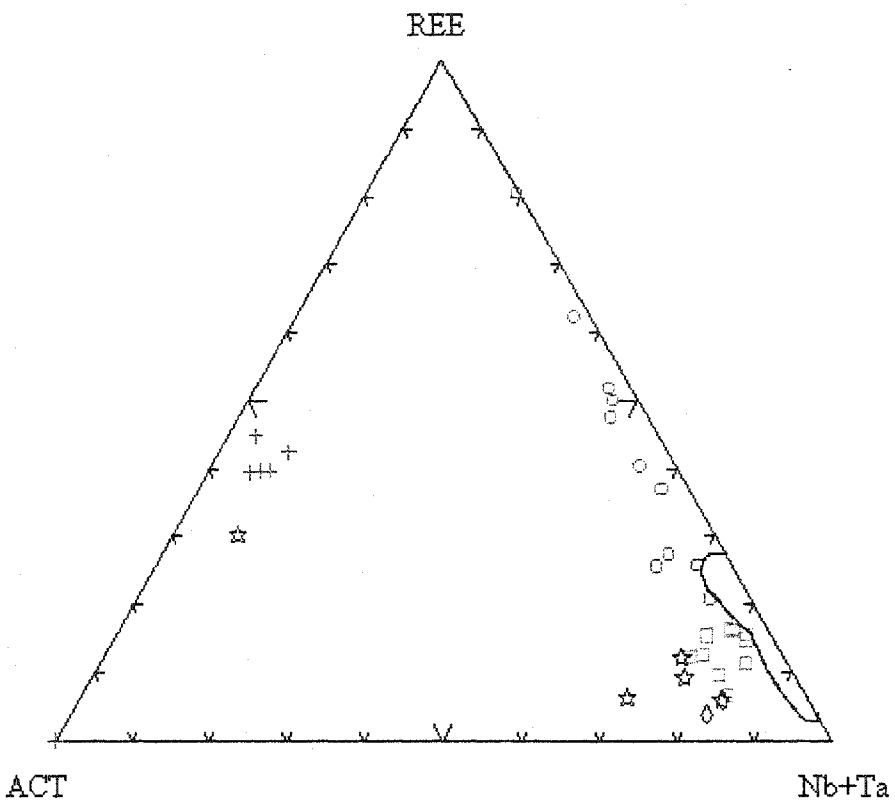

Figure 4.8. A ternary compositional diagram with apices (ACT)-(REE)-(Nb+Ta) for zirconolites from carbonatites worldwide.

+ : Phalaborwa, ○ : Schryburt Lake, □ : Kovdor, ◇ : Kaiserstuhl, ✡ : Sokli

Shaded field represents the NIOCAN and Bond Zone zirconolite compositional field.

Williams (1996) concludes that textural information indicates that zirconolite crystallizes later than, and in some cases replaces, pyrochlore and baddeleyite. In comparison with Oka zirconolites, both are found as accessory minerals, in association with pyrochlores and baddeleyite. The strong compositional zoning that is found in Kovdor zirconolites is not seen in NIOCAN and Bond Zone zirconolites. Zirconolites from both localities have high Nb, and display Ti-site substitutions. Neither zirconolites have Ca-site substitutions occurring. NIOCAN and Bond Zone zirconolites have enriched REE relative to Kovdor zirconolites.

4.3.2. Schyburt Lake, Ontario, Canada

A mineralogical and petrological study of the Schryburt Lake carbonatite, demonstrated the occurrence of baddeleyite, calzirtite, uranopyrochlore, and a complexly-zoned Nb-, Nd-rich zirconolite (Platt, pers. com. 2003). REE_2O_3 contents range from 5.5 to 21.6%, Nd being the most abundant REE (up to 7.56 % wt. % Nd_2O_3) (Platt, unpublished data). Figure 4.8 best displays the REE enrichment in the Schryburt Lake zirconolites, along with the large range of Nb+Ta.

A very strong negative correlation is found in figure 4.5, indicating the presence of a Ca-site substitution with REE. In some of the zirconolite grains analysed, the sum of (Y+REE) cations exceeds 50% of the Ca structural site, and on the basis of recommendations regarding rare earth mineral nomenclature, these grains have been regarded as a new mineral species, zirconolite-Nd (Platt, pers. com.). A negative correlation is evident in figure 4.6, indicating the presence of a Ti-site substitution with Ta+Nb.

Few similarities can be identified between the NIOCAN and Bond Zone zirconolites and the Schryburt Lake zirconolites: the latter have complex zonation and REE-enrichment, Ca is being replaced by REE, and Ti is being replaced with Ta+Nb.

4.3.3. Phalaborwa carbonatite complex, South Africa

Williams *et al.* (1996) describes zirconolite from Phalaborwa occurring with baddeleyite and zircon. The zirconolite is TiO_2-enriched, REE- and Nb_2O_5-poor. No correlation is found in figure 4.5, a bivariate diagram with Ca v.s. REE, indicating no substitution at the Ca-site is present. No correlation is found between Ti and Ta+Nb in figure 4.6, indicating no substitution at the Ti-site is present. Phalaborwa zirconolites do not show the same compositional characteristics as other zirconolites from carbonatites, and are not directly comparable to the NIOCAN and Bond Zone zirconolites from Oka.

4.3.4. Sokli carbonatite complex, Finland

The zirconolites from Sokli are found as discrete prisms in hydrothermal phoscorites. They are associated with pyrochlore, and are considered to have apparently formed at the expense of pyrochlore, or as inclusions in pyrochlore. They are generally REE-, ACT-poor and Nb-, Ti-rich with the exception of one REE-, ACT-enriched sample. They plot in the (Nb+Ta) corner of the ternary compositional diagram in figure 4.8, in common with zirconolites from Kovdor. Sokli zirconolites do not exhibit Ca-site substitutions (figure 4.5). In figure 4.6, a slight negative correlation is noted, indicating a substitution at the Ti-site with Nb. Compositional variations of the zirconolites from Oka and Sokli are similar, however, zirconolites from Solki are considered to be a product of hydrothermal nature. No characteristics of hydrothermal activity are seen at Oka and therefore cannot be regarded as a product of hydrothermal product.

4.3.5. Kaiserstuhl carbonatite complex, Germany

At Kaiserstuhl, zirconolite occurs with calzirtite, baddeleyite, Nb-perovskite and pyrochlore. In figure 4.8, the Kaiserstuhl zirconolites plot at the (Nb+Ta) corner, with very low

REE and ACT content. No correlation is evident in figure 4.5 due to insufficient data, and no conclusions can be drawn with respect to Ca-site substitution. Figure 4.6 shows a slight correlation between Ti and Ta+Nb, which could be confirmed by more analyses. Both the Oka and Kaiserstuhl carbonatites contain rare accessory minerals such as zirconolite, calzirtite, baddeleyite, Nb-perovskite and pyrochlore, and further comparisons on the composition and paragenesis of these minerals could be beneficial.

4.4. Discussion

Zirconolite has been recognized for the first time in the NIOCAN and Bond Zone deposit at Oka. This has the highest Nb content of all zirconolites from previously studied carbonatites. Slight compositional zoning is present, reflecting only slight changes in Nb and LREE content. The wide compositional ranges observed for several elements (e.g. Nb) in the NIOCAN and Bond Zone zirconolite reflects the ease with which its crystal structure can accommodate large differences in the size and charge of the cations, resulting in the large range in compositions present.

Textural relationships with apatite, magnetite, perovskite and pyrochlore imply that the Nb-rich zirconolites at NIOCAN and Bond Zone are the product of a late-stage formation. Baddeleyite and calzirtite are commonly found exhibiting the same textural relationships.

Gière *et al.* (1998) states that the overall composition of zirconolite reflects the general geochemical characteristics of the geological surroundings. NIOCAN and Bond Zone zirconolites are Nb-rich, as are the perovskite, pyrochlore and niocalite analyzed in this study. Preference of the LREE's over the HREE's is found throughout the pyrochlores, perovskites and zirconolites. Ce is the dominant LREE in each of these minerals, with La and Nd also present.

The textural relationships and the geochemical characteristics of zirconolite from the NIOCAN and Bond Zone deposit infer the mineral formed from a reaction phase, with one or both of the following zirconolite-forming reactions possible (from Gière *et al.*, 1998):

calzirtite + 8 perovskite + 5 CO_2 $\leftrightarrow$ 5 zirconolite + 5 calcite

baddeleyite + 2 perovskite + CO_2 $\leftrightarrow$ zirconolite + calcite

Chapter 5: Mineralogy and composition of Niocalite minerals

5.1. Niocalite

5.1.1. Introduction

The relatively rare Nb-silicate niocalite $(Ca,Nb)_4Si_2O_7(O,OH,F)_2$ was first described from the Oka carbonatite by Nickel (1956). Nickel *et al.* (1958) presented a complete chemical analysis of the new Nb-mineral. Niocalite was first described from Oka as occurring within a coarse, crystalline strontian calcite containing magnetite and apatite. Other Nb-bearing minerals, notably pyrochlore and niobian perovskite were found occurring in the area, however were characteristically absent in the niocalite-bearing rock itself (Nickel *et al.*, 1958). Nickel *et al.* (1958) reported that in some samples of calciocarbonatite, niocalite constituted about 10% of the total rock.

Niocalite belongs to a family of minerals which includes cuspidine, hiortdahlite, låvenite and wöherlite. Structural similarities between this family can only be resolved by detailed single crystal x-ray studies. The general formula for these minerals on the basis of 36 oxygens is $X_{16}(Si_2O_7)_4(O,OH,F)_8$, X corresponding to $(Na)^{+}(Ca,Mg,Mn,Fe)^{2+}(REE)^{3+}(Zr,Ti,Hf)^{4+}(Nb,Ta)^{5+}$. The distribution of cations only within this family can be generalized to:

cuspidine	$(Ca)_4(Ca)_8(Ca)_2(Ca)_2$
niocalite	$(Ca)_4(Ca)_8(Ca)_2(Nb)_2$
wöherlite	$(Na)_4(Ca)_8(Zr)_2(Nb)_2$
hiortdahlite	$(Na,Ca)_4(Ca)_8(Zr)_2(M)_2$
låvenite	$(Na)_4(Na,Ca)_8(Zr)_2(Zr,Ti)_2$

(*M* represents a mixing site, in hiortdahlite, with an average charge of three; Merlino and Perchiazzi, 1985). The minerals of this family are distinguished by variations in their Ca, Na, Nb (+Ta) and Zr+Ti(+Hf) contents.

There are only two reported occurrences of niocalite in the literature, Oka (described above), and in the silicate-carbonate rocks of the central calciocarbonatite intrusion in the Kaiserstuhl alkaline-carbonatite complex. REE-bearing niocalite has been provisionally identified as tiny inclusions in gregoryite phenocrysts from natrocarbonatite lava, at Oldoinyo Lengai (Church and Jones, 1995); compositional data were not presented for these inclusions.

5.2. NIOCAN and Bond Zone Niocalite minerals

Previous work on niocalite from the Bond Zone at Oka (Nickel *et al.*, 1958) reports euhedral, unzoned, discrete niocalite grains occurring in the calciocarbonatite. Although other Nb-bearing minerals (pyrochlore, Nb-rich perovskite) had been identified at the complex, no association had been identified between niocalite and the other Nb-minerals. The euhedral, discrete, niocalite grains (devoid of zoning) reported from earlier studies, have been identified in the NIOCAN and Bond Zone deposits. In addition, this study has revealed an association of niocalite with other Nb-bearing minerals. Niocalite has been found occurring in close contact to Ce-pyrochlore, Nb-rich zirconolite and Nb-rich perovskite (figure 5.1). It also occurs as overgrowths on subhedral, highly altered ceriopyrochlore grains (figure 5.1).

Appendix II.4 contains niocalite compositional data (EMPA) from the NIOCAN and Bond Zone deposits, Kaiserstuhl alkaline and carbonatite rocks (Keller and Williams, 1995), and previous data from the Bond Zone (Keller and Williams, 1995). Table 5.1 shows representative compositions of niocalite from the NIOCAN and Bond Zone deposit. The data compares well with those originally reported by Keller and Williams (1995) and Nickel (1958). Low amounts

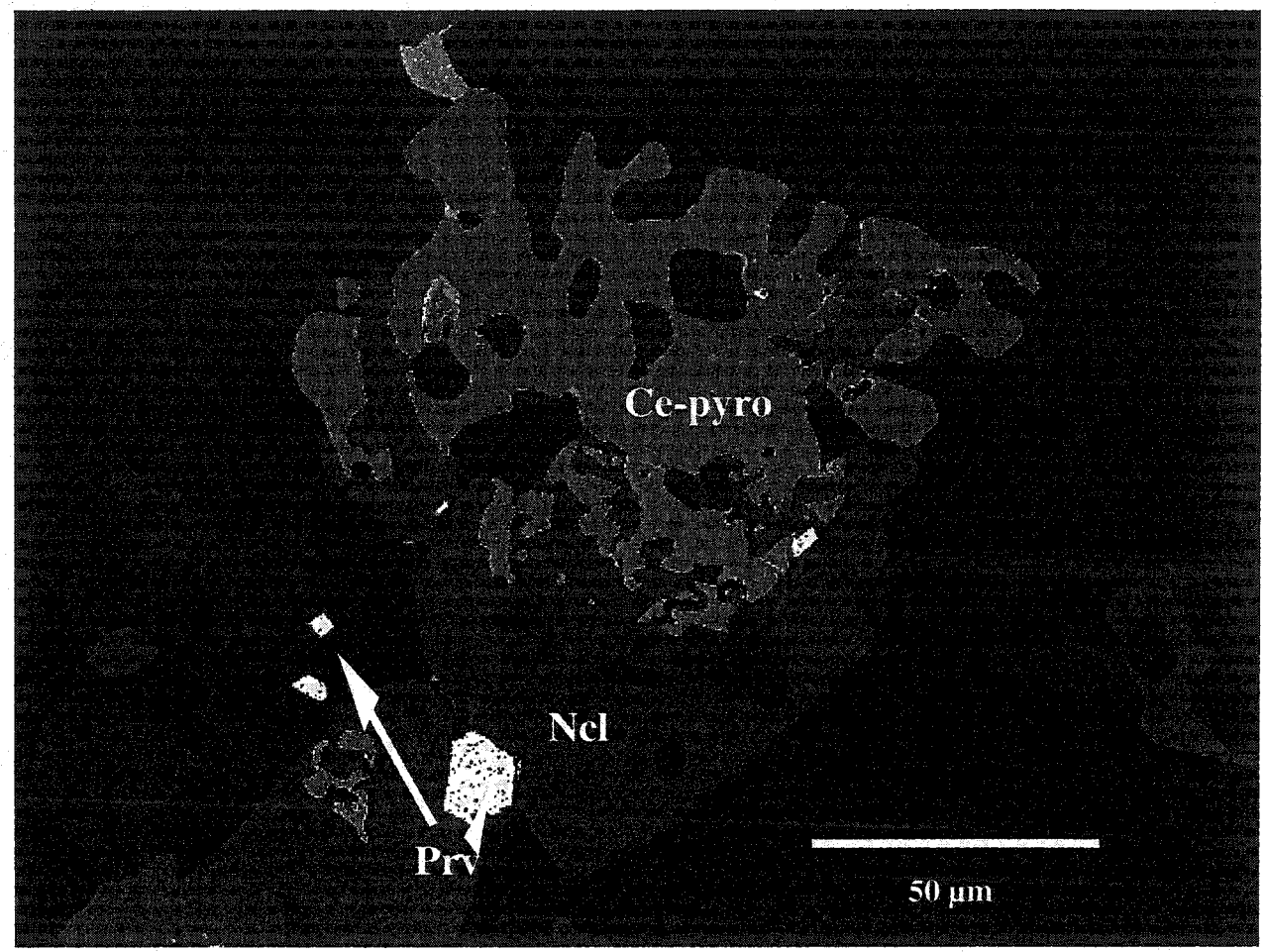

Figure 5.1. False-colour image of niocalite overgrowth on ceriopyrochlore, in coexistence with Nb-rich perovskite. Scale as shown.

Table 5.1. Representative compositions of niocalite from NIOCAN and Bond Zone

	N1	N3	N5	N11	N19
SiO_2	31.59	31.12	31.17	30.17	30.96
TiO_2	0.00	0.00	0.14	0.00	0.00
ZrO_2	0.00	0.00	1.21	1.05	0.00
Nb_2O_5	17.84	18.63	17.43	18.09	18.29
Al_2O_3	0.00	0.10	0.26	0.06	0.35
La_2O_3	0.00	0.00	0.00	0.00	0.18
Ce_2O_3	0.31	0.25	0.39	0.67	0.52
Nd_2O_3	0.33	0.23	0.07	0.48	0.56
FeO	0.00	0.46	0.25	0.00	0.11
MnO	0.72	0.07	0.97	0.89	0.96
MgO	0.00	0.00	0.00	0.00	0.40
CaO	46.71	47.89	47.23	43.99	45.46
SrO	0.14	0.80	1.42	0.92	0.00
Na_2O	0.86	0.47	0.38	1.26	1.27
Total	98.50	100.02	100.92	97.58	99.41

of LREE, mainly Ce are present in the Oka niocalite. Eby (1975) and Hornig (1988) also recognised the presence of LREE in niocalite from Oka. Niocalite analyses from NIOCAN and Bond Zone plot directly in the compositional field defined by Keller and Williams (1995), with moderate Nb+Ta and low Na (figure 5.2). Niocalite analyses in figure 5.3, all plot in the compositional field with the exception of one analyses enriched in Na, plotting towards the compositional field of wöhlerite, defined by Keller and Williams (1995). Wöhlerite has been found occurring in the Bond Zone at Oka (Nickel, 1958), however was not identified from NIOCAN and Bond Zone in this study. These new data compare reasonably well with those originally reported by Nickel *et al.* (1958) and Keller and Williams (1995).

5.3. Kaiserstuhl Niocalite minerals

Niocalite and wöherlite coexist together at the Kaiserstuhl alkaline-carbonatite complex. Niocalite is associated with, and, in some cases, intergrown with the Na, Ca, Zr silicate wöherlite (Keller and Williams, 1995). The minerals are found interstitial to major mineral phases of the rocks. Irregular zoning is noted in the Kaiserstuhl niocalite and wöherlite. Analysis reveals the zoning to correspond to intermediate compositions between niocalite and wöherlite (Keller and Williams, 1995).

Many similar Nb- and Zr-bearing minerals found occurring at both complexes. Kaiserstuhl is the host to Nb- and Zr-bearing minerals such as pyrochlore, Nb-rich perovskite, Nb-rich zirconolite and calzirtite. Kaiserstuhl niocalite plots in the compositional fields for niocalite in figures 5.2, 5.3 and 5.4, and is compositionally similar to the analyses of NIOCAN and Bond Zone niocalite.

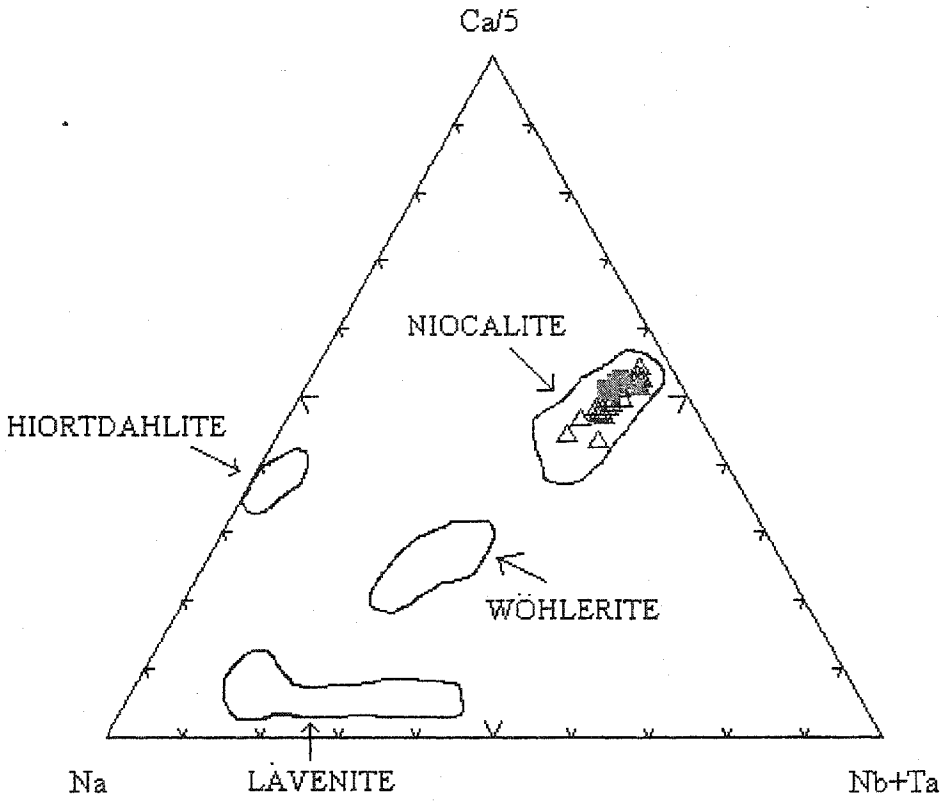

Figure 5.2. Ternary compositional diagram [Na-(Ca/5)-(Nb+Ta)] for the NIOCAN and Bond Zone niocalite minerals (△). Compositional fields for the other members of the niocalite family are shown (yellow). Niocalite analyses from Kaiserstuhl ■ (Keller and Williams, 1995), and previous niocalite analyses from Bond Zone at Oka ▲ (Nickel *et al.*, 1958) are also shown.

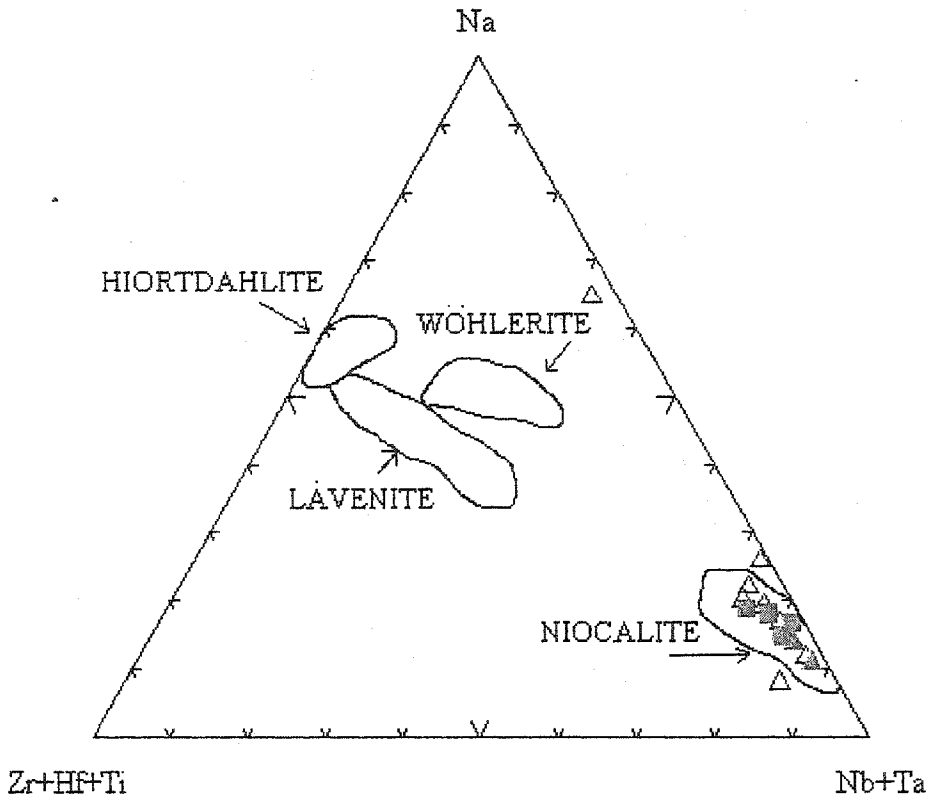

Figure 5.3. Ternary compositional diagram [(Zr+Hf+Ti)-(Na)-(Nb+Ta)] for the NIOCAN and Bond Zone niocalite minerals △ . Compositional fields for the other members of the niocalite family are shown (yellow). Niocalite analyses from Kaiserstuhl ■ (Keller and Williams, 1995), and previous niocalite analyses from Bond Zone at Oka ▲ (Nickel *et al.*, 1958) are also shown.

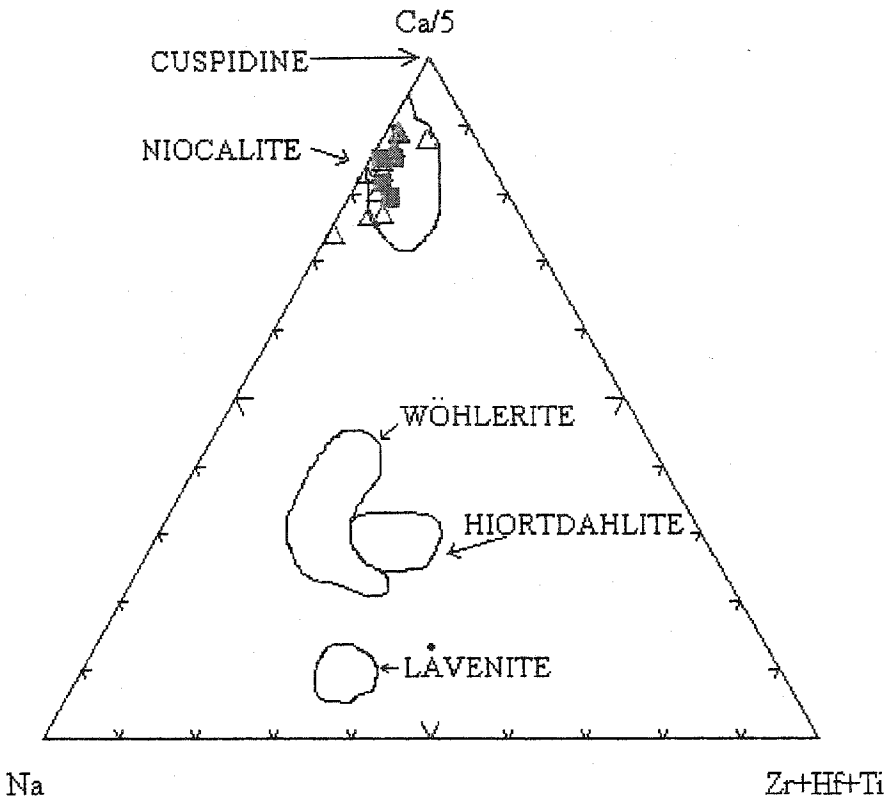

Figure 5.4. Ternary compositional diagram [Na-(Ca/5)-(Zr+Hf+Ti)] for the NIOCAN and Bond Zone niocalite minerals △. Compositional fields for the other members of the niocalite family are shown (yellow). Niocalite analyses from Kaiserstuhl ■ (Keller and Williams, 1995), and previous niocalite analyses from Bond Zone at Oka ▲(Nickel *et al.*, 1958) are also shown.

5.4. Discussion

Niocalite has been analysed from the NIOCAN and Bond Zone deposit at Oka, and analyses compare well with previous work on the Bond Zone niocalite. Previous studies report niocalite occurring as discrete, euhedral grains devoid of zoning (Nickel *et al.*, 1958), however, niocalite from the Bond Zone is found occurring as anhedral overgrowths on cerium pyrochlore and ceriopyrochlore grains, in textural association with Nb-rich perovskite. Although wöherlite has been identified as occurring in the Bond Zone and St. Lawrence Columbian deposits at Oka (Nickel *et al.*, 1958), it was not identified in this study, indicating a possible absence of wöherlite in the NIOCAN deposit. There are only two occurrences of niocalite; Oka and Kaiserstuhl, and analyses from both compare reasonably well with one another.

Chapter 6: Conclusion

Data presented in chapters 1-5 permit the following generalizations regarding the compositional variation and paragenesis of Nb-bearing minerals in the Oka carbonatite complex:

Pyrochlore

NIOCAN and Bond Zone pyrochlore-group minerals exhibit extremely wide compositional variations. The majority of these are cerium pyrochlores with thorium and uranium varieties also being present. Pyrochlores can be zonation-free or show discontinuous and/or patchy zonation. Two or more compositional and/or textural varieties occur in close proximity to each other. This observation implies that such pyrochlores cannot have crystallized together in their current host rock. Many pyrochlores exhibit *A*-site deficiency, resulting from leaching of *A*-site cations caused by diverse alteration processes during and after crystallization.

Perovskite

NIOCAN and Bond Zone perovskites occur as euhedral- to -subhedral crystals which exhibit patchy and slight compositional zonation. They are commonly fractured and contain inclusions of calcite and magnetite. The significant characteristic of the perovskite-group minerals at the NIOCAN and Bond Zone deposits is their extreme enrichment in Nb, coupled with low REE contents. Latrappite and Nb-rich perovskite have been identified as occurring at Oka. Their compositions do not reflect solid solutions toward loparite, and can be expressed in the quaternary system perovskite-Ca_2FeNbO_6-$Ca_2Nb_2O_7$-lueshite.

Zirconolite

Zirconolite has been recognized for the first time in the NIOCAN and Bond Zone carbonatites at Oka. Zirconolite is most commonly found located in the fractures and cavities of calcite and apatite, and occasionally found rimming pyrochlore and biotite grains. Rarely, the

zirconolite exhibits zoning, which reflects slight variations in Nb and $LREE^{3+}$ content. The zirconolites are Nb-rich, and have the highest Nb content of all zirconolites from previously studied carbonatites.

Niocalite

The euhedral, discrete, niocalite grains reported from earlier studies have been identified from the NIOCAN and Bond Zone carbonatites at Oka. In addition, this study has revealed an association of niocalite with other Nb-bearing minerals. Niocalite has been found occurring in close contact to Ce-pyrochlore, Nb-rich zirconolite and Nb-rich perovskite. It also occurs rarely as overgrowths on subhedral, highly-altered ceriopyrochlore grains.

The textures and compositions of the Nb-minerals occurring at Oka suggest that they did not crystallize in equilibrium in their current host rock. Crystallization of these minerals could not have been contemporaneous, as they could not have been liquidus phases at the same time. It is probable that the minerals were derived from other regions within the complex, possibly other magma chambers. These being disturbed and their contents mixed with other batches of magma. Transportation of this mixed assemblage produced their current host rock.

Until recently, little was known about the factors that determine whether pyrochlore or perovskite crystallizes from carbonatite magmas. Jago and Gittens (1993) undertook experiments to determine the solubility of Nb, and pyrochlore in carbonate liquids that approximate in composition to carbonatite magmas. Using the system $CaCO_3$-Na_2CO_3-pyrochlore, Jago and Gittens (1993) found the solubility of Nb_2O_5 in water-bearing calcitic liquids is at least 5 wt. %, rising as high as 7.5 wt. %, but diminishing to less than 0.75 wt. % in liquids that more closely resemble carbonatite magmas. Results indicate that in fluorine-free liquids, Nb forms lueshite or other perovskite-group minerals. Furthermore, pyrochlore

crystallizes only from liquids containing at least 1 wt. % F. Jago and Gittens (1993) conclude that most carbonatite magmas contain at least small amounts of fluorine, this being concentrated during magmatic crystallization, and reaching the 1 wt. % level at an early stage of carbonatite evolution, and therefore crystallizing pyrochlore at this early stage.

Further work on the solubility of Nb in the ternary system $CaCO_3$-$Ca(OH)_2$-$NaNbO_3$ (calcite-portlandite-lueshite) at 0.1 GPa was undertaken by Mitchell and Kjarsgaard (2002). Results indicate that Nb is extremely soluble in water-bearing melts in this system. The maximum solubility of Nb_2O_5 in this system is estimated to be 48 wt. % (650 ° at 0.1 GPa) (Mitchell and Kjarsgaard, 2002). The experiments show that perovskite-structured compounds rather than pyrochlore crystallize from these fluorine-free, water-rich melts. Mitchell and Kjarsgaard (2002) conclude that the H_2O/F ratio of the melt and not the presence of alkalies alone determines whether or not perovskite- or pyrochlore- structured minerals are precipitated from carbonatite magmas, in agreement with the observations of Jago and Gittens (1993).

These data suggest that pyrochlore is probably an early liquidus phase in F-bearing magmas and perovskite probably forms later on in the evolution of the carbonatite. These observations imply pyrochlore- and perovskite-group minerals which coexist in a section must represent the results of magma mixing. Perovskite, after crystallizing in one batch of magma could be transported and/or mixed with different pyrochlores and/or perovskites in other batches of magma. Therefore, the final assemblage of Nb-minerals that is observed is the result of magma mixing. The textural and compositional variations that are observed in the Nb-minerals of the Oka carbonatite complex record the effects of complex interactions and/or variations in bulk composition of these magmatic episodes. Some minerals exhibit primary growth features,

i.e.- continuous compositional zoning, while others reflect the instability in their host magma, i.e.- overgrowth, *A*-site vacancy development, patchy replacement textures.

The crystallization history of the Oka carbonatite magma cannot be deduced from the observed mineral assemblage. The calciocarbonatite does not represent a liquid composition, it has a bulk composition which is determined by mixing material derived from several batches of magma. The magmas which gave rise to NIOCAN and Bond Zone seem more evolved than those forming the pyrochlore-group minerals in the St. Lawrence Columbium deposits, as the pyrochlores from St. Lawrence Columbian are "less-evolved" relative to NIOCAN and Bond Zone pyrochlores.

The major conclusion of this work is that the calciocarbonatites at NIOCAN and Bond Zone are hybrid rocks. No simple hypothesis can be devised to explain the significant concentrations of pyrochlores in particular sections of host rock. Enrichment of specific zones is probably dependent upon rheological factors rather than compositional controls.

References

Bayliss, P., Mazzi, F., Munno, R., and T.J. White. 1989. Mineral nomenclature: zirconolite. Mineralogical Magazine, **53**:565-569.

Bellatreccia, F., Ventura, G.D., Caprilli, E., Williams, C.T., and G.C. Parodi. 1999. Crystal-chemistry of zirconolite and calzirtite from Jacupiranga, Sao Paulo (Brazil). Mineralogical Magazine, **63**: 649-660.

Chakhmouradian, A.R., and R.H. Mitchell. 1997. Compositional variation of perovskite-group minerals from the carbonatite complexes of the Kola Alkaline Province, Russia. The Canadian Mineralogist, **35**:1293-310.

Chakhmouradian, A. R. and R. H. Mitchell. 1998a. Lueshite, pyrochlore and monazite-(Ce) from apatite-dolomite carbonatite, Lesnaya Varaka complex, Kola Peninsula, Russia. Mineralogical Magazine, **62**:769-782.

Chakhmouradian, A. R. and R. H. Mitchell. 1998b. Compositional variation of perovskite-group minerals from the Khibina Complex, Kola Peninsula, Russia. The Canadian Mineralogist, **36**:953-970.

Church, G.A. and A.P. Jones. 1995. Silicate-carbonate immiscibility at Oldoinyo, Lengai. Journal of Petrology, **36**:869-889.

de Hoog, J.C.M., and M.J. van Bergen. 2000. Volatile-induced transport of HFSE, REE, Th, and U in arc magmas: evidence from zirconolite-bearing vesicles in potassic lavas of Lewotolo volcano (Indonesia). Contributions to Mineralogy and Petrology, **139**:485-502.

Eby, G.N. 1975. Abundance and distribution of the rare-earth elements and yttrium in the rocks and minerals of the Oka carbonatite complex, Quebec. **39**:597-620.

Gière, R., and C.T. Wiiliams. 1992. REE-bearing minerals in a Ti-rich vein from the Adamello contact aureole (Italy). Contributions to Mineralogy and Petrology, **112**: 3-100.

Gière, R., Williams, C.T., and G.R. Lumpkin. 1998. Chemical characteristics of natural zirconolite. Schweiz. Mineral. Petrogr. Mitt. **78**:433-459.

Gold. D.P. 1963. The relationship between the limestones and the alkaline igneous rocks of Oka and St. Hilaire, Quebec. Unpub. Ph.D. Thesis, McGill University., Montreal.

Gold, D.P. 1967. Alkaline ultrabasic rocks in the Montreal area, Quebec. *In*, P.J. Wylie, Ed., *Ultramafic and Related Rocks*. John Wiley and Sons, Inc., New York, pp. 288-302.

Gold, D.P. 1969. The Oka Carbonatite and alkaline complex, 43-63, in Guidebook for the Geology of Monteregian Hills. G. Pouliot. Edit. Min. Assoc. Canada, June 1969.

Gold, D.P. 1972. The Monteregian Hills: Ultra-alkaline rocks and the Oka carbonatite complex. *In:* The 24th International Geological Congress, Excursion Guide, 1-47.

Haggerty, S.E., and A.N. Mariano. 1983. Strontian-loparite and strontio-chevkinite: two new minerals in rheomorphic fenites from the Parana Basin Carbonatites, South America. Contributions to Mineralogy and Petrology., **84**:365-381.

Hammond, A. 1999. Pyrochlore from the Prairie Lake Carbonatite Complex. Lakehead University, *unpublished.*

Hogarth, D.D. 1989. Pyrochlore, apatite and amphibole: distinctive minerals in carbonatite. In: Carbonatites: Genesis and Evolution (Edited by Bell,K.) pp 105-148. Chapman and Hall, London.

Hogarth, D.D. and J.E.T. Horne. 1989. Non-metamict uranoan pyrochlore and uranpyrochlore from tuff near Ndale, Fort Portal area, Uganda. Mineralogical Magazine, **53**:257-262.

Hogarth, D.D., Williams, C.T., and P. Jones. 2000. Primary zoning in pyrochlore group minerals from carbonatites. Mineralogical Magazine, **64**:683-697.

Hornig, I. 1988. Spurenelementuntersuchungen an Karbonatiten mit Hilfe der ICP-Atomemissionsspektroskopie. PhD. Thesis, Univ. Freiburg, 237 pp.

Jago, B.C., and J. Gittins. 1993. Pyrochlore crystallization in carbonatites: the role of fluorine. South African Journal of Geology, **96**:149-159.

Kalogeropoulos, S.I. 1977. Geochemistry and mineralogy of the St. Lawrence Pyrochlore Deposit, Oka, P.Q. unpub. M.Sc. Thesis, Queen's University, Kingston, ON.

Kapustin, Yu. L. 1980. Mineralogy of Carbonatites. Amerind Pub.Co. Pvt. Ltd. New Delhi.

Keller, J., and C.T. Williams. 1995. Niocalite and wöhlerite from the alkaline and carbonatite rocks at Kaiserstuhl, Germany. Mineralogical Magazine, **59**:561-566.

Keller, J. 1984. Der jungtertiare Valkanismus Südwestdeutschlands: Exkursionen in Kaiserstuhl und Hegau. Fortschritte der Mineralogie, **62**: 2-35.

Knudsen, C. 1989. Pyrochlore-group minerals from the Qaqarssuk carbonatite complex. *In: Lanthanides, tantalum & niobium.* Eds. P. Möller, P. Černý & F. Saupé. Springer Verlag, Berlin, pg 80-99.

Lindqvist, K., and Pentti Rehtijärvi. 1979. Pyrochlore from the Sokli carbonatite complex, Northern Finland. Bulletin of the Geological Society of Finland, **51**:81-93.

Lottermoser, B.G. and B.M. England. 1988. Compositional variation in pyrochlores from the Mt. Weld Carbonatite Laterite, Western Australia. Mineralogy and Petrology, **38**:37-51.

Lumpkin, G. R. and R.C. Ewing. 1995. Geochemical alteration of pyrochlore group minerals: Pyrochlore subgroup. American Mineralogist, **80**:732-743.

Lumpkin, G.R. and A.N. Mariano. 1996. Natural occurrence and stability of pyrochlore in carbonatites, related hydrothermal systems, and weathering enviroments. Mat. Res. Soc. Symp. Proc. Vol. 412, 831-836.

McCallum, M.E. 1989. Oxide minerals in the Chicken Park kimberlite, northern Colorado. *In:* Kimberlites and related rocks (ed. J. Ross). Geol. Soc. Austr. Spec. Publ., **14**:241-263.

Merlino, S. and N. Perchiazzi. 1985. The crystal structure of hiortdahlite I. Tschermaks. Mineral. Petrogr. Mitt. **34**:297-310.

Mitchell, R. 1986. Kimberlites: Mineralogy, Geochemistry and Petrology, Plenum Press, New York.

Mitchell, R., and Bergman, S.C. 1991. Petrology of Lamproites, New York.

Mitchell, R. and Kjarsgaard, B.A. 2002. Solubility of niobium in the system $CaCO_3$-$Ca(OH)_2$-$NaNbO_3$ at 0.1 GPa pressure. Contributions to Mineralogy and Petrology, **144**:93-97.

Mitchell, R.H., and Vladykin, N.V. 1993. Rare earth-bearing tausonite and potassium barium titanates from the Little Murun potassic alkaline complex, Yakutia, Russia. Mineralogical Magazine., **57**:651-654.

Mitchell, R.H., Choi, J.B., Hawthorne, F.C., McCammon, C.A., and Burns, P.C. 1998. Latrappite: a re-investigation. The Canadian Mineralogist, **36**:107-116.

Mitchell, R.H. 1996. Perovskites: a revisted classification scheme for an important rare earth element host in alkaline rocks. *In*: Rare Earth Minerals: Chemistry, origin and ore deposits. *Edited by*: Adrian P. Jones, Frances Wall, C. Terry Williams. Chapman & Hall, London.

Mitchell, R.H. 2002. Perovskites: Modern and Ancient. Almaz Press, Thunder Bay, Ontario, Canada.

Nasraoui, M. and Bilal, E. 2000. Pyrochlores from the Lueshe carbonatite complex (Democratic Republic of Congo): a geochemical record of different alteration stages. Journal of Asian Earth Sciences, **18**:237-251.

Nickel, E.H. 1964. Latrappite- a proposed new name for the perovskite-type calcium niobate mineral from the Oka area of Quebec. Canadian Mineralogist, **8**:121-122.

Nickel, E.H. 1956. Niocalite: a new calcium-niobium silicate mineral. American Mineralogist. **41**:785-786.

Nickel, E.H., Rowland, J.F., and Maxwell, J.A. 1958. The composition and crystallography of niocalite. Canadian Mineralogist, **6**:264-72.

Nickel, E.H., and R.C. McAdam. 1963. Niobian perovskite from Oka, Quebec; A new classification for minerals of the perovskite group. Canadian Mineralogist, **7**:683-697.

Petruk, W. and De'Alton, Owens. 1975. Electron microprobe analyses for pyrochlores from Oka, Quebec. Canadian Mineralogist, **13**:282-285.

Platt, R.G. 1994. Perovskite, loparite and Ba-Fe hollandite from the Schryburt Lake carbonatite complex, northwestern Ontario, Canada. Mineralogical Magazine, **58**:49-57.

Shafiqullah, M., Tupper, W.M., and Cole, J.S.S. 1970. K-Ar age of the carbonatite complex, Oka, Quebec. Canadian Mineralogist, **10**:541-552.

Simandl, G.J., Jones, P.C. and M. Rotella. 2001. Blue River Carbonatites, British Columbia-Primary exploration targets for tantalum. Exploration and Mining in British Columbia, Minerals and Mines Branch Publication.

Ulrych, J., Piveč, E., Povondra, P., and J. Rutsek. 1988. Perovskite from melitite rocks. Osečná complex, northern Bohemia, Czechoslovakia. N.Jb. Mineral. Monatsh., 81-95.

Vlasov, K.A. 1966. Geochemistry and Mineralogy of Rare Elements and Genetic Types of Their Deposits II. Mineralogy of Rare Elements. Israel Program for Scientific Translations. Jerusalem.

Viladkar, S.G., and I. Ghose. 2002. U-rich pyrochlore in carbonatite of Newania, Rajasthan. N.Jb. Miner. Mh, **3**:97-106.

Vorobyev, E. I., Konyev, K.A., and Y.V. Malyshok. 1984. Tausonit, geologicheskiye usloviya obrazovaniya I mineralnii paragenezisi. (Tausonite, geological conditions of formation and mineral paragenesis.) Nauka Press, Novosibirsk (*in Russian*).

Williams, C.T. 1996. The occurrence of niobium zirconolite, pyrochlore and baddeleyite in the Kovdor carbonatite complex, Kola Pennisula, Russia. Mineralogical Magazine, **60**:639-646.

Williams, C.T., and R. Gière. 1996. Zirconolite: a review of localities worldwide, and a compilation of its chemical compositions. Bull. Nat. Hist. Mus. Lond. **52**:1-24.

Williams, C.T., Wall, F., Woolley, A.R., and S. Phillipo. 1997. Compositional variation in pyrochlore from the Bingo carbonatite, Zaïre. Journal of African Earth Sciences, **3**:137-145.

APPENDIX I

Drill Locations from the Oka carbonatite complex

The Oka Carbonatite Complex, Drill Locations

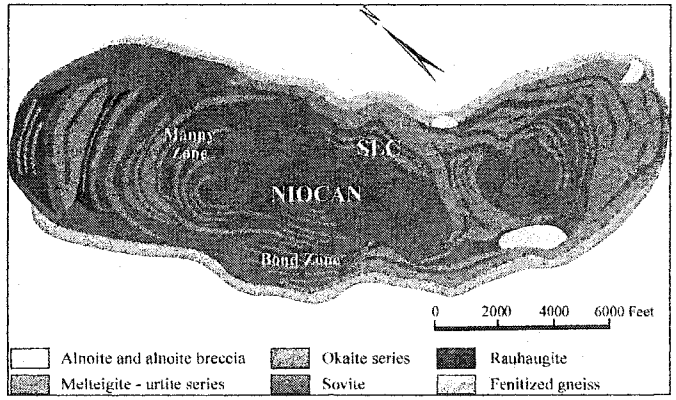

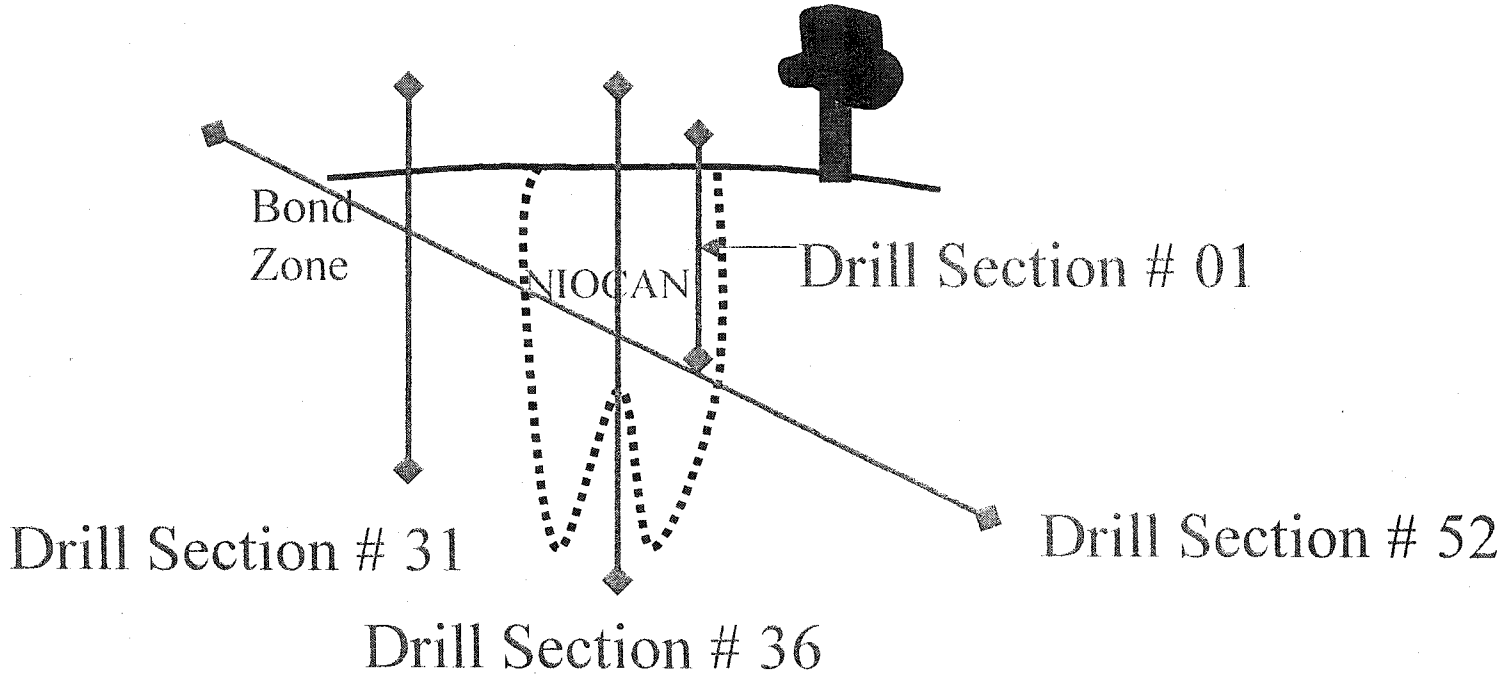

APPENDIX II
SEM-EDS analyses of NIOCAN and Bond Zone minerals

II.1 Pyrochlore

Drill Core # 52

	14.4b-a	14.4b-b	14.4b-c	14.4b-d	14.4b-e	14.4b-f	14.4b-g	14.4b-h	14.4b-I	14.4b-j	14.4b-k	14.4b-l
Oxides												
Na_2O	3.47	3.47	3.23	3.2	3.11	3.36	3.4	1.75	1.75	1.79	3.22	4.06
Al_2O_3	0.14	0.06	0.21	0.18	0.08	0.44	0.49	0.45	0.44	0.37	0.23	0.32
SiO_2	0.17	0.16	0.35	0.33	0.1	0.3	0.2	0.31	0.34	0.35	0.31	0.09
K_2O	0	0	0	0	0	0	0	0	0	0	0	0
CaO	13.6	13.66	13.94	13.86	12.78	13.9	13.66	10.15	10.16	10.17	14.34	15.09
TiO_2	3.23	3.3	5.09	5.09	3.53	3.72	3.37	2.31	2.26	2.15	4.77	3.09
MnO	0.48	0.52	0.46	0.61	0.67	0.51	0.56	0.76	0.87	0.85	0.7	0.21
Fe_2O_3	2.54	2.54	2.33	2.36	2.85	2.5	2.47	1.86	1.98	1.91	1.94	1.85
SrO	0.45	0.44	0.34	0.39	0.49	0.76	0.6	0.12	0.14	0.18	0.32	0.7
Y_2O_3	0	0	0	0	0	0	0	0	0	0	0	0
ZrO_2	5.35	5.27	4.52	4.57	7.22	5.32	5.29	16.18	16.24	16.27	4.91	3.32
Nb_2O_5	51.16	51.28	48.78	48.95	46.5	50.52	51.3	34.47	34.6	34.41	48.65	58.11
BaO	0.27	0.31	0.11	0.06	0.37	0.09	0.2	0.05	0.05	0.07	0.13	0.14
La_2O_3	1.09	1.17	1.18	1.06	1.2	1	0.82	1.45	1.36	1.25	1	0.86
Ce_2O_3	5.53	5.37	6.34	6.16	4.99	5.9	5.43	6.4	6.26	6.2	6.36	6.44
Pr_2O_3	0	0	0	0	0	0	0	0	0	0	0	0
Nd_2O_3	1.5	1.43	1.85	1.96	1.61	1.1	1.35	2.39	2.34	2.27	1.51	1.2
PbO	0	0	0	0	0	0	0	0	0	0	0	0
Ta_2O_5	0.42	0.36	0.23	0.33	0.42	0.11	0.1	0.3	0.08	0.04	0.73	0.05
ThO_2	10.96	11.01	9.94	9.86	14.39	10.53	10.67	20.52	20.84	21.05	10.9	2.03
UO_2	0.27	0.09	0.01	0.07	0.2	0.55	0.26	0.27	0.61	0.51	0.01	0.24
F	0	0	0	0	0	0	0	0	0	0	0	0
Sum	100.63	100.44	98.91	99.04	100.51	100.61	100.17	99.74	100.32	99.84	100.03	97.8
Sum *A*	1.8077	1.812	1.804	1.793	1.813	1.793	1.769	1.704	1.71	1.731	1.864	1.764
A-def	0.193	0.188	0.196	0.207	0.187	0.207	0.231	0.296	0.29	0.269	0.136	0.236
Sum *B*	2	2	2	2	2	2	2	2	2	2	2	2
O	6.69	6.703	6.637	6.617	6.734	6.601	6.554	6.718	6.732	6.786	6.811	6.423

Drill Core # 52

	14.4b-m	14.4b-n	14.4b-o	14.4b-p	14.4b-q	48.25a-a	48.25a-b	48.25a-c	48.25a-e	48.25a-f	504.9-a	204.35-a
Oxides												
Na_2O	2.79	3.4	2.66	2.75	2.85	2.09	3.85	3.52	2.19	2.19	4.5	3.75
Al_2O_3	0.35	0.43	0.51	0.49	0.5	0.34	0.14	0	0	0	0	0
SiO_2	0.21	0.23	0.65	0.78	0.95	1.62	1.65	3.09	1.21	1.14	0	1.5
K_2O	0	0	0	0	0	0	0	0	0	0	0	0
CaO	13.8	14.67	14.08	13.52	13.55	17.94	14.75	14.9	15.89	15.9	10.74	13.77
TiO_2	4.51	3.24	3.98	2.61	2.54	10.27	6.49	6.72	9.71	9.73	5.1	5.78
MnO	0.74	0.57	0.73	0.61	0.67	0	0	0	0	0	1.08	0.16
Fe_2O_3	2.58	2.42	2.83	1.99	2.23	2.47	3.55	3.49	2.58	2.58	2.38	1.97
SrO	0.35	0.58	0.28	0.53	0.38	0	0	0	0	0	0	0.26
Y_2O_3	0	0	0	0	0	0	0	0	0	0	0	0
ZrO_2	5.45	4.72	6.48	9.22	9.27	0	0	0	4.31	4.18	7.06	2.47
Nb_2O_5	47.19	52.27	46.4	46.25	45.83	40.22	39.61	38.74	35.91	36.27	49.25	44.23
BaO	0.18	0.31	0.06	0.3	0.36	0	0	0	0	0	0	0
La_2O_3	1.08	0.88	0.93	0.75	0.82	0	0	0	0	0	2.31	0
Ce_2O_3	5.97	4.89	7.66	5.94	5.74	8.77	4.62	4.43	5.87	5.93	13.76	6.71
Pr_2O_3	0	0	0	0	0	0	0	0	0	0	0	0
Nd_2O_3	1.73	1.11	1.95	1.56	1.29	0	0	0	0.81	0.95	3.07	0
PbO	0	0	0	0	0	0	0	0	0	0	0	0
Ta_2O_5	0	0	0	0	0	2.67	9.52	8.3	3.35	3.29	0	5.02
ThO_2	12.73	11.63	8.31	10.21	10.31	0	0	0	0	0	0	0.61
UO_2	0.42	0.08	0.41	2.05	2.32	13.1	15.38	17.4	17.43	18.31	0	12.05
F	0	0	0	0	0	0	0	0	0	0	0	0
Sum	100.08	101.43	97.92	99.56	99.61	99.49	99.56	100.59	99.26	100.47	99.25	98.28
Sum *A*	1.822	1.838	1.762	1.757	1.758	1.927	1.901	1.852	1.858	1.875	1.796	1.846
A-def	0.178	0.162	0.238	0.243	0.242	0.073	0.099	0.148	0.142	0.125	0.204	0.154
Sum *B*	2	2	2	2	2	2	2	2	2	2	2	2
O	6.764	6.735	6.498	6.574	6.534	6.873	6.656	6.593	6.74	6.814	6.387	6.676

Drill Core #52

	48.25b-1	48.25b-2	48.25b-3	109.5-a	109.5-b	109.5-c	109.5-d	109.5-e	109.5-f	109.5-g	109.5-h	109.5i
Oxides												
Na_2O	0	2.75	2.67	2.02	2.17	1.99	2.43	1.89	1.84	2.21	2.5	1.98
Al_2O_3	0	0	0	0.83	0.17	0.21	0.13	0.04	0.28	0	0	0
SiO_2	1.99	1.88	2.42	1.22	1.55	2.19	2.18	0.88	1.05	1.5	0.77	1.4
K_2O	0	0	0	0	0	0	0	0	0	0	0	0
CaO	18.34	19.56	19.19	17.72	18.02	17.48	17.63	17.97	17.7	16.66	16.89	16.92
TiO_2	8.36	8.82	8.89	9.52	9.49	9.87	9.69	9.64	9.35	9.11	9.53	8.8
MnO	0	0	0	0.66	0.58	0.56	0.63	0.39	0.38	0.79	0.53	0.35
Fe_2O_3	1.66	1.49	1.32	2.76	2.08	1.85	1.89	1.98	1.89	1.93	2.88	1.97
SrO	0	0	0	1.9	0	0	0	0	0	0	0	0
Y_2O_3	0	0	0	0	0	0	0	0	0	0	0	0
ZrO_2	1.75	1.08	1.4	0	0	0	0	0	0	0	0	0
Nb_2O_5	49.73	50.15	48.44	48.15	47.97	46.45	46.93	49.36	48.76	45.43	44.97	47.01
BaO	0	0	0	0	0	0	0	0	0	0	0	0
La_2O_3	0	0	0	0	0	0	0	0	0	1.49	0.19	1.46
Ce_2O_3	10.83	10.6	10	11.38	11.5	10.46	11.08	10.55	11.03	10.45	9.48	11.07
Pr_2O_3	0	0	0	0	0	0	0	0	0	0	0	0
Nd_2O_3	1.28	0	0	1.42	2.25	2.03	2.11	2.16	1.57	2.15	1.86	1.68
PbO	0	0	0	0	0	0	0	0	0	0	0	0
Ta_2O_5	0	0	0	0	0	0	0	0	0	1.96	0.79	1.21
ThO_2	0	0	0	0.93	2.43	4.39	2.54	1.94	3.16	1.29	2.69	1.82
UO_2	1.02	1.02	1.91	2.17	1.59	0.6	1.74	2.6	2.25	4.13	5.25	3.82
F	0	0	0	0	0	0	0	0	0	0	0	0
Sum	94.96	97.35	96.24	100.68	99.8	98.09	98.98	99.4	99.26	99.1	98.34	99.49
Sum *A*	1.479	1.852	1.825	1.803	1.862	1.783	1.854	1.807	1.799	1.889	1.918	1.848
A-def	0.521	0.148	0.175	0.197	0.138	0.217	0.146	0.193	0.201	0.111	0.082	0.152
Sum *B*	2	2	2	2	2	2	2	2	2	2	2	2
O	6.147	6.555	6.489	6.462	6.727	6.55	6.652	6.702	6.689	6.861	6.825	6.839

	Drill Core #52		Pyrochlores									
	109.5-j	109.5-k	109.5-l	109.5-m	109.5-1	109.5-2	109.5-3	109.5-4	109.5-5	119a-1	119a-2	155.5-a
Oxides												
Na_2O	2.1	2.95	1.95	2.19	1.91	2.49	2.37	1.67	2.02	0.79	1.1	3.5
Al_2O_3	0	0	0	0	0	0	0	0	0	0	0.7	0
SiO_2	1.41	1.01	0.95	1.21	0.59	1.08	1.06	1.46	1.57	2.34	2.34	1.06
K_2O	0	0	0	0	0	0	0	0	0	0	0	0
CaO	16.98	17.25	17.41	17.11	16.82	16.81	16.87	16.07	16.91	15.74	33.24	16.7
TiO_2	8.79	9.45	9.31	9.07	8.83	9.29	9.16	9.26	8.9	11.84	47.26	7.79
MnO	0.35	0.43	0.09	0.5	0.45	0.39	0.37	0.39	0.51	0	0	0
Fe_2O_3	1.97	1.69	1.94	0.6	1.88	1.71	1.74	1.85	2.09	2.23	3.74	0.64
SrO	0	0	0	0	0	0	0	0	0	0	0	0
Y_2O_3	0	0	0	0	0	0	0	0	0	0	0	0
ZrO_2	0	0	0	0	0	0.96	1.32	0.65	1.43	7.63	0	2.82
Nb_2O_5	46.47	48.02	47.76	47.6	46.75	46.52	46.59	47.71	48.01	29.09	3	53.51
BaO	0	0	0	0	0	0	0	0	0	0	0	0
La_2O_3	1.31	1.39	1.22	1.36	1.26	0.62	0.89	2.36	1.31	0	1.85	0
Ce_2O_3	11.15	12.53	11.59	12.04	11.49	11.31	11.19	11.14	11.1	2.08	5.99	9.25
Pr_2O_3	0	0	0	0	0	0	0	0	0	0	0	0
Nd_2O_3	1.45	3.02	1.04	1.79	1.4	2.13	1.91	3.46	2.09	0	2.32	0
PbO	0	0	0	0	0	0	0	0	0	0	0	0
Ta_2O_5	1.07	1.32	0.74	0.09	0	0	0	0	0	0	0	0
ThO_2	1.89	0.62	2.37	3.39	1.49	1.57	1.76	0.66	2.06	0	0	0
UO_2	3.85	0.7	1.72	1.67	3.09	2.41	2.54	3.11	3.07	27.98	0	0
F	0	0	0	0	0	0	0	0	0	0	0	0
Sum	98.79	100.38	98.09	98.62	96.96	97.29	97.77	99.79	101.07	99.72	101.54	95.27
Sum *A*	1.878	1.974	1.826	1.978	1.839	1.892	1.877	1.755	1.794	1.704	1.934	1.703
A-def	0.122	0.026	0.174	0.022	0.161	0.108	0.123	0.245	0.206	0.296	0.066	0.297
Sum *B*	2	2	2	2	2	2	2	2	2	2	2	2
O	6.877	6.936	6.757	7.2	6.788	6.8	6.787	6.674	6.665	6.562	5.434	6.238

Drill Core #52

	155.5-b	155.5-c	155.5-d	155.5-e	155.5-f	155.5-g	155.5-p3-1	155.5-p4-a	155.5-p4-b	155.5-5a	155.5-5b
Oxides											
Na_2O	3.72	4.34	3.62	2.96	5.5	3.94	0	3.45	3.32	2.38	3.09
Al_2O_3	0	0	0	0	0	0	0	0	0	0	0
SiO_2	0.95	0.89	0.64	0.4	0.32	0.49	0.45	0.6	0.5	3.97	4.32
K_2O	0	0	0	0	0	0	0.01	0	0	0	0
CaO	15.81	18.26	16.96	16.87	16.6	16.43	16.3	16.11	15.51	15.63	14.98
TiO_2	7.68	6.61	6.85	8.5	7.13	6.75	7.07	6.56	6.83	10.88	11.25
MnO	0	0	0	0	0	0	0.22	0	0	0.42	0.4
Fe_2O_3	0.53	1.5	1.24	1.03	2.54	1.22	1.02	0.95	1.37	2.28	2.53
SrO	0	0	0	0	0	0	0	0	0	0	0
Y_2O_3	0	0	0	0	0	0	0	0	0	0	0
ZrO_2	2.04	0.46	2.27	1.93	2.8	2.63	0.85	0.93	1.46	3.59	2.38
Nb_2O_5	56.43	55.7	55.17	53.27	54.96	55.38	56.4	55.03	54.81	35.42	35.37
BaO	0	0	0	0	0	0	0	0	0	0	0
La_2O_3	0	0	0	0	0	0	0	0	0	0	0
Ce_2O_3	11.36	8.4	8.4	10.16	6.87	8.58	9.8	9.76	7.77	3.14	2.26
Pr_2O_3	0	0	0	0	0	0	0	0	0	0	0
Nd_2O_3	0	0	0	0	0	0	0	0	0	0	0
PbO	0	0	0	0	0	0	0	0	0	0	0
Ta_2O_5	0	0	0	0	0	0	0	0	0	0	0
ThO_2	0	0	0	0	0	0	0	1.25	3.17	0	0
UO_2	0	0	0	0	0	0	1.77	0	0	23.24	24.15
F	0	0	0	0	0	0	0	0	0	0	0
Sum	98.52	96.16	95.15	95.12	96.72	95.42	93.89	94.64	94.74	100.95	100.73
Sum *A*	1.684	1.917	1.725	1.69	1.832	1.731	1.334	1.761	1.656	1.773	1.796
A-def	0.316	0.083	0.275	0.31	0.168	0.269	0.666	0.239	0.344	0.227	0.204
Sum *B*	2	2	2	2	2	2	2	2	2	2	2
O	6.279	6.59	6.274	6.286	6.139	6.257	6.062	6.491	6.254	6.484	6.427

Drill Core # 52	
	204.35-b
Oxides	
Na_2O	3.57
Al_2O_3	0.1
SiO_2	1.84
K_2O	0
CaO	13.85
TiO_2	6.92
MnO	0.12
Fe_2O_3	1.87
SrO	0.25
Y_2O_3	0
ZrO_2	2.19
Nb_2O_5	40.99
BaO	0
La_2O_3	0
Ce_2O_3	6.52
Pr_2O_3	0
Nd_2O_3	0
PbO	0
Ta_2O_5	6.09
ThO_2	0.95
UO_2	13.67
F	0
Sum	98.93
Sum *A*	1.854
A-def	0.146
Sum *B*	2
O	6.693

	Drill Core #52											
	155.5-7d	155.5-7e	478-p4-1	478-p4-2	478-p4-3	478-p4-4	478-p6-1	478-p6-2	478-p6-3	478-p8-1	478-p8-2	204.35-b
Oxides												
Na_2O	0	0	5.69	6.53	6.59	6.34	6.2	6.34	5.5	6.17	5.22	3.57
Al_2O_3	0	0	0	0	0	0	0	0	0	0	0	0.1
SiO_2	0	0	0	0	0	0	0	0	0	0	0	1.84
K_2O	0	0	0	0	0	0	0	0	0	0	0	0
CaO	7.22	16.17	11.42	12.35	12.02	11.91	9.8	11.29	11.17	10.95	9.99	13.85
TiO_2	11.44	5.95	7.17	4.61	5.16	5.45	5.48	5.08	5.95	5.47	6.36	6.92
MnO	0.36	0.5	0.78	0.38	0.65	0.56	0	0	0	0	0	0.12
Fe_2O_3	2	1.13	0.41	0.38	0.82	0.42	1.4	1.01	1.53	0.94	1.56	1.87
SrO	2.25	1.36	0	0	0	0	0	0	0	0.7	0.7	0.25
Y_2O_3	0	0	0	0	0	0	0	0	0	0	0	0
ZrO_2	5.41	2.74	0	0	0	0	4.22	3.47	3.26	2.61	4.04	2.19
Nb_2O_5	34.6	61.64	54.79	60.64	58.39	58.96	55.79	57.65	53.18	56.67	49.92	40.99
BaO	0	0	0.32	0	0	0	0	0	0	0	0	0
La_2O_3	0	0	2.23	0.93	0.62	1.72	2.11	1.11	1.44	0	0	0
Ce_2O_3	2.91	8.79	8.16	5.06	5.96	6.55	12.13	10.31	8.47	9.87	9.46	6.52
Pr_2O_3	0	0	0	0	0	0	0	0	0	0	0	0
Nd_2O_3	0	0	1.88	0.41	1.06	1.07	1.59	0.93	1.16	0.88	1.78	0
PbO	0	0	0	0	0	0	0	0	0	0	0	0
Ta_2O_5	6.37	0.85	0	0	0	0	0	0	0	2.44	1.88	6.09
ThO_2	0	0	5.04	4.04	3.98	4.07	0	0	5.32	6.03	6.54	0.95
UO_2	24.46	1.08	1.08	0	0	0	0	0	0	0	0	13.67
F	0	0	0	0	0	0	0	0	0	0	0	0
Sum	97.02	100.21	98.97	95.33	95.25	97.05	98.72	97.19	96.98	102.73	97.45	98.93
Sum *A*	1.053	1.266	1.964	1.891	1.936	1.923	1.744	1.788	1.784	1.816	1.73	1.854
A-def	0.947	0.734	0.036	0.109	0.064	0.077	0.256	0.212	0.216	0.184	0.27	0.146
Sum *B*	2	2	2	2	2	2	2	2	2	2	2	2
O	5.553	5.912	6.886	6.58	6.611	6.689	6.194	6.26	6.365	6.485	6.276	6.693

Drill Core #52

	155.5-5c	155.5-5d	155.5-t1	155.5-t2	155.5-t3	155.5-6a	155.5-6b	155.5-6c	155.5-6d	155.5-7a	155.5-7b	155.5-7c
Oxides												
Na_2O	4.21	3.19	1.13	3.61	3.13	0	0	0	0	0	0	0
Al_2O_3	0	0	0	0	0	0	0	0	0	0	0	0
SiO_2	0	0	1.97	1.92	2.4	0	0	0	0	0	0	0
K_2O	0	0	0	0	0	0	0	0	0	0	0	0
CaO	17.04	17.61	12.69	13.43	14.62	17.89	18.47	13.66	15.67	5.19	7.66	4.09
TiO_2	7.26	7.42	9.42	8.79	9.96	9.41	9.55	9.31	9.41	12.27	11.58	14.07
MnO	0.95	1.28	0	0	0	0.62	0.14	0.37	0.45	0.5	0	0
Fe_2O_3	0.95	1.28	1.61	1.2	1.52	0.7	0.94	3.02	1.73	1.41	1.11	1.61
SrO	0	0	0	0	0	0	0.57	0.66	0.68	2.68	1.41	2.84
Y_2O_3	0	0	0	0	0	0	0	0	0	0	0	0
ZrO_2	1.12	1.38	3.4	1.68	2.47	1.98	1.13	5.83	5.36	5.84	4.98	5.48
Nb_2O_5	57.39	56.98	42.75	44.58	41.47	53.23	52.63	38.78	38.61	35.5	37.5	34.9
BaO	0	0	0	0	0	0	0	0	0	0	0	0
La_2O_3	0	0	0	0	0	0	0	0	0	0	0	0
Ce_2O_3	9.62	10.15	4.13	5.93	3.43	9.14	10.33	3.3	3.35	5.02	3.09	5.71
Pr_2O_3	0	0	0	0	0	0	0	0	0	0	0	0
Nd_2O_3	0	0	0	0	0	0	0	0	0	0	0	0
PbO	0	0	0	0	0	0	0	0	0	0	0	0
Ta_2O_5	0	0	1.15	2.67	2.93	0.99	1.25	4.6	4.92	6.04	6.97	7.41
ThO_2	0	0	0	0	0	0	0	0	0	0	0	0
UO_2	0.53	0	18.63	13.59	18.66	0.94	0.1	22.24	19.71	25.2	24.89	24.08
F	0	0	0	0	0	0	0	0	0	0	0	0
Sum	99.07	99.29	96.88	97.4	100.59	94.9	95.11	101.77	99.89	99.65	99.19	100.19
Sum *A*	1.89	1.811	1.359	1.708	1.708	1.413	1.476	1.391	1.556	0.972	1.018	0.836
A-def	0.11	0.189	0.641	0.292	0.292	0.587	0.524	0.609	0.444	1.028	0.982	1.164
Sum *B*	2	2	2	2	2	2	2	2	2	2	2	2
O	6.654	6.575	5.968	6.377	6.393	6.102	6.226	6.169	6.558	5.47	5.598	5.093

	Drill Core #36											
	270.85-e	332.5-a	332.5-b	332.5-c	332.5-d	332.5-e	503.4-a	503.4-b	503.4-c	147.35-a	147.35-b	147.35-c
Oxides												
Na_2O	2.97	3.47	3.64	3.57	1.8	0	3.86	4.55	3.68	2.96	3.15	3.13
Al_2O_3	0.07	0	0	0	0	0	0	0.21	0.54	0.11	0.03	0.22
SiO_2	0.47	0.35	0.24	0.3	2.26	2.15	0	0.74	0	0.81	0.18	0.62
K_2O	0	0	0	0	0	0	0	0	0	0	0	0
CaO	12.71	17.7	17.6	17.53	16.09	13.23	17.42	16.92	16.48	13.23	13.14	13.16
TiO_2	3.72	3.05	3.28	3.14	12.19	12.42	5.14	1.84	4.87	3.13	3.02	3.09
MnO	0.87	0.37	0.43	0.47	0	0	0	0	0	0.42	0.76	0.77
Fe_2O_3	2.98	2.63	2.53	2.47	2.01	1.16	1.64	2.76	1.73	2.41	2.36	2.34
SrO	0	0	0	0	0	0	0	0	0	0	0	0
Y_2O_3	0	0	0	0	0	0	0	0	0	0	0	0
ZrO_2	7.35	0	0	0	6.42	6.08	0	0.41	1.55	3.48	3.27	3.21
Nb_2O_5	44.23	59.94	60.66	60.6	30.87	29.36	60.02	62.11	54.39	52.89	53.44	53.33
BaO	0	0	0	0	0	0	0	0	0	0	0	0
La_2O_3	1.46	1.28	1.57	1.46	0	0	1.33	0.62	0.92	2.48	2.15	2.19
Ce_2O_3	8.97	9.78	10.16	10	2.35	2.36	8.01	6	7.78	11.73	11.79	11.9
Pr_2O_3	0	0	0	0	0	0	0	0	0	0.35	1.3	1.29
Nd_2O_3	2.46	1.03	0.86	0.73	0	0	0.83	0.34	0.69	2.23	2.85	2.75
PbO	0	0	0	0	0	0	0.13	0.52	0.45	0	0	0
Ta_2O_5	0.16	0	0	0	0	0	0	0	1.82	0	0	0
ThO_2	8.86	0	0	0	0	0	0	0.45	0	1.41	1.38	1.54
UO_2	0.01	0	0	0	29.03	28.64	0.35	1.29	1.77	0	0	0
F	0	0	0	0	0	0	0	0	0	0	0	0
Sum	97.29	99.6	100.97	100.27	102.02	95.4	98.73	98.81	96.67	97.64	98.82	99.54
Sum *A*	1.837	1.918	1.928	1.915	1.868	1.497	1.86	1.834	1.828	1.74	1.849	1.814
A-def	0.163	0.082	0.072	0.085	0.132	0.503	0.14	0.166	0.172	0.26	0.151	0.186
Sum *B*	2	2	2	2	2	2	2	2	2	2	2	2
O	6.69	6.875	6.897	6.876	6.851	6.413	6.703	6.503	6.544	6.578	6.861	6.751

Drill Core # 36

	132.3-p2-4	358.3-p3-1	358.3-p3-2	358.3-p3-3	358.3-p3-4	358.3-p3-5	358.3-p4-1	358.3-p4-4	270.85-a	270.85-b	270.85-c	270.85-d
Oxides												
Na_2O	2.75	2.78	2.96	2.88	3.58	2.71	2.97	2.76	3.53	3.75	3.07	2.97
Al_2O_3	0	0.4	0.15	0.38	0.07	0.11	0.2	0.13	0.07	0.05	0.09	0.09
SiO_2	0	1.75	2.15	2.84	2.63	1.74	1.86	2.06	0.34	0.48	0.23	0.66
K_2O	0	0	0	0	0	0	0	0	0	0	0	0
CaO	10.94	15.67	15.11	14.89	16.88	17.01	16.45	14.88	11.46	11.03	13.18	12.94
TiO_2	4.17	7.56	8.06	7.69	4.82	6.61	5.42	7.27	4.21	4.54	3.67	3.69
MnO	0	0.24	0.24	0.13	0.11	0.12	0	0	0.99	1.02	0.68	0.65
Fe_2O_3	2.95	2.13	1.97	1.91	1.33	1.62	1.51	7.27	2.7	2.52	2.77	2.77
SrO	0	0	0	0	0	0	0	0	0	0	0	0
Y_2O_3	0	0	0	0	0	0	0	0	0	0	0	0
ZrO_2	4.85	0	0	0	0	0	0	0	6.25	6.07	6.06	5.89
Nb_2O_5	45.47	43.28	41.88	41.43	52.88	50.74	47.42	41.45	43.81	43.78	44.78	44.02
BaO	0	0	0	0	0	0	0	0	0.21	0.09	0.1	0.23
La_2O_3	0.58	0	0	0	0	0	0	0	1.24	1.56	1.1	0.91
Ce_2O_3	6.62	6.74	5.72	6.3	9.26	10.34	9.36	8.14	7.23	8.17	6.32	6.64
Pr_2O_3	0	0	0	0	0	0	0	0	0	0	0	0
Nd_2O_3	0.44	0.83	0.52	1.15	1.32	2.04	1.17	1.13	2	2.09	1.59	1.71
PbO	0	0	0	0	0	0	0	0	0	0	0	0
Ta_2O_5	0	0	3.25	2.36	3.85	3.91	4.52	3.13	0.38	0.06	0.69	0.02
ThO_2	18.17	4.32	0	0	0	0	0	0	12.42	10.96	11.4	10.67
UO_2	0	12.48	15.65	16.26	0.4	0.49	0.6	8.75	0.28	0.07	0.51	0.8
F	0	0	0	0	0	0	0	0	0	0	0	0
Sum	96.94	98.18	97.66	98.22	97.13	97.44	91.48	96.97	96.81	96.23	96.42	94.38
Sum *A*	1.696	1.988	1.879	1.873	1.8	1.759	1.826	1.626	1.872	1.874	1.868	1.848
A-def	0.304	0.012	0.121	0.127	0.2	0.241	0.174	0.374	0.128	0.126	0.132	0.152
Sum *B*	2	2	2	2	2	2	2	2	2	2	2	2
O	6.695	7.117	6.818	6.809	6.5	6.499	6.562	5.824	6.782	6.739	6.806	6.743

	Drill Core # 36											
	27.2-1	27.2-2	27.2-3	27.2-p3	57.8-1	57.8-2	132.3-1	132.3-2	132.3-4	132.3-p2-1	132.3-p2-2	132.3-p2-3
Oxides												
Na_2O	4.41	4.6	4.46	4.47	4.64	3.51	3.82	3.85	3.73	3.72	2.9	4.54
Al_2O_3	0	0	0	0	0	0	0.55	0.18	0	0	0	0
SiO_2	0	0	0	0	0.31	0.19	0	0	0.84	0.64	0.27	0.74
K_2O	0	0	0	0	0	0	0	0	0	0	0	0
CaO	10.77	11.36	11.3	10.7	11.2	11.61	13.13	10.94	12.93	11.86	11.33	13.57
TiO_2	5.98	3.74	3.82	3.82	5.3	3.02	3.81	5.29	4.15	4.23	3.89	4.25
MnO	0	0	0	0	0	0	0.8	2.17	0	0	0	0
Fe_2O_3	2.53	2.05	2.01	2.07	1.26	2.76	1.83	2.17	1.83	2.39	3.41	1.54
SrO	0	0	0	0	0	0	0	0	0	0	0	0
Y_2O_3	0	0	0	0	0	0	0	0	0	0	0	0
ZrO_2	4.75	5.73	5.63	5.78	2.61	4.71	3.43	4.4	4.62	4.66	5.84	1.56
Nb_2O_5	48.48	51.07	50	50.39	54.06	54.18	53.35	51.92	52.43	51.63	44.05	56.2
BaO	0	0	0	0	0	0	0	0	0	0	0	0
La_2O_3	1.42	2.26	1.85	1.95	0	0	1.6	1.53	1.62	0.56	0.96	0.35
Ce_2O_3	9.17	9.59	9.71	9.16	14.06	15.75	11.84	10.53	10.98	9.93	6.21	8.23
Pr_2O_3	0	0	0	0	0	0	0	0	0	0	0	0
Nd_2O_3	2.11	1.34	1.48	2.27	0	0	2.8	2.22	1.5	2.34	1.34	1.84
PbO	0	0	0	0	0	0	0	0	0	0	0	0
Ta_2O_5	0	0	0	0	0	0	1.42	0	0	0	0	0
ThO_2	8.76	8.31	8.06	7.43	0	0	1.41	4.32	3.66	4.32	18.55	3.67
UO_2	0	0	0	0	0	0	0	0	0	0	0	0
F	0	0	0	0	0	0	0	0	0	0	0	0
Sum	98.38	100.05	98.32	98.04	93.44	95.73	99.79	99.52	98.29	96.28	98.75	96.49
Sum *A*	1.744	1.839	1.84	1.779	1.689	1.597	1.828	1.731	1.73	1.638	1.759	1.79
A-def	0.256	0.161	0.16	0.221	0.311	0.403	0.172	0.269	0.27	0.362	0.241	0.21
Sum *B*	2	2	2	2	2	2	2	2	2	2	2	2
O	6.4	6.682	6.684	6.544	6.247	6.158	6.649	6.42	6.461	6.219	6.75	6.518

Drill Core #31

	101-1	101-b	101-c	101-d	162.9	162.9-a	162.9-b	155.15-a	155.15-b	155.15-c	155.15-d	155.15-e
Oxides												
Na_2O	5.58	5.33	4.79	5.48	3.17	0.29	0.42	3.66	2.64	3.75	3.36	3.19
Al_2O_3	0.03	0.04	0.2	0.28	0	0.08	0.36	0	0	0	0	0
SiO_2	0.24	0.27	0.09	0.5	0.89	11.68	9.64	1.52	3.72	1.39	4.49	1.71
K_2O	0.06	0.03	0.03	0	0	0	0	0	0	0	0	0
CaO	16.4	15.31	14.9	16.21	15.4	6.19	6.1	12.74	13.45	14.31	13.25	13.34
TiO_2	4.62	6.94	8.57	5.53	7.95	8.05	7.9	11.06	10.48	8.99	9.84	12.33
MnO	0	0	0	0	0.52	0.39	0.55	0.47	0.66	0.42	0.42	0
Fe_2O_3	0.1	0.1	0.26	0.31	1.39	1.97	1.65	0.71	1.73	1.48	1.03	0.46
SrO	0.78	0.9	0.77	0.82	0	3.41	3.48	0	0	0	0	0
Y_2O_3	0	0	0	0	0	0	0	0	0	0	0	0
ZrO_2	2.42	1.05	1.82	2.14	4.21	5.72	6.46	2.87	4.14	3.26	3.78	2.42
Nb_2O_5	62.47	59.65	56.72	62.64	47.14	36.84	37.99	42.89	35.62	44.79	38.22	43.13
BaO	0.17	0.17	0.26	0.15	0	0	0	0	0	0	0	0
La_2O_3	0.02	0.54	0.66	0.35	1.77	0.34	0	2.44	2.56	1.81	2.27	2.15
Ce_2O_3	1.61	3.21	5.23	2.35	14.45	8.15	7.63	15.42	14.2	13.08	13.71	14.86
Pr_2O_3	0	0	0	0	0	0	0	0	0	0	0	0
Nd_2O_3	0.15	0.27	0.27	0.31	2.49	0.56	0.74	2.53	2.91	2.04	2.54	2.18
PbO	0	0	0	0	0	0.38	0.62	0	0	0	0	0
Ta_2O_5	0	0	0	0	0	2.85	4.19	0	0	0	0	0
ThO_2	0	0	0	0	0.65	2.07	3.41	1.81	4.1	2.31	3.59	2.83
UO_2	0	0	0	0	0.47	3.05	2.99	1.27	1.78	1.55	1.29	0.65
F	0	0	0	0	0	0	0	0	0	0	0	0
Sum	94.3	93.81	94.57	97.07	100.24	92.02	94.13	99.41	98	99.18	98.78	99.2
Sum *A*	1.783	1.743	1.677	1.713	1.911	0.712	0.749	1.88	1.844	1.93	1.821	1.767
A-def	0.217	0.257	0.323	0.287	0.089	1.288	1.251	0.12	0.156	0.07	0.179	0.233
Sum *B*	2	2	2	2	2	2	2	2	2	2	2	2
O	6.241	6.17	6.038	6.081	6.795	4.081	4.223	6.682	6.546	6.733	6.434	6.481

	Drill Core # 31		Pyrochlores									
	155.15-f	171.42	178.1	211A-a	211A-d	211A-e	211A-f	211A-g	350.2-a	350.2-b	350.2-c	350.2-d
Oxides												
Na_2O	4.15	2.09	0.23	5.55	1.46	2.27	1.53	0.12	3.91	4.56	6.67	6.96
Al_2O_3	0	0.17	0	0.38	0	0.21	0.12	0.08	0.2	0.21	0	0
SiO_2	1.19	1.3	0.84	0.51	1.85	2.59	1.41	0.81	0.92	1.05	0.54	0.66
K_2O	0	0	0	0	0	0	0	0	0	0	0	0
CaO	12.76	12.44	14.19	16.51	17.28	16.54	16.26	17.19	11.64	12.06	17.01	17.26
TiO_2	11.35	15.65	8.89	32.68	7.82	9.72	9.5	8.95	10.11	9.98	6.28	5.5
MnO	0.57	1.1	0.69	0	0.16	0.19	0.48	0.43	0.91	0.3	0	0
Fe_2O_3	0.36	0.4	1.44	1.99	1.83	1.69	1.9	1.77	1.84	1.26	0.53	0.24
SrO	0	0	0.17	0.67	0	0	0	0.13	0.26	0.21	0	0
Y_2O_3	0	0	0	0	0	0	0	0	0	0	0	0
ZrO_2	2.3	0.3	3.48	0.32	5.1	5.22	5.91	4.41	5.29	3.35	6.09	1.66
Nb_2O_5	44.18	37.63	43.66	20.75	43.51	36.23	35.64	44.23	39.55	41.93	61.46	64.74
BaO	0	0.06	0	1.05	0.2	0.56	0.53	0	0.24	0.14	0	0
La_2O_3	2.39	2.22	1.43	3.96	1.46	0.84	1.35	1.56	0.85	0.83	0	0.11
Ce_2O_3	15.32	14.19	12.61	7.07	10.28	8.95	9.77	10.59	5.59	6.46	1.48	1.29
Pr_2O_3	0	0	0	0	0	0	0	0	0	0	0	0
Nd_2O_3	2.67	3.05	0	1.54	1.84	1.41	1.94	2.23	1.27	1.28	0	0
PbO	0	0	0	0	0	0.64	0.27	0.08	0	0.73	0	0.41
Ta_2O_5	0	0	1.11	0.84	0	4.58	6.48	3.19	0	0	0	0
ThO_2	1.76	1.2	3.55	0	2.22	2.69	1.99	1.68	0.79	0.74	0	0.62
UO_2	0.88	0	0.42	0	2.92	5.91	6.37	0.32	14.41	13.99	0	0
F	0	0	0	0	0	0	0	0	0	0	0	0
Sum	99.88	92.59	95.09	94.05	97.92	99.98	101.69	99.6	98.9	99.05	100.06	99.45
Sum *A*	1.945	1.674	1.475	1.84	1.77	1.817	1.795	1.552	1.782	1.898	1.741	1.869
A-def	0.055	0.326	0.525	0.16	0.23	0.183	0.205	0.448	0.218	0.102	0.259	0.131
Sum *B*	2	2	2	2	2	2	2	2	2	2	2	2
O	6.796	6.256	6.228	5.361	6.595	6.477	6.604	6.29	6.358	6.624	5.905	6.272

	Drill Core # 31			Pyrochlores								
	13.8-1	13.8-2	13.8-3	13.8-4	13.8-a	13.8-b	13.8-c	211.2-pd	211.2-p1	211.2-p6	211.2-p6b	211.2-p6c
Oxides												
Na_2O	2.52	1.24	1.4	1.22	1.54	1.28	1.79	5.38	0	5.05	1.36	5.03
Al_2O_3	0	0	0	0	0	0	0	0	0	0	0	0
SiO_2	3.42	1.71	1.36	1.8	1.41	1.36	1.56	1.77	0.98	1.35	1.5	1.12
K_2O	0	0	0	0	0	0	0	0	0	0	0	0
CaO	21.63	18.07	17.02	19	18.23	17.61	18.84	24.91	14.04	24.76	34.77	20.67
TiO_2	4.1	8.3	7.33	7.11	7.71	7.91	6.81	26.78	7.88	27.81	39.58	33.99
MnO	0	0	0	0	0	0	0	0	0	0	0	0
Fe_2O_3	1.38	1.91	2.24	1.86	2.13	1.89	2.44	5.76	1.84	5.62	5.33	4.32
SrO	0	0	0	0	0	0	0	0	0.59	0	0	0
Y_2O_3	0	0	0	0	0	0	0	0	0	0	0	0
ZrO_2	1.75	6.32	9.6	4.25	5.6	9.79	0	0	1.44	0	0	0
Nb_2O_5	58.1	41.24	36.79	45.37	41.43	35.13	47.4	27.75	49.13	26.59	13.18	19.48
BaO	0	0	0	0	0	0	0	0	0.21	0	0	0
La_2O_3	0	0	0	0	0	0	1.13	0	0	0	0	0
Ce_2O_3	3.89	8.11	3.7	10.66	7.86	5.1	11.8	3.43	10.07	4.33	2.27	7.03
Pr_2O_3	0	0	0	0	0	0	0	0	0	0	0	0
Nd_2O_3	0.07	0.78	0.86	1.05	1.12	0	1.36	1.31	1.34	0.99	0.75	1.63
PbO	0	0	0	0	0	0	0	0	0	0	0	0
Ta_2O_5	0	0	0	0	0	0	2.77	0	6.66	0	0	0
ThO_2	0	0	0	0	0	0	0.78	0	0	0	0.26	0.32
UO_2	0.4	12.29	20.5	6.74	10.94	20.9	1.57	0	0	0	0	0
F	0	0	0	0	0	0	0	0	0	0	0	0
Sum	97.26	99.97	100.8	99.06	97.97	100.97	98.25	97.09	94.18	97.82	99	93.59
Sum *A*	1.708	1.784	1.819	1.831	1.865	1.897	1.916	2.003	1.189	1.987	1.991	1.814
A-def	0.292	0.216	0.181	0.169	0.135	0.103	0.084	-0.003	0.811	0.013	0.009	0.186
Sum *B*	2	2	2	2	2	2	2	2	2	2	2	2
O	6.283	6.679	6.78	6.806	6.803	6.969	6.94	5.58	5.602	5.57	5.608	5.181

Drill Core # 31

	350.2-e	350.2-f	350.2-g	350.2-h
Oxides				
Na_2O	6.43	6.46	6.5	6.33
Al_2O_3	0	0	0	0
SiO_2	0.59	0.83	1.06	1.02
K_2O	0	0	0	0
CaO	16.76	16.84	16.33	16.85
TiO_2	6.3	6.87	6.24	6.75
MnO	0	0	0	0
Fe_2O_3	0.11	0.02	0.36	0.2
SrO	0	0	0	0
Y_2O_3	0	0	0	0
ZrO_2	5.52	3.57	6.5	2.41
Nb_2O_5	61.6	61.05	60.03	61.15
BaO	0	0	0	0
La_2O_3	0	0.13	1.088	0.38
Ce_2O_3	1.62	2.43	2.91	2.52
Pr_2O_3	0	0	0	0
Nd_2O_3	0	0	0	0
PbO	0.38	0.27	0.18	0.42
Ta_2O_5	0	0	0	0
ThO_2	0.01	0	0	0
UO_2	0	0	0	0
F	0	0	0	0
Sum	99.32	98.46	101.2	98.03
Sum *A*	1.731	1.786	1.74	1.797
A-def	0.269	0.214	0.26	0.203
Sum *B*	2	2	2	2
O	5.947	6.078	5.947	6.122

	Drill Core # 01		Pyrochlores						
	125.5a-1	125.5a-2	125.5a-3	125.5a-a	125.5a-b	125.5a-c	125.5a-d	125.5a-e	125.5a-f
Oxides									
Na_2O	2.69	2.78	3	3.02	3.62	3.72	3.78	3.95	3.87
Al_2O_3	0	0	0	0	0	0	0	0	0
SiO_2	0.29	0.57	0.31	0.33	0.1	0.22	0.13	0.22	0.16
K_2O	0	0	0	0	0	0	0	0	0
CaO	13.37	12.48	14.16	14.51	14.23	14.32	14.36	14.54	14.22
TiO_2	4.26	3.51	2.28	5.35	3.98	4.19	4.18	3.57	3.56
MnO	0.32	0.61	0.01	0.41	0.32	0.08	0.08	0	0.3
Fe_2O_3	2.27	2.46	2.66	1.51	1.78	1.65	1.69	1.54	1.57
SrO	0	0	0	0	0	0	0	0	0
Y_2O_3	0	0	0	0	0	0	0	0	0
ZrO_2	5.53	6.92	4.37	4.09	3.24	3.33	3.36	3.01	3.25
Nb_2O_5	46.59	44.89	56.98	52.3	57.11	57.05	57.04	57.32	58.12
BaO	0	0	0	0	0	0	0	0	0
La_2O_3	0	0	0	0	0	0	0	0	0
Ce_2O_3	10.28	8.74	11.28	12.54	9.76	10.04	10.14	10.37	10.27
Pr_2O_3	0	0	0	0	0	0	0	0	0
Nd_2O_3	0	0	0	0	0	0	0	0	0
PbO	0	0	0	0	0	0	0	0	0
Ta_2O_5	0	0	0	0	0	0	0	0	0
ThO_2	8.05	10.87	0.49	0	0	0	0	0	0
UO_2	0	0	0	0	0	0	0	0	0
F	0	0	0	0	0	0	0	0	0
Sum	93.65	93.83	95.54	94.06	94.14	94.6	94.76	94.52	95.32
Sum *A*	1.755	1.737	1.581	1.692	1.64	1.642	1.657	1.719	1.678
A-def	0.245	0.263	0.419	0.308	0.36	0.358	0.343	0.281	0.322
Sum *B*	2	2	2	2	2	2	2	2	2
O	6.598	6.55	6.16	6.35	6.203	6.197	6.222	6.368	6.296

APPENDIX II
SEM-EDS analyses of NIOCAN and Bond Zone minerals

II.2. Perovskite

	Drill Core #52		Perovskite								
Oxides	52-36.8-gr2	52-36.8-gr1	52-36.8-1	52-36.8-2	52-36.8-3	52-48.25a1	52-48.25a2	52-48.25a3	52-119b(1)	52-119b(2)	52-54.0(1)
Na_2O	4.50	5.15	2.33	3.69	2.64	4.02	4.00	2.66	3.47	3.08	3.70
MgO	0.00	0.19	0.25	0.14	0.00	2.05	1.89	1.37	0.00	0.00	0.47
Al_2O_3	0.00	0.21	0.23	0.08	0.14	0.49	0.40	0.49	0.35	0.48	0.00
SiO_2	0.00	0.00	0.78	0.83	1.34	0.00	0.00	0.00	0.98	0.62	0.00
K_2O	0.00	0.00	0.00	0.00	0.00	0.00	0.00	0.00	0.00	0.00	0.00
CaO	27.85	27.82	31.43	28.56	30.56	29.70	29.49	32.32	29.21	29.34	27.94
TiO_2	25.74	25.68	29.95	23.71	28.50	20.95	20.95	28.56	30.16	35.53	23.15
MnO	0.41	0.41	0.38	0.09	0.20	0.00	0.00	0.00	0.00	0.00	0.33
Fe_2O_3	0.40	1.49	7.35	7.26	7.48	9.05	8.50	7.86	5.93	3.60	7.46
SrO	0.37	0.47	0.32	0.10	2.18	0.00	0.00	0.00	0.01	0.20	0.57
ZrO_2	0.00	0.00	0.00	0.00	0.00	1.57	1.56	1.44	0.00	0.00	0.00
Nb_2O_5	34.11	34.45	22.95	30.46	25.51	31.39	31.67	23.71	25.67	22.19	29.51
BaO	0.00	0.00	0.00	0.00	0.00	0.00	0.00	0.00	0.00	0.00	0.00
La_2O_3	2.60	1.43	0.91	2.39	0.00	0.00	0.00	0.00	0.88	0.26	1.01
Ce_2O_3	2.71	1.43	1.86	2.81	2.89	0.00	0.00	0.00	2.16	2.49	1.07
Nd_2O_3	0.00	0.62	0.48	0.44	0.00	0.00	0.00	0.00	0.60	0.64	0.65
Sm_2O_3	0.00	0.00	0.00	0.00	0.00	0.00	0.00	0.00	0.00	0.00	0.82
PbO	0.00	0.00	0.00	0.00	0.00	0.00	0.00	0.00	0.00	0.00	0.00
Ta_2O_5	0.00	0.00	0.00	0.00	0.00	0.00	0.00	0.00	0.71	0.99	2.31
ThO_2	0.00	0.00	0.00	0.00	0.00	0.00	0.00	0.00	0.55	0.00	0.20
UO_2	0.00	0.00	0.00	0.00	0.00	0.00	0.00	0.00	0.00	0.00	0.00
Sum	98.69	99.25	99.22	100.56	101.44	99.22	98.46	98.41	100.67	99.42	99.20
*Sum A**	1.06	1.07	1.02	1.03	1.01	1.04	1.03	1.02	1.00	0.98	1.17
*Sum B**	0.92	0.94	1.03	1.00	1.01	1.07	1.05	1.05	1.00	1.01	0.87
End-member Components:											
$CaThO_3$	0.00	0.00	0.00	0.00	0.00	0.00	0.00	0.00	0.00	0.00	0.00
Tausonite	0.47	0.59	0.42	0.13	2.87	0.00	0.00	0.00	0.01	0.26	0.72
Loparite	9.05	5.43	4.73	9.25	3.04	0.00	0.00	0.00	5.08	3.94	5.28
Lueshite	18.88	22.78	10.14	15.20	12.22	20.50	20.46	13.34	15.70	14.16	17.35
Latrappite	0.93	3.41	17.73	17.27	17.99	22.15	20.86	18.92	14.26	8.68	18.49
Perovskite	47.58	51.01	54.48	41.76	50.45	45.62	46.02	57.97	53.12	61.80	42.40
$Ca_2Nb_2O_7$	23.09	16.78	12.50	16.39	13.43	11.73	12.67	9.78	11.83	11.60	15.71

	Drill Core # 52		Perovskite									
Oxides	D2-3(a)	D2-3(b)	D2-5(a)	D2-5(b)	D2-5c	D2-5(d)	D2-5(e)	52-30.3a	52-30.3b	52-30.3c	52-30.3d	52-36.88[1]
Na_2O	1.18	1.38	2.08	1.12	0.82	0.09	0.19	4.94	4.71	4.18	4.16	2.97
MgO	0.00	0.00	0.00	0.00	0.00	0.00	0.00	0.00	0.00	0.00	0.00	0.00
Al_2O_3	1.10	1.00	0.95	1.10	0.95	0.90	1.03	0.10	0.16	0.21	0.14	0.02
SiO_2	0.33	0.38	0.67	0.35	0.78	0.03	0.25	0.43	0.54	0.58	0.59	0.40
K_2O	0.00	0.00	0.00	0.00	0.00	0.00	0.00	0.00	0.00	0.00	0.00	0.00
CaO	33.19	32.80	30.34	33.18	35.54	36.83	36.15	25.89	25.39	26.36	27.94	30.47
TiO_2	38.90	38.58	41.95	45.30	44.84	46.93	47.70	32.50	33.47	28.72	28.42	34.58
MnO	0.06	0.07	0.16	0.00	0.59	0.05	0.02	0.00	0.30	0.06	0.11	0.41
Fe_2O_3	5.25	5.12	4.84	4.09	4.70	3.88	3.77	2.98	3.15	5.08	5.23	5.83
SrO	0.00	0.00	0.00	0.00	0.00	0.00	0.00	0.48	0.51	0.49	0.48	0.59
ZrO_2	0.45	0.00	0.00	0.34	0.00	0.82	0.90	0.00	0.00	0.00	0.00	0.00
Nb_2O_5	14.46	14.49	10.41	7.65	7.63	5.09	4.98	24.14	21.97	27.44	27.84	19.63
BaO	0.00	0.00	0.00	0.00	0.32	0.00	0.00	0.00	0.00	0.00	0.00	0.00
La_2O_3	1.70	1.69	2.74	2.97	1.49	1.60	1.65	2.60	3.02	2.26	1.67	2.06
Ce_2O_3	2.40	2.35	5.35	3.89	2.16	2.59	2.93	3.39	4.16	3.11	1.93	3.36
Nd_2O_3	1.00	0.88	1.24	0.89	0.00	1.07	0.64	0.76	0.46	0.42	0.38	0.00
Sm_2O_3	0.00	0.00	0.00	0.00	0.00	0.00	0.00	0.00	0.34	0.00	0.00	0.13
PbO	0.00	0.00	0.21	0.00	0.00	0.00	0.00	0.00	0.00	0.00	0.00	0.00
Ta_2O_5	0.00	0.00	0.00	0.00	0.00	0.00	0.00	0.00	0.00	0.00	0.00	0.00
ThO_2	0.00	0.00	0.00	0.00	0.31	0.65	0.20	0.00	0.00	0.00	0.00	0.00
UO_2	0.00	0.00	0.00	0.00	0.00	0.00	0.00	0.00	0.00	0.00	0.00	0.00
Sum	100.02	98.74	100.94	100.85	100.13	100.53	100.41	98.21	98.18	98.91	98.89	100.45
Sum A*	1.00	1.01	1.01	1.01	1.01	1.02	1.00	1.15	1.13	1.14	1.15	1.12
Sum B*	1.00	1.00	1.01	1.00	1.01	0.99	1.00	0.87	0.89	0.88	0.87	0.92
End-member Components:												
$CaThO_3$	0.00	0.00	0.00	0.00	0.00	0.38	1.12	0.00	0.00	0.00 x		0.00
Tausonite	0.00	0.00	0.00	0.00	0.00	0.00	0.00	0.60	0.65	0.65		0.74
Loparite	7.61	7.42	13.34	11.70	4.34	0.90	1.89	10.34	12.31	9.38		8.42
Lueshite	3.24	4.30	5.68	1.40	2.45	0.00	0.00	20.21	18.77	17.93		11.45
Latrappite	12.34	12.06	11.31	9.28	10.71	0.00	0.00	6.85	7.34	12.28		13.43
Perovskite	66.63	66.95	66.58	73.19	79.55	98.72	97.99	55.88	55.75	47.90		58.58
$Ca_2Nb_2O_7$	10.17	9.28	3.09	4.43	2.95	0.00	0.00	6.11	5.18	12.18		7.39

	Drill Core #52		Perovskite									
Oxides	52-30.3 s4	52-36.8(a1)	52-36.8(a2)	52-36.8(a3)	52-36.8[A]	52-36.8[B]	52-36.8AA	52-36.8AB	52-36.8AC	52-36.8AD	52-36.8AE	52-36.8AF
Na_2O	3.88	1.50	2.31	2.22	2.06	1.38	1.16	1.15	2.26	0.57	1.95	1.52
MgO	0.00	0.00	0.00	0.00	0.00	0.00	0.00	0.00	0.00	0.00	0.00	0.00
Al_2O_3	0.16	0.40	0.21	0.40	0.19	0.57	0.11	0.68	0.55	0.58	0.33	0.11
SiO_2	0.96	0.86	1.28	0.44	0.37	0.60	0.00	0.34	0.27	0.31	0.37	0.55
K_2O	0.00	0.00	0.00	0.00	0.00	0.00	0.00	0.00	0.00	0.00	0.00	0.00
CaO	27.71	31.77	32.05	30.38	30.58	29.13	30.52	30.31	31.90	30.80	30.10	30.38
TiO_2	27.14	27.85	31.77	41.00	48.46	44.55	46.37	16.96	37.39	49.51	45.27	48.33
MnO	0.00	0.00	0.17	0.36	0.00	0.00	0.15	0.00	0.25	0.01	0.28	0.00
Fe_2O_3	5.83	6.02	5.99	4.72	2.75	3.98	3.96	3.58	5.23	3.78	3.24	2.76
SrO	0.16	0.65	0.21	0.57	0.36	0.29	0.81	0.13	0.36	0.36	0.52	0.53
ZrO_2	0.00	0.00	0.00	0.00	0.00	0.00	0.27	0.00	0.00	0.00	0.00	0.32
Nb_2O_5	28.64	15.51	22.16	11.60	5.47	5.71	2.90	3.02	16.42	1.79	5.49	4.03
BaO	0.00	0.00	0.00	0.00	0.00	0.00	0.00	0.00	0.00	0.00	0.00	0.00
La_2O_3	1.60	2.16	1.79	3.49	3.42	6.21	4.44	5.60	2.58	4.23	4.70	4.22
Ce_2O_3	1.46	2.69	2.04	5.24	5.64	6.50	6.80	7.60	3.34	6.47	6.79	6.14
Nd_2O_3	1.01	0.62	0.17	1.54	0.89	0.85	1.40	1.21	1.13	1.85	0.72	1.24
Sm_2O_3	0.00	0.00	0.00	0.00	0.00	0.00	0.27	0.00	0.17	0.40	0.42	0.00
PbO	0.00	0.00	0.00	0.00	0.00	0.00	0.00	0.00	0.00	0.00	0.00	0.00
Ta_2O_5	0.00	0.00	0.00	0.00	0.00	0.00	0.00	0.00	0.00	0.00	0.00	0.00
ThO_2	0.00	0.00	0.00	0.00	0.00	0.00	0.00	0.00	0.00	0.00	0.00	0.00
UO_2	0.00	0.00	0.00	0.00	0.00	0.00	0.00	0.00	0.00	0.00	0.00	0.00
Sum	98.55	100.03	100.15	101.96	100.19	99.77	99.16	100.58	101.85	100.64	100.18	100.13
Sum A*	1.14	1.05	1.00	1.01	1.02	1.01	1.03	1.01	1.01	0.97	1.05	1.00
Sum B*	0.87	0.95	0.96	0.95	0.99	0.98	0.99	0.98	0.99	1.01	0.97	0.99
End-member Components:												
$CaThO_3$	0.00	0.00	0.00	0.00	0.00	0.00	0.00	0.00	0.00	0.00	0.00	0.00
Tausonite	0.21	0.85	0.27	0.71	0.53	0.46	1.25	0.20	0.44	0.59	0.82	0.80
Loparite	6.62	8.78	6.54	14.89	18.64	14.57	11.94	12.05	10.55	6.24	20.44	15.25
Lueshite	17.43	4.54	8.99	5.54	0.90	0.00	0.00	0.00	7.09	0.00	0.00	0.00
Latrappite	14.16	14.37	13.89	10.72	0.00	0.00	0.00	0.00	11.78	0.00	0.00	0.00
Perovskite	47.85	61.71	64.71	63.67	79.93	84.97	86.81	87.75	62.10	93.17	78.74	83.96
$Ca_2Nb_2O_7$	13.72	9.76	5.61	4.47	0.00	0.00	0.00	0.00	8.05	0.00	0.00	0.00

	Drill Core # 52		Perovskite									
Oxides	52-36.8(1)	52-36.8(2)	52-36.8(3)	52-36.8(4)	52-36.8(5)	52-119b6	52-119b7	52-119b8	D2oka1	D2oka2	D2oka-01	D2oka-02
Na_2O	2.80	3.56	4.28	4.27	2.13	2.15	2.13	2.03	0.41	0.21	1.26	1.45
MgO	0.00	0.00	0.00	0.00	0.00	0.00	0.00	0.00	0.00	0.00	0.00	0.00
Al_2O_3	0.31	0.23	0.15	0.22	0.25	0.00	0.00	0.00	0.99	0.93	0.89	0.95
SiO_2	0.45	0.87	0.70	0.18	0.18	1.10	0.00	0.92	0.31	0.13	0.88	1.01
K_2O	0.00	0.00	0.00	0.00	0.00	0.00	0.00	0.00	0.00	0.00	0.00	0.00
CaO	28.81	28.02	26.29	26.29	29.39	32.28	32.41	30.97	35.71	35.67	31.12	30.93
TiO_2	32.01	25.62	25.82	25.82	44.80	32.64	32.65	23.79	45.33	45.48	40.29	41.01
MnO	0.00	0.20	0.04	0.32	0.14	0.00	0.00	0.00	0.00	0.07	0.10	0.22
Fe_2O_3	6.54	6.88	6.22	5.86	3.71	6.88	6.87	8.06	3.98	4.24	5.17	4.75
SrO	0.00	0.00	0.00	0.00	0.00	0.00	0.00	0.00	0.00	0.00	0.00	0.00
ZrO_2	0.41	0.44	0.11	0.00	0.22	0.00	1.15	0.00	0.60	0.99	0.13	0.13
Nb_2O_5	22.08	29.74	31.94	32.00	6.54	20.50	20.48	27.80	6.82	7.01	10.79	10.52
BaO	0.00	0.00	0.00	0.00	0.00	0.00	0.00	0.00	0.00	0.00	0.00	0.00
La_2O_3	1.54	0.10	0.49	0.00	2.62	0.00	0.00	0.00	1.66	1.69	2.95	3.24
Ce_2O_3	3.50	1.28	1.99	1.00	7.55	2.39	2.46	1.86	3.41	3.37	4.85	5.36
Nd_2O_3	0.61	0.49	0.60	0.75	3.66	0.00	0.00	0.63	0.00	0.00	1.26	1.11
Sm_2O_3	0.00	0.00	0.00	0.00	0.00	0.00	0.00	0.00	0.00	0.00	0.00	0.00
PbO	0.00	0.00	0.00	0.00	0.00	0.00	0.00	0.00	0.00	0.00	0.00	0.00
Ta_2O_5	0.00	0.00	0.00	0.00	0.00	1.17	1.07	1.63	0.00	0.00	0.00	0.00
ThO_2	0.14	0.00	0.00	0.00	0.00	0.00	0.00	0.00	0.00	0.00	0.42	0.14
UO_2	0.00	0.00	0.00	0.00	0.00	0.00	0.00	0.00	0.00	0.00	0.00	0.00
Sum	99.20	97.53	98.63	96.71	101.19	99.11	99.22	97.69	99.22	99.79	100.11	100.82
*Sum A**	0.99	0.99	0.98	0.98	1.02	1.00	1.01	1.01	1.02	1.00	1.00	1.00
*Sum B**	1.03	1.03	1.03	1.03	1.00	1.03	1.03	1.02	1.00	1.00	1.00	1.00
End-member Components:												
$CaThO_3$	0.00	0.00	0.00	0.00	0.00	0.00	0.00	0.00	0.00	0.00	0.00	0.00
Tausonite	0.00	0.00	0.00	0.00	0.00	0.00	0.00	0.00	0.00	0.00	0.00	0.00
Loparite	8.39	2.23	4.15	1.95	22.38	2.43	2.59	2.76	4.25	2.15	13.63	14.52
Lueshite	11.66	18.18	21.28	22.24	0.00	10.00	9.81	9.85	0.00	0.00	1.72	2.27
Latrappite	16.21	17.56	15.81	15.08	0.00	16.60	16.52	20.52	0.00	0.00	12.34	11.17
Perovskite	52.58	46.95	43.47	45.55	77.62	60.25	60.34	45.97	95.71	97.85	64.86	65.28
$Ca_2Nb_2O_7$	11.15	15.09	15.30	15.18	0.00	10.72	10.75	20.90	0.00	0.00	7.44	6.77

	Drill Core #52		Perovskite									
Oxides	52-36.8[2]	52-36.8[3]	52-36.8[4]	52-36.8[5]	52-36.8[6]	52-36.8[7]	52-36.8[8]	52-36.8[9]	52-36.8[10]	52-30.3 s1	52-30.3 s2	52-30.3 s3
Na_2O	3.08	3.62	4.07	4.41	4.60	4.40	4.74	3.49	2.20	4.29	4.54	3.93
MgO	0.00	0.00	0.00	0.00	0.00	0.00	0.00	0.00	0.00	0.00	0.00	0.00
Al_2O_3	0.61	0.31	0.14	0.18	0.00	0.00	0.12	0.27	0.20	0.00	0.00	0.07
SiO_2	0.88	0.57	0.69	0.69	0.68	0.74	0.96	1.06	0.66	0.22	0.84	1.13
K_2O	0.00	0.00	0.00	0.00	0.00	0.00	0.00	0.00	0.00	0.00	0.00	0.00
CaO	26.42	28.93	27.95	27.12	27.19	27.17	27.47	29.06	30.86	24.72	27.10	28.28
TiO_2	26.78	24.13	26.06	25.76	24.50	24.31	27.30	25.12	35.21	42.48	26.37	27.43
MnO	0.00	0.00	0.29	0.00	0.25	0.36	0.30	0.00	0.00	0.00	0.21	0.13
Fe_2O_3	7.15	6.49	5.61	5.94	5.77	6.68	5.42	7.20	5.34	1.98	5.87	5.02
SrO	0.58	0.40	0.09	0.16	0.03	0.31	0.27	0.39	0.45	0.54	0.28	0.00
ZrO_2	0.00	0.00	0.00	0.00	0.00	0.00	0.00	0.00	0.00	0.00	0.00	0.00
Nb_2O_5	30.21	32.38	32.52	33.10	34.08	33.10	31.14	30.48	17.86	12.42	29.74	29.34
BaO	0.00	0.00	0.00	0.00	0.00	0.00	0.00	0.00	0.00	0.00	0.00	0.00
La_2O_3	1.79	1.92	0.99	1.12	1.12	1.29	0.88	1.27	2.85	5.07	2.31	1.95
Ce_2O_3	2.63	1.81	1.75	1.65	1.31	1.68	1.27	1.56	4.03	6.42	2.89	0.95
Nd_2O_3	0.00	0.00	0.00	0.00	0.00	0.00	0.00	0.00	0.00	1.34	0.29	1.21
Sm_2O_3	0.00	0.08	0.45	0.00	0.00	0.00	0.00	0.00	0.00	0.00	0.00	0.00
PbO	0.00	0.00	0.00	0.00	0.00	0.00	0.00	0.00	0.00	0.00	0.00	0.00
Ta_2O_5	0.00	0.00	0.00	0.00	0.00	0.00	0.00	0.00	0.00	0.00	0.00	0.00
ThO_2	0.00	0.00	0.00	0.00	0.00	0.00	0.00	0.00	0.00	0.00	0.00	0.00
UO_2	0.00	0.00	0.00	0.00	0.00	0.00	0.00	0.00	0.00	0.00	0.00	0.00
Sum	100.13	100.64	100.61	100.13	99.53	100.04	99.87	99.90	99.66	99.48	100.44	99.44
Sum A*	1.08	1.14	1.14	1.14	1.16	1.16	1.15	1.15	1.10	1.07	1.17	1.15
Sum B*	0.89	0.84	0.86	0.86	0.85	0.86	0.87	0.87	0.91	0.94	0.86	0.86
End-member Components:												
$CaThO_3$	0.00	0.00	0.00	0.00	0.00	0.00	0.00	0.00	0.00	0.00	0.00	0.00
Tausonite	0.84	0.52	0.12	0.21	0.04	0.41	0.35	0.52	0.57	0.67	0.36	6.98
Loparite	7.92	6.69	4.78	4.59	4.19	5.05	3.49	4.85	10.93	19.67	8.88	17.04
Lueshite	14.28	15.71	18.90	20.90	21.79	20.70	22.34	16.06	7.09	13.82	19.27	11.87
Latrappite	18.85	15.44	13.57	14.50	13.96	16.31	12.90	17.50	12.39	4.51	13.79	49.39
Perovskite	37.81	42.80	45.55	43.86	43.95	41.99	49.36	44.77	58.88	62.06	49.76	14.79
$Ca_2Nb_2O_7$	20.50	18.85	17.08	15.94	16.07	15.53	11.57	16.31	10.14	0.00	7.95	0.00

	Drill Core #52		Perovskite
Oxides	52-36.8AG	52-36.8BA	
Na_2O	1.38	1.35	
MgO	0.00	0.00	
Al_2O_3	0.17	0.19	
SiO_2	0.61	0.02	
K_2O	0.00	0.00	
CaO	30.47	30.90	
TiO_2	48.08	44.93	
MnO	0.00	0.00	
Fe_2O_3	2.77	3.33	
SrO	0.38	0.65	
ZrO_2	0.24	0.00	
Nb_2O_5	4.17	7.25	
BaO	0.00	0.00	
La_2O_3	4.62	3.89	
Ce_2O_3	6.37	6.19	
Nd_2O_3	1.12	0.85	
Sm_2O_3	0.00	0.00	
PbO	0.00	0.00	
Ta_2O_5	0.00	0.00	
ThO_2	0.00	0.00	
UO_2	0.00	0.00	
Sum	100.38	99.55	
Sum A*	1.00	1.04	
Sum B*	0.99	0.96	
End-member Components:			
$CaThO_3$	0.00	0.00	
Tausonite	0.57	0.81	
Loparite	14.00	16.23	
Lueshite	0.00	1.02	
Latrappite	0.00	7.62	
Perovskite	85.42	69.33	
$Ca_2Nb_2O_7$	0.00	4.99	

APPENDIX II
SEM-EDS analyses of NIOCAN and Bond Zone minerals

II.3. Zirconolite

Zirconolite legend

Sum Ca^{2+} = (*A*-site) = Ca + Na + Ce + Nd + Sm + Th

Sum Zr^{4+} = (*B*-site) = Zr + Hf

Sum Ti^{4+} = (*C*-site) = Ti + Mn + Fe + Mg + Nb + Ta + Al + Si

	Zirconolite											
	01-125b(8)	01-125p2(1)	01-125p1(1)	31-211.0(1)	31-211.2a	31-211.2b	31-211p6(1)	31-211p6(2)	31-211p6(3)	31-211p6(4)	31-211p6(5)	31-211p6(6)
MgO	n.d.	n.d.	0.49	1.76	n.d.	n.d.	n.d.	n.d.	n.d.	n.d.	n.d.	n.d.
Al_2O_3	0.40	n.d.	n.d.	1.16	n.d.	n.d.	n.d.	n.d.	n.d.	n.d.	n.d.	n.d.
SiO_2	n.d.	n.d.	0.62	1.71	n.d.	n.d.	n.d.	n.d.	n.d.	n.d.	n.d.	n.d.
CaO	11.08	11.00	13.00	10.93	10.95	14.32	11.00	10.37	9.71	11.19	11.19	11.09
TiO_2	8.89	8.75	13.05	13.09	19.09	13.51	13.72	15.03	13.17	12.91	12.63	12.59
MnO	3.76	3.50	2.80	n.d.	1.72	2.39	2.94	3.19	1.49	2.86	3.17	3.00
FeO	6.95	7.51	6.08	6.84	5.70	8.28	5.62	5.17	6.49	5.98	5.51	5.76
ZrO_2	34.20	35.01	36.58	38.29	33.15	37.76	37.52	35.05	39.13	36.88	35.97	36.08
Nb_2O_5	31.10	28.84	25.74	21.37	16.37	24.00	22.07	21.50	24.35	22.68	24.57	23.85
La_2O_3	n.d.	n.d.	0.26	n.d.	n.d.	n.d.	n.d.	n.d.	n.d.	n.d.	n.d.	n.d.
Ce_2O_3	3.71	3.70	1.33	1.82	5.92	n.d.	5.16	6.03	2.82	4.51	4.54	4.92
Nd_2O_3	n.d.	1.64	0.26	0.19	n.d.	n.d.	n.d.	n.d.	n.d.	n.d.	n.d.	n.d.
Sm_2O_3	n.d.	n.d.	n.d.	0.27	n.d.	n.d.	n.d.	n.d.	n.d.	n.d.	n.d.	n.d.
HfO_2	n.d.	n.d.	n.d.	n.d.	n.d.	n.d.	n.d.	n.d.	n.d.	n.d.	n.d.	n.d.
Ta_2O_5	n.d.	n.d.	n.d.	2.76	2.00	n.d.	2.83	3.17	2.02	2.76	2.85	2.65
ThO_2	n.d.	n.d.	0.20	n.d.	n.d.	n.d.	n.d.	n.d.	n.d.	n.d.	n.d.	n.d.
UO_2	n.d.	n.d.	n.d.	n.d.	n.d.	n.d.	n.d.	n.d.	n.d.	n.d.	n.d.	n.d.
$(Na,K)_2O$	n.d.	n.d.	n.d.	0.20	n.d.	n.d.	n.d.	n.d.	n.d.	n.d.	n.d.	n.d.
Total	**100.19**	**99.95**	**100.41**	**100.12**	**94.90**	**100.26**	**100.86**	**99.51**	**99.18**	**99.77**	**100.43**	**99.84**
Cations to 7 oxygens												
Sum Ca^{2+}	0.9	0.9	0.9	0.8	1.0	1.0	0.9	0.9	0.8	0.9	0.9	0.9
Sum Zr^{4+}	1.1	1.2	1.1	1.2	1.1	1.2	1.2	1.1	1.3	1.2	1.2	1.2
Sum Ti^{4+}	2.0	2.0	2.0	2.0	2.0	1.9	1.9	1.9	1.9	1.9	1.9	1.9
TOTAL CATIONS	**4.0**	**4.0**	**4.0**	**4.0**	**4.0**	**4.1**	**4.0**	**4.0**	**3.9**	**4.0**	**4.0**	**4.0**

	31-211p6(7)	31-211Aa1	31-211Aa2	31-211Aa3	31-211ba	31-211bb	31-211bc	31-211b-a	31-211b-b	31-211b-c	31-211p4(1)
MgO	n.d.	0.41	0.21	0.14	n.d.	n.d.	n.d.	0.51	0.50	0.44	0.43
Al_2O_3	n.d.	0.66	0.63	0.69	n.d.	n.d.	n.d.	n.d.	n.d.	n.d.	n.d.
SiO_2	n.d.	0.78	0.50	0.54	n.d.	n.d.	n.d.	n.d.	n.d.	n.d.	n.d.
CaO	10.79	11.64	13.89	13.39	12.66	12.77	12.43	9.18	9.33	9.37	8.20
TiO_2	12.72	16.39	19.91	19.65	15.29	15.46	15.21	17.88	17.54	17.53	16.77
MnO	3.28	2.28	1.65	1.56	2.89	3.08	2.64	2.52	3.47	3.43	2.93
FeO	5.65	7.80	7.47	7.23	4.97	4.86	4.90	5.78	5.76	5.75	6.49
ZrO_2	36.08	32.15	33.86	33.76	33.91	33.84	34.05	34.42	34.14	34.00	38.53
Nb_2O_5	23.22	20.15	21.57	20.97	19.13	19.07	18.66	16.11	16.78	16.78	19.34
La_2O_3	n.d.	0.58	n.d.	n.d.	1.25	1.02	0.93	1.47	0.99	1.02	0.54
Ce_2O_3	4.21	1.99	n.d.	n.d.	4.36	3.96	3.92	5.55	4.51	4.58	3.33
Nd_2O_3	n.d.	0.84	n.d.	n.d.	1.91	2.22	2.16	2.26	3.00	3.07	2.16
Sm_2O_3	n.d.	0.26	0.10	0.10	n.d.	n.d.	n.d.	n.d.	n.d.	n.d.	n.d.
HfO_2	n.d.	1.04	0.31	0.53	n.d.	n.d.	n.d.	n.d.	n.d.	n.d.	n.d.
Ta_2O_5	3.74	n.d.	n.d.	n.d.	1.56	1.60	1.83	1.43	1.96	1.69	1.51
ThO_2	n.d.	0.29	0.13	0.11	0.76	0.83	0.62	2.64	2.39	2.54	1.02
UO_2	n.d.	n.d.	n.d.	n.d.	n.d.	n.d.	n.d.	1.01	0.40	0.50	0.73
$(Na,K)_2O$	n.d.	0.22	0.37	0.34	n.d.	n.d.	n.d.	n.d.	n.d.	n.d.	n.d.
Total	**99.69**	**96.38**	**100.60**	**99.01**	**99.22**	**98.71**	**97.35**	**100.76**	**100.72**	**100.69**	**101.98**
Cations to 7 oxygens											
Sum Ca^{2+}	0.9	0.9	0.9	0.9	1.1	1.1	1.1	0.9	0.9	0.9	0.7
Sum Zr^{4+}	1.2	1.1	1.0	1.0	1.1	1.1	1.1	1.1	1.1	1.1	1.2
Sum Ti^{4+}	1.9	2.2	2.2	2.1	1.8	1.9	1.8	2.0	2.0	2.0	2.0
TOTAL CATIONS	**4.0**	**4.1**	**4.1**	**4.1**	**4.0**	**4.1**	**4.0**	**4.0**	**4.0**	**4.0**	**3.9**

	31-211p4(4)	31-350p1a	31-350p1b	36-132.3a	36-132.3b	36-160.2a	36-160.2b	36-358.3-1	36-358.3-2	36-358.3-3	52-119a(a)
MgO	0.49	0.29	0.30	n.d.	n.d.	n.d.	n.d.	n.d.	n.d.	n.d.	n.d.
Al_2O_3	n.d.	0.37	0.28	n.d.	n.d.	n.d.	n.d.	n.d.	n.d.	n.d.	n.d.
SiO_2	n.d.	n.d.	n.d.	n.d.	n.d.	n.d.	n.d.	n.d.	n.d.	n.d.	n.d.
CaO	8.44	10.98	11.00	10.03	10.33	10.07	9.99	14.02	13.45	12.94	11.79
TiO_2	12.99	9.61	7.41	10.84	7.31	7.23	7.30	29.36	28.98	24.78	8.41
MnO	2.10	2.35	2.72	3.89	3.29	3.28	3.32	n.d.	n.d.	n.d.	n.d.
FeO	7.01	6.89	7.17	6.24	7.75	7.37	7.42	6.76	6.64	7.18	1.05
ZrO_2	38.40	30.53	31.78	32.80	35.61	34.64	34.89	31.63	32.73	32.91	74.34
Nb_2O_5	23.69	25.33	28.16	27.47	28.83	29.09	28.91	11.73	10.88	15.14	5.55
La_2O_3	0.42	0.42	0.57	n.d.	n.d.	n.d.	n.d.	2.34	0.76	1.66	n.d.
Ce_2O_3	2.11	2.26	2.28	4.86	4.88	5.11	5.23	n.d.	n.d.	n.d.	n.d.
Nd_2O_3	1.59	1.29	1.14	3.19	2.58	n.d.	n.d.	1.94	2.40	2.46	n.d.
Sm_2O_3	n.d.	n.d.	n.d.	n.d.	n.d.	n.d.	n.d.	n.d.	n.d.	n.d.	n.d.
HfO_2	n.d.	n.d.	n.d.	n.d.	n.d.	n.d.	n.d.	n.d.	n.d.	n.d.	n.d.
Ta_2O_5	2.71	1.45	1.39	n.d.	n.d.	n.d.	n.d.	n.d.	n.d.	n.d.	n.d.
ThO_2	1.53	n.d.	n.d.	1.41	n.d.	2.52	2.50	n.d.	n.d.	n.d.	n.d.
UO_2	1.15	0.73	0.74	n.d.	n.d.	n.d.	n.d.	n.d.	n.d.	n.d.	n.d.
$(Na,K)_2O$	n.d.	n.d.	n.d.	n.d.	n.d.	n.d.	n.d.	0.22	0.26	n.d.	n.d.
Total	**102.64**	**92.49**	**94.94**	**100.71**	**100.58**	**99.31**	**99.57**	**99.06**	**96.10**	**97.07**	**101.11**
Cations to 7 oxygens											
Sum Ca^{2+}	0.7	1.0	0.9	0.9	0.9	0.9	0.9	1.0	1.0	1.0	calzirtite
Sum Zr^{4+}	1.2	1.0	1.1	1.1	1.2	1.2	1.2	1.0	1.0	1.0	
Sum Ti^{4+}	2.0	2.0	2.0	2.0	1.9	1.9	1.9	2.1	2.1	2.0	
TOTAL CATIONS	**3.9**	**4.0**	**4.0**	**4.0**	**4.0**	**4.0**	**4.0**	**4.1**	**4.1**	**4.0**	

	52-119b-1	52-478(1)	52-478(2)	52-478(3)	52-478(4)	52-478(5)	52-478(6)	52-478p31	52-478a	52-478b	52-478c	52-478(a)
MgO	n.d.	n.d.	n.d.	n.d.	n.d.	n.d.	n.d.	n.d.	n.d.	n.d.	n.d.	n.d.
Al_2O_3	0.33	n.d.	n.d.	n.d.	n.d.	n.d.	n.d.	n.d.	n.d.	n.d.	n.d.	n.d.
SiO_2	n.d.	n.d.	n.d.	n.d.	n.d.	n.d.	n.d.	n.d.	n.d.	n.d.	n.d.	n.d.
CaO	12.49	11.95	11.25	11.16	8.88	9.29	11.46	8.92	10.77	10.46	10.76	10.05
TiO_2	10.70	10.52	10.50	11.34	11.75	11.53	28.44	6.20	9.68	10.00	9.64	10.53
MnO	0.30	2.62	2.74	2.44	3.99	3.65	0.52	4.02	3.16	2.82	3.15	2.94
FeO	1.42	6.90	7.30	7.40	7.49	6.70	5.09	13.17	7.30	7.03	7.22	6.97
ZrO_2	75.63	36.90	36.14	34.38	36.08	35.75	37.04	45.04	36.45	36.42	36.65	35.75
Nb_2O_5	n.d.	28.92	29.13	29.26	24.01	25.13	13.59	22.91	28.22	28.67	27.87	27.66
La_2O_3	n.d.	n.d.	n.d.	n.d.	n.d.	n.d.	n.d.	n.d.	n.d.	n.d.	n.d.	n.d.
Ce_2O_3	n.d.	2.19	2.46	2.89	2.24	5.40	2.66	n.d.	3.11	1.43	3.05	3.91
Nd_2O_3	n.d.	1.67	0.97	1.99	4.58	2.98	1.79	n.d.	1.92	2.90	1.53	2.37
Sm_2O_3	n.d.	n.d.	n.d.	n.d.	n.d.	n.d.	n.d.	n.d.	n.d.	n.d.	n.d.	n.d.
HfO_2	n.d.	n.d.	n.d.	n.d.	n.d.	n.d.	n.d.	n.d.	n.d.	n.d.	n.d.	n.d.
Ta_2O_5	n.d.	n.d.	n.d.	n.d.	n.d.	n.d.	n.d.	n.d.	n.d.	n.d.	n.d.	n.d.
ThO_2	n.d.	n.d.	n.d.	n.d.	n.d.	n.d.	n.d.	n.d.	n.d.	n.d.	n.d.	n.d.
UO_2	n.d.	n.d.	n.d.	n.d.	n.d.	n.d.	n.d.	n.d.	n.d.	n.d.	n.d.	n.d.
$(Na,K)_2O$	n.d.	n.d.	n.d.	n.d.	n.d.	n.d.	n.d.	n.d.	n.d.	n.d.	n.d.	n.d.
Total	**100.88**	**101.70**	**100.50**	**100.90**	**99.01**	**100.43**	**100.60**	**100.30**	**100.61**	**99.73**	**99.37**	**100.18**
Cations to 7 oxygens												
Sum Ca^{2+}	calzirtite	0.9	0.9	0.9	0.8	0.9	0.9	0.7	0.9	0.9	0.9	0.9
Sum Zr^{4+}		1.2	1.2	1.1	1.2	1.2	1.1	1.5	1.2	1.2	1.2	1.2
Sum Ti^{4+}		1.9	1.9	2.0	2.0	1.9	2.0	2.0	1.9	1.9	1.9	1.9
TOTAL CATIONS		**3.9**	**4.0**	**4.0**	**4.0**	**4.0**	**4.0**	**4.1**	**4.0**	**4.0**	**4.0**	**4.0**

	52-478(b)	52-478(c)	52-514.2A	BZ-1a	BZ-1b	BZ-1c	BZ-1d	BZ-1e	52-478p11	52-478p12	52-478p13	52-478p14
MgO	n.d.	n.d.	n.d.	0.56	0.41	0.62	0.03	0.35	n.d.	n.d.	n.d.	n.d.
Al_2O_3	n.d.	n.d.	n.d.	n.d.	n.d.	n.d.	n.d.	n.d.	n.d.	n.d.	n.d.	n.d.
SiO_2	n.d.	n.d.	n.d.	n.d.	n.d.	n.d.	n.d.	n.d.	n.d.	n.d.	n.d.	n.d.
CaO	10.20	10.42	11.51	8.98	9.29	9.59	8.28	9.19	11.11	12.06	11.36	12.08
TiO_2	8.75	9.26	10.15	12.55	12.53	12.46	11.91	12.14	11.60	11.28	11.24	11.60
MnO	2.49	2.91	2.97	3.67	3.61	3.59	2.80	3.15	3.10	2.58	2.63	2.05
FeO	6.62	6.51	7.54	5.24	5.41	4.91	5.71	5.78	6.31	6.73	6.49	7.07
ZrO_2	36.49	36.50	36.28	37.10	37.20	37.87	39.74	39.15	33.73	34.98	33.70	36.15
Nb_2O_5	28.01	27.61	28.49	24.60	24.45	25.73	24.93	24.47	27.84	26.31	27.98	28.34
La_2O_3	n.d.	n.d.	n.d.	n.d.	n.d.	n.d.	n.d.	n.d.	n.d.	n.d.	n.d.	n.d.
Ce_2O_3	2.45	3.33	2.63	2.93	3.16	3.05	3.06	2.55	1.45	1.96	1.83	0.95
Nd_2O_3	5.24	2.82	2.45	2.69	2.44	2.34	2.54	1.92	3.55	4.55	3.25	1.46
Sm_2O_3	n.d.	n.d.	n.d.	n.d.	n.d.	n.d.	n.d.	n.d.	n.d.	n.d.	n.d.	n.d.
HfO_2	n.d.	n.d.	n.d.	n.d.	n.d.	n.d.	n.d.	n.d.	n.d.	n.d.	n.d.	n.d.
Ta_2O_5	n.d.	n.d.	n.d.	n.d.	n.d.	n.d.	n.d.	n.d.	0.60	0.35	0.63	0.17
ThO_2	n.d.	n.d.	n.d.	0.52	0.81	0.74	0.62	1.69	n.d.	n.d.	n.d.	n.d.
UO_2	n.d.	n.d.	n.d.	n.d.	n.d.	n.d.	n.d.	n.d.	n.d.	n.d.	n.d.	n.d.
$(Na,K)_2O$	n.d.	n.d.	n.d.	1.06	0.76	0.76	n.d.	0.41	n.d.	n.d.	n.d.	n.d.
Total	**100.25**	**99.36**	**101.03**	**99.92**	**100.07**	**101.67**	**99.60**	**100.79**	**99.30**	**100.80**	**99.11**	**99.87**
Cations to 7 oxygens												
Sum Ca^{2+}	0.9	0.9	0.9	0.8	0.8	0.8	0.7	0.8	0.9	1.0	0.9	0.9
Sum Zr^{4+}	1.2	1.2	1.2	1.2	1.2	1.2	1.3	1.3	1.1	1.1	1.1	1.2
Sum Ti^{4+}	1.8	1.9	1.9	2.1	2.0	2.0	1.8	1.9	2.0	1.9	1.9	1.9
TOTAL CATIONS	**4.0**	**4.0**	**4.0**	**4.1**	**4.2**	**4.0**	**3.9**	**4.0**	**4.0**	**4.0**	**4.0**	**4.0**

	52-478p15	52-478p16	52-48.25(3)	52-48.25(2)	52-48.25(1)
MgO	n.d.	n.d.	n.d.	n.d.	n.d.
Al_2O_3	n.d.	n.d.	1.14	1.12	0.73
SiO_2	n.d.	n.d.	n.d.	n.d.	n.d.
CaO	11.81	11.72	10.00	10.42	10.04
TiO_2	11.56	11.49	11.13	9.74	18.21
MnO	2.30	2.22	2.86	3.26	3.46
FeO	7.39	7.32	5.64	6.41	4.48
ZrO_2	35.88	35.85	35.11	35.79	33.91
Nb_2O_5	27.07	27.09	24.38	25.93	11.52
La_2O_3	n.d.	n.d.	n.d.	n.d.	n.d.
Ce_2O_3	1.79	1.88	4.08	3.91	5.52
Nd_2O_3	2.02	2.04	2.58	2.91	5.46
Sm_2O_3	n.d.	n.d.	n.d.	n.d.	n.d.
HfO_2	n.d.	n.d.	0.72	0.54	0.56
Ta_2O_5	0.44	0.40	n.d.	n.d.	n.d.
ThO_2	n.d.	n.d.	0.94	1.53	4.56
UO_2	n.d.	n.d.	0.11	0.08	0.04
$(Na,K)_2O$	n.d.	n.d.	n.d.	n.d.	n.d.
Total	**100.27**	**100.00**	**98.69**	**101.64**	**98.51**
Cations to 7 oxygens					
Sum Ca^{2+}	0.9	0.9	0.9	0.9	1.1
Sum Zr^{4+}	1.2	1.2	1.2	1.2	1.2
Sum Ti^{4+}	1.9	1.9	1.9	1.9	1.8
TOTAL CATIONS	**4.0**	**4.0**	**4.0**	**4..0**	**4.1**

APPENDIX II
SEM-EDS analyses of NIOCAN and Bond Zone minerals

II.4. Niocalite

Legend

Analysis	Locality	Reference
N1 – N20	NIOCAN and Bond Zone , Oka	this work
K-1, K-2, K-3, K-4	Kaiserstuhl, Germany	Keller and Williams, 1995
Oka-1, Oka-2	Bond Zone, Oka	Keller and Williams, 1995

Niocalite

	N1	N2	N3	N4	N5	N6	N7	N8	N9	N10	N11	N12
SiO_2	31.59	31.12	31.12	30.02	31.17	30.81	30.50	29.36	29.74	29.55	30.17	30.90
TiO_2	0.00	0.00	0.00	0.13	0.14	0.00	0.13	0.00	0.00	0.00	0.00	0.00
ZrO_2	0.00	0.00	0.00	0.00	1.21	0.98	0.25	1.40	0.85	0.62	1.05	0.00
Nb_2O_5	17.84	18.02	18.63	17.25	17.43	17.72	17.63	17.39	17.51	17.71	18.09	17.57
Ta_2O_5	0.00	0.00	0.00	0.00	0.00	0.00	0.00	0.00	0.00	0.00	0.00	0.00
Al_2O_3	0.00	0.12	0.10	0.00	0.26	0.21	0.15	0.02	0.00	0.00	0.06	0.00
La_2O_3	0.00	0.00	0.00	0.67	0.00	0.00	0.00	0.00	0.00	0.00	0.00	0.89
Ce_2O_3	0.31	0.65	0.25	1.54	0.39	0.56	0.63	0.07	0.67	0.40	0.67	1.21
Nd_2O_3	0.33	0.68	0.23	0.19	0.07	0.00	0.33	0.14	0.26	0.33	0.48	0.00
FeO	0.00	0.14	0.46	0.00	0.25	0.55	0.11	0.00	0.00	0.00	0.00	0.42
MnO	0.72	1.51	0.07	0.98	0.97	0.90	0.70	1.12	0.92	0.76	0.89	0.67
MgO	0.00	0.00	0.00	0.00	0.00	0.00	0.00	0.00	0.00	0.00	0.00	0.60
CaO	46.71	47.14	47.89	43.75	47.23	46.60	46.37	43.28	43.98	44.08	43.99	45.51
SrO	0.14	0.68	0.80	0.00	1.42	1.27	0.74	0.88	0.81	0.72	0.92	0.00
Na_2O	0.86	0.49	0.47	0.98	0.38	0.00	0.55	1.10	1.02	0.85	1.26	1.67
F	n.a.	n.a.	n.a.	n.a.	n.a.	n.a.	n.a.	n.a.	n.a.	n.a.	n.a	n.a.
Total	**98.50**	**100.55**	**100.02**	**95.51**	**100.92**	**99.60**	**98.09**	**94.76**	**95.76**	**95.02**	**97.58**	**99.67**
Cations to 36 oxygens												
Na^{+}	0.444	0.251	0.241	0.527	0.194	0.000	0.288	0.596	0.548	0.459	0.665	0.863
Ca^{2+}	13.319	13.340	13.541	13.010	13.300	13.297	13.399	12.961	13.052	13.156	12.836	12.990
Fe^{2+}	0.000	0.031	0.102	0.000	0.055	0.122	0.025	0.000	0.000	0.000	0.000	0.094
Mn^{2+}	0.162	0.338	0.016	0.230	0.216	0.203	0.160	0.265	0.216	0.179	0.205	0.151
Mg^{2+}	0.000	0.000	0.000	0.000	0.000	0.000	0.000	0.000	0.000	0.000	0.000	0.238
Sr^{2+}	0.022	0.104	0.122	0.000	0.216	0.196	0.116	0.143	0.130	0.116	0.145	0.000
La^{3+}	0.000	0.000	0.000	0.069	0.000	0.000	0.000	0.000	0.000	0.000	0.000	0.087
Ce^{3+}	0.030	0.063	0.024	0.156	0.038	0.054	0.062	0.007	0.068	0.041	0.067	0.118
Nd^{+}	0.031	0.064	0.021	0.019	0.007	0.000	0.032	0.014	0.026	0.033	0.047	0.000
Zr^{4+}	0.000	0.000	0.000	0.000	0.155	0.127	0.033	0.191	0.115	0.084	0.139	0.000
Nb^{5+}	2.146	2.151	2.223	2.164	2.070	2.134	2.150	2.198	2.193	2.230	2.230	2.116
Ta^{5+}	0.000	0.000	0.000	0.000	0.000	0.000	0.000	0.000	0.000	0.000	0.000	0.000
Ti^{4+}	0.000	0.000	0.000	0.027	0.028	0.000	0.026	0.000	0.000	0.000	0.000	0.000
Si^{4+}	8.408	8.220	8.213	8.332	8.193	8.206	8.226	8.208	8.238	8.232	8.220	8.233
Al^{3+}	0.000	0.037	0.031	0.000	0.081	0.066	0.048	0.007	0.000	0.000	0.019	0.000
F^{-}	n.a.	n.a.	n.a.	n.a.	n.a.	n.a.	n.a.	n.a.	n.a.	n.a.	n.a.	n.a.

	N13	N14	N15	N16	N17	N18	N19	N20	N21	K-1	K-2	K-3
SiO_2	30.74	31.17	31.38	31.59	30.96	29.28	30.96	30.28	30.32	30.01	29.79	29.35
TiO_2	0.00	0.00	0.00	0.00	0.00	0.00	0.00	0.00	0.28	0.06	0.10	0.10
ZrO_2	0.00	0.00	0.00	0.00	0.00	0.27	0.00	0.00	0.00	0.23	0.53	1.21
Nb_2O_5	18.09	18.27	18.69	18.23	18.29	19.73	18.29	17.67	16.76	16.77	16.27	16.85
Ta_2O_5	0.00	0.00	0.00	0.00	0.00	0.00	0.00	0.00	0.00	0.14	0.79	0.23
Al_2O_3	0.00	0.00	0.00	0.01	0.00	0.00	0.35	0.00	0.00	n.d.	n.d.	n.d.
La_2O_3	0.00	0.00	0.00	0.39	0.18	0.00	0.18	0.00	0.00	0.53	0.38	0.23
Ce_2O_3	0.81	0.24	0.26	0.42	0.52	0.39	0.52	0.97	0.00	1.30	0.78	0.38
Nd_2O_3	0.01	0.70	0.70	0.13	0.56	0.28	0.56	0.00	0.00	0.33	0.29	<0.15
FeO	0.37	0.00	0.06	0.19	0.11	0.29	0.11	0.32	0.36	0.44	0.53	0.27
MnO	0.84	0.66	0.53	1.02	0.96	0.90	0.96	0.88	0.72	0.49	0.48	0.62
MgO	0.55	0.54	0.48	0.01	0.40	0.09	0.40	0.00	0.23	0.18	0.18	0.21
CaO	45.02	47.04	46.83	46.71	45.46	42.86	45.46	45.60	43.58	46.19	46.28	46.76
SrO	0.00	0.00	0.36	0.00	0.00	0.00	0.00	0.00	0.00	0.21	0.20	0.18
Na_2O	2.08	1.37	1.40	1.03	1.28	1.62	1.27	1.06	0.78	0.81	0.71	1.00
F	n.a.	n.a.	n.a.	n.a.	n.a.	n.a.	n.a.	n.a.	n.a.	1.68	2.25	1.90
Total	**98.88**	**99.99**	**100.69**	**100.03**	**99.07**	**96.08**	**99.41**	**96.78**	**93.03**	**98.66**	**98.60**	**98.74**
Cations to 36 oxygens												
Na^+	1.078	0.700	0.712	0.527	0.662	0.868	0.654	0.561	0.423	0.418	0.368	0.517
Ca^{2+}	12.895	13.283	13.150	13.193	12.997	12.690	12.938	13.328	13.059	13.230	13.221	13.360
Fe^{2+}	0.083	0.000	0.013	0.042	0.025	0.067	0.024	0.073	0.084	0.098	0.118	0.060
Mn^{2+}	0.190	0.147	0.118	0.228	0.217	0.211	0.216	0.203	0.171	0.111	0.108	0.140
Mg^{2+}	0.219	0.212	0.188	0.010	0.159	0.037	0.158	0.000	0.096	0.072	0.072	0.083
Sr^{2+}	0.000	0.000	0.055	0.000	0.000	0.000	0.000	0.000	0.000	0.033	0.031	0.028
La^{3+}	0.000	0.000	0.000	0.390	0.018	0.000	0.018	0.000	0.000	0.052	0.037	0.023
Ce^{3+}	0.079	0.023	0.025	0.420	0.051	0.039	0.051	0.970	0.000	0.127	0.076	0.037
Nd^+	0.001	0.066	0.066	0.130	0.053	0.028	0.530	0.000	0.000	0.032	0.028	0.000
Zr^{4+}	0.000	0.000	0.000	0.000	0.000	0.036	0.000	0.000	0.000	0.029	0.068	0.157
Nb^{5+}	2.186	2.177	2.214	2.173	2.206	2.465	2.197	2.179	2.119	2.027	1.961	2.031
Ta^{5+}	0.000	0.000	0.000	0.000	0.000	0.000	0.000	0.000	0.000	0.010	0.057	0.017
Ti^{4+}	0.000	0.000	0.000	0.000	0.000	0.000	0.000	0.000	0.059	0.012	0.020	0.020
Si^{4+}	8.218	8.216	8.225	8.328	8.262	8.092	8.225	8.261	8.481	8.023	7.942	7.826
Al^{3+}	0.000	0.000	0.000	0.010	0.000	0.000	0.110	0.000	0.000	0.000	0.000	0.000
F^-	n.a.	n.a.	n.a.	n.a.	n.a.	n.a.	n.a.	n.a.	n.a.	1.420	1.897	1.602

	K-4	Oka1	Oka1
SiO_2	29.38	29.77	29.90
TiO_2	0.10	0.15	0.26
ZrO_2	0.66	0.33	n.d.
Nb_2O_5	17.20	17.14	18.86
Ta_2O_5	0.29	0.57	n.d.
Al_2O_3	n.d.	<0.1	n.d.
La_2O_3	0.17	0.24	n.d.
Ce_2O_3	0.56	0.67	n.d.
Nd_2O_3	0.27	0.26	n.d.
FeO	0.24	0.34	0.49
MnO	0.73	0.99	0.99
MgO	0.14	0.23	0.70
CaO	46.30	46.39	46.96
SrO	0.28	0.29	n.d.
Na_2O	0.94	0.67	0.55
F	2.02	1.79	1.73
Total	**98.74**	**99.08**	**100.6**

Cations to 36 oxygens			
Na^{+}	0.486	0.345	0.279
Ca^{2+}	13.241	13.224	13.158
Fe^{2+}	0.054	0.076	0.107
Mn^{2+}	0.165	0.223	0.219
Mg^{2+}	0.056	0.092	0.273
Sr^{2+}	0.043	0.044	0.000
La^{3+}	0.017	0.024	0.000
Ce^{3+}	0.055	0.065	0.000
Nd^{+}	0.026	0.024	0.000
Zr^{4+}	0.086	0.043	0.000
Nb^{5+}	2.075	2.062	2.230
Ta^{5+}	0.021	0.042	0.000
Ti^{4+}	0.020	0.030	0.051
Si^{4+}	7.841	7.920	7.819
Al^{3+}	0.000	0.000	0.049
F^{-}	1.705	1.502	1.431

APPENDIX III
NIOCAN and Bond Zone drill core logs

Mineral symbols

Symbol	Mineral
Ap	Apatite
Bad	Baddeleyite
Brt	Barite
Bt	Biotite
Cal	Calcite
Ce-Pyro	Cerium Pyrochlore
(Ce)Pyro	Ceriopyrochlore
Gn	Galena
Ilm	Ilmenite
Mag	Magnetite
Mtc	Monticellite
Prv	Perovskite
Py	Pyrite
Pyro	Pyrochlore (Calcium)
Sd	Siderite
Sp	Sphalerite
Str	Strontianite
Th-Pyro	Thorium Pyrochlore
(Th)Pyro	Thorpyrochlore
U-Pyro	Uranoan Pyrochlore
(U)Pyro	Uranpyrochlore
Znrt	Zirconolite

Ceriopyrochlore = Ce exceeds 20 at. % of *A*-site occupancy
Thorpyrochlore = Th exceeds 20 at. % of *A*-site occupancy
Uranpyrochlore = U exceeds 20 at. % of *A*-site occupancy

Drill Core

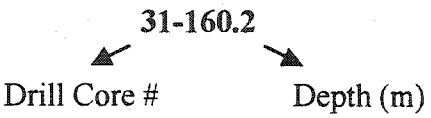

Drill core	Rock type	Textural features	Major minerals	Accessory minerals	Paragenetic features
01-125.5a	Magnetite Calciocarbonatite	• Coarse grained • Inequigranular	Cal, Ce-Pyro, Mag, Ilm, Ap	Sp, Mtc, Brt	• Large Ce-pyro's (0.6 mm) exhibit zoning reflecting REE concentration increasing from core to rim • Brt is found infilling fractures of Cal
01-125.5b	Magnetite Calciocarbonatite	• Coarse grained • Inequigranular	Cal, Mag, Ce-Pyro, Ap	Mtc, Sp, Bt, Brt, Zrnt, Bad	• Zrnt and Bad are found as inclusions within Ap grains • Brt is found in fractures of Cal • Large Ce-pyro (0.6 mm) are zoned reflecting the REE concentrations increasing from core to rim
31-13.8	Calciocarbonatite	• Medium- to-coarse grained • Inequigranular	Cal, (U)Pyro, Ap, Ce-pyro	Mag, Mtc, Sp	• Subhedral- to –anhedral (U)Pyro (20μm-50μm) exhibiting a dark mantling rim upon a light core in BSE images. Analysis indicated an increase in UO_2 from the rim to the core • Homogeneous subhedral Ce-Pyro (20μm-70μm) appear to have no relationship to the (U)Pyro
31-61.0	Calciocarbonatite	• Medium- to-coarse grained • Inequigranular	Cal, Ap, Pyro	Bt, Py, Sd, Sp	• Small (18μm-60μm) euhedral Pyro's appear homogeneous in BSE imaging, occur in clusters surrounded by Cal • Large (0.6 mm-0.9 mm) euhedral- to – subhedral Pyro's, also homogeneous in BSE imaging
31-86.83	Calciocarbonatite	• Medium grained • Inequigranular	Cal, Ap	Bt, Brt	• Absence of Nb-mineralization
31-86.85	Calciocarbonatite	• Medium grained • Inequigranular	Cal, Ap, Bt	Brt	• Absence of Nb-mineralization
31-101	Calciocarbonatite	• Coarse grained • Inequigranular	Cal, Ap, Pyro, Mag, Sp	Bt, Brt	• Small (15μm-60μm) subhedral- to – anhedral Pyro's exhibit patchy discolouration • Analyses of Pyro's shows a low REE content

Drill core	Rock type	Textural features	Major minerals	Accessory minerals	Paragenetic features
31-157	Calciocarbonatite	• Medium grained • Inequigranular	Cal, Ap, Mag	Bad, Mtc, Sp, Prv	• Ap exhibits two distinct zones reflecting REE concentrations (dark core-light rim) • Prv appears mottled in the BSE image • Bad is found in fractures of Cal
31-162.9	Calciocarbonatite	• Medium- to-coarse grained • Inequigranular	Cal, Ap, Mag, Ilm, Bt	Ce-Pyro, (Ce)Pyro, Brt, Zrnt	• (Ce)Pyro is subhedral and metamict, riddled with impurities, as inferred from low analysis totals and significant *A*-site vacancies • Ce-Pyro is also subhedral and exhibits patchy alteration, shown in BSE imaging
31-166.15	Pyrochlore Calciocarbonatite	• Coarse grained • Inequigranular	Cal, Ap, Mag, Ce-Pyro	Bt, Brt, Py	• Subhedral altered Ce-Pyro exhibit patchy zoning, correlating with REE contents
31-171.42	Pyrochlore Calciocarbonatite	• Fine- to-medium grained • Inequigranular	Cal, Ap, Ce-Pyro, Mag, Th-pyro	Ilm, Brt, Bt, (Ce)Pyro	• Subhedral altered Ce-Pyro and (Ce)Pyro exhibit patchy zoning, correlating with REE contents • Mag and Ilm are found associated together, often intergrown with each other
31-178.1	Pyrochlore Calciocarbonatite	• Porphyritic texture	Cal, Ap, Mag, Ce-Pyro, Bt	Zrnt	• Small anhedral Zrnt are found infilling fractures within the calcite, and along boundaries of Ap and Cal • Large phenocrysts of Mag, Ap, and subhedral altered Ce-Pyro are found in a groundmass of Cal • Ce-Pyro exhibit patchy zoning correlating with REE contents
31-203.3	Calciocarbonatite	• Medium grained • Inequigranular	Cal, Ap, Bt, Mag, Mtc	Sp, Brt, Prv, Bad	• Small (20μm) Prv are found with slight patchy alteration correlating with REE contents • Sp and Bad are found interstitial to larger Bt grains

Drill core	Rock type	Textural features	Major minerals	Accessory minerals	Paragenetic features
31-211.0	Calciocarbonatite	• Porphyritic texture	Cal, Ap, Mag	Prv, Zrnt, Bt, Ilm, Str	• Zrnt and Str often occur rimming the Bt grains • Small (40-70μm) Prv occurs in clusters, showing slight alteration
31-211b	Monticellite Calciocarbonatite	• Porphyritic texture	Cal, Mag, Ap, Mtc	Bt, Ce-Pyro, Sp, Prv, Zrnt, Brt, Str	• Small subhedral (60μm) highly-altered Ce-Pyro occur with inclusions of Cal, Brt and Str • Mtc, Ap, and Mag occur as phenocrysts in a groundmass of interlocking fine grained Cal
31-350.2	Pyrochlore Calciocarbonatite	• Coarse grained • Granular texture	Cal, Ap, Mag, Bt	U-Pyro, Ce-Pyro, Pyro, Gn, Bad, Zrnt, Brt	• Subhedral U-Pyro show slight patchy zoning representing changes in REE content • Subhedral small (20-50μm) clusters of Ce-Pyro • Euhedral, unaltered, homogeneous Pyro, found with no association to the Ce-Pyro or the U-Pyro
52-14.4b	Pyrochlore Calciocarbonatite	• Coarse grained • Inequigranular	Cal, Ap, Mag, Th-Pyro, (Th)Pyro, Ce-Pyro	Bt, Brt, Ncl	• Ce-pyro are mantled, exhibiting alteration around the rim, including bleached zones and fractures at the rim • Th-Pyro and (Th)Pyro are small, euhedral, and show concentric zoning, reflecting REE concentrations that increase from core to rim
52-36.8	Calciocarbonatite	• Medium grained • Inequigranular	Cal, Mtc, Ap	Ncl, Str, Sp, Ilm, Mag., Prv	• Small euhedral Ncl are found interstitial to Prv and Mag • Str and Sp are found infilling fractures in Cal

Drill core	Rock type	Textural features	Major minerals	Accessory minerals	Paragenetic features
52-37.45	Pyrochlore Calciocarbonatite	• Medium grained • Equigranular	Cal, Ap, Mag, Ce-Pyro	Py, U-Pyro, Gn, Ncl, Prv, Brt, Badd	• Euhedral Prv is found surrounding anhedral Mag and anhedral Ap • U-Pyro and Ce-Pyro are subhedral, oscillatory zoned and are found in clusters
52-48.25a	Monticellite Calciocarbonatite	• Medium grained • Equigranular	Cal, Ap, Mag, Mtc	Py, Ce-Pyro, U-Pyro, Gn, Ncl, Prv	• Euhedral- to –subhedral oscillatory zoned U-Pyro and Ce-Pyro are unaltered, with analysis revealing low *A*-site vacancies • Ncl, Prv, U-Pyro, and Ce-Pyro all are found to occur together
52-48.25b	Monticellite carbonatite	• Medium grained • Equigranular	Mtc, Ap, Cal	Ncl, Bt, Ce-Pyro, Py, Mag	• Ap exhibits concentric zoning with high REE contents along the rim of the crystals • Euhedral Ncl and subhedral Ce-Pyro occur clustered together
52-101.75	Calciocarbonatite	• Coarse grained • Inequigranular • Layering	Cal, Ap, Mag	(U)Pyro, Ce-Pyro, Bt	• (U)Pyro display discoloured turbid patches and are extremely altered, and also occur as inclusions within REE-rich Ap • Ce-Pyro are also found as inclusions within zoned REE-rich apatites however do not show alteration
52-109.5	Calciocarbonatite	• Coarse grained • Inequigranular	Cal, Ap, Mag	Py, Ce-Pyro	• Subhedral Ce-Pyro are absent of zoning
52-119a	Biotite Monticellite Calciocarbonatite	• Coarse grained • Inequigranular	Cal, Bt, Mtc, Ap	Py, Mag, Ce-Pyro, Brt, Calz, Sp	• Subhedral Ce-Pyro exhibit bleached zones and are riddled with impurities • Calz is found infilling fractures within Cal grains
52-119b	Monticellite Calciocarbonatite	• Coarse grained • Inequigranular	Cal, Mtc, Ap, Mag	Prv, Calz, Zrnt, Ce-Pyro, U-Pyro, Brt	• Subhedral Ce-Pyro exhibit bleached zones and are riddled with impurities • Calz and Zrnt are found associated with each other, often appearing clustered together interstitial to Cal

Drill core	Rock type	Textural features	Major minerals	Accessory minerals	Paragenetic features
52-155.15	Pyrochlore Calciocarbonatite	• Medium grained • Equigranular • Layering	Cal, Ce-Pyro, Ap	Bt, Py	• Small clusters (0.1-0.22 mm) of subhedral Ce-Pyro exhibit low temperature alteration • Ap inclusions were identified within Ce-Pyro grains • Larger Ce-Pyro (1.4 mm) exhibit fractures that have been filled in with Cal, have patchy zoning and low temperature alteration around the rim of the grains
52-204.35a	Calciocarbonatite	• Coarse grained • Inequigranular	Cal, Ap, Mag, Bt	U-Pyro, Zrnt, Brt	• Zrnt are found attached to U-Pyro grains • U-Pyro are large (1.0-1.5mm) show some fractures, and are turbid
52-219.65	Calciocarbonatite	• Coarse grained • Inequigranular	Cal, Ap, Mag	(U)Pyro, Calz, Bt, Bad, Zrnt	• Calz are found attached to the (U)Pyro grains, while Zrnt is found in close association with the (U)Pyro • (U)Pyro exhibits patchy zoning and infilling of fractures with calcite and apatite
52-478	Pyrochlore Calciocarbonatite	• Coarse grained • Inequigranular	Cal, Ap, Mag, Ce-Pyro	Zrnt, Sp, Brt, Mtc, Bt	• Small (50μm) subhedral grains • Invariant in composition, grains have Zrnt inclusions and exhibit discoloured zones and patches • Inclusions of oscillatory zoned REE-rich apatites are also found within a few larger Ce-Pyro
52-514	Calciocarbonatite	• Coarse grained • Inequigranular	Cal, Ap, Mag	Brt, Bt, Ce-Pyro, Th-pyro	• Small (50μm) Ce-pyro are subhedral and moderately fractured

APPENDIX IV

Representative compositions of pyrochlore group minerals from carbonatites and alkaline complexes worldwide.

Appendix IV Legend

Analyses	Locality	General Reference	Rock Type	Pyrochlore classification
Lu-mg1	Lueshe	Nasraoui and Bilah, 2000	calciocarbonatite	Pyrochlore
Lu-h2	Lueshe	Nasraoui and Bilah, 2000	calciocarbonatite	Strontium pyrochlore
Lu-w1	Lueshe	Nasraoui and Bilah, 2000	calciocarbonatite	Cerium pyrochlore
Nd-U1	Ndale	Hogarth and Horne, 1989	calcite-rich tuff	Uranpyrochlore
Ver-1, Fir-1	Blue River	Simandl *et al.* 2001	magnesiocarbonatite	Tantalum pyrochlore
Sok-1	Sokli	Lindqvist *et al.* 1979	calciocarbonatite	Pyrochlore
Sok-2	Sokli	Lindqvist *et al.* 1979	calciocarbonatite	Uranpyrochlore
Bin-1, Bin-4, Bin-6, Bin-8, Bin-9	Bingo	Williams *et al.* 1997	calciocarbonatite	Pyrochlore
Bin-2, Bin-5, Bin-10, Bin-11, Bin-12, Bin-13	Bingo	Williams *et al.* 1997	calciocarbonatite	Bariopyrochlore
Bin-3	Bingo	Williams *et al.* 1997	calciocarbonatite	Uranoan pyrochlore
Bin-7,	Bingo	Williams *et al.* 1997	calciocarbonatite	Strontium pyrochlore
Kola1, Kola2, Kola3	Lesnaya Varaka	Chakhmouradian *et al.* 1998	apatite-dolomite carbonatite	Thorium pyrochlore
Kov-1, Kov-3	Kovdor	C.T. Williams, 1996	alkaline complex	Uranpyrochlore
Kov-2	Kovdor	C.T. Williams, 1996	alkaline complex	Uranoan pyrochlore
Chi-1	Chilwa Island	Hogarth *et al.* 2000	calciocarbonatite	Pyrochlore
Fen-1	Fen	Hogarth *et al.* 2000	calciocarbonatite	Uranoan pyrochlore
Fen-2	Fen	Hogarth *et al.* 2000	calciocarbonatite	Uranpyrochlore
Fen-3, Fen-4	Fen	Hogarth *et al.* 2000	calciocarbonatite	Pyrochlore
Qaq-1	Qaqarssuk	C. Knudsen, 1989	calciocarbonatite	Pyrochlore
Qaq-2	Qaqarssuk	C. Knudsen, 1989	calciocarbonatite	Uranpyrochlore
Mt-W-A, Mt-W-B	Mt. Weld	Lottermoser and England, 1988	Laterite carbonatite	Cerium pyrochlore
Mt-W-C, Mt-W-D	Mt. Weld	Lottermoser and England, 1988	Laterite carbonatite	Stontium pyrochlore
Mt-W-E, Mt-W-E2	Mt. Weld	Lottermoser and England, 1988	Laterite carbonatite	Pyrochlore
PL-1, PL-2, PL-3, PL-4, PL-5, PL-6, PL-7, PL-8, PL-9, PL-10	Prairie Lake	Hammond, 1999	calciocarbonatite	Uranpyrochlore
Lovo-1	Lovozero	Chakhmouradian and Mitchell, 2002	alkaline complex	Pyrochlore
Lovo-2, Lovo-3	Lovozero	Chakhmouradian and Mitchell, 2002	alkaline complex	Uranpyrochlore
Lovo-4	Lovozero	Chakhmouradian and Mitchell, 2002	alkaline complex	Thorium pyrochlore
Lovo-5, Lovo-6	Lovozero	Chakhmouradian and Mitchell, 2002	alkaline complex	Cerium pyrochlore
New-1 to 6	Newania	Viladkar and Ghose, 2002	dolomite carbonatite	Uranoan pyrochlore

	Lu-Mg1	Lu-h2	Lu-w1	Nd-U1	Ver-1	Fir-1	Sok-1	Sok-2
Na_2O	7.900	2.400	0.260	5.290	7.190	7.680	3.720	1.160
Al_2O_3	0.000	0.000	1.390	0.000	0.000	0.000	0.030	0.160
SiO_2	0.000	1.830	0.210	0.000	0.000	0.000	0.050	0.610
K_2O	0.010	0.280	2.840	0.000	0.000	0.000	0.000	0.000
CaO	14.69	8.800	1.280	8.690	13.73	14.87	16.63	9.290
TiO_2	3.340	2.930	2.400	9.270	2.680	1.620	4.450	0.570
MnO	0.010	0.000	0.000	0.000	0.000	0.000	0.070	0.080
Fe_2O_3	0.060	1.870	4.160	0.640	0.100	0.020	2.470	1.300
SrO	1.330	5.830	1.320	0.160	0.460	0.810	0.000	0.000
Y_2O_3	0.000	0.000	0.000	0.170	0.130	0.140	0.000	0.000
ZrO_2	0.030	0.020	0.000	0.280	0.000	0.000	2.200	3.350
Nb_2O_5	66.94	64.30	63.13	32.30	60.33	66.21	52.19	48.94
BaO	0.110	0.015	0.160	0.000	0.000	0.000	0.000	0.000
La_2O_3	0.320	1.470	0.120	0.120	0.110	0.100	0.000	0.000
Ce_2O_3	0.680	3.060	10.63	0.210	0.270	0.250	1.380	1.010
Pr_2O_3	0.000	0.000	0.000	0.000	0.000	0.000	0.000	0.000
Nd_2O_3	0.000	0.000	0.000	0.000	0.000	0.000	0.000	0.000
PbO	0.000	0.000	0.000	0.000	0.060	0.010	0.000	0.000
Ta_2O_5	0.270	0.000	0.000	15.76	6.890	4.490	0.800	10.01
ThO_2	0.090	0.000	0.000	0.070	0.180	0.730	3.670	2.080
UO_2	0.160	0.000	0.000	26.44	4.280	0.030	0.300	27.52
F	5.100	1.730	2.790	0.190	4.170	5.150	5.700	1.600
Sum	**101.14**	**94.54**	**92.19**	**99.51**	**100.65**	**102.13**	**93.66**	**107.58**
Na	0.928	0.270	0.027	0.775	0.892	0.919	0.478	0.157
K	0.001	0.021	0.198	0.000	0.000	0.000	0.000	0.000
Ca	0.953	0.546	0.075	0.703	0.942	0.984	1.181	0.694
Mn	0.001	0.000	0.000	0.000	0.000	0.000	0.004	0.005
Sr	0.047	0.127	0.027	0.026	0.017	0.029	0.000	0.000
Y	0.000	0.000	0.000	0.012	0.004	0.005	0.000	0.000
Ba	0.000	0.003	0.003	0.000	0.000	0.000	0.000	0.000
La	0.010	0.031	0.002	0.001	0.003	0.002	0.000	0.000
Ce	0.020	0.065	0.213	0.005	0.006	0.006	0.033	0.026
Pr	0.000	0.000	0.000	0.000	0.000	0.000	0.000	0.000
Nd	0.000	0.000	0.000	0.000	0.000	0.000	0.000	0.000
Pb	0.000	0.000	0.000	0.000	0.001	0.000	0.000	0.000
Th	0.000	0.000	0.000	0.000	0.003	0.010	0.055	0.033
U	0.000	0.000	0.000	0.201	0.061	0.000	0.004	0.427
Site A	**1.960**	**1.060**	**0.546**	**1.980**	**1.929**	**1.956**	**1.756**	**1.341**
A-def	**0.040**	**0.940**	**1.454**	**0.020**	**0.071**	**0.044**	**0.244**	**0.651**
Al	0.000	0.000	0.090	0.000	0.000	0.000	0.002	0.013
Si	0.020	0.106	0.011	0.000	0.000	0.000	0.003	0.043
Ti	0.150	0.128	0.099	0.165	0.129	0.075	0.222	0.030
Fe	0.000	0.082	0.171	0.012	0.005	0.001	0.123	0.068
Zr	0.000	0.006	0.000	0.000	0.000	0.000	0.071	0.114
Nb	1.830	1.684	1.560	1.742	1.746	1.848	1.564	1.543
Ta	0.000	0.000	0.000	0.081	0.120	0.075	0.014	0.190
Site B	**2.000**	**2.000**	**2.000**	**2.000**	**2.000**	**2.000**	**2.000**	**2.000**
F	0.977	0.317	0.482	0.320	0.844	1.006	1.195	0.353

	Kov-1	Kov-2	Kov-3	Chi-1	Fen-1	Fen-2	Fen-3	Fen-4
Na_2O	3.910	5.360	5.140	5.180	2.380	0.000	6.440	6.580
Al_2O_3	0.000	0.000	0.000	0.050	0.140	0.190	0.000	0.000
SiO_2	0.000	0.000	0.000	0.110	0.130	0.560	0.050	0.050
K_2O	0.000	0.000	0.000	0.100	0.000	0.000	0.000	0.000
CaO	9.180	11.29	10.33	16.45	16.01	8.700	15.75	17.10
TiO_2	3.820	5.140	4.660	2.920	8.790	9.470	2.670	3.420
MnO	0.050	0.050	0.090	0.050	0.290	0.680	0.000	0.000
Fe_2O_3	1.350	0.890	0.750	0.900	1.260	1.650	0.870	0.360
SrO	0.300	0.230	0.240	0.450	0.370	0.980	0.230	0.260
Y_2O_3	0.050	0.050	0.050	0.000	0.090	0.200	0.340	0.320
ZrO_2	3.090	2.510	3.020	0.350	0.100	0.100	3.240	1.640
Nb_2O_5	38.57	45.32	43.20	63.96	41.55	45.36	63.20	65.16
BaO	0.000	0.000	0.000	0.060	0.130	0.640	0.000	0.000
La_2O_3	0.110	0.100	0.100	0.210	0.050	0.050	0.250	0.130
Ce_2O_3	0.180	0.120	0.280	1.940	0.100	0.130	2.360	1.190
Pr_2O_3	0.000	0.000	0.000	0.100	0.000	0.000	0.000	0.000
Nd_2O_3	0.000	0.000	0.000	0.150	0.000	0.000	0.290	0.050
PbO	1.140	0.920	1.210	0.460	2.140	1.960	0.000	0.000
Ta_2O_5	14.57	9.420	9.720	0.080	6.190	6.190	0.080	0.050
ThO_2	1.810	2.100	0.830	1.440	0.100	0.100	0.990	1.010
UO_2	20.42	15.91	18.75	0.100	17.53	19.84	0.100	0.100
F	0.470	1.020	1.030	2.420	1.640	0.460	4.970	4.790
Sum	**98.92**	**99.80**	**98.82**	**97.72**	**99.30**	**98.94**	**99.59**	**100.20**
Na	0.566	0.722	0.719	0.625	0.325	0.000	0.759	0.769
K	0.000	0.000	0.000	0.008	0.000	0.000	0.000	0.000
Ca	0.734	0.840	0.799	1.096	1.209	0.594	1.026	1.105
Mn	0.000	0.000	0.006	0.003	0.017	0.037	0.000	0.000
Sr	0.008	0.006	0.007	0.016	0.015	0.036	0.008	0.009
Y	0.000	0.000	0.000	0.000	0.003	0.007	0.011	0.010
Ba	0.000	0.000	0.000	0.001	0.004	0.016	0.000	0.000
La	0.003	0.000	0.000	0.005	0.001	0.001	0.006	0.003
Ce	0.005	0.003	0.007	0.044	0.003	0.003	0.053	0.026
Pr	0.000	0.000	0.000	0.002	0.000	0.000	0.000	0.000
Nd	0.000	0.000	0.000	0.003	0.000	0.000	0.006	0.001
Pb	0.023	0.017	0.024	0.008	0.041	0.034	0.000	0.000
Th	0.031	0.033	0.014	0.020	0.002	0.001	0.014	0.014
U	0.339	0.246	0.301	0.001	0.275	0.281	0.001	0.001
Site A	**1.709**	**1.867**	**1.876**	**1.833**	**1.895**	**1.010**	**1.884**	**1.939**
A-def	**0.291**	**0.133**	**0.124**	**0.167**	**0.105**	**0.990**	**0.116**	**0.061**
Al	0.000	0.000	0.000	0.004	0.012	0.014	0.000	0.000
Si	0.000	0.000	0.000	0.007	0.009	0.036	0.003	0.003
Ti	0.214	0.268	0.253	0.137	0.466	0.454	0.122	0.155
Fe	0.076	0.046	0.041	0.042	0.067	0.079	0.040	0.016
Zr	0.112	0.085	0.106	0.011	0.003	0.003	0.096	0.048
Nb	1.302	1.422	1.409	1.799	1.324	1.307	1.738	1.777
Ta	0.296	0.178	0.191	0.001	0.119	0.107	0.001	0.001
Site B	**2.000**	**2.000**	**2.000**	**2.000**	**2.000**	**2.000**	**2.000**	**2.000**
F	0.111	0.224	0.235	0.476	0.366	0.093	0.956	0.913

	PL-1	PL-2	PL-3	PL-4	PL-5	PL-6	PL-7	PL-8
Na_2O	0.000	0.000	4.890	0.890	2.330	0.720	0.640	0.000
Al_2O_3	0.870	0.640	0.000	0.580	0.000	1.440	0.660	0.000
SiO_2	7.520	5.540	0.870	3.230	1.650	8.150	3.180	4.930
K_2O	0.400	0.410	0.000	0.000	0.000	0.000	0.000	0.000
CaO	12.98	13.22	16.62	13.77	18.94	13.74	12.18	10.48
TiO_2	10.77	11.37	11.91	11.42	11.68	11.77	12.32	9.67
MnO	0.000	0.000	0.000	0.000	0.220	0.280	0.000	0.310
Fe_2O_3	1.020	1.080	0.000	0.470	0.280	0.470	0.310	2.730
SrO	5.090	5.200	0.770	2.040	2.780	3.470	3.400	2.550
Y_2O_3	0.000	0.000	0.000	0.000	0.000	0.000	0.000	0.000
ZrO_2	0.000	0.000	0.000	0.000	1.140	0.800	1.000	0.000
Nb_2O_5	38.32	41.14	42.62	34.57	36.86	33.28	30.31	40.01
BaO	0.000	0.000	0.000	0.000	0.000	0.000	0.000	0.000
La_2O_3	0.000	0.000	0.000	0.000	0.000	0.000	0.000	0.000
Ce_2O_3	0.830	1.000	1.130	1.220	0.880	0.000	0.000	1.250
Pr_2O_3	0.000	0.000	0.000	0.000	0.000	0.000	0.000	0.000
Nd_2O_3	0.000	0.000	0.000	0.000	0.000	0.000	0.000	0.000
PbO	0.000	0.000	1.880	0.790	1.280	0.000	2.070	1.600
Ta_2O_5	0.000	0.000	0.000	0.000	0.000	0.000	2.420	2.430
ThO_2	0.000	0.770	0.770	0.000	0.000	0.000	0.000	1.470
UO_2	13.78	14.01	16.28	13.13	9.640	23.48	18.05	17.68
F	0.000	0.000	0.000	0.000	0.000	0.000	0.000	0.000
Sum	**91.58**	**94.38**	**97.74**	**82.11**	**87.68**	**97.6**	**86.24**	**95.11**
Na	0.000	0.000	0.652	0.121	0.324	0.081	0.088	0.000
K	0.029	0.031	0.000	0.000	0.000	0.000	0.000	0.000
Ca	0.801	0.827	1.224	1.036	1.457	0.854	0.927	0.680
Mn	0.000	0.000	0.000	0.000	0.013	0.014	0.000	0.016
Sr	0.170	0.176	0.031	0.083	0.116	0.117	0.140	0.090
Y	0.000	0.000	0.000	0.000	0.000	0.000	0.000	0.000
Ba	0.000	0.000	0.000	0.000	0.000	0.000	0.000	0.000
La	0.000	0.000	0.000	0.000	0.000	0.000	0.000	0.000
Ce	0.017	0.021	0.028	0.031	0.023	0.000	0.000	0.028
Pr	0.000	0.000	0.000	0.000	0.000	0.000	0.000	0.000
Nd	0.000	0.000	0.000	0.000	0.000	0.000	0.000	0.000
Pb	0.000	0.000	0.035	0.000	0.000	0.025	0.000	0.040
Th	0.000	0.010	0.012	0.000	0.000	0.000	0.000	0.020
U	0.177	0.182	0.249	0.205	0.154	0.303	0.285	0.238
Site A	**1.194**	**2.231**	**1.247**	**1.492**	**2.112**	**1.368**	**1.479**	**1.098**
A-def	**0.806**	**0.000**	**0.743**	**0.508**	**0.000**	**0.632**	**0.521**	**0.902**
Al	0.059	0.044	0.000	0.048	0.000	0.098	0.055	0.000
Si	0.433	0.323	0.060	0.227	0.118	0.473	0.226	0.299
Ti	0.466	0.499	0.616	0.603	0.630	0.513	0.658	0.441
Fe	0.044	0.047	0.000	0.025	0.015	0.021	0.017	0.124
Zr	0.000	0.000	0.000	0.000	0.040	0.023	0.035	0.000
Nb	0.998	1.086	1.325	1.097	1.196	0.873	0.963	1.096
Ta	0.000	0.000	0.000	0.000	0.000	0.000	0.047	0.040
Site B	**2.000**	**2.000**	**2.000**	**2.000**	**2.000**	**2.000**	**2.000**	**2.000**

	Bin-1	Bin-2	Bin-3	Bin-4	Bin-5	Bin-6	Bin-7	Bin-8
Na_2O	4.730	0.090	0.140	8.170	0.050	5.860	1.600	0.200
Al_2O_3	0.050	0.840	1.520	0.050	1.700	0.050	0.130	0.140
SiO_2	1.310	9.420	14.80	0.250	4.590	1.080	1.600	1.450
K_2O	0.090	0.070	0.350	0.050	0.250	0.090	0.080	0.070
CaO	13.82	4.160	5.670	15.55	0.200	14.08	11.71	9.74
TiO_2	0.820	2.510	3.350	2.870	1.770	0.820	0.980	1.400
MnO	0.050	0.740	0.070	0.050	0.050	0.060	0.050	2.620
Fe_2O_3	1.010	2.160	2.260	0.510	3.300	1.080	1.620	5.850
SrO	1.890	2.980	5.730	1.100	0.580	1.340	3.470	0.180
Y_2O_3	0.000	0.000	0.000	0.000	0.000	0.000	0.000	0.000
ZrO_2	1.810	1.100	0.700	2.330	3.120	2.610	4.140	0.630
Nb_2O_5	65.11	48.02	40.92	65.20	62.94	64.50	64.02	65.12
BaO	0.570	12.39	5.360	0.090	9.880	0.170	1.090	0.930
La_2O_3	0.070	0.270	0.310	0.060	0.060	0.190	0.090	0.620
Ce_2O_3	0.280	2.330	1.050	0.180	0.320	0.210	0.270	2.010
Pr_2O_3	0.000	0.000	0.000	0.000	0.000	0.000	0.000	0.000
Nd_2O_3	0.000	0.000	0.000	0.000	0.000	0.000	0.000	0.000
PbO	1.080	0.550	0.100	0.100	0.100	0.100	2.670	0.100
Ta_2O_5	0.100	0.100	0.100	0.110	0.520	0.110	0.130	0.100
ThO_2	0.230	0.300	0.100	0.100	1.090	0.100	0.140	0.340
UO_2	0.320	2.920	8.160	0.120	0.820	0.120	0.140	0.830
F	3.400	0.300	0.230	4.500	0.820	4.500	1.950	0.100
Sum	**96.54**	**91.25**	**90.62**	**101.04**	**91.14**	**99.15**	**95.01**	**92.13**
Na	0.555	0.010	0.014	0.947	0.000	0.690	0.179	0.021
K	0.007	0.005	0.023	0.000	0.016	0.007	0.006	0.005
Ca	0.897	0.246	0.306	0.996	0.011	0.916	0.723	0.567
Mn	0.000	0.035	0.003	0.000	0.000	0.003	0.000	0.121
Sr	0.066	0.095	0.168	0.038	0.017	0.047	0.116	0.006
Y	0.000	0.000	0.000	0.000	0.000	0.000	0.000	0.000
Ba	0.014	0.268	0.106	0.002	0.191	0.004	0.025	0.020
La	0.002	0.006	0.006	0.001	0.001	0.004	0.002	0.012
Ce	0.006	0.047	0.019	0.004	0.006	0.005	0.006	0.040
Pr	0.000	0.000	0.000	0.000	0.000	0.000	0.000	0.000
Nd	0.000	0.000	0.000	0.000	0.000	0.000	0.000	0.000
Pb	0.018	0.008	0.000	0.000	0.000	0.000	0.041	0.000
Th	0.003	0.004	0.000	0.000	0.012	0.000	0.002	0.004
U	0.004	0.036	0.092	0.002	0.009	0.002	0.002	0.010
Site A	**1.571**	**0.760**	**0.736**	**1.994**	**0.263**	**1.994**	**1.101**	**0.806**
A-def	**0.429**	**1.240**	**1.264**	**0.006**	**1.737**	**0.006**	**0.899**	**1.194**
Al	0.009	0.032	0.043	0.000	0.099	0.000	0.009	0.003
Si	0.092	0.160	0.761	0.066	0.227	0.080	0.079	0.075
Ti	0.042	0.077	0.048	0.037	0.066	0.037	0.057	0.052
Fe	0.070	0.132	0.115	0.049	0.122	0.046	0.238	0.205
Zr	0.116	0.083	0.042	0.077	0.075	0.053	0.017	0.014
Nb	1.668	1.515	0.988	1.770	1.404	1.783	1.600	1.649
Ta	0.002	0.002	0.003	0.000	0.007	0.000	0.000	0.002
Site B	**2.000**	**2.000**	**2.000**	**2.000**	**2.000**	**2.000**	**2.000**	**2.000**
F	0.651	0.052	0.037	0.851	0.000	0.751	0.355	0.000

	Lovo-1	Lovo-2	Lovo-3	Lovo-4	Lovo-5	Lovo-6	Qaq-1	Qaq-2
Na_2O	6.900	5.240	1.010	6.730	5.960	6.030	8.190	0.320
Al_2O_3	0.000	0.000	0.000	0.000	0.000	0.000	0.000	0.000
SiO_2	0.360	0.000	0.000	0.000	0.510	0.660	2.490	0.810
K_2O	0.000	0.000	0.000	0.000	0.000	0.000	0.000	0.000
CaO	14.79	5.470	2.690	15.61	8.770	8.710	14.31	5.560
TiO_2	9.430	9.010	9.450	9.270	9.040	8.800	3.690	3.880
MnO	0.010	0.000	0.000	0.000	1.110	0.980	0.000	0.000
Fe_2O_3	0.080	0.000	0.070	0.090	0.420	0.530	0.490	1.720
SrO	3.670	3.000	1.910	1.730	0.950	0.720	0.000	1.160
Y_2O_3	0.000	0.000	0.000	0.000	0.000	0.000	0.000	0.000
ZrO_2	0.000	0.000	0.000	0.000	0.000	0.000	0.070	0.460
Nb_2O_5	59.67	45.88	46.00	59.66	62.17	62.76	64.15	30.07
BaO	0.000	0.000	0.000	0.000	1.110	1.270	0.000	2.050
La_2O_3	0.470	1.170	2.040	0.630	1.870	1.680	0.370	0.440
Ce_2O_3	0.980	2.890	3.520	1.270	2.820	3.010	1.410	0.730
Pr_2O_3	0.000	0.000	0.000	0.000	0.230	0.370	0.000	0.000
Nd_2O_3	0.000	1.040	0.470	0.660	1.010	1.060	0.350	0.020
PbO	0.000	0.000	0.000	0.000	0.000	0.000	0.000	0.000
Ta_2O_5	0.230	1.940	1.570	0.000	0.000	0.340	0.020	23.07
ThO_2	0.000	0.000	0.000	3.560	1.550	0.550	0.240	0.070
UO_2	0.890	20.73	26.35	0.000	0.870	1.670	0.350	20.32
F	0.000	0.000	0.000	0.000	0.000	0.000	0.000	0.000
Sum	**97.48**	**96.37**	**95.08**	**99.21**	**98.39**	**99.14**	**96.13**	**90.68**
Na	0.774	0.725	0.138	0.767	0.647	0.647	0.987	0.051
K	0.000	0.000	0.000	0.000	0.000	0.000	0.000	0.000
Ca	0.917	0.418	0.203	0.983	0.526	0.516	0.953	0.490
Mn	0.000	0.000	0.000	0.000	0.053	0.046	0.000	0.000
Sr	0.123	0.124	0.078	0.059	0.031	0.023	0.000	0.055
Y	0.000	0.000	0.000	0.000	0.000	0.000	0.000	0.000
Ba	0.000	0.000	0.000	0.000	0.024	0.028	0.000	0.066
La	0.010	0.031	0.053	0.014	0.039	0.034	0.008	0.013
Ce	0.021	0.075	0.091	0.027	0.058	0.061	0.032	0.022
Pr	0.000	0.000	0.000	0.000	0.005	0.007	0.000	0.000
Nd	0.000	0.026	0.012	0.014	0.020	0.021	0.008	0.001
Pb	0.000	0.000	0.000	0.000	0.000	0.000	0.000	0.000
Th	0.000	0.000	0.000	0.048	0.020	0.007	0.003	0.001
U	0.011	0.329	0.413	0.000	0.011	0.021	0.005	0.372
Site A	**1.856**	**1.728**	**0.988**	**1.912**	**1.434**	**1.411**	**1.996**	**1.071**
A-def	**0.144**	**0.272**	**1.012**	**0.088**	**0.566**	**0.589**	**0.004**	**0.929**
Al	0.000	0.000	0.000	0.000	0.000	0.000	0.000	0.000
Si	0.021	0.000	0.000	0.000	0.029	0.037	0.155	0.067
Ti	0.410	0.483	0.501	0.410	0.381	0.366	0.172	0.240
Fe	0.003	0.000	0.004	0.004	0.018	0.022	0.023	0.106
Zr	0.000	0.000	0.000	0.000	0.000	0.000	0.000	0.000
Nb	1.562	1.479	1.465	1.586	1.572	1.570	1.650	1.071
Ta	0.004	0.038	0.030	0.000	0.000	0.005	0.000	0.516
Site B	**2.000**	**2.000**	**2.000**	**2.000**	**2.000**	**2.000**	**2.000**	**2.000**
F	0.000	0.000	0.000	0.000	0.000	0.000	0.000	0.000

	PL-9	PL-10	Mt-W-A	Mt-W-B	Mt-W-C	Mt-W-D	Mt-W-E	Mt-W-E2
Na_2O	2.080	0.300	5.600	7.200	2.600	3.300	7.900	5.700
Al_2O_3	0.000	1.780	0.000	0.000	0.000	0.000	0.000	0.000
SiO_2	2.050	5.850	0.000	0.000	0.000	0.000	0.000	0.000
K_2O	0.000	0.310	0.000	0.000	0.000	0.000	0.000	0.000
CaO	13.68	14.88	2.800	0.500	4.600	6.000	14.80	12.50
TiO_2	15.34	8.740	2.100	2.600	3.500	2.400	2.900	0.000
MnO	0.000	0.000	0.000	0.000	0.000	0.000	0.000	0.000
Fe_2O_3	0.370	1.340	0.300	0.000	0.500	2.300	0.000	0.300
SrO	0.840	4.220	5.200	0.000	14.00	10.40	3.100	3.400
Y_2O_3	0.000	0.000	0.000	0.000	0.000	0.000	0.000	0.000
ZrO_2	3.280	0.000	0.000	0.000	0.000	0.000	0.000	0.000
Nb_2O_5	25.35	30.50	63.30	62.70	67.10	57.20	67.90	68.10
BaO	0.000	0.000	0.000	0.000	0.000	0.000	0.000	0.000
La_2O_3	0.000	0.000	0.000	0.000	0.000	0.000	0.000	0.000
Ce_2O_3	1.690	0.820	13.20	23.60	0.000	1.800	0.000	0.000
Pr_2O_3	0.000	0.000	0.000	0.000	0.000	0.000	0.000	0.000
Nd_2O_3	0.000	0.000	0.000	0.000	0.000	0.000	0.000	0.000
PbO	3.300	2.360	0.000	0.000	0.000	0.000	0.000	0.000
Ta_2O_5	2.260	0.000	0.000	0.000	0.000	0.000	0.000	0.000
ThO_2	1.570	3.200	0.000	0.000	0.000	0.000	0.000	0.000
UO_2	24.84	18.19	0.000	0.000	0.000	0.000	0.000	0.000
F	0.000	0.000	0.000	0.000	0.000	0.000	0.000	0.000
Sum	**96.65**	**92.79**	**92.60**	**96.80**	**92.30**	**83.40**	**96.70**	**89.00**
Na	0.293	0.040	0.704	0.848	0.311	0.437	0.864	0.675
K	0.000	0.027	0.000	0.000	0.000	0.000	0.000	0.000
Ca	1.064	1.088	0.194	0.032	0.304	0.439	0.894	0.818
Mn	0.000	0.017	0.000	0.000	0.000	0.000	0.000	0.000
Sr	0.035	0.167	0.260	0.000	0.500	0.412	0.101	0.120
Y	0.000	0.000	0.000	0.000	0.000	0.000	0.000	0.000
Ba	0.000	0.000	0.000	0.000	0.000	0.000	0.000	0.000
La	0.000	0.000	0.000	0.000	0.000	0.000	0.000	0.000
Ce	0.045	0.020	0.298	0.500	0.000	0.042	0.000	0.000
Pr	0.000	0.000	0.000	0.000	0.000	0.000	0.000	0.000
Nd	0.000	0.000	0.000	0.000	0.000	0.000	0.000	0.000
Pb	0.026	0.065	0.000	0.000	0.000	0.000	0.000	0.000
Th	0.026	0.050	0.000	0.000	0.000	0.000	0.000	0.000
U	0.401	0.276	0.000	0.000	0.000	0.000	0.000	0.000
Site A	**1.930**	**1.729**	**1.392**	**1.381**	**1.116**	**1.332**	**1.853**	**1.614**
A-def	**0.070**	**0.271**	**0.608**	**0.619**	**0.884**	**0.668**	**0.147**	**0.386**
Al	0.000	0.143	0.000	0.000	0.000	0.000	0.000	0.000
Si	0.149	0.399	0.000	0.000	0.000	0.000	0.000	0.000
Ti	0.838	0.448	0.102	0.118	0.162	0.123	0.122	0.013
Fe	0.020	0.069	0.014	0.000	0.023	0.118	0.000	0.000
Zr	0.116	0.000	0.000	0.000	0.000	0.000	0.000	0.000
Nb	0.832	0.941	1.855	1.721	1.872	1.767	1.730	1.881
Ta	0.045	0.000	0.000	0.000	0.000	0.000	0.000	0.000
Site B	**2.000**	**2.000**	**1.972**	**1.840**	**2.057**	**2.009**	**1.859**	**1.894**

	Bin-9	Bin-10	Bin-11	Bin-12	Bin-13	Kola-1	Kola-2	Kola-3
Na_2O	0.200	0.080	0.400	0.440	0.080	7.240	7.270	6.870
Al_2O_3	0.050	0.720	1.390	1.400	0.800	0.000	0.000	0.000
SiO_2	1.340	15.04	11.42	10.93	11.11	0.000	0.000	0.000
K_2O	0.050	0.200	0.210	0.240	0.250	0.000	0.000	0.000
CaO	10.18	6.230	6.480	6.480	4.050	13.68	12.77	12.57
TiO_2	1.230	1.270	3.100	2.990	2.800	2.620	3.000	2.720
MnO	2.660	0.090	0.140	0.240	0.130	0.000	0.000	0.000
Fe_2O_3	4.850	3.030	2.760	2.600	1.580	0.110	0.110	0.210
SrO	0.240	6.140	4.980	5.000	2.110	1.150	1.140	1.070
Y_2O_3	0.000	0.000	0.000	0.000	0.000	0.000	0.000	0.000
ZrO_2	0.520	1.700	1.080	1.220	0.530	0.000	0.000	0.000
Nb_2O_5	65.05	43.17	44.00	42.91	47.65	67.35	65.93	64.97
BaO	1.880	5.640	7.910	7.290	13.10	0.000	0.000	0.000
La_2O_3	0.440	0.330	0.230	0.280	0.180	0.110	0.420	0.000
Ce_2O_3	2.110	0.600	3.370	3.130	0.890	1.850	2.070	1.940
Pr_2O_3	0.000	0.000	0.000	0.000	0.000	0.000	0.000	0.000
Nd_2O_3	0.000	0.000	0.000	0.000	0.000	0.400	1.030	0.940
PbO	0.100	0.100	0.100	2.380	0.100	0.000	0.000	0.000
Ta_2O_5	0.130	0.200	0.100	0.100	0.100	0.000	0.000	0.000
ThO_2	0.460	0.100	0.150	0.160	0.100	2.430	3.420	3.880
UO_2	0.240	7.680	2.630	2.560	6.990	0.000	0.000	0.000
F	0.100	0.110	0.620	0.750	0.180	0.000	0.000	0.000
Sum	**91.58**	**92.18**	**90.61**	**90.69**	**92.46**	**96.94**	**97.16**	**96.17**
Na	0.022	0.008	0.041	0.046	0.008	0.864	0.877	0.844
K	0.000	0.013	0.014	0.017	0.017	0.000	0.000	0.000
Ca	0.612	0.338	0.367	0.377	0.233	0.902	0.851	0.853
Mn	0.126	0.004	0.006	0.011	0.006	0.000	0.000	0.000
Sr	0.008	0.180	0.152	0.158	0.066	0.041	0.041	0.039
Y	0.000	0.000	0.000	0.000	0.000	0.000	0.000	0.000
Ba	0.041	0.112	0.164	0.155	0.276	0.000	0.000	0.000
La	0.009	0.006	0.004	0.006	0.004	0.002	0.010	0.000
Ce	0.000	0.011	0.065	0.062	0.018	0.042	0.047	0.045
Pr	0.000	0.000	0.000	0.000	0.000	0.000	0.000	0.000
Nd	0.000	0.000	0.000	0.000	0.000	0.009	0.023	0.021
Pb	0.000	0.000	0.000	0.035	0.000	0.000	0.000	0.000
Th	0.006	0.000	0.002	0.002	0.000	0.034	0.048	0.056
U	0.003	0.086	0.031	0.031	0.084	0.000	0.000	0.000
Site A	**0.872**	**0.759**	**0.846**	**0.900**	**0.712**	**1.894**	**1.897**	**1.858**
A-def	**1.128**	**1.241**	**1.154**	**1.100**	**1.288**	**0.106**	**0.103**	**0.142**
Al	0.090	0.087	0.090	0.051	0.055	0.000	0.000	0.000
Si	0.747	0.602	0.594	0.598	0.521	0.000	0.000	0.000
Ti	0.127	0.123	0.122	0.113	0.104	0.121	0.140	0.130
Fe	0.086	0.110	0.106	0.064	0.090	0.005	0.005	0.010
Zr	0.017	0.028	0.032	0.014	0.030	0.000	0.000	0.000
Nb	0.933	1.050	1.055	1.159	1.200	1.874	1.854	1.860
Ta	0.000	0.000	0.000	0.001	0.002	0.000	0.000	0.000
Site B	**2.000**	**2.000**	**2.000**	**2.000**	**2.000**	**2.000**	**2.000**	**2.000**
F	0.000	0.018	0.104	0.129	0.031	0.000	0.000	0.000

	New-1	New-2	New-3	New-4	New-5	New-6	New-7	New-8
SiO_2	0.130	0.170	0.600	0.230	0.850	0.510	1.340	0.780
TiO_2	5.740	7.070	4.150	4.230	4.700	3.460	3.650	4.770
Fe_2O_3	3.830	2.440	4.000	3.930	3.750	1.890	2.140	2.090
MnO	0.000	0.000	0.000	0.060	0.000	0.000	0.000	0.020
MgO	0.020	0.020	0.010	0.120	0.080	0.010	0.020	0.100
CaO	6.180	6.800	4.920	4.160	5.340	6.760	6.150	7.500
BaO	7.580	4.780	7.650	8.740	9.680	0.200	0.190	0.200
SrO	3.300	3.150	4.300	4.510	3.330	1.340	1.120	1.450
Na_2O	0.000	1.620	0.280	0.300	0.120	1.300	0.490	3.110
ZrO_2	0.200	0.170	0.230	0.100	0.220	0.220	0.300	0.370
Nb_2O_5	43.57	42.35	43.82	44.71	44.17	51.01	50.32	48.32
La_2O_3	0.140	0.100	0.150	0.170	0.190	0.190	0.140	0.180
Ce_2O_3	0.570	0.280	0.520	0.670	0.550	0.590	0.550	0.580
Nd_2O_3	0.140	0.070	0.070	0.220	0.120	0.160	0.170	0.170
Sm_2O_3	0.010	0.010	0.010	0.030	0.030	0.020	0.010	0.030
Gd_2O_3	0.010	0.000	0.010	0.010	0.010	0.000	0.000	0.000
Ta_2O_5	3.990	4.250	4.900	4.710	3.700	6.290	6.180	4.750
PbO	1.800	2.500	2.120	1.700	1.610	2.620	2.450	2.500
UO_2	20.39	21.47	19.66	19.54	19.70	22.56	22.92	20.52
F	0.250	0.330	0.340	0.420	0.170	0.330	0.440	0.250
Sum	**100.03**	**99.49**	**99.64**	**100.44**	**100.30**	**101.47**	**100.55**	**99.70**
Mn	0.000	0.000	0.000	0.001	0.000	0.000	0.000	0.004
Mg	0.001	0.002	0.001	0.050	0.004	0.001	0.002	0.050
Ca	0.469	0.526	0.377	0.319	0.404	0.492	0.435	0.549
Ba	0.211	0.135	0.214	0.245	0.268	0.005	0.005	0.005
Sr	0.136	0.138	0.178	0.187	0.137	0.053	0.043	0.057
Na	0.000	0.227	0.039	0.042	0.016	0.171	0.063	0.412
La	0.004	0.003	0.004	0.004	0.005	0.005	0.003	0.005
Ce	0.015	0.007	0.014	0.018	0.014	0.015	0.013	0.015
Nd	0.004	0.002	0.002	0.006	0.003	0.004	0.004	0.004
Sm	0.001	0.001	0.001	0.007	0.001	0.001	0.000	0.002
Gd	0.001	0.000	0.001	0.001	0.001	0.000	0.000	0.000
Pb	0.034	0.049	0.041	0.033	0.031	0.048	0.044	0.046
U	0.322	0.345	0.313	0.312	0.310	0.341	0.337	0.312
Site A	**1.197**	**1.435**	**1.815**	**1.225**	**1.194**	**1.136**	**0.949**	**1.461**
A-def	**0.803**	**0.565**	**0.185**	**0.775**	**0.806**	**0.864**	**1.051**	**0.539**
Si	0.009	0.012	0.043	0.016	0.060	0.035	0.089	0.053
Ti	0.306	0.384	0.223	0.228	0.250	0.177	0.181	0.245
Fe	0.204	0.133	0.215	0.212	0.199	0.097	0.106	0.108
Zr	0.007	0.006	0.008	0.003	0.008	0.007	0.010	0.012
Nb	1.397	1.382	1.416	1.448	1.412	1.568	1.503	1.493
Ta	0.077	0.083	0.095	0.092	0.071	0.116	0.111	0.088
Site B	**2.000**	**2.000**	**2.000**	**2.000**	**2.000**	**2.000**	**2.000**	**2.000**
F	0.056	0.075	0.077	0.095	0.038	0.037	0.036	0.050

APPENDIX V

SEM-EDS analyses for pyrochlore-group minerals from the St. Lawrence Columbium deposit

St. Lawrence Columbium pyrochlore legend

Sample #	General reference	comments
C	Petruk and Owens, (1975)	Homogeneous pyrochlore grains
D	Petruk and Owens, (1975)	Homogeneous pyrochlore grains
K	Petruk and Owens, (1975)	Homogeneous pyrochlore grains
A (Zone 1)	Petruk and Owens, (1975)	Zoned Cerium pyrochlore
A (Zone 2)	Petruk and Owens, (1975)	Zoned Cerium pyrochlore
B (Zone 1)	Petruk and Owens, (1975)	Zoned Cerium pyrochlore
B (Zone 2)	Petruk and Owens, (1975)	Zoned Cerium pyrochlore
U-pyro	Petruk and Owens, (1975)	Uranoan pyrochlore
60-1	Kalogeropoulos, (1977)	Cerium pyrochlore
60-5	Kalogeropoulos, (1977)	Cerium pyrochlore
70-2	Kalogeropoulos, (1977)	Cerium pyrochlore
70-3	Kalogeropoulos, (1977)	Cerium pyrochlore
80-4	Kalogeropoulos, (1977)	Cerium pyrochlore
90-2r	Kalogeropoulos, (1977)	Cerium pyrochlore
90-3	Kalogeropoulos, (1977)	Cerium pyrochlore
90-5	Kalogeropoulos, (1977)	Cerium pyrochlore
2ON-1	Kalogeropoulos, (1977)	Cerium pyrochlore
2ON-4C	Kalogeropoulos, (1977)	Cerium pyrochlore
2ON-6	Kalogeropoulos, (1977)	Cerium pyrochlore
2ON-8b	Kalogeropoulos, (1977)	Cerium pyrochlore
2O-1	Kalogeropoulos, (1977)	Cerium pyrochlore
2O-5R	Kalogeropoulos, (1977)	Cerium pyrochlore
30-2	Kalogeropoulos, (1977)	Cerium pyrochlore
30-4	Kalogeropoulos, (1977)	Cerium pyrochlore

	C	D	K	A (Zone 1)	A (Zone 2)	B (Zone 1)	B (Zone 2)	U-Pyro
Na_2O	6.01	3.69	5.76	6.37	6.11	5.38	5.67	4.68
CaO	17.05	18.29	15.19	15.06	14.87	17.06	15.58	14.17
MnO	0.07	0.24	0.21	0.10	0.06	0.04	0.03	0.11
SrO	0.68	0.27	0.44	0.48	0.61	0.72	0.73	0.61
FeO	0.66	1.38	1.21	1.10	0.37	1.09	0.69	2.28
U_3O_8	0.00	0.00	0.24	0.00	0.84	0.00	0.36	8.82
Ce_2O_3	3.28	6.47	6.17	5.11	4.02	2.56	4.87	5.51
Nd_2O_3	0.25	0.79	0.45	0.41	0.46	0.21	0.50	0.84
La_2O_3	0.69	0.97	1.08	0.97	0.96	0.67	0.92	1.15
Nb_2O_5	65.33	59.02	62.19	64.07	63.31	64.47	62.36	56.37
Ta_2O_5	0.12	0.16	0.45	0.37	0.56	0.39	0.39	2.23
TiO_2	4.21	5.57	3.84	3.26	4.08	3.41	4.68	3.57
ZrO_2	0.00	0.41	0.19	0.14	0.08	0.11	0.11	0.32
SiO_2	0.00	0.00	0.00	0.00	0.00	0.00	0.00	0.00
Total	**98.35**	**97.26**	**97.43**	**97.44**	**96.33**	**96.11**	**96.39**	**100.67**
Na	0.710	0.460	0.710	0.770	0.740	0.650	0.690	0.600
Ca	1.120	1.260	1.030	1.010	1.000	1.150	1.050	1.010
Mn	0.004	0.010	0.010	0.010	0.004	0.002	0.002	0.010
Sr	0.020	0.010	0.020	0.020	0.020	0.030	0.030	0.020
Fe^{2+}	0.030	0.070	0.050	0.040	0.020	0.060	0.040	0.050
U	0.000	0.000	0.004	0.000	0.010	0.000	0.004	0.130
Ce	0.070	0.150	0.140	0.120	0.090	0.060	0.100	0.130
Nd	0.010	0.020	0.010	0.010	0.010	0.004	0.010	0.020
La	0.010	0.020	0.030	0.020	0.020	0.020	0.020	0.030
Total in *A*	**1.98**	**2.00**	**2.00**	**2.00**	**1.91**	**1.96**	**1.98**	**2.00**
***A*-def**	**0.02**	**0.00**	**0.00**	**0.00**	**0.09**	**0.04**	**0.02**	**0.00**
Nb	1.800	1.710	1.790	1.820	1.800	1.830	1.770	1.690
Ta	0.010	0.002	0.010	0.010	0.010	0.010	0.010	0.040
Ti	0.190	0.270	0.170	0.150	0.190	0.160	0.220	0.180
Zr	0.000	0.010	0.010	0.004	0.002	0.004	0.004	0.020
Fe^{3+}	0.000	0.004	0.020	0.020	0.000	0.000	0.000	0.070
Total in *B*	**2.00**	**2.00**	**2.00**	**2.00**	**2.00**	**2.00**	**2.00**	**2.00**

	60-1	60-5	70-2	70-3	80-4	90-2r	90-3	90-5
Nb_2O_5	60.49	58.47	51.21	54.69	59.71	49.21	52.99	50.50
Ta_2O_3	1.63	1.25	2.01	1.62	0.32	0.36	0.52	0.00
TiO_2	2.36	4.09	8.45	5.82	5.20	7.44	6.83	7.13
ZrO_2	0.00	0.00	0.60	0.00	0.00	0.84	0.50	0.77
Al_2O_3	0.34	0.15	0.24	0.36	0.00	0.37	0.20	0.21
Fe_2O_3	2.25	2.30	1.48	1.94	0.55	2.34	2.36	2.12
SnO_2	0.00	0.00	0.00	0.00	0.00	0.00	0.00	0.00
CaO	18.02	16.53	17.12	17.20	15.50	17.98	17.20	18.78
Na_2O	4.62	3.87	4.43	4.38	5.85	2.63	2.25	2.68
MnO	0.00	0.00	0.00	0.00	0.00	0.00	0.00	0.00
Ce_2O_3	4.83	7.41	7.98	8.58	3.60	10.86	10.30	9.70
La_2O_3	0.39	1.15	1.84	1.62	0.51	2.63	0.38	0.33
Pr_2O_3	0.00	0.00	0.00	0.00	0.00	0.00	0.00	0.00
Nd_2O_3	0.72	2.18	1.38	1.41	2.08	2.75	1.00	1.95
Eu_2O_3	0.17	0.00	0.81	0.00	0.16	0.00	0.00	0.00
Gd_2O_3	1.28	0.73	0.00	0.00	0.76	0.49	0.00	0.48
Y_2O_3	0.00	0.00	0.00	0.00	0.00	0.00	0.00	0.00
ThO_2	0.00	0.74	0.59	0.52	0.76	0.17	0.00	0.21
U_2O_3	0.00	0.00	0.00	0.00	0.00	0.81	1.14	1.19
F	2.48	2.42	3.04	2.89	4.76	0.02	1.34	2.56
SiO_2	0.00	0.00	0.00	0.00	0.00	1.01	1.17	0.55
Total	**100.99**	**99.99**	**101.84**	**101.53**	**99.76**	**101.21**	**100.15**	**99.45**
Ca	1.220	1.115	1.156	1.173	1.057	1.261	1.170	1.323
Na	0.566	0.472	0.541	0.540	0.722	0.334	0.277	0.342
Mn	0.000	0.000	0.000	0.000	0.000	0.000	0.000	0.000
Ce	0.112	0.171	0.184	0.200	0.084	0.260	0.239	0.233
La	0.009	0.027	0.043	0.038	0.012	0.063	0.009	0.008
Pr	0.000	0.000	0.000	0.000	0.000	0.000	0.000	0.000
Nd	0.016	0.049	0.031	0.032	0.047	0.064	0.023	0.046
Eu	0.004	0.000	0.017	0.000	0.003	0.000	0.000	0.000
Gd	0.027	0.015	0.000	0.000	0.016	0.010	0.000	0.010
Y	0.000	0.000	0.000	0.000	0.000	0.000	0.000	0.000
Th	0.000	0.000	0.008	0.008	0.011	0.003	0.000	0.003
U	0.000	0.000	0.000	0.000	0.000	0.011	0.015	0.017
Total in *A*	**1.953**	**1.86**	**1.981**	**1.991**	**1.954**	**2**	**1.734**	**1.983**
***A*-def**	**0.047**	**0.140**	**0.019**	**0.009**	**0.046**	**0.000**	**0.266**	**0.017**
Nb	1.728	1.665	1.459	1.574	1.719	1.457	1.521	1.501
Ta	0.028	0.021	0.034	0.028	0.005	0.006	0.009	0.000
Ti	0.112	0.194	0.400	0.278	0.249	0.366	0.326	0.353
Zr	0.000	0.000	0.018	0.000	0.000	0.027	0.105	0.025
Al	0.025	0.011	0.018	0.027	0.000	0.028	0.105	0.016
Fe	0.106	0.109	0.070	0.093	0.026	0.115	0.113	0.105
Sn	0.000	0.000	0.000	0.000	0.000	0.000	0.000	0.000
Total in *B*	**2.00**	**2.00**	**2.00**	**2.00**	**2.00**	**2.00**	**2.00**	**2.00**

	2ON-1	2ON-4C	2ON-6	2ON-8b	2O-1	2O-5R	30-2	30-4
Nb_2O_5	49.87	59.31	50.56	52.80	54.48	53.84	50.00	49.10
Ta_2O_3	0.00	0.00	0.17	0.00	2.20	1.09	2.20	3.84
TiO_2	7.21	2.12	5.80	7.11	6.50	5.41	4.99	5.22
ZrO_2	0.00	0.00	0.19	0.13	0.26	0.65	0.78	0.94
Al_2O_3	0.90	0.30	0.33	0.24	0.11	1.36	0.00	0.00
Fe_2O_3	1.81	2.84	2.11	1.53	2.46	2.68	2.88	2.93
SnO_2	3.43	0.00	3.00	0.00	0.00	0.00	0.00	0.00
CaO	16.48	17.01	15.41	16.22	18.04	18.40	16.07	16.43
Na_2O	3.50	4.20	2.91	4.04	2.76	2.69	3.11	2.34
MnO	0.00	0.53	0.00	0.28	0.16	0.00	0.00	0.00
Ce_2O_3	8.93	6.60	9.05	8.73	8.35	9.25	10.14	10.13
La_2O_3	1.33	0.84	2.02	0.61	1.20	1.40	1.76	1.74
Pr_2O_3	0.53	0.34	1.19	0.65	0.21	0.70	0.67	0.84
Nd_2O_3	1.33	0.86	2.07	1.88	1.38	0.89	2.02	3.54
Eu_2O_3	0.15	0.00	0.17	0.23	0.25	0.00	0.00	0.00
Cd_2O_3	0.64	0.44	0.73	0.68	0.46	0.93	0.77	0.56
Y_2O_3	0.00	0.17	0.33	0.00	0.00	0.00	0.00	0.00
ThO_2	0.00	0.00	0.66	0.21	0.00	0.00	0.00	0.44
U_2O_3	0.00	0.88	0.00	0.00	0.00	0.49	0.36	0.18
F	0.96	1.17	1.98	2.41	1.02	0.98	2.16	2.46
SiO_2	0.89	0.00	0.62	0.00	0.20	0.70	1.28	1.35
Total	**100.32**	**98.76**	**100.53**	**98.43**	**99.48**	**101.55**	**99.6**	**102.35**
Ca	1.112	1.179	1.081	1.132	1.234	1.208	1.167	1.180
Na	0.427	0.527	0.370	0.510	0.342	0.319	0.409	0.304
Mn	0.000	0.051	0.000	0.027	0.015	0.000	0.000	0.000
Ce	0.206	0.156	0.217	0.208	0.195	0.219	0.251	0.249
La	0.031	0.020	0.049	0.015	0.028	0.032	0.044	0.043
Pr	0.012	0.008	0.028	0.015	0.049	0.016	0.016	0.020
Nd	0.030	0.019	0.048	0.044	0.031	0.019	0.049	0.085
Eu	0.003	0.000	0.038	0.005	0.005	0.000	0.000	0.000
Gd	0.013	0.009	0.016	0.015	0.010	0.000	0.017	0.012
Y	0.000	0.003	0.007	0.000	0.000	0.006	0.000	0.000
Th	0.000	0.000	0.010	0.003	0.000	0.190	0.000	0.007
U	0.000	0.012	0.000	0.000	0.000	0.848	0.005	0.002
Total in *A*	**1.835**	**1.978**	**1.830**	**1.974**	**1.866**	**1.838**	**1.960**	**1.903**
A-def	**0.165**	**0.022**	**0.170**	**0.026**	**0.134**	**0.162**	**0.040**	**0.097**
Nb	1.420	1.736	1.497	1.554	1.515	1.491	1.532	1.488
Ta	0.000	0.000	0.003	0.000	0.038	0.018	0.040	0.070
Ti	0.341	0.103	0.286	0.348	0.312	0.249	0.254	0.263
Zr	0.000	0.000	0.006	0.004	0.008	0.019	0.026	0.031
Al	0.067	0.023	0.025	0.018	0.008	0.098	0.000	0.000
Fe	0.086	0.138	0.104	0.075	0.119	0.123	0.147	0.147
Sn	0.086	0.000	0.078	0.000	0.000	0.000	0.000	0.000
Total in *B*	**2.00**	**2.00**	**2.00**	**2.00**	**2.00**	**2.00**	**2.00**	**2.00**

APPENDIX VI

Representative compositions of zirconolite minerals from carbonatite complexes worldwide

Legend

Analyses	Locality	General Reference
KO-16, KO-19, KO-21, KO-22, KO-24, KO-26, KO-29	Kovdor carbonatite complex, Russia	Kapustin (1980); Kukharenko *et al.* (1965)
KA-71, KA-72	Kaiserstuhl, Germany	Keller (1984)
SL-36, SL-38, SL-40, SL-42, SL-44, SL-46, SL-48, SL-50, Sl-52, SL-54, SL-56	Schryburt Lake carbonatite complex, Canada	Williams and Platt (unpublished)
PH-60, PH-61, PH-62, PH-63, PH-64, PH-65	Phalaborwa carbonatite complex, South Africa	Williams, unpublished data
SO-66, SO-67, SO-68, SO-69, SO-70	Sokli carbonatite complex, Finland	Hornig-Kjarsgaard, unpublished data

	KO-16	KO-19	KO-21	KO-22	KO-24	KO-25	KO-26	KO-29	KO-31	KO-33	KA-71	KA-72
MgO	n.d.	0.80	0.74	0.76	0.39	0.27	0.58	0.30	0.54	0.48	0.85	n.d.
Al_2O_3	3.47	<0.5	<0.5	<0.5	<0.5	<0.5	<0.5	<0.5	<0.05	<0.05	n.d.	n.d.
SiO_2	n.d.	<0.5	<0.5	<0.5	<0.5	<0.5	<0.5	<0.5	<0.05	<0.05	n.d.	n.d.
CaO	10.12	10.82	10.72	11.47	12.72	12.74	12.30	11.85	12.12	12.25	11.38	12.50
TiO_2	14.86	17.25	16.54	14.70	21.05	23.54	18.68	22.77	18.72	17.18	13.56	22.70
Cr_2O_3	n.d.	n.d.	n.d.	n.d.	n.d.	n.d.	n.d.	n.d.	n.d.	n.d.	n.d.	n.d.
MnO	n.d.	0.30	0.27	0.26	0.13	0.05	0.20	0.34	0.16	0.20	0.94	0.20
FeO	4.00	7.57	7.77	7.27	7.31	7.10	7.66	6.79	7.46	7.40	7.41	2.28
Fe_2O_3	2.88	n.d.	n.d.	n.d.	n.d.	n.d.	n.d.	n.d.	n.d.	n.d.	n.d.	5.32
Y_2O_3	n.d.	0.05	0.17	0.09	0.23	0.13	0.25	0.18	0.31	0.15	n.d.	n.d.
ZrO_2	32.94	28.81	29.27	28.64	30.53	31.18	30.29	30.72	31.24	29.88	30.51	34.80
Nb_2O_5	19.82	19.01	19.85	20.68	17.45	14.54	18.25	14.47	18.04	20.78	22.07	15.70
La_2O_3	n.d.	0.25	0.45	0.17	0.17	0.26	0.21	0.18	0.40	0.22	n.d.	n.d.
Ce_2O_3	3.06	1.52	1.40	0.97	1.62	1.42	1.61	1.46	1.62	1.47	0.77	0.90
Pr_2O_3	n.d.	0.38	0.19	0.16	0.39	0.14	0.41	0.41	0.48	0.17	n.d.	n.d.
Nd_2O_3	n.d.	1.13	1.40	0.82	1.15	1.31	1.58	1.16	1.49	1.14	1.10	n.d.
Sm_2O_3	n.d.	0.32	0.31	n.d.	0.18	0.33	0.20	0.18	0.40	0.35	0.27	n.d.
Gd_2O_3	n.d.	0.21	0.22	0.14	0.26	0.24	0.34	0.35	0.34	0.18	n.d.	n.d.
Tb_2O_3	n.d.	n.d.	n.d.	n.d.	n.d.	n.d.	n.d.	n.d.	n.d.	n.d.	n.d.	n.d.
Dy_2O_3	n.d.	0.20	0.22	<0.15	0.16	<0.15	0.18	<0.15	0.19	<0.15	n.d.	n.d.
Ho_2O_3	n.d.	n.d.	n.d.	n.d.	n.d.	n.d.	n.d.	n.d.	n.d.	n.d.	n.d.	n.d.
Er_2O_3	n.d.	<0.15	<0.15	<0.15	<0.15	<0.15	<0.15	<0.15	<0.15	<0.15	n.d.	n.d.
Tm_2O_3	n.d.	n.d.	n.d.	n.d.	n.d.	n.d.	n.d.	n.d.	n.d.	n.d.	n.d.	n.d.
Yb_2O_3	n.d.	n.d.	n.d.	n.d.	n.d.	n.d.	n.d.	n.d.	n.d.	n.d.	n.d.	n.d.
Lu_2O_3	n.d.	n.d.	n.d.	n.d.	n.d.	n.d.	n.d.	n.d.	n.d.	n.d.	n.d.	n.d.
HfO_2	n.d.	0.52	0.48	0.48	0.70	0.62	0.72	0.67	0.72	0.55	n.d.	n.d.
Ta_2O_5	2.08	1.75	2.46	4.97	2.03	1.66	3.27	2.78	3.91	2.80	3.08	n.d.
WO_3	n.d.	<0.25	<0.25	<0.25	<0.25	<0.25	<0.25	<0.25	<0.25	<0.25	n.d.	n.d.
PbO	n.d.	0.18	<0.1	<0.1	<0.1	<0.1	0.20	<0.1	<0.1	<0.1	n.d.	n.d.
ThO_2	3.21	6.26	5.42	5.51	1.18	1.36	1.09	2.46	2.04	2.26	5.13	4.10
UO_2	1.82	0.13	0.23	0.28	0.41	0.56	0.40	1.07	0.24	0.51	1.22	1.40
$(Na,K)_2O$	0.89	n.d.	n.d.	n.d.	n.d.	n.d.	n.d.	n.d.	n.d.	n.d.	n.d.	n.d.
Total	102.11	97.46	98.11	97.37	98.08	97.45	98.40	98.14	100.42	97.95	98.29	99.50

Cations to 7 oxygens

	KO-16	KO-19	KO-21	KO-22	KO-24	KO-25	KO-26	KO-29	KO-31	KO-33	KA-71	KA-72
Ca^{2+}	0.719	0.799	0.788	0.854	0.897	0.895	0.880	0.840	0.856	0.882	0.839	0.850
$(Y+REE)^{3+}$	0.074	0.101	0.109	0.060	0.101	0.094	0.117	0.098	0.127	0.094	0.053	0.021
Pb^{2+}	n.d.	0.003	n.d.	n.d.	0.001	0.001	0.004	n.d.	n.d.	n.d.	n.d.	n.d.
Th^{4+}	0.048	0.098	0.085	0.087	0.018	0.020	0.017	0.037	0.031	0.035	0.080	0.058
U^{4+}	0.027	0.002	0.004	0.004	0.006	0.008	0.006	0.016	0.004	0.008	0.019	0.020
SUM Ca^{2+}	0.868	1.004	0.985	1.006	1.022	1.018	1.022	0.991	1.017	1.017	0.991	0.950
Zr^{4+}	1.065	0.969	0.979	0.971	0.979	0.997	0.988	0.991	1.004	0.978	1.024	1.077
Hf^{4+}	n.d.	0.010	0.009	0.010	0.013	0.012	0.014	0.013	0.014	0.011	n.d.	n.d.
SUM Zr^{4+}	1.065	0.979	0.988	0.980	0.992	1.008	1.000	1.004	1.018	0.989	1.024	1.077
Ti^{4+}	0.741	0.894	0.853	0.788	1.041	1.160	0.938	1.133	0.926	0.888	0.702	1.084
Si^{4+}	n.d.	n.d.	n.d.	n.d.	n.d.	n.d.	n.d.	n.d.	n.d.	n.d.	n.d.	n.d.
Mg^{2+}	n.d.	0.082	0.076	0.079	0.038	0.026	0.058	0.030	0.053	0.048	0.087	n.d.
Mn^{2+}	n.d.	0.018	0.016	0.015	0.007	0.003	0.011	0.019	0.009	0.011	0.055	0.011
Fe^{2+}	0.222	0.436	0.446	0.423	0.402	0.389	0.428	0.376	0.411	0.416	0.427	0.121
Fe^{3+}	0.144	n.d.	n.d.	n.d.	n.d.	n.d.	n.d.	n.d.	n.d.	n.d.	n.d.	0.254
Al^{3+}	0.271	n.d.	n.d.	n.d.	n.d.	n.d.	n.d.	n.d.	n.d.	n.d.	n.d.	n.d.
Cr^{3+}	n.d.	n.d.	n.d.	n.d.	n.d.	n.d.	n.d.	n.d.	n.d.	n.d.	n.d.	n.d.
Nb^{5+}	0.589	0.593	0.615	0.650	0.519	0.431	0.551	0.433	0.538	0.631	0.687	0.451
Ta^{5+}	0.037	0.033	0.046	0.094	0.036	0.030	0.059	0.050	0.070	0.051	0.058	n.d.
SUM Ti^{4+}	2.003	2.056	2.051	2.029	2.044	2.039	2.044	2.041	2.009	2.025	2.015	1.920
TOTAL	**3.936**	**4.038**	**4.024**	**4.014**	**4.059**	**4.065**	**4.067**	**4.036**	**4.045**	**4.031**	**4.031**	**3.947**

	SL-36	SL-38	SL-40	SL-42	SL-44	SL-46	SL-48	SL-50	SL-52	SL-54	SL-56
MgO	0.31	0.33	0.47	0.22	0.48	0.21	0.19	0.18	0.30	0.28	0.35
Al_2O_3	0.11	<0.05	<0.05	<0.05	<0.05	<0.05	0.09	<0.05	0.09	<0.05	0.12
SiO_2	0.48	<0.05	<0.05	0.05	0.16	0.27	0.07	0.15	0.31	0.19	0.46
CaO	9.19	10.50	10.68	11.78	10.49	5.79	9.11	6.93	7.35	9.78	8.71
TiO_2	29.12	23.20	18.34	22.52	19.39	22.40	25.93	21.84	22.90	23.64	20.51
Cr_2O_3	n.d.	n.d.	n.d.	n.d.	n.d.	n.d.	n.d.	n.d.	n.d.	n.d.	n.d.
MnO	0.20	0.13	0.47	0.21	0.40	0.55	0.21	0.47	0.32	0.27	1.07
FeO	8.77	6.98	6.74	7.37	8.22	7.90	7.48	7.46	7.80	7.04	6.56
Fe_2O_3	n.d.	n.d.	n.d.	n.d.	n.d.	n.d.	n.d.	n.d.	n.d.	n.d.	n.d.
Y_2O_3	1.28	0.53	0.56	0.49	0.61	1.26	1.08	1.41	0.95	0.51	0.48
ZrO_2	32.78	30.51	30.73	30.15	28.87	28.36	30.33	29.49	29.50	30.00	32.62
Nb_2O_5	2.82	13.10	18.92	15.48	17.75	9.11	9.91	10.53	11.91	13.21	13.82
La_2O_3	0.45	0.19	0.32	0.14	0.37	0.53	0.33	0.36	0.34	0.23	0.19
Ce_2O_3	5.03	2.09	2.15	2.09	2.64	5.27	3.29	4.13	3.78	2.95	1.99
Pr_2O_3	1.10	0.27	0.38	0.57	0.41	1.25	0.89	1.05	0.92	0.66	0.61
Nd_2O_3	4.99	2.25	2.03	2.49	3.22	7.27	4.54	5.91	5.51	3.89	2.04
Sm_2O_3	1.03	0.61	0.43	0.80	0.90	1.90	1.33	1.89	1.46	0.98	0.49
Gd_2O_3	0.91	0.46	0.41	0.40	0.40	1.25	0.79	1.12	0.87	0.59	0.26
Tb_2O_3	n.d.	n.d.	n.d.	n.d.	n.d.	n.d.	n.d.	n.d.	n.d.	n.d.	n.d.
Dy_2O_3	0.45	0.30	0.19	0.25	<0.15	0.57	0.56	0.68	0.61	0.25	0.69
Ho_2O_3	n.d.	n.d.	n.d.	n.d.	n.d.	n.d.	n.d.	n.d.	n.d.	n.d.	n.d.
Er_2O_3	<0.15	0.22	0.19	<0.15	<0.15	0.20	0.22	0.37	<0.15	<0.15	<0.15
Tm_2O_3	n.d.	n.d.	n.d.	n.d.	n.d.	n.d.	n.d.	n.d.	n.d.	n.d.	n.d.
Yb_2O_3	<0.18	<0.18	<0.18	<0.18	<0.18	<0.18	<0.18	<0.18	<0.18	<0.18	<0.18
Lu_2O_3	n.d.	n.d.	n.d.	n.d.	n.d.	n.d.	n.d.	n.d.	n.d.	n.d.	n.d.
HfO_2	0.57	0.70	0.57	0.67	0.72	0.58	0.65	0.59	0.66	0.64	0.60
Ta_2O_5	0.29	<0.25	1.04	0.66	<0.25	<0.25	<0.25	0.30	<0.25	<0.25	<0.25
WO_3	<0.25	<0.25	<0.25	<0.25	<0.25	<0.25	<0.25	<0.25	<0.25	<0.25	<0.25
PbO	<0.1	0.23	0.25	0.19	<0.1	<0.1	<0.1	0.14	0.14	0.14	0.23
ThO_2	<0.1	0.93*	0.64	1.45	1.58	0.54	0.77	1.07	1.88	0.55	3.67
UO_2	0.10	2.04	2.13	0.41	0.03	0.51	0.53	0.42	0.46	0.97	0.49
$(Na,K)_2O$	n.d.	n.d.	n.d.	n.d.	n.d.	n.d.	n.d.	n.d.	n.d.	n.d.	n.d.
Total	97.98	95.77	97.64	98.19	96.64	95.72	98.30	96.49	98.06	96.77	95.96

Cations to 7 oxygens

	SL-36	SL-38	SL-40	SL-42	SL-44	SL-46	SL-48	SL-50	SL-52	SL-54	SL-56
Ca^{2+}	0.654	0.779	0.776	0.835	0.765	0.445	0.651	0.525	0.540	0.705	0.643
$(Y+REE)^{3+}$	0.377	0.173	0.168	0.175	0.216	0.514	0.322	0.442	0.366	0.250	0.171
Pb^{2+}	n.d.	0.004	0.005	0.003	0.001	0.001	n.d.	0.003	0.003	0.003	0.004
Th^{4+}	n.d.	0.014	0.010	0.022	0.024	0.009	0.012	0.017	0.029	0.008	0.058
U^{4+}	0.001	0.031	0.032	0.008	0.000	0.008	0.008	0.007	0.007	0.015	0.008
SUM Ca^{2+}	1.033	1.002	0.991	1.041	1.006	0.977	0.993	0.994	0.945	0.981	0.883
Zr^{4+}	1.062	1.011	1.017	0.972	0.958	0.992	0.987	1.017	0.986	0.985	1.095
Hf^{4+}	0.011	0.014	0.011	0.013	0.014	0.012	0.012	0.012	0.013	0.012	0.013
SUM Zr^{4+}	1.073	1.025	1.028	0.985	0.972	1.004	0.999	1.029	0.999	0.997	1.108
Ti^{4+}	1.455	1.186	0.936	1.120	0.992	1.208	1.301	1.162	1.181	1.197	1.062
Si^{4+}	0.032	n.d.	n.d.	0.003	0.011	0.019	0.005	0.011	0.021	0.013	0.032
Mg^{2+}	0.031	0.033	0.048	0.022	0.049	0.022	0.019	0.019	0.031	0.028	0.036
Mn^{2+}	0.011	0.007	0.027	0.012	0.023	0.033	0.012	0.028	0.019	0.015	0.062
Fe^{2+}	0.378	0.397	0.382	0.408	0.468	0.474	0.417	0.441	0.447	0.396	0.378
Fe^{3+}	n.d.	n.d.	n.d.	n.d.	n.d.	n.d.	n.d.	n.d.	n.d.	n.d.	n.d.
Al^{3+}	0.009	n.d.	n.d.	n.d.	n.d.	0.003	0.007	n.d.	0.007	n.d.	0.010
Cr^{3+}	n.d.	n.d.	n.d.	n.d.	n.d.	n.d.	n.d.	n.d.	n.d.	n.d.	n.d.
Nb^{5+}	0.085	0.403	0.580	0.463	0.546	0.295	0.299	0.377	0.369	0.402	0.430
Ta^{5+}	0.005	n.d.	0.019	0.012	0.003	n.d.	0.003	0.011	0.001	0.001	0.004
SUM Ti^{4+}	2.004	2.026	1.992	2.039	2.091	2.061	2.064	2.008	2.076	2.056	2.014
TOTAL	**4.110**	**4.053**	**4.011**	**4.065**	**4.069**	**4.042**	**4.056**	**4.031**	**4.020**	**4.036**	**4.005**

	PII-60	PII-61	PII-62	PII-63	PII-64	PII-65	SO-66	SO-67	SO-68	SO-69	SO-70
MgO	<0.05	<0.05	<0.05	<0.05	<0.05	0.17	0.15	1.06	1.07	1.13	0.52
Al_2O_3	<0.05	<0.05	<0.05	<0.05	<0.05	n.d.	n.d.	0.13	0.15	0.18	0.03
SiO_2	<0.05	<0.05	<0.05	<0.05	<0.05	n.d.	0.13	0.05	0.03	0.03	0.18
CaO	12.36	12.02	11.48	9.75	11.31	11.28	12.07	10.32	9.18	9.09	11.16
TiO_2	36.15	35.39	34.68	34.33	35.71	34.93	34.45	14.14	14.10	14.40	19.79
Cr_2O_3	n.d.	n.d.	n.d.	n.d.	n.d.	n.d.	n.d.	n.d.	n.d.	n.d.	n.d.
MnO	0.19	0.21	0.21	0.35	0.26	n.d.	n.d.	n.d.	n.d.	n.d.	n.d.
FeO	6.49	6.85	6.57	10.20	6.32	n.d.	n.d.	8.89	7.27	8.56	8.16
Fe_2O_3	n.d.	n.d.	n.d.	n.d.	n.d.	6.88	6.64	n.d.	n.d.	n.d.	n.d.
Y_2O_3	0.32	0.32	0.17	0.36	0.28	n.d.	0.45	0.24	0.41	0.34	0.46
ZrO_2	35.15	33.71	34.55	31.65	33.67	32.90	32.23	26.17	26.08	26.76	27.35
Nb_2O_5	0.19	0.29	0.23	0.38	0.19	n.d.	0.45	18.50	17.01	16.50	15.68
La_2O_3	<0.07	0.13	0.11	<0.07	<0.07	n.d.	n.d.	n.d.	n.d.	n.d.	n.d.
Ce_2O_3	0.74	0.91	0.77	1.04	0.77	n.d.	0.33	1.59	2.42	1.31	2.49
Pr_2O_3	<0.14	<0.14	<0.14	<0.14	<0.14	n.d.	n.d.	n.d.	n.d.	n.d.	n.d.
Nd_2O_3	0.57	0.85	0.75	1.08	0.61	n.d.	0.95	n.d.	n.d.	n.d.	n.d.
Sm_2O_3	0.33	0.36	0.27	0.31	0.26	n.d.	n.d.	n.d.	n.d.	n.d.	n.d.
Gd_2O_3	0.32	0.17	0.23	0.33	0.23	n.d.	n.d.	n.d.	n.d.	n.d.	n.d.
Tb_2O_3	n.d.	n.d.	n.d.	n.d.	n.d.	n.d.	n.d.	n.d.	n.d.	n.d.	n.d.
Dy_2O_3	0.28	0.21	0.26	0.33	0.15	n.d.	n.d.	n.d.	n.d.	n.d.	n.d.
Ho_2O_3	n.d.	n.d.	n.d.	n.d.	n.d.	n.d.	n.d.	n.d.	n.d.	n.d.	n.d.
Er_2O_3	<0.16	<0.16	<0.16	<0..16	<0.16	n.d.	n.d.	n.d.	n.d.	n.d.	n.d.
Tm_2O_3	n.d.	n.d.	n.d.	n.d.	n.d.	n.d.	n.d.	n.d.	n.d.	n.d.	n.d.
Yb_2O_3	n.d.	n.d.	n.d.	n.d.	n.d.	n.d.	n.d.	n.d.	n.d.	n.d.	n.d.
Lu_2O_3	n.d.	n.d.	n.d.	n.d.	n.d.	n.d.	n.d.	n.d.	n.d.	n.d.	n.d.
HfO_2	0.51	0.70	0.85	0.55	0.76	1.22	0.90	1.08	0.76	0.70	0.40
Ta_2O_5	<0.2	0.39	<0.2	0.32	<0.2	n.d.	n.d.	5.67	5.68	5.83	0.21
WO_3	<0.2	<0.2	<0.2	<0.2	<0.2	n.d.	n.d.	n.d.	n.d.	n.d.	n.d.
PbO	0.65	0.33	0.68	0.17	0.21	n.d.	n.d.	n.d.	n.d.	n.d.	n.d.
ThO_2	3.46	4.18	4.03	5.58	3.67	4.36	4.85	5.89	7.65	10.80	5.57
UO_2	1.41	1.44	1.51	1.87	1.68	1.37	1.44	n.d.	n.d.	n.d.	n.d.
$(Na,K)_2O$	n.d.	n.d.	n.d.	n.d.	n.d.	n.d.	n.d.	n.d.	n.d.	n.d.	n.d.
Total	99.11	98.48	97.34	98.59	98.09	93.11	95.04	93.73	91.81	95.63	92

Cations to 7 oxygens

	PH-60	PH-61	PH-62	PH-63	PH-64	PH-65	SO-66	SO-67	SO-68	SO-69	SO-70
Ca^{2+}	0.829	0.818	0.792	0.676	0.780	0.783	0.830	0.804	0.739	0.713	0.847
$(Y+REE)^{3+}$	0.060	0.070	0.060	0.083	0.056	0.000	0.045	0.052	0.083	0.048	0.082
Pb^{2+}	0.011	0.008	0.012	0.003	0.004	n.d.	n.d.	n.d.	n.d.	n.d.	n.d.
Th^{4+}	0.049	0.060	0.059	0.082	0.054	0.064	0.071	0.097	0.131	0.180	0.090
U^{4+}	0.020	0.020	0.022	0.027	0.024	0.020	0.021	n.d.	n.d.	n.d.	n.d.
SUM Ca^{2+}	0.969	0.975	0.944	0.871	0.917	0.867	0.966	0.953	0.953	0.941	1.019
Zr^{4+}	1.073	1.044	1.084	0.999	1.057	1.040	1.009	0.927	0.956	0.955	0.945
Hf^{4+}	0.009	0.013	0.016	0.010	0.014	0.023	0.016	0.022	0.016	0.015	0.008
SUM Zr^{4+}	1.082	1.057	1.099	1.010	1.071	1.062	1.025	0.950	0.972	0.970	0.953
Ti^{4+}	1.702	1.691	1.678	1.672	1.729	1.702	1.663	0.773	0.797	0.793	1.055
Si^{4+}	n.d.	n.d.	n.d.	n.d.	n.d.	n.d.	0.008	0.004	0.002	0.002	0.013
Mg^{2+}	0.001	0.002	0.002	0.002	0.002	0.016	0.014	0.115	0.120	0.123	0.055
Mn^{2+}	0.010	0.011	0.011	0.019	0.014	n.d.	n.d.	n.d.	n.d.	n.d.	n.d.
Fe^{2+}	0.340	0.364	0.354	0.552	0.340	n.d.	n.d.	0.540	0.457	0.524	0.484
Fe^{3+}	n.d.	n.d.	n.d.	n.d.	n.d.	0.336	0.321	n.d.	n.d.	n.d.	n.d.
Al^{3+}	n.d.	n.d.	n.d.	n.d.	n.d.	n.d.	n.d.	0.011	0.013	0.016	0.003
Cr^{3+}	n.d.	n.d.	n.d.	n.d.	n.d.	n.d.	n.d.	n.d.	n.d.	n.d.	n.d.
Nb^{5+}	0.005	0.008	0.007	0.011	0.005	n.d.	0.013	0.608	0.578	0.546	0.502
Ta^{5+}		0.007	0.003	0.006	0.003	n.d.	n.d.	0.112	0.118	n.d.	0.004
SUM Ti^{4+}	2.058	2.083	2.054	2.263	2.094	2.054	2.019	2.163	2.083	2.120	2.115
TOTAL	**4.109**	**4.114**	**4.097**	**4.143**	**4.082**	**3.984**	**4.010**	**4.065**	**4.009**	**4.031**	**4.088**